Spectroscopic
Atlas for
Amateur Astronomers

A Guide to the Stellar
Spectral Classes

Richard Walker

Version 3.0   03/2012

Table of Contents

Change log of the atlas versions

<u>Version 1.3</u>: Corrections of some labeling-/typing errors and temperature of the O-class stars, some English language corrections.

<u>Version 1.4</u>: Corrections of some labeling and typing errors. *sect. 1:* correction of citation error regarding *Spectroweb*.

<u>Version 1.5</u>: *Sect*. *7.4, (8) WR133,* expansion velocity of the stellar wind, *EW* value replaced by *FWHM* value.
sect. 8.3 (9.3): chart of the theoretical B-class continuum, correction of the wrongly labeled Ca II line (thanks to Robin Leadbeater!).

<u>Version 2.0</u>: New: *Sect. 12:* Be Shell stars and some adjustments to *sect. 11*.
New: *Sect. 18 − 21:* Spectral sequence of the *Mira Variables* on the *AGB* with the classes *M(e), S-* and carbon stars *C*.
General revision of the title structure, the table of contents and the *sect. 31* "Bibliography and Internet".

<u>Version 3.0</u>:
Sect. 3.5: Additional Abbreviations,
Sect. 3.7: New: Formula for metallicity.
Sect. 7:   General revision and expansion to the early O Class.
Sec. 10:   P Cygni, higher resolved profile sections (900L grating) in the green and blue range of the spectrum.
Sect. 13: New: *Herbig Ae/Be* and *T Tauri Protostars*
Sect. 21: Correction of the wrongly labelled *BD Camelopardalis:* new HD 22649
Sect. 24: General revision of the section, new: determination of the excitation classes of emission nebulae and table 85: SNR M1/ NGC 1952.
Sect. 25: Reflexion spectra: former Tables 85 and 86 ==> new Tables 90 and 91
            New: Comet C/2009 P1 Garradd, Table 94
Sect. 27: New: Nigth Sky Spectrum Table 96
Sect. 28: Table 106, Calibration spectrum of the glow starter OSRAM ST 111
Sect. 31: List of bright Planetary Nebulae sorted by excitation classes.
All Parameter tables of the individual spectral classes: Correction of the wrong (german) abbreviation "*Mrd*" by *bn* (thanks to Dave Dowhos!).

Directory of Tables

Table	Page	Topic	Objects	Wavelength domain	Gra-ting
23	59	Metallicity: Vega vs. Sirius	Vega α Lyr Sirius A α CMa	3920 – 4700	900L
30	62	Development of spectral features within the F-class	Adhafera ζ Leo Procyon α CMi	3830 – 6700	200L
31	64	Effects of the luminosity on spectra of the early F-class	Porrima γ Vir Caph β Cas Mirfak α Per	3920 – 4750	900L
40	67	Development of spectral features within the G-class	Muphrid η Boo Vindemiatrix ε Vir	3800 – 6600	200L
41	68	Detailed spectrum of an early G-class star	Sun	3800 – 7200 3900 – 4800	200L 900L
42	69	Detailed spectrum of an early G-class star	Sun	4700 – 5700 5650 – 6700	900L
50	73	Development of spectral features within the K-class	Arcturus α Boo Alterf λ Leo	3900 – 6800	200L
51	74	Detailed spectrum of an early K-class star	Pollux α Gem	3900 – 6800 3800 – 4800	200L 900L
52	76	Effects of the luminosity on spectra of the late K-class	Alsciaukat α Lyncis 61 Cygni B	4000 – 4900	900L
53	77	Detailed spectrum of a later K-class star	Aldebaran α Tau	5150 – 5900 5850 – 6700	900L
60	80	Development of spectral features within the M-class	Antares α Sco Ras Algethi α Her	3900 – 7200	200L
63	84	Mira Variable M(e), comparison to a late classified M-Star	Mira o Ceti Ras Algethi α Her	3900 – 7200	200L
65	87	Extreme S-Class star, comparison to a Mira Variable M(e)	R Cygni Mira o Ceti	4100 – 7300	200L
66	89	Development of spectral features within the *S*-Class	Omikron1 Orionis Chi Cygni R Cygni	4100 – 7300	200L
66A	90	Comparison of an „*intrinsic*" and „*extrinsic*" S-Class star	BD Camelopardalis HR Pegasi	4300 – 7200	200L
67	95	Comparison of differently classified carbon stars	WZ Cassiopeiae Z Piscium W Orionis	4600 – 7300	200L
67A	96	*Merril Sanford Bands,* details at a higher resolved spectrum	W Orionis	4730 – 5400	900L
70	99	Comparison of Spectra: Spiral galaxy vs. star of the late G-class	Andromeda M31 Vindemiatrix ε Vir	3900 – 6700	200L
80	108	Emission Nebula: *H II Region*	M42	3800 – 7300	200L
80A	109	Intensity profiles of Hβ and [OIII] (λ5007) in the central area of M42	M42	n.a.	200L
81	110	Emission Nebula: *Planetary Nebula*	IC418 Spirograph Neb	4100 – 7100	200L
82	111	Emission Nebula: *Planetary Nebula*	NGC6210 Turtle Neb.	3850 – 6600	200L
83	112	Emission Nebula: *Planetary Nebula*	NGC7009 Saturn Neb	3800 – 6700	200L

Table	Page	Topic	Objects	Wavelength domain	Gra-ting
84	113	Emission Nebula: *Planetary Nebula*	M57 Ring Nebula	4600 – 6800	200L
84A	114	Intensity profiles of [O III] and [N II] in the longitudinal axis of M57	M57 Ring Nebula	n.a.	200L
85	115	Emission Nebula: *SNR*	M1 / NGC 1952	4600 – 6800	200L
90	118	Reflexion spectra of solar system bodies	Mars, Venus	4300 – 7800	200L
91	119	Reflexion spectra of solar system bodies	Jupiter, Saturn	4400 – 7800	200L
94	120	Comet spectrum	C/2009 P1 Garradd	3800 – 6400	200L
95	122	Spectral absorptions due to the earth's atmosphere	Earth's atmosphere	6800 – 7800	900L
96	124	Night sky spectrum	Light Pollution Airglow	4000 – 7400	200L
101	127	Gas discharge lamp	Neon glow lamp	5800 – 8100	900L
102	128	Gas discharge lamp	ESL Osram Sunlux	3900 – 6400	200L
103	129	Gas discharge lamp	Xenon strobe tube	3900 – 8100	200L 900L
104	130	Gas discharge lamp	High pressure sodium vapor lamp	4700 – 7250	200L
105	131	Gas discharge lamp	High power xenon lamp	4900 – 6900	200L
106	132	Gas discharge lamp	Glow Starter OSRAM ST 111	4000 – 7700 3900 – 4800	200L 900L
110	134	Swan Bands / Hydrocarbon gas flames: Comparison of superposed spectra	Butane-gas-torch Comet Hyakutake WZ Cassiopeiae	3800 – 6400	200L

1   Introduction

Probably most amateur astronomers have a common experience at the beginning of their spectrographic ˝career˝. Full of expectations they test the new device for the first time and look with great pride at the first self recorded spectrum. This first enthusiasm then quickly gives way to the perplexity, how these numerous lines shall now be identified and even analyzed.

Fortunately, some recommendable introductory literature, e.g. [1], for amateurs to the interpretation of stellar spectra is available in English. However, a real ˝*Spectral Atlas*˝, which systematically covers the classes *O, B, A, F, G, K, M*, by commenting most of the lines, visible in a medium resolved spectral profile was still missing. In the Internet we find many professional papers, mostly focused on small sections of a spectral profile. Nevertheless, they often contribute valuable puzzle pieces to the exciting ˝detective work˝ of line identification.

Very well documented is the spectrum of the Sun (G2 V), where almost all of the lines are identified and commented. Here, at least two easily readable and freely downloadable atlases are available on the net [80], [81]. These sources can even help, with the necessary precautions, to identify spectral lines of adjacent spectral classes.

Spectral atlases from professional sources, published on the internet, and covering all important spectral classes can rarely be found. Amazingly, even in such professional papers, usually only a few intense lines, mostly in very lowly resolved spectra, are commented. However, the focus of many practical applications, even in professional works, is mostly reduced to relatively few, highly intense and isolated lines, e.g. for determination of the rotation speed or the metal abundance. In such publications the ultraviolet, the blue- and red- to far infrared part of the spectra are preferably treated - the sections "green" and "yellow" however only rarely.

In Appendix 33.3 some excerpts from several historical as well as state of the art spectral atlases are shown. Probably the best known, and highly important one, even for the history of science, is the out of print standard work "*An atlas of stellar spectra, with an outline of spectral classification*" by Morgan, Keenan and Kellman [50]. This seminal work from 1943 can now be downloaded from the Internet but is limited to the short-wavelength part of the visible spectrum, reflecting the state of technology in the 1940's. It presents photographic spectral strips, commented with handwritten notes! Made in a similar style is the ˝*Revised MK Spectral Atlas for Stars Earlier Than the Sun*˝ from 1978 by Morgan, Abt, and Tapscott [51].

Some spectral atlases were available in the past but are out of print today. The most comprehensive ˝reference work˝ is surely ˝*Bonner Spektralatlas*˝, the title of the English edition: ˝*Atlas for Objective Prism Spectra*˝ by Waltraut C. Seitter, 1975 [5]). This atlas, covering the spectral types from *O5* to *M2,* is out of print today, but recently available as download [5]! Still based on photographic spectral strips it's the only reviewed work, documenting most of the lines between about λ 3400 − 5000, which are visible with low to medium resolving spectrographs. In the *green-red* range this atlas partly shows quite large gaps. It's striking, that despite this work undoubtedly being outdated, it has never been adapted to today's requirements, but is still referenced in various current papers. Written in a similar style, but much less detailed, are also the atlases [6], [7] and [8]. A stroke of luck that Martin Brunold [705] collected all these books and has kindly provided me with a review (see Appendix 33.3).

Nowadays calibrated and intensity-normalized profiles, plotted against the wavelength are required to meet the current standards. Fairly recent (2000) is "*A Digital Spectral Classification Atlas*" by R.O. Gray [52]. However it's limited to a lowly resolved, short-wave part of the visible spectrum. Furthermore several atlases exist, focusing on specific

wavelength ranges. Some of them are listed in the bibliography. For some of the brighter stars monographs are available, with fully commented spectra of e.g. Sirius, Procyon and Aldebaran. Unfortunately, such papers are mostly available as "abstracts" only. The download prices for the full versions are usually pretty high.

Very useful *is Spectroweb* [59], to find on the home page of *Dr. Alex Lobel*, Royal Observatory of Belgium. It's an interactive internet platform providing highly resolved and almost completely commented profiles of some bright stars, belonging to the middle and late spectral classes *F, G, K, M*. Due to the enormous line density it's, particularly for beginners, very difficult to make the link to the highly blended lines of their own, in most cases lowly resolved profiles. Here at last it becomes clear, why spectral atlases need to be created for specific degrees of resolution.

Recently the pocket guide *"A Spectroscopic Atlas of Bright Stars"* [9] was published. It's essentially a collection of non-normalized pseudo-continua of bright stars, showing a few, intense spectral lines. These have been recorded by Jack Martin under the London night sky on conventional (chemical) film with a slitless transmission grating spectrograph.

This huge diversity of information explains why different sources have been used for the line identification. References for each and every line would not be feasible. However, for each spectral class, the mainly used sources are referenced. An alternative option would be to compare the spectra with synthetically generated profiles, based on models of stellar atmospheres. This allows for example the software *"Spectrum"* from *R.O. Gray*, which runs on Linux with a command-oriented interface. The installation for non Linux users, and also the operation are demanding. So this is probably a realistic option for very few amateurs only.

This atlas is primarily intended to be used as a tool for the line identification – as a supplement to my *" Spectroscopic Applications for Amateur Astronomers"* [30] and the practical part *," The processing and analysis of spectral profiles ..."* [31]. In these documents also detailed information on the classification system of the spectra and the Hertzsprung-Russel diagram (*HRD*) are included (currently available in German only). Knowledge of these topics are presupposed here and therefore treated briefly only.

From the beginning it was clear, that this atlas would not be reduced to an isolated collection of some labeled spectral tables. Therefore, each spectral class is presented with their main characteristics and typical features. The atlas will be continuously updated if new information or characteristic spectra are available. This intended future expansion was considered in the numbering system of the tables. After such updates, direct or "hot links" on the file will necessarily lead to the void. Therefore, I strongly recommend linking to the atlas only to: http://www.ursusmajor.ch/astrospektroskopie/richard-walkers-page/index.html

Many thanks to *Martin Huwiler, Urs Flükiger* and *Dr. Helen Wider* for proofing the German edition, and Urs again for kindly providing his homepage for downloading!

Richard Walker, CH 8911 Rifferswil   © richiwalker@bluewin.ch

2 Selection, Preparation and Presentation of the Spectra

2.1 Selection of spectra

Main criteria for the selection of the spectra have been the documentation of the spectral characteristics of the classes *O, B, A, F, G, K, M*, and further the demonstration of certain effects e.g. due to the different luminosity classes. The consideration of bright "common knowledge stars" was of secondary importance. In principle, every spectral class, including some extraordinary star types, is presented at least with an "early" and a "late" representative spectrum to show the development of characteristic features in the profile. Commented in separate chapters are spectra of emission nebulae, composite spectra of extragalactic objects, reflection spectra of solar system bodies, absorption bands generated by the earth's atmosphere and some profiles of terrestrial light sources.

2.2 Recording and Resolution of the Spectra

The spectra have been recorded with the DADOS spectrograph [603], equipped with reflection gratings of 200- or 900 Lines/mm. Unless otherwise noted, the recording was made through the 8 inch Schmidt-Cassegrain *Celestron C8,* the *25 μm slit* of the DADOS spectrograph, and finally with the monochrome camera *Meade DSI III Pro*. The spectra on the following *Tables*: *5* (WR133), *70* and *84* have been recorded together with *Martin Huwiler* through the CEDES 36 inch telescope of the *Mirasteilas* observatory in Falera (see Appendix 33.4).

The processing of the spectra with *Vspec* indicates the following dispersions: 900L grating about 0.65 Å/pixel and 200L grating some 2.55 Å/pixel. Data of the Sony Chip ICX285AL: 1.4 Mega-pixel, 2/3" Monochrome CCD, Pixelsize 6.45μm x 6.45μm [606]. For longer exposure times a dark frame was subtracted. The processing of a "flatfield" was omitted.

The *R-value*, defines the resolution of the spectrograph. According to the DADOS Manual it corresponds to $R_{200L} = 647$ at 6160 Å and $R_{900L} = 3,000$ at 5610 Å. My own measurements in this wavelength domain, using several averaged *FWHM* values of Neon emissionlines, yielded R-values in the order of $R_{200L} = 900$, respectively $R_{900L} = 4,000$. Generally these resolutions have proven to be ideal for the presentation of the stellar spectral sequence. Substantially higher R-values would be soon comparable to reading a newspaper with the microscope. Therefore it's not surprising that Gray/Corbally [2] denote profiles with a resolution of ~ 3 Å as *"classification resolution spectra"*. Even the professional astronomy uses spectrographs with lower resolutions for certain tasks.

2.3 The Processing of the Spectra

The monochrome *fits* images have been processed with the standard procedure of *IRIS* [550]. In most cases, about 5−7 spectral profiles have been stacked, to achieve noise reduction. The generating and analizing of the final profile was performed with *Vspec* [551]. The procedure is described in detail in the *IRIS* and *Vspec* manuals. For the software functions, applied to process the spectra in this atlas, a step by step description is available in [31] (German only).

With one exception (M31) in all broadband spectra (200L) the pseudo-continuum was removed. The profiles have been rectified − divided by the course of their own continuum. Thus, the intensity of the spectrallines becomes visually comparable over the entire range and further it results a flat (rectified), space-saving and easily readable profile. The *relative depth or height* of a line *in relation* to the height of the according continuum level is crucial for the intensity comparison. The profile of a *pseudo-continuum* presents strong lines at the *blue or red end* of the spectrum optically as relatively *too weak* and vice versa, weak lines in the *middle part, -as too high*.

But just this reasonable correction may confuse the beginners, if they try to find lines of their uncorrected pseudo-continuum in the flat, rectified atlas profile. The following graphic illustrates this effect with the superposition of the uncorrected pseudo-continuum (blue) and the atlas profile of the solar spectrum (red).
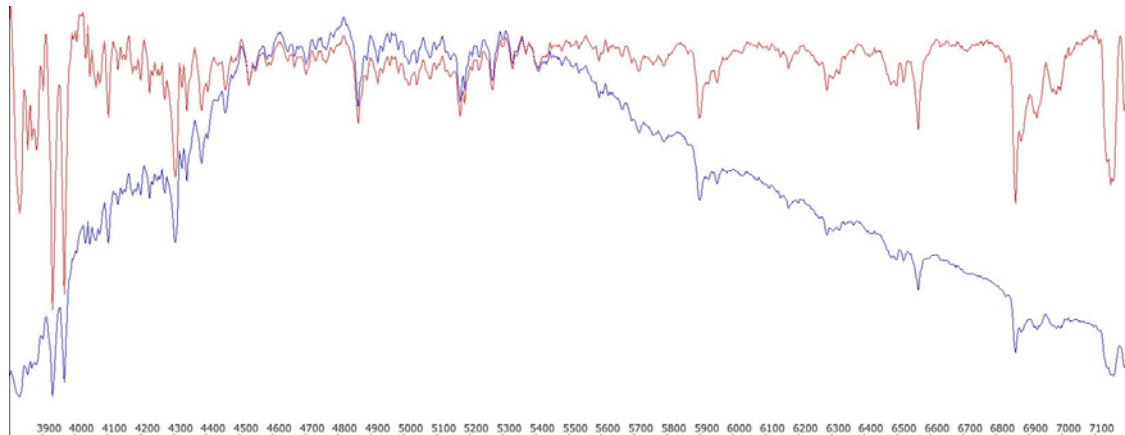
In rare cases with an increased noise level (by faint objects), the profile was sometimes smoothed, using filters such as the *Vspec* MMSE filter (minimum mean squared error).The goal of this process was here exclusively to improve the *readability* of the documented lines. A reduction of the telluric H_2O/O_2 absorption in the yellow/red range of the spectral profile was omitted. Therefore the line documentation in this domain was restrained accordingly.

2.4   Calibration of the Wavelength

Most of the spectra have been calibrated *relatively*, based on *known lines* and *not absolutely* with the calibration lamp. This prevents that the profile, as a result of possible high radial velocities (Doppler Effect), is shifted on the wavelength axis. The focus here is the presentation of the spectral class and not the documentation of the individual star. Only for spectra of late spectral classes and extraordinary stars the calibration was carried out with the lamp. The *unit for the wavelength* is here generally *Angstrom* [Å]. These values are shown according to convention [2] with the prefix [λ]. E.g. *5000 Å* correspond to *λ 5000*.

2.5   Normalization of the Intensity

An *absolute* flux calibration of the intensity profile would be very time consuming and is *not* necessary for the purpose of this atlas. But the continuum intensity of the rectified profiles was always normalized to unity, so that the medium continuum level yields about $I_c = 1$. An absorption line is usually saturated to the maximum if it reaches from the continuum level down to the wavelength axis $I_c = 0$. At the applied low to medium resolutions, in stellar spectra this can rarely, if at all, be seen. Hence, for space saving reasons, in most of the cases, not the entire range of saturation is presented. Instead the corresponding level on the wavelength axis is indicated with amounts mainly in a range of *0.3–0.6*. In case of montages showing several spectra in one chart, the single profiles have been normalized to unity, based on the same continuum section, to enable a rough comparison of the line intensities.
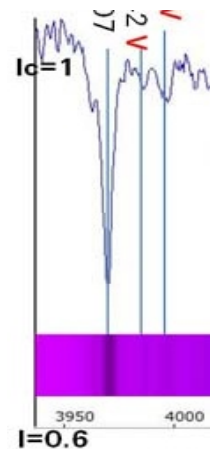
2.6   Line Identification

For the sometimes complex identification process of spectral lines nearly all referenced information sources have been used. Some intensive, but in all the listed sources *not*

documented lines, have been determined with *Vspec (Tools/Elements/line ident)*. The values, implemented in this tool, are based on the *ILLSS Catalogue, Coluzzi 1993*. This procedure was applied very restrictively, i.e. in few cases with a clear profile, high line intensity and missing, plausible alternative elements in the immediate neighborhood. The labeling of such items is declared with a red "**V**".

The wavelengths of spectral lines are here usually labeled with an accuracy of two decimal places. These values were complemented from the *Vspec* tool, because in ancient sources (e.g. *BSA*), the indicated accuracy is only rounded to 1 Å. Labelings, lacking decimal places, here mostly indicate, that the line is a "blend", formed by several elements/ions with comparable intensity. Typically affected are metal absorption lines in spectra of the middle to late spectral classes. However, if in such cases the intensity of a blended line is clearly dominated by a certain element or ion it's also used to label the whole blend.

2.7   Presentation

All spectra are at least documented by a broadband profile (200L grating). In the presence of interesting lines or according information, higher resolved spectra are attached (900L grating). The line profiles are supplemented on the wavelength axis by synthetically produced spectral strips (Vspec). Their color gradient shall chiefly serve as a rough visual reference for the wavelength domain.

Generally, only such details are commented, which are really recognizable in the profiles. Molecular absorption bands are marked with this icon: ▮▮▮ .

For densly labeled tables, I recommend to zoom it on the screen – even if inaccuracies of my drawings become relentlessly ovious this way. Due to this "online aspect", I avoided to separate the tables and the explanatory text in to different parts of the atlas. Due to numerous slim lines, hardcopies of this document require a *high printer resolution*.

3   Terms, Definitions and Abbreviations

3.1   Parameters and Identification of the Stars

The information to the spectral and brightness classes comes largely from the *Bright Stars Catalogue* [505] or *James Kaler* [506], the distance information, if there available, from the *Karkoschka Atlas* [10]. The information to the "surface temperature" of the stars stems from a variety of sources, e.g. [506]. These temperatures usually refer to the layer of the stellar *photosphere*, which is mainly responsible for the formation of the spectral lines.

The *rotation velocity* of a star refers here to the part of the surface velocity v, wich is projected to the direction of the earth − $v \sin i$ − and can spectrographically be determined by using the Doppler principle (details and procedures see [30], [31]). These values are mainly derived from the *Bright Stars Catalogue* [505] or by *James Kaler* [506].

Brighter stars are referred in the atlas with the *proper name* and in the *Bayer system* with small Greek letters, combined with the abbreviated latin constellation name, e.g. *Sirius α CMa* (see the corresponding lists in appendix 33.1). Fainter stars, lacking proper names, are identified with the *Bayer system*, or if necessary, with the *Flamsteed number*, e.g. *φ Sagittarii* or *61 Cygni*.

3.2   Galactic Nebulae and Star Clusters

Such parameters are from NED [501], the *NASA/IPAC Extragalactic Database* or *Karkoschka* [10].

3.3   Extragalactic Objects

Parameters of galaxies and quasars, e.g. the *Z*-values of the redshift are from NED [501], the *NASA/IPAC Extragalactic Database*. From understandable reasons, information about the masses of such objects is missing there. Current estimates are still very uncertain, and accordingly the subject of debate − not least about the existence of dark matter. Therefore these values come from recent publications.

3.4   "Early" and "Late" Spectral Types

At the beginning of the 20th Century, a hypothesis *wrongly* postulated that the spectral sequence from *O* to *M* represents the chronological development stages in the life of a star from very hot to cold. This missleading thesis has subsequently influenced the terminology, which is still in use today. Therefore the classes *O, B, A* are still called *˝early-˝*, and *K, M* as *"late"* types. In this Atlas the classes *F* and *G* are referred as *˝middle˝*.

This terminology is logically also applied *within* a class. So e.g. *M0* is called an *"early"* and *M8* a *"late"* M-type. In consequence e.g. *A2* is *"earlier"* than *A7*.

3.5   Abbreviations and Units

AU: Astronomical unit, 149.6M km
AGB: Asymptotic Giant Branch (HRD)

BSA: Bonner Spektralatlas
ESO: European Southern Observatory
ESL: Energy saving lamp
EW: Equivalent width of a spectral line [30]
FWHM: **F**ull **w**idth at **h**alf **m**aximum height [30]
HB: Horizontal Branch (HRD)
HRD: Hertzsprung-Russel Diagram

HST: Hubble Space Telescope

MK: Morgan, Keenan, Kellman: spectral classification system and spectral atlas

PN: Planetary Nebula

PMS: Pre-Main sequence Star. Young Protostar not yet established on main sequence

RGB: Red Giant Branch (HRD)

SB1: SB 1 system. Spectroscopic binary stars with strongly different bright components. Only the spectrum of the brighter component can therefore be observed.

SB2: SB 2 system. Spectroscopic binary stars with two similar bright components. A *composite spectrum* of both components is therefore observed.

SN: Supernova

VLT: Very Large Telescope, ESO telescope group at Cerro Paranal, Chile

WR: Wolf-Rayet stars

SuW: German astronomical journal: *Sterne und Weltraum*

K: Kelvin temperature unit K ≈ °Celsius + 273°

Å: unit of wavelength Angstrom. 1 Å = 10^{-10}m

ly: light year 1 ly = 9,46 x 10^{12} km   *parsec:* 1 parsec = 3.26 ly

Labeling of the Balmer Series: *Hα, Hß, Hγ, Hδ, Hε, H8, H9, H10* etc: Further lines after *Hε* are labeled with the affected shell number, involved in the according electron transition.

200L / 900L: reflection grating of the DADOS spectrograph with 200 or 900 lines/mm.

V: Apparent magnitude of a celestial body

V: Spectral line identified with help of the *Vspec* Tool

▓ : Molecular absorption band

⊙: Comparison to the sun: M⊙: solar mass, L⊙: Luminosity of the sun

3.6   Identifiying of the Elements and Ions

As usual in astrophysics, all the elements, except of *hydrogen* and *helium*, are called *"metals"* and identified in the astrophysical form - for details see [30].

The term "*Ionisation stage*" refers here to the number of electrons, which an ionized atom has lost to the space (Si IV, Fe II, H II, etc.). The Roman numeral **I** is used for spectral lines associated with the *neutral* element, numeral **II** for those from the *first* ionization stage, − **III** for those from the *second-*, and so on. This must not be confused with the term "*Degree of ionisation*" in plasma physics. It defines for a gas mixture the *ratio* of atoms (of a certain element) that are ionised into charged particles, reagarding the temperature, density and the required ionisation energy of the according element. This "*Degree*" is determined in astrophysics with the famous *Saha equation*.

So-called "Forbidden lines" are written within brackets, eg [O III].

3.7   The Metal Abundance

Of great importance is the logarithmic *iron to hydrogene ratio* $\boldsymbol{Fe/H}$ considering the number of atoms (not the mass!) as a unit of *metal abundance* ("metallicity") in a stellar atmosphere.

$$Fe/H = \log\frac{(Fe/H)_{Star}}{(Fe/H)_{Sun}}$$

$\boldsymbol{Fe/H}$ values, smaller than found in the atmosphere of the Sun, are considered to be *metal poor* and carry a *negative sign* (−).The existing range is from approximately +0.5 to −5.4 (SuW 7/2010).

4   The Fraunhofer Lines

Fraunhofer has characterised the more prominent of the solar absorption lines with the letters *A* to *K* − this at a time when the physical relationships were still unknown. Later, additional lines were supplemented with small letters. These line designations are still in use even in current professional papers.

In this atlas some of the Fraunhofer lines are labled in the solar spectrum and neighboring spectral classes. The table shows the listed Fraunhofer lines, rounded to 1 Å (Sources: Table: NASA, Graphic: Wikipedia).

Line ident.	Element	Wavelength Å
A − Band	O_2	7594 - 7621
B − Band	O_2	6867 - 6884
C	H (α)	6563
a − Band	O_2	6276 - 6287
D 1, 2	Na	5896 & 5890
E	Fe	5270
b 1, 2, 3	Mg	5184/73/69
F	H (β)	4861
d	Fe	4668
e	Fe	4384
f	H (γ)	4340
G − Band	CH	4300 - 4310
g	Ca	4227
h	H (δ)	4102
H	Ca II	3968
K	Ca II	3934
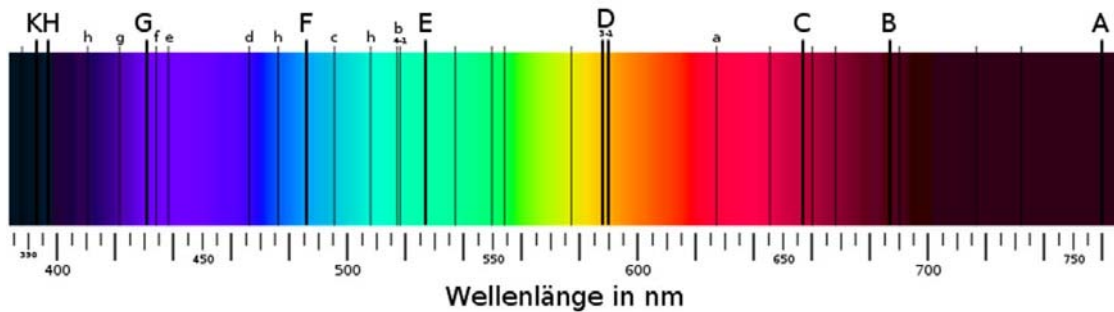
Below: Original drawing of the solar spectrum by *Joseph Fraunhofer*. In contrast, the convention today requires the blue region of the spectrum to be left and vice versa the red to be right. Stunningly *visionary* appears to me the sketched, estimated intensity profile of the pseudo-continuum above the spectral strip! This type of plotted profiles, today of course normalised/calibrated and overprinted with the spectral lines, we can find again in publications only since about the last 40 years!
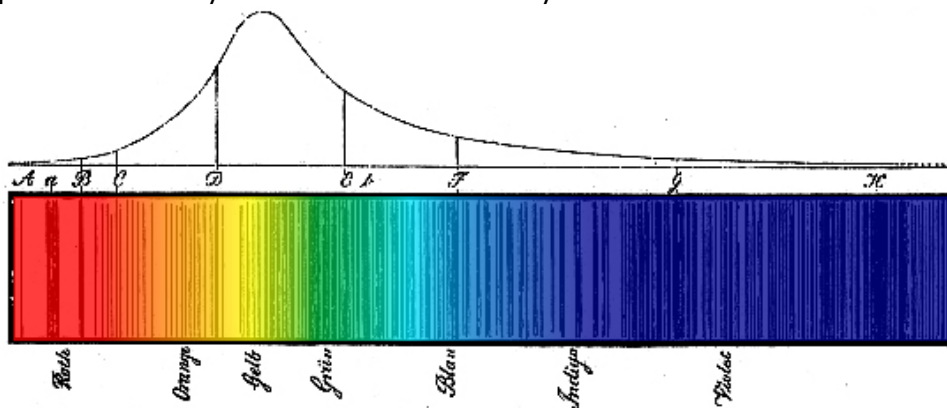
5 Overview and Characteristics of Stellar Spectral Classes

5.1 The Temperature Sequence

The rough, one-dimensional determination of the spectral classes *O, B, A, F, G, K, M*, is easy and even feasible for slightly advanced amateurs. This sequence of letters is further subdivided into decimal subclasses which follows directly the decreasing photospheric temperature, starting with the extremely hot O-type of several 10,000's K, and proceeding down to the cold *M*-class with about 2,400 − 3,500 K. The Sun is classified as *G2* with 5,800 K.

Spectral distinction criteria are prominent features such as lines in absorption or emission, which appear prominently in certain classes, and are entirely absent in others. The following charts show a montage with sample spectra of the entire class sequence of *O − M*. Here the original profiles of the stars are shown (200L grating), which are also used to present the individual spectral classes. This way, this resolution already enables the identification of the intense and therefore most documented spectral lines. Further also the influence of some elements, ions or molecules to the different spectral types becomes roughly visible.

Table 01 shows superposed the synthetically produced spectral strips − Table 02 shows the same but with the according intensity profiles.

What is already clearly noticeable here?

− In the upper third of the table (B2−A5), the strong lines of the H-Balmer series, i.e. *Hα, Hβ, Hγ*, etc. They appear most pronounced in the class *A2* and are weakening from here towards earlier and later spectral classes.

− In the *lower quarter* of the table *(K5−M5)* the eye-catching shaded bands of molecular absorption spectra, mainly due to titanium oxide *(TiO)*.

− Just underneath the half of the table some spectra *(F5−K0)*, showing only few prominent features, but charged with a large number of fine metal lines. Striking features here are only the *Na I* double line (Fraunhofer D1, 2) and in the "blue" part the impressive Fraunhofer lines of *Ca II* (K + H), gaining strength towards later spectral classes. *Fraunhofer H* at λ 3968 starts around the *early F-class* to *overprint* the weakening *Hε* hydrogen line at λ 3970. In addition, the *H*-Balmer series is further weakening towards later classes.

− Finally on the top of the table the extremely hot O-class with very few fine lines, mostly ionised helium (He II) and multiply ionized metals. The H-Balmer series appears here quite weak, as a result of the extremely high temperatures. The telluric H_2O and O_2 absorption bands are reaching high intensities here, because the strongest radiation of the star takes place in the ultraviolet whereas the telluric absorption bands are located in the undisturbed domain near the infrared part of the spectrum. By contrast the maximum radiation of the *late* spectral classes takes place in the infrared part, enabling the stellar *TiO* absorption bands to overprint here the telluric lines.

− In the spectra of hot stars (~ classes from early A − O) the double line of *neutral* sodium *Na I* (Fraunhofer $D_{1,2}$) must imperatively be of *interstellar* origin. Neutral sodium *Na I* has a very low ionisation energy of just 5.1 eV (see table in sect. 30) and can therefore exist only in the atmospheres of relatively cool stars. The wavelengths of the ionised *Na II* lie already in the ultraviolet range and are therefore not detectable by amateur equipment.

TABLE 01

Overview on the spectral classes

Spectral lines (top labels): Hε 3970, Hδ 4101, Hγ 4340, He I 4388, He I 4471, C III 4647/51, Hβ 4861, He I 4922, He I 5016, He I 50486, He II 5411, He I 5876, Na I 5890/95, Telluric O₂, Hα 6562, He I 6678

Class	Star	Temperature
O9.5	Alnitak	25'000°K
B1	Spica	22'000°K
B7	Regulus	15'000°K
A1	Sirius	10'000°K
A7	Altair	7'550°K
F0	Adhafera	7'030°K
F5	Procyon	6'330°K
G2	Sun	5'700°K
G8	Vindemiatrix	4'990°K
K1.5	Arcturus	4'290°K
K5	Alterf	3'950°K
M1.5	Antares	3'600°K
M5	Rasalgethi	3'300°K

Wavelength scale: 4000, 4200, 4400, 4600, 4800, 5000, 5200, 5400, 5600, 5800, 6000, 6200, 6400, 6600

Bottom labels: K H — Ca II, Ca I 4227, CH 4300, TiO, Mg I 5167-83 „Mg Triplet", TiO, TiO, TiO, TiO, TiO

©Richard Walker 2010/05

TABLE 02   <u>**Overview on the spectral classes**</u>

©Richard Walker 2010/05

Line labels (top axis): Hε 3970 · Hδ 4101 · Hγ 4340 · He I 4388 · He I 4471 · C III 4647/51 · Hβ 4861 · He I 4922 · He I 5016 · He I 5048 · He II 5411 · He I 5876 · Na I 5890/95 · Telluric O₂ · Hα 6563 · He I 6678

Wavelength axis: 4000 4200 4400 4600 4800 5000 5200 5400 5600 5800 6000 6200 6400 6600

Class	Star	Temp
O9.5	Alnitak	25'000°
B1	Spica	22'000°
B7	Regulus	15'000°
A1	Sirius	10'000°
A7	Altair	7'550°
F0	Adhafera	7'030°
F5	Procyon	6'330°
G2	Sun	5'700°
G8	Vindemiatrix	4'990°
K1.5	Arcturus	4'290°
K5	Alterf	3'950°
M1.5	Antares	3'600°
M5	Rasalgethi	3'300°

Additional line labels: Fe I/Ca I 4526 – 29 · Fe I/Ca I 4455 - 59 · Fe I/Ca I 5270 · Fe I 5328

Bottom wavelength axis: 4000 4200 4400 4600 4800 5000 5200 5400 5600 5800 6000 6200 6400 6600

Bottom band labels: K H · Ca I 4227 · CH 4300 · TiO · TiO · TiO · Mg I 5167-83 „Mg Triplet" · TiO · TiO · TiO · TiO · TiO · TiO · Ca II

5.2   The Luminosity Classes

Within the same spectral class, stars can show huge different absolute luminosities, due to different stages of their development. Since 1943, the spectral classes have therefore been expanded by an additional dimension in Roman numerals – the so called six *luminosity classes*. The Sun is classified with *G2V* since it's (fortunately) still located on the *Main Sequence* of the *HRD* with the luminosity class *V*.

Luminosity class	Star type
I	Luminous Super Giants
Ia-0, Ia, Iab, Ib	Subdivision of the Super Giants according to decreasing luminosity
II	Bright Giants
III	Normal Giants
IV	Sub Giants
V	Dwarfs or Main Sequence Stars
VI	Subdwarfs (rarely used, as specified by prefix)
VII	White Dwarfs (rarely used, as specified by prefix)

5.3   Suffixes, Prefixes, and Special Classes

With additional small letters, placed as prefix or suffix, extraordinary phenomena, such as a relative overabundance of a metal or the appearance of emission lines in the spectrum are specified. Some additives however are overdetermining, as e.g. *Giants*, unlike the *Subdwarfs* and *White Dwarfs*, are already specified by the luminosity class. Such labels are therefore hardly ever in use. Further with additional capital letters some special classes are specified.

Examples: Sirius A: *A1 Vm*, metal-rich *Main Sequence Star* (Dwarf) spectral class *A1*

Sirius B: *DA2*, White Dwarf or „Degenerate" of spectral class *A2*

Omikron Andromedae: *B6 IIIep*,

Omikron Ceti (Mira): *M7 IIIe*

Kapteyn's star: *sd M1 V,*   Subdwarf of spectral class M1 V

P Cygni: *B2 Ia pe*

Suffixes	
s	Sharp lines
b	Broad lines
c	Extraordinary sharp lines
comp	Composite spectrum
e	H- emission lines in B- and O- stars
f	He- and N- emission lines in O- Stars
em	Metallic emission lines
k	Interstellar absorptionlines
m	Strong metal lines
n / nn	Diffuse lines/ strongly diffuse lines eg due to high rotation speed
wk	Weak lines
p, pec	Peculiar spectrum
sh	Shell
v	Variation in spectrum
Fe, Mg...	Relatively high or low (−) abundance of the specified element

Prefixes	
d	Dwarf
sd	Subdwarf
g	Giant

Special Classes	
Q	Novae
P	Planetary Nebulae
D	Dwarf, +additional letter for *O, B, A* spectral class
W	Wolf-Rayet Star + additional letter for *C-, N-* or *O-* lines *(see sect. 8)*
S	Stars with zirconium oxide absorption bands *(see sect. 21)*
C	Carbon stars *(see sect. 22)*
L, T,	Brown dwarfs
Y	Theoretical class for brown dwarfs < 600 K

Nowadays the special classes *P (Planetary Nebulae)* and *Q (Novae)* are barely in use!

The suffixes are not always applied consistently. We often see other versions. In the case of shell stars e.g. *pe*, or *shell* is in use.

6 Appearance of Elements and Molecules in the Spectra

The spectrum of a star is primarily determined by the *temperature* of the photosphere. This temperature defines directly the spectral class in the *HRD*. From secondary importance is the density of the stellar atmosphere, primarily depending on the *luminosity class*, and further the specific *abundance* of certain metals. Another influential parameter is the *rotation speed* of the star, which, as a result of the Doppler Effect, broadens the spectral lines and reduces their intensity.

For the spectroscopy the following chart is from similar importance as the HRD. It shows roughly the appearance and the intensity (EW) of characteristic spectral lines, depending on the spectral class, respectively the "surface temperature" of a star. The latter determines for a certain element the *stage* and *degree* of ionisation. The theoretical foundations have been developed in 1925 by *Cecilia Payne-Gaposhkin* (1900-1979), according to *Otto Struve* "undoubtedly the most brilliant Ph.D. thesis ever written in astronomy". She was the first to apply the laws of atomic physics to the study of the temperature and density of stellar bodies and to conclude that hydrogen and helium, the two lightest elements, are also the two most common in the universe. She also disproved the old hypothesis that the chemical composition of the Sun is the same as of the earth. In addition to this scientific career, she was a mother of three children.

This chart is not only of great value for determining the spectral class, but also prevents by the line identification from large interpretation errors. Thus it becomes immediately clear that the *photosphere* of the Sun (spectral type G2V) is a few thousand degrees too cold to show helium *He I* in a normal (photospheric) solar spectrum. It also shows that the hydrogen lines of the Balmer series remain visible in varying degrees of intensity in nearly all spectral classes. Only in the late M- classes, they are increasingly overprinted by strong absorption bands of mainly *TiO*. The examples Sirius (A0) and Regulus (B7V) show however that the influence of the *Fe* lines goes much further to the left, as indicated in this diagram.
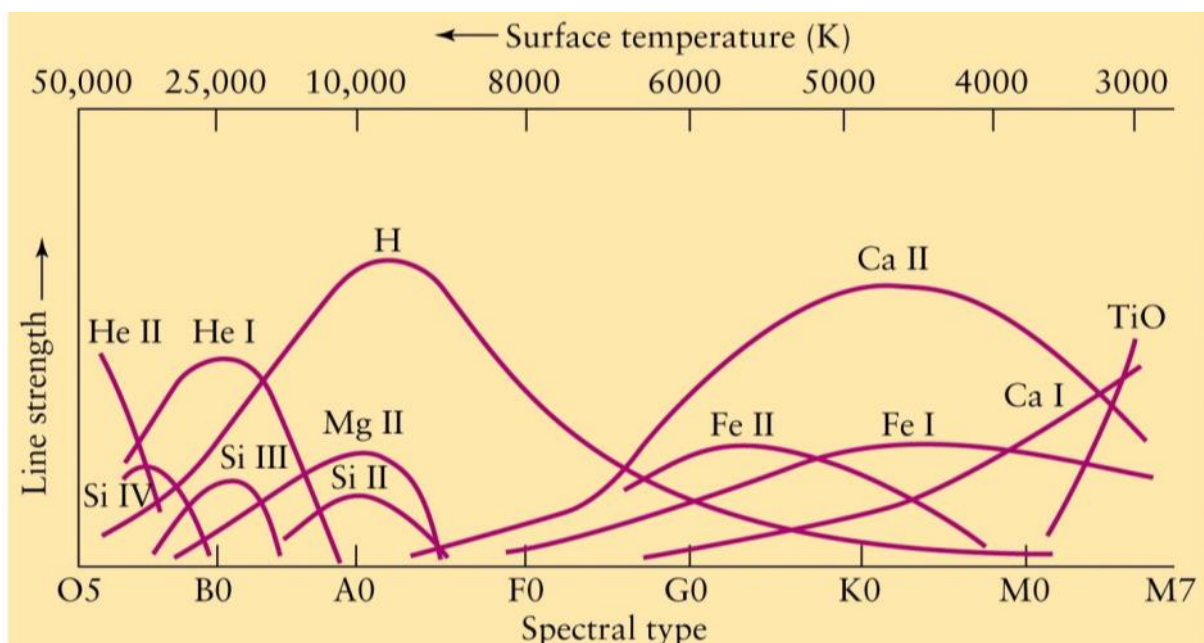
7 Spectral Class O

7.1 Overview

The O-Class comprises the hottest, most massive and shortest-living stars of the universe. At the end of their short lives, they will all end, due to their huge masses, in a *SN* explosion. Subsequently the only remains will consist of a very small, extremely compact *Neutron Star* or even a *Black Hole*. These blue shining, extreme types of stars are very rare. For the Milky Way only about 20,000 representatives of the O-type are estimated. As a result of their tremendous luminosity two bright representatives of this class are visible in a distance of some 1,000 ly in the constellation Orion: *Alnitak (ζ Ori)* 1.8^m and Mintaka 2.2^m (δ Ori). All these stars are *late O*-Types. Bright representatives of earlier *O*-types are only found in the southern sky, such as *Naos (ζ Puppis)*

HD	Name	Spec. Class	V^m
24912	Menkhib, ξ Per	O7.5 III e	4.1
30614	α Cam	O9.5 Ia e	4.3
36486	Mintaka, δ Ori	O9.5 II+B0III	2.4
36861	Meissa, λ Ori	O8 III	3.4
37022	Θ^1 Ori C	O6 pe v	5.1
37043	Nair al Saif, ι Ori	O9 III	2.8
37468	σ Ori,	O9.5 V	3.8
37742	Alnitak, ζ Ori	O9.5 Ib	1.8
47839	15 Mon	O7 Ve	4.6
57060	29 CMa	O7	5.0
57061	30 CMa	O9 Ib	4.4
66811	Naos, ζ Pup	O4 I f(n) p	2.3
149757	ζ Oph	O9.5 V n	2.6
203064	68 Cyg	O7 III n(f)	5.0

2.3^m. The list on the right shows O- stars with an apparent magnitude V from about 5^m upwards, which are spectroscopically accessible even for averagely equipped amateurs.

Two other Orion stars *ε- (Alinlam),* and *κ- (Saiph)*, are classified as *B0*, just scarcely missing the O-Class. Significantly fainter, but also much further distant, is the multiple *Trapezium star θ^1 Ori*. Its *C*-component θ^1 Ori C is a spectral type *O6pe V* and plays a key role for the ionisation of central parts in the Orion nebula M42.

This striking accumulation of extremely massive stars – known as so-called <u>OB Associations</u> – is not yet fully understood. Other slightly smaller clusters are located in the constellation *Scorpion, Perseus* and *Swan*. Together with other groups, they form the so-called *"Gould Belt"*, which is inclined some 20° to the galactic plane and has a diameter of about 2,000 ly. Our Sun is located somewhat off-center but still roughly within the ring plane [700].
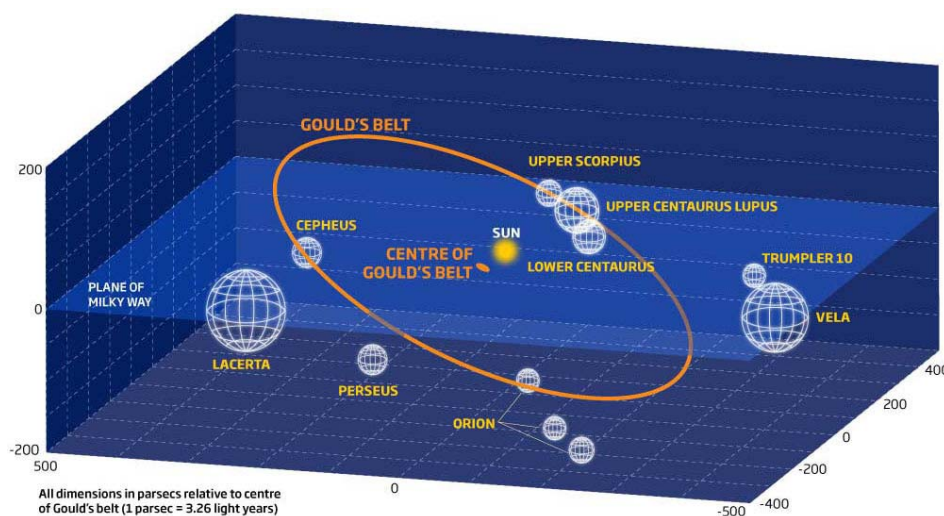
Chart: New Scientist

7.2   Parameters of the Early to Late O-Class Stars

The following table shows the data *exclusively for the Main Sequence Stars* of the *O*-class compared to the Sun (⊙) and according to [701] and other sources.

Mass M/M⊙	Stay on *Main Sequence* [y]	Temperature photosphere [K]	Radius R/R⊙	Luminosity L/L⊙
60 – 20	1M – 10M	50,000 –25,000	15 – 9	800,000 – 90,000

The O-class is open-ended. Currently, the top ranking is *O3* with a surface temperature of about 50,000 K [1]. The late *O9* class has been subdivided into decimal subclasses.

7.3   Spectral Characteristics of the O-Class

Spectra of the O-class are dominated by relatively low intense absorptions of singly or multiply ionised elements. The extremely high temperatures cause in addition to neutral helium He I, also lines of ionised helium (*He II*). In the early O-classes *He II* may also appear as *emission line*. In earlier times the appearance of He II in the spectrum was used as the main criterion for the definition of the O-class [2]. Today, in higher-resolved spectra, it can be detected already in the B0 class. Further appear also multiply ionised metals, as *C III, N III, [O III]* and *Si IV*. Due to the extreme temperatures, the *degree of ionisation* is here too high for the *H*-Balmer Series and their line intensity therefore only weak [30]. If *H*-lines appear in emission, the suffix "e" is added to the class letter (*Oe*). If *He* and/or *N* are seen in emission, the suffix "f" is added. *"Of"* stars seem to form the link between the O-Class and the Wolf-Rayet Stars, probably also to the LBV stars (see *sect. 8/10*).

The maximum intensity of the real continuum is in the UV range. The graph shows the theoretical continuum for a synthetic O9V standard star (Vspec *Tools/Library*).
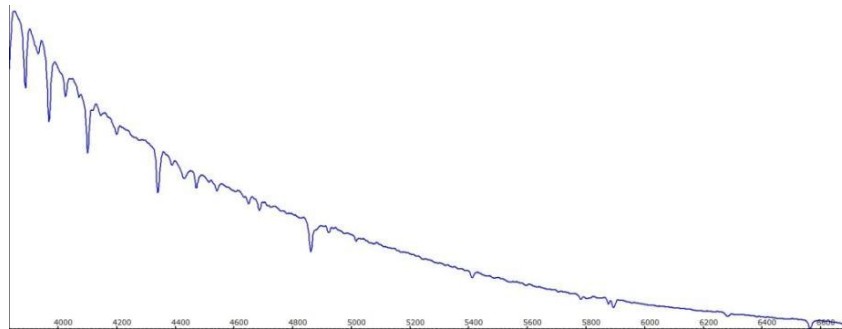
7.4   General Remarks to the Classification of O-Stars

In no other spectral class, even among reputable databases, such different classifications can be found as in the O-class. Perhaps this can also be justified by the typically higly variable spectral features. This particularly affects the suffixes. But even by the decimal subclasses we see significant differences. Further in the early O-classes indications for the luminosity class are often missing.

7.5   Commented spectra

Table 1: *Alnitak* (ζ Ori) and *Mintaka* (δ Ori)

This table shows two broadband spectra (200L grating) providing an overview on the spectral features of the late O-class.

Alnitak (1200 ly) belongs to the spectral class *O9.5 Ib*, representing the lower level of the so-called *Super Giants*. The Wikipedia picture shows the size of the star compared to the Sun.
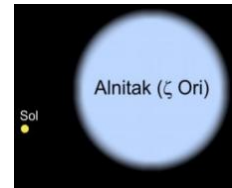
Mintaka (1200 ly) is classified slightly below with *O9.5 II (Bright Giant)*. Both stars are dominant components in multiple star systems and their surface temperature is about 25,000 K. In spite of the minimal class difference even in these low-resolution spectra, some differences can be observed (see comment below).

Table 2: Detailed spectrum of *Alnitak* (ζ Ori)

This table shows for *Alnitak* (1200 ly), a late O-Type star, two higher resolved spectra in the blue- and red wavelength domains (900L grating). Here, the main distinguishing feature between the two spectra of *Table 1* is clearly visible. The *Hα* line at λ 6562 forms here a textbook example of a *P-Cygni profile* with a red shifted emission- and a blue-shifted absorption line. This is always an indication for radially ejected matter by the star, a common process for some members of this extreme stellar class. The wavelength shift results here to about 7 Å. According to the Doppler law this yields a gas-expansion velocity $v_r \approx 320\ km/s$.
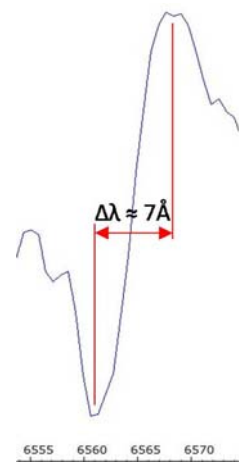
$$v_r = \frac{\Delta\lambda}{\lambda_0} \cdot c$$

λ_0 = Wavelength of the line, $c = 300'000\ km/s$ (speed of light)

For further information, refer to *Table 13* for *P Cygni* or [30].

Line identification:

Die line identification is based amongst others on [1], [5], [51], [56], [57]

Table 3: $\Theta^1 Ori\ C$, HD37022 V=+5.13^m and *68 Cygni*   HD203064 V=+5.04^m

This table shows two apparently faint representatives of the early to mid-O-class, which are easily accessible for the averagely equipped amateur (200L grating).

$\Theta^1 Ori\ C$ (~1400 ly) is the brightest component of the famous Trapezium in M42. This stellar giant with its ever-changing spectral characteristics is being investigated intensively. The interferometric study [351] provides a good overview on these efforts. The data concerning the spectral type show a wide variation range eg *O4−O6 pv* [500], *O5−O7* [351] or *O6* [506]. The stellar mass is, depending on the source, estimated to about 31-34 solar masses. Like nearly all other stars of the Trapezium, also Θ1Ori C has at least one companion of spectral type O9.5, maybe also B0,

with an orbital period of about 11 years. Recently, still another, very closely orbiting companion, with about one solar mass and a period of ~ 50 days is presumed. The data for the surface temperature vary approximately in the range of the proposed spectral types between 39'000K and 45'000K. The C- component generates some 80% of the total amount of photons [223], exciting the H II region of the Orion Nebula (see tables 80/80A)!
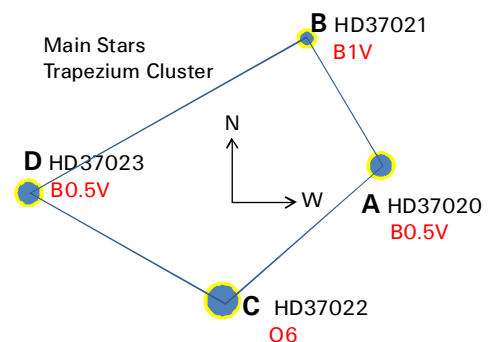
Most of the absorption lines appear here similar to those of Alnitak and Mintaka. Hβ is striking, because in the surrounding nebula generated from the broad emission line, photospheric absorption dip of the star grows. The two [O III] emissions must be generated by the nebula, because the hot and dense stellar atmospheres can impossibly generate "forbidden" lines. The Hα emission is produced by the recombination of the surrounding H II region (see sect. 24), totally veiling here the stellar line.

It is stronly recommended to record $\Theta^1 Ori\ C$ with autoguiding to ensure the tracking on the correct trapezium star. The orientation of the slit axis should be optimised accordingly. The sketch above should facilitate the orientation. The exposure time for the profile in Table 3 is 340 seconds.

68 Cygni (~2300 ly) is surrounded by the weakly developed H II region _Sharpless 119_. It is the brightest of total 6 ionising stars. Most of the sources classify this star with 30 solar masses and a surface temperature of about 35'000K as O7 III n (f) [505]. "Of" stars are considered as a transitional phase on the way to Wolf Rayet stars and show eg He and N lines in emission - a clear indication that material is repelled. As classification lines for the Of-type the blend N III λλλ 4634−40−42 and He II λ 4686 are used [2]. Since only NIII appears here in emission, _68 Cygni_ is considered as a "mild" Of star, and the suffix "f" is therefore set in parentheses (f) [2]. In the intensive Of -phase both features, NIII and He II, are seen in emission. Compared to the O9-types the C IV lines (λλ 5801/5812) are quite intensive here. This indicates that _68 Cygni,_ as well as $\Theta^1 Ori\ C,$ are stars of the rather early O-class. C IV requires with 47.9 eV almost twice the ionisation energy as He II.

According to [505] 68 Cygni passed about 1959-70, a phase with Hα in emission. Because of the high proper motion, it is regarded as so called "runaway star" and originates probably from the OB2 region of Cepheus. As a possible scenario, the acceleration by the supernova explosion of a companion is discussed. Perhaps the remaining black hole with ~3 M⊙ still orbits around the star very closely. Observed fluctuations of equivalent widths at certain spectral lines indicate a possible orbital period of about 5 days. The prior information is mainly based on [352].

TABLE 1

He I 6678.15

Hα 6562.82

Telluric O$_2$

Interstellar   Interstellar

Na I 5889/95
He I 5875.6

Mintaka δ Ori O9.5 II   Alnitak ζ Ori O9.5 Ib

O III 5592.37

He II 5411.52

He I 5047.74
He I 5015.68

He I 4921.93
Hβ 4861.33

He I 4713.15
C III 4647 /51

He II 4541.59

He I 4471.48

He I 4387.9

Hγ 4340.47

He II/N III 4200
He I 4143.76
Hδ 4101.74
He I 4025.5
Hε 3970.07

6600 6500 6400 6300 6200 6100 6000 5900 5800 5700 5600 5500 5400 5300 5200 5100 5000 4900 4800 4700 4600 4500 4400 4300 4200 4100 4000

I=0.7   I=0.7

TABLE 2

He I 4713.15

He II 4685.68

C III 4647 - 51

N II/NIII 4630-34

OII 4609/10 **V**
O II 4596.17
O II 4590.97
Si III 4574.78
Si III 4567.87
Si III 4552.65
He II 4541.59

N III 4511/15

Mg II 4481
He I 4471.48

O II 4416.98
O II 4414.91

He I 4387.9
N III 4379.09
O II 4366.9 **V**

Hγ 4340.47

O II 4315/17

O II 4302.81 **V**

O II 4276-95

O II 4254

He II/N III 4200
O II 4185.46

Fe II 4151.6 **V**
He I 4143.76

He I 4120.81

Si IV 4116.1
Hδ 4101.74

Si IV 4088.86

O II 4075.87

O II 4070

He I 4025.5

He I 4009.27
N II 3995
O II 3983
Hε 3970.07
He I/O III 3962/65

Alnitak ζ Ori   O9.5 Ib

I=0.6

He I 6678.15

Hα 6562.82

Telluric O$_2$

N II 5932/42

Na I 5895.92

Interstellar

Na I 5889.95
He I 5876.0

C IV 5812.14
C IV 5801.51

I=0.6

©Richard Walker 2010/05

TABLE 3

He I 6678.15

Hα 6562.82

Telluric O$_2$

Interstellar   Interstellar   N II 5932/42

Na I 5889/95

He I 5875.6
C IV 5812.14
C IV 5801.51

C III 5696

O III 5592.37

He II 5411.52

Emission lines Orion Nebula M42

68 Cygni O7III n(f)

Θ^1 Ori C   O6 pv

He I 5047.74
He I 5015.68

He I 4921.93
Hβ 4861.33

He I 4713.15
He II 4685.68
N III 4634-42   C III 4647 /51
N V 4604-4620
He II 4541.59
N III 4511/15
He I 4471.48
Diffuse ISM Band

He I 4387.9
Hγ 4340.47
O II 4276-95

He II/N III 4200
He I 4143.76
Hδ 4101.74

He I 4025.5
Hε 3970.07

H8 3889.05
H9 3835.38

8 Wolf Rayet Stars

The French astronomers *Charles Wolf* and *Georges Rayet* discovered in 1867 very rare stars, whose spectra are standing out by massively broadened, intense *helium emission lines* and the *almost complete absence of hydrogen*. These objects are grouped in an *extra class*, marking the *final stage* of massive O and early B stars. In this phase, the star blasts away its entire outer hydrogen shell with velocities of > 2000 km/s and subsequently reveals its extremely hot, former nuclear fusion zones where, in addition to helium, various metals have been formed.

On this final trip to the *SN* type *1b* or *1c*, the star exposes now in a chronological sequence one after the other of its former nuclear fusion zones, similar to the peeling of an onion. Therefore, the spectrum now differs completely from the previous O- or early B-stage. The broad lines of ionised helium *He II* appear together with the emissions of the highly ionised metals on the surface layer of the star, which characterise the classification of *WR* stars - a strong indication for the extremely high temperatures and the corresponding excitation energies *(see sect. 30)*. Hydrogen emission lines can hardly be detected in WR stars!

WN: WR stars with nitrogene emissions
WC: WR with carbon emissions
WO: WR with oxygene emissions (extremely rare).

Similar to normal spectral classes also WR stars are subdivided into decimal subclasses. The HST image (NASA) shows the star *WR 124* (class *WN8*) with about 20 solar masses. It's located in the constellation *Arrow* blasting away its shell with about 2000 km/s. The remains of such bizarre stellar "monsters" with about 10–80 solar masses and surface temperatures of 30,000–100,000 K will most probably implode in to a *Black Hole* during the final *SN* explosion.
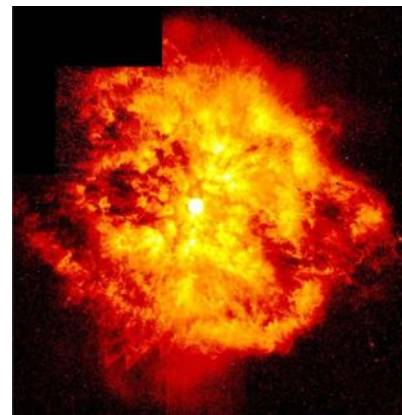
About 10% of the *central stars* in *Planetary Nebulae* show similar spectra, which are also classified as *WR* types *(WRPN)*. However, their absolute magnitude is significantly lower and they finally end up much less spectacular as *White Dwarfs*. Anyway these objects are too faint for amateur equipments.

With an apparent brightness of 1.74^m and the spectral type *WC8*, *γ Velorum* in the southern sky is the brightest representative of the *WR* stars. On the northern hemisphere mainly in the constellation *Cygnus*, a concentration of such extreme stars can be found, which are members of the *Cygnus OB associations*. Here 23 WR stars are located – 14 are classified as *WN*-type, 8 as *WC*-, and just one as *WO*- type. The two brightest reach an apparent magnitude in the range of 6–7^m and are therefore well accessible with a slit spectrograph, even for moderate sized amateur telescopes. By chance they just represent the two main types *WN* and *WC*!

Both categories show within their subclasses dramatically different profiles. Therefore here follows a list with emission lines, already identified in WR-stars [Å] – "lines of classification" according to *Karel van der Hucht* [232]:

WN Stars:

He I 3888, He I 4027, He I 4471, He I 4921, He I 5875, He II 4200, He II 4340,
He II 4541, He II 4686, He II 4861, He II 5411, He II 6560, N II 3995, N III 4634–4641
N III 5314, N IV 3479–3484, N IV 4058, N V 4603, N V 4619, N V 4933–4944.

WC Stars:

C II 4267, C III 5696, C III/C IV 4650, C IV 5801−12, O V 5572−98
He lines: see WN stars.

Table 5: *Wolf-Rayet Stars WR 133 and WR 140*

The montage of two overview spectra (200L grating) presents the subtypes *WN* and *WC* of *Wolf-Rayet Stars*. The appearance, as well as the intensity of the emission lines, inform about the chemical composition and the huge excitation energy of the individual WR star. See *sect. 30: Required ionisation energies for the individual elements*.

WR 133 spectral class *WN4:*   HD 190918

J2000   RA: 20h 05' 57.3''   Dec: +35° 47' 18.2"   V=+6.78^m

Some 6,500 ly distant, the very well explored *WR 133* in the constellation Cygnus hides itself inconspicuously within the central members of the open cluster NGC 6871. Despite to the use of "Goto Telescopes" here is a certain risk to record the wrong star − what is instantly recognisable in the spectrum. In particular, the bright *He II* "emission knots" can hardly be overlooked.
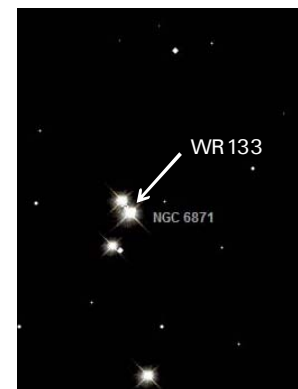
WR 133 forms a spectroscopic binary (SB2) with an *O9 I Supergiant* in an orbital period of about 112 days. Therefore, we see a composite spectrum, which is however clearly dominated by the emission lines of the *WR star* (labeled *red* in *Table 5*). Striking here are the numerous lines of differently high ionised *nitrogen*, responsible for the classification *WN*. However one faint carbon emission shows up here, *C IV* at λ 5801-12 [230]. This spectral feature is significantly weaker than by the *WC* type *WR 140* (see below).

The very close-by *O9* companion star generates here some absorptions of helium- and some *H*-Balmer lines (labeled *black* in *Table 5*), as well as the sodium double line, which is of interstellar origin [344]. The continuum is here, in comparison to *WR 140* presented below, relatively intense. The publications [232] and [233] show the determination of the decimal subclass mainly by the comparison of the individual line intensities.

The strong *He II* emission at λ 6560 poses a *considerable risk* to be _misinterpreted_ as *Hα* line at λ 6562! The most intense line here is clearly the *He II* at λ 4686. The expansion velocity of the stellar wind can be estimated from the *FWHM* values of the two intense *He II* emissions. If these figures are put in to the Doppler formula and the results are finally corrected by the *instrumental broadening* [30], velocities of $v_r \approx 1800\ km/s$ at λ 4686 and $v_r \approx 1500\ km/s$ at λ 6560 are resulting. In the order of magnitude, these figures agree quite well with literature values ($v_r < 2000\ km/s$). The spectrum was recorded with the 90 cm (36 inch) CEDES Cassegrain Telescope in Falera − exposure: 4x30 sec. The line identification is based amongst others on [230] [231] [232] [233] [344].

_WR 140_   spectral class _WC7:_   HD 193793

J2000   RA: 20h 20′ 28″   Dec: +43° 51′ 16.3″   V=+6.93[m]

Also located in the constellation Cygnus and some 4,700 ly distant, _WR140_ is a member of a spectroscopic binary (SB2) with an _O4 V Main SequenceStar_ in a _highly excentric orbit_ with a period of some 2,900 days. During the periastron passages this binary system usually attracts the worldwide attention of professional- and amateur astronomers, mainly observing effects, caused by the colliding stellar winds _(colliding wind binary)_ [346] [347].The map shows the star pattern in the immediate vicinity of the WR star. It's relatively isolated and therefore much easier to find than WR 133.
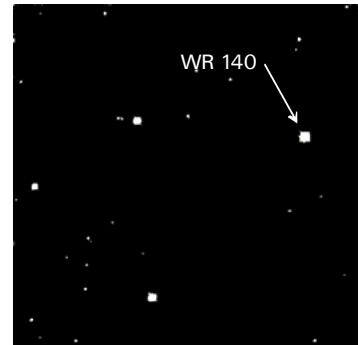
This composite spectrum is clearly dominated by the _WR star._ One of the reasons is presumably the time of the last periastron passage of January 2009. At the time of recording it dated already back more than 1½ years. In contrast to the very close binary system _WR 133_, absorption lines are barely visible here, besides the well known telluric lines and the double line of sodium, which could also be of interstellar origin. The numerous different lines of highly ionised carbon show clearly, that _WR 140,_ with the classification _WC7,_ is a representative of the _carbon type_ among the _WR_ stars. Nitrogen is not detectable. The intense _C III/C IV_ emission at λ 4650 is blended with the _He II_ line at λ 4686. This feature is even the most striking of the spectrum, followed by the _C IV_ emission line at λ 5801-12 and the _C III_ "hump" at λ 5696. The _He II_ emission at λ 6560 is relatively weak. The spectrum was recorded with the _Celestron C8_ − exposure: 10x90 sec.

The line identification is based amongst others on [230] [231] [232] [233] [344].

Due to these striking emission lines in the spectra, _WR_ stars are sometimes also called _"Laser Stars"_ [200].

TABLE 5

WR 133   HD190918   WN 4

N V 7102 - 29

Telluric O$_2$ 6870

He II 6560.1

Telluric

Na I5890/96
He I 5875
C IV 5801-12

He II 5411.52

N V 4933/44

Hβ 4861.33

He II 4685.7

N V 4619.4

N V 4603.2

He I 4471

Hγ 4340.47

N III 4097
N IV 4057.8
He I 4026.2
Hε 3970.1
H8 3889.1

I=0.7

WR 140   HD 193793   WC 7

C III 7037

Telluric O$_2$ 6870

He II 6560.1

Telluric

Na I5890/96
C IV 5801 - 12

C III 5696

He II 4685.7
CIII / CIV 4650

I=0.7
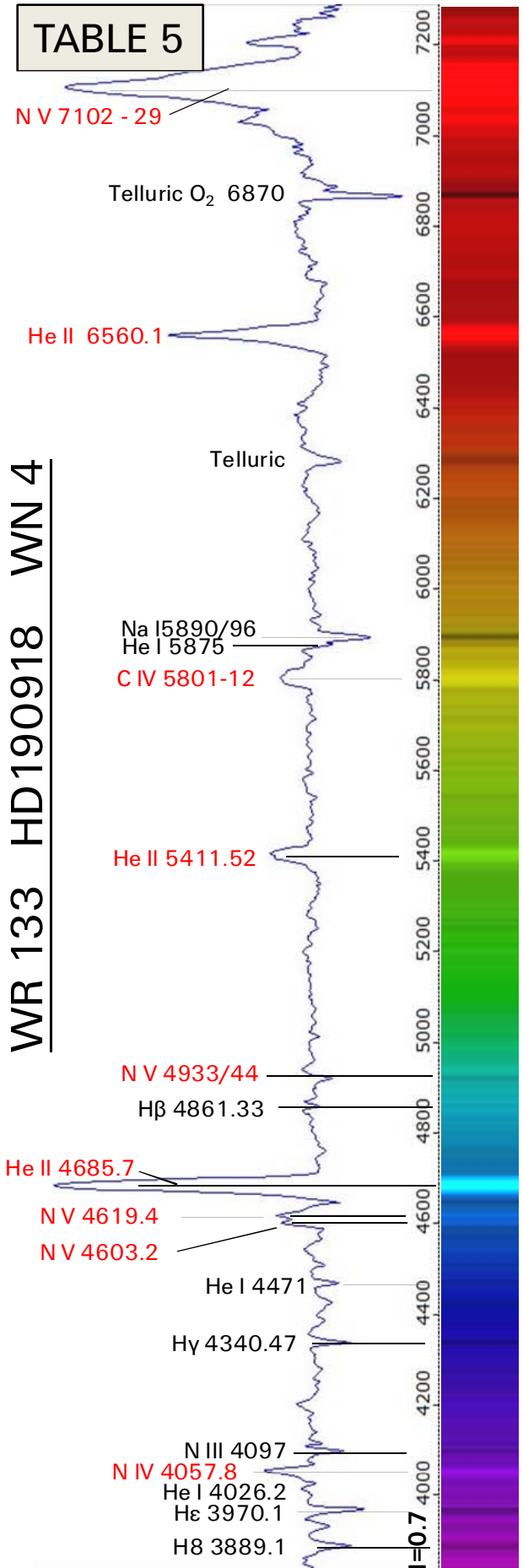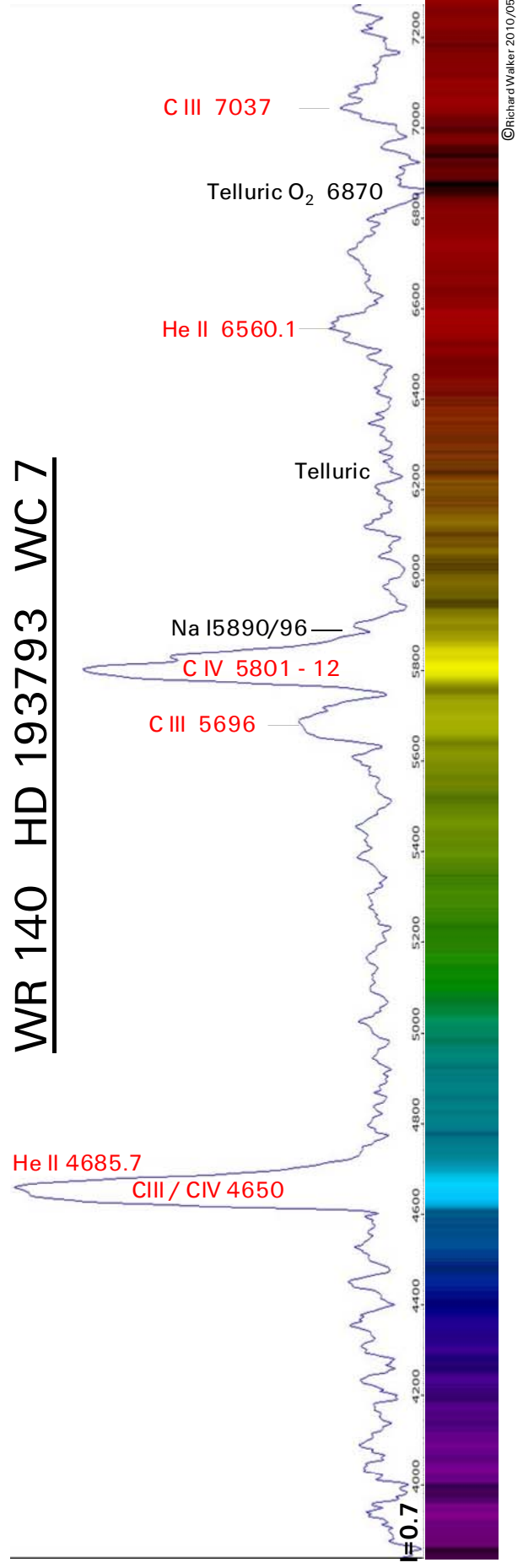
9   Spectral Class B

9.1   Overview

Below the extreme O-category seamlessly follows the B-class. Several of the bright Orion stars are early *B0*-types and differ therefore from the above presented late *O9.5* stars, only by small nuances within the spectral profiles. These blue-white luminous B-stars are less massive and hot and therefore living much longer. Further they are much more numerous, dominating a considerable part of the brighter constellations. Here some examples: all bright members of the *Pleiades*, all the bright *Orion stars* except Alnitak, Mintaka and Betelgeuse, all bright stars in the head of the *Scorpion*, except the reddish Antares. Further mentionable are *Regulus, Spica, Alpheratz*, and the weaker blue component of the well known double star *Albireo B* (B8V). Even the famous, unstable giant *P Cygni*, as well as most of the *Be-* and *Shell stars* belong to the B-class.

9.2   Parameters of the Early to Late B-Class Stars

The following table shows the data, exclusively valid for the *Main Sequence Stars* of the *B*-class, compared to the Sun (☉) and according to [701] and other sources (*). Here, the *enormous spread* becomes evident, covered by this class from the *B0–B9* types. Particularly impressive is the difference in the luminosity – that is about a factor of 550! The huge luminosity is one of the reasons, why the some 1000 ly distant, mostly *early B-class stars* in the Orion constellation, are able to show such a great brightness. Within this class, in the range of about 8–10 solar masses, it's decided whether single stars explode as a *SN* or end up as *White Dwarfs*.

Mass M/M☉	Stay on *Main Sequence* [y]	Temperature photosphere [K]	Radius R/R☉	Luminosity L/L☉
18 – 3	10M – 400M	25,000 (*) – 10,500	8.4 – 3.0	52,000 – 95

9.3   Spectral Characteristics of the B-Class

This class is characterised by the absorption lines of neutral helium, *He I*, reaching their maximum intensity at about class *B2* and weakening downwards the subclasses to *B9*. Further dominating are spectral lines of singly ionised metals *O II, Si II, Mg II*. Against later subclasses, the Fraunhofer K line of *Ca II* becomes faintly visible and the H-Balmer series gets significantly stronger. Due to lower temperatures and thereby decreasing *degree of ionisation* the simply ionised *He II* is only visible in the top *B0* subclass, but limited here to the *Main Sequence Stars* of the luminosity class *V*. Absorption lines of higher ionised silicon *Si III* and *Si IV* appear until down to type *B2*.

Higly abundant in the B–class are so called *"Fast Rotators"*. Such stars with high rotation speed (about 150–400 km/s) influence the appearance of the spectrum significantly. For details, see the comments to the tables below.

The maximum intensity of the real continuum is still in the UV range, but with a significantly higher share in the visible spectrum. The following graph shows the theoretical continuum for a *B6 IV* standard star *(Vspec Tools/Library)*. Marked with a read arrow is here the small kink of the emerging but still very weak Fraunhofer K-line of singly ionised calcium *Ca II*.
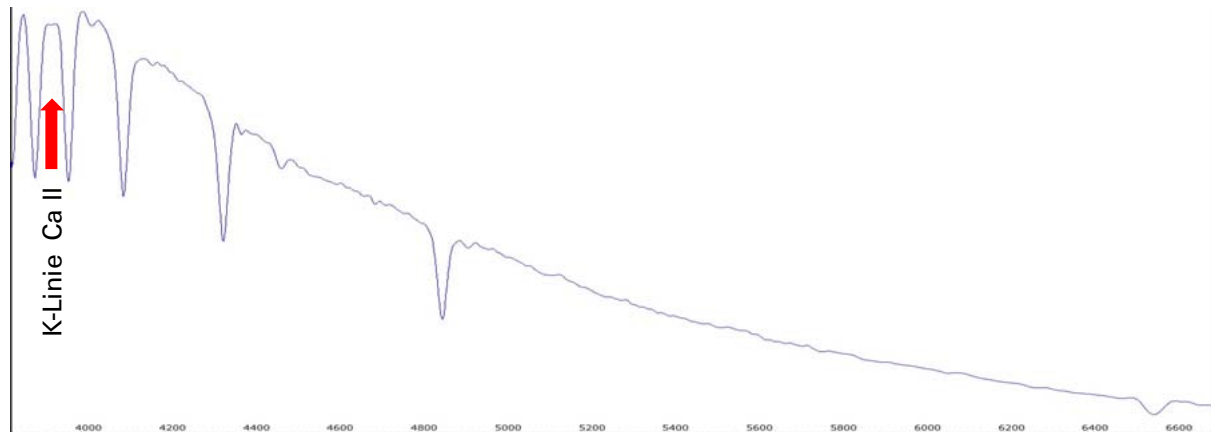
9.4 Commented Spectra

Table 10: Alnilam (ε Ori) and Gienah Corvi (γ Crv)

The development of the B-subclasses is demonstrated here by a montage of two overview spectra (200L grating) representing an early and late subtype.

Alnilam (1200 ly) belongs to the spectral class *B0 Iab*, and is a so-called *Supergiant*. The surface temperature is about 25,000 K. The star ejects permanently matter, visible here by the somewhat stunted *P Cygni profile* of the *Hα* line. About this detail, a PhD thesis exists [340], which analyses a time series of the line-profile change. For more information, refer to *Table 13*, *P Cygni*.

Gienah Corvi (165 ly) is classified with *B8IIIp Hg Mn*. It's in the Giant stage and shows overabundances of mercury *Hg* and manganese *Mn* (at this resolution not visible in the profile). For a giant, it has a remarkably high apparent rotation speed of some 150 km/s [506]. This flattens the spectral lines, as the following example of Regulus will show more detailed. According to [506] this effect explaines, why the overabundances of some metals have been discovered here so late.

The comparison of these spectra clearly demonstrates the remarkable change in the spectra within the enormous span from the early to the late *B*-Class. The *He I* lines of *Gienah Corvi* are only very faint. Moreover, they are now blended by numerous, still weak, singly ionised or even neutral metal absorptions, such as *Fe I/II, Mg II, Ca I/II*. These lines appear very diffuse, additionally flattened by the enormous rotation speed. Clearly visible however is the striking increase in the intensity of the *H*-Balmer series towards the late subclasses.

Here appears, for the first time and tentatively only, the Fraunhofer *K-line*, *Ca II* at λ 3933. The remarkable small kink in the continuum peak between *Hε* and *H8*, will grow dramatically within the following *A*-class and becomes the most dominant spectral feature for the middle- to late spectral types! Their "twin-sister", the Fraunhofer *H-line* at λ 3968, has still no chance to compete against the strong Balmer absorption line *Hε* at λ 3970.

TABLE 10

He I 6678.15

Hα 6562.82

Telluric O₂

Na I 5895.92   Interstellar
Na I 5889.95
He I 5876

N II 5932/42

O III 5592.37

He II 5411.52

He I 5047.74
He I 5015.68

He I 4921.93

Fe II 4923.92

Hβ 4861.33

He I 4713.15
C III 4647 - 51
OII 4590/96
Si III 4567.87
Si III 4552.65

He I 4471.48

OII 4415/17
He I 4387.9

Fe I/II 4383/84

Hγ 4340.47
OII 4276 - 95

OII 4185/90
He I 4143.76

Fe II 4233/34
Ca I 4226.73
Fe II 4172/78

Hδ 4101.74
He I 4025.5
Hε 3970.07

Ca II 3933.66

Alnilam ε Ori B0 Iab

Gienah Corvi γ Crv
B8IIIp Hg Mn

I=0.7

I=0.5

<u>Table 11:</u> Effect of the luminosity on spectra of the B-class: *Regulus* (α Leo), *φ Sagittarii* and *Rigel* (β Ori).

Regulus (77 ly) is classified as *B7V* and is, like our Sun, as so-called *Dwarf* still remaining on the *Main Sequence* of the HRD. It's the dominant component of a quadruple star system with a surface temperature at the poles of about 15,000 K. Its very high apparent rotation speed at the equator is about 315 km/s, which is not exceptional for stars of the late B-class. *Albireo B* (B8Ve) for example has an apparent rotational speed of some 250 km/s [506]. Thereby the spectral lines of *Regulus* are strongly widened and the star itself gets impressively flattened. (Computer drawing by *W. Huang*: Regulus in size compared to the Sun). The *Hα* line is already well developed in this late *B*-class.
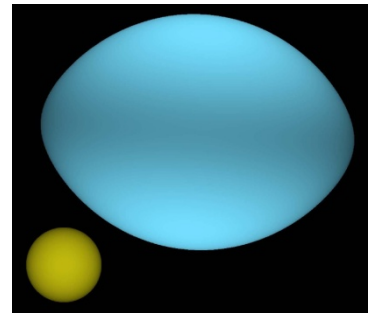
φ Sagittarii (230 ly) is classified with *B8III* and therefore a so-called *Normal Giant*. Its surface temperature is about 12,300 K and the apparent rotation speed is indicated by *Kaler* [506] with relatively low 52 km/s. This has hardly a noticeable influence on the *line width* in this spectrum.

Rigel (800 ly) is classified as *B8 Iab*, belonging to the *Super Giants*. It has a small companion, which is even visible in amateur telescopes, but hardly affects this spectrum of medium resolution (Photo NASA). The surface temperature is about 11,500 K. The apparent rotation speed is indicated in the range of about 40−60 km/s, depending on the info source.

The comparison of these three spectra, equally normalised, shows a clear decrease of the width and intensity of the *H-Balmerlines* with increasing luminosity. Conversely to this, the metal lines in the giants become more intense and narrower at the same time, caused by the less dense stellar atmosphere and thus a lower *pressure-* and *collision broadening*. For the *Regulus* spectrum, an additional role plays the so-called *rotational broadening*. With its apparent rotation speed of 315 km/s it's a real *"Fast rotator"*. This value is about 5 − 6 times higher than by *Rigel* and *φ Sagittarii*. Due to this effect particularly the fine metal lines of the Regulus spectrum become additionally broadened and their intensity considerably reduced.

F. Royer [401] has shown this effect in a chart for the A-class stars and the *Mg II* line at λ 4481 (marked in Table 11 with a red ellipse). Due to this effect, the absorption lines of *Regulus* become additionaly "ironed out". Remarkable that the *Mg II* line in *Table 11* shows a slightly different behavior than the directly adjacent *He I* absorption at λ 4471.
Caveat: This synthetic spectrum is calculated for a much higher resolution than shown in *Table 11*. Therefore the lines appear in the DADOS spectrum considerably wider, as a result of the greater *instrumental broadening*!

TABLE 11

Effect of the luminosity on spectra of the B-class

Rigel β Ori B8 Iab

φ Sagittarius B8 III

Regulus α Leo B7V

He I 4713.15

Fe II 4629.34

Fe II 4583.99

Fe II 4549

Fe II 4522.63

Mg II 4481.33
He I 4471.48

He I 4387.93

Fe II 4351.8
Hγ 4340.47

Fe II 4303.17 **V**

C II 4267.27

Fe II 4233/34

Fe II 4179
Fe II 4172.45

He I 4143.76
Si I 4130.89
Si I 4128.07
He I 4120.81
Hδ 4101.74

Ti II 4054
Fe I 4046

He I 4026

He I 4009.27

Hε 3970.07

Ca II 3933.66

Rigel

φ Sgr

Regulus

©Richard Walker 2010/05
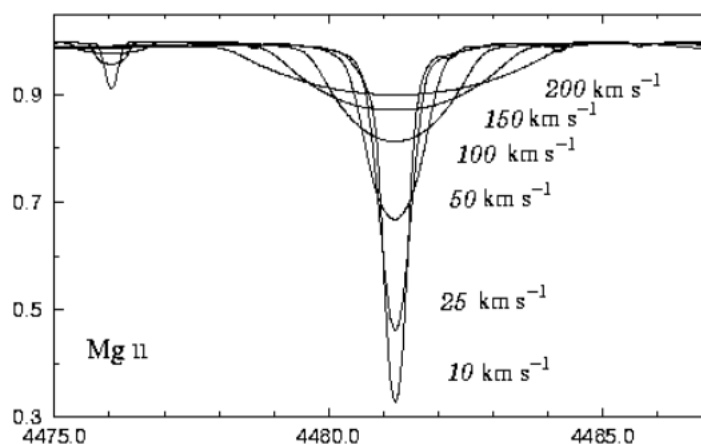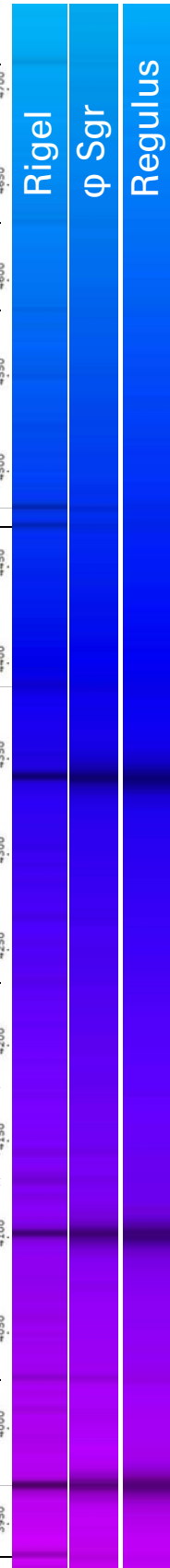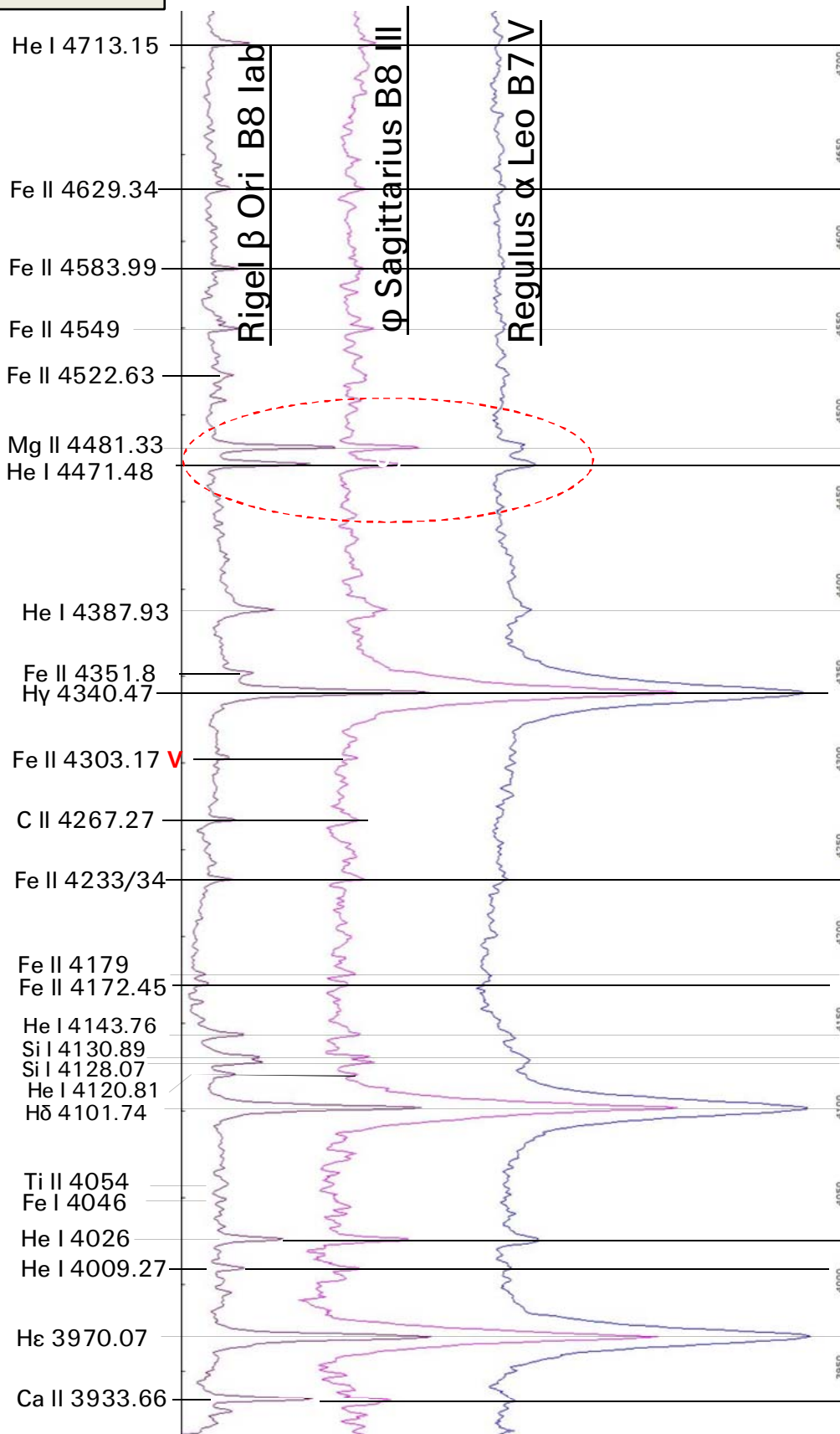
Table 12: Detailed spectrum of *Spica* (α Vir)

Overview spectrum (200L grating) and higher resolved profiles (900L grating)

Spica (260 ly) is a spectroscopic binary with an orbital period of about four days. The dominant *A*-component is in the Giant stage and has a surface temperature of about 22,000 K, corresponding to the spectral type *B1 III-IV*. The smaller *B*-component with the spectral type *B2V* is still on the *Main Sequence* and with a temperature of about 18,500 K significantly less hot and luminous. This very close orbit of the two stars causes, due to the Doppler effect, a periodic splitting of spectral lines (SB2 system), which is not recognisable in these profiles here. Ionised helium *He II* is here no more recognisable however still several absorption lines of multiply ionised metals.

Line identification:

The line identification is based amongst others on [1], [51], [56], [57]

TABLE 12

Spica α Vir
B1III-IV+B2V

He I 6678.15

Hα 6562.82

Telluric O₂

Na I 5895.92
Na I 5889.95

He I 5876

He I 5047,74
He I 5015.67

He I 4921.93

Hβ 4861.33

He I 4713.15

C III/ O II

Si III

He I 4471.48

He I 4387.9

Hγ 4340.47

He I 4143.76

Hδ 4101.74
He I 4025.5

Hε 3970.07
H8 3889.05

H9 3835.38

I=0.6

He I 4713.15

O II 4676.23

C III 4647 /51
O II 4639 - 52

Si III 4591/96
Si III 4574.78
Si III 4567.87
Si III 4552.65

Mg II 4481.13
He I 4471.48
N II 4447.03
He I 4437.55
O II 4416.98
O II 4414.91

He I 4387.9

O II 4366.9

Hγ 4340.47

O II 4317/ 20
O II 4302.81 V
O II 4285.7
O II 4276.7
C II 4267.27
O II 4253.98

O II 4189.79
C III 4187
He I 4168.97
O II 4153.3
He I 4143.76

He I 4120.81

Hδ 4101.74

C III/O II 4068-76

He I 4025.5
He I 4009.27

Hε 3970.07

He I 3926.53

I=0.5

Hα 6562.82

I=0.6

Na I 5895.92
Na I 5889.95
He I 5876

Si III 5739

I=0.6

He I 5047,74

He I 5015.67

He I 4921.93

Hβ 4861.33

I=0.5

© Richard Walker 2010/05

10 LBV Stars

P Cygni is one of the so-called *Luminous Blue Variables* (LBV), most probably progenitors of *WR stars!* It's an unstable and variable *Supergiant* of spectral class *B2 Ia pe*, with a surface temperature of about 19,000 K. Its distance is according Karkoschka some 5000 ly. What we analyse here with our spectrographs, apparently "realtime", tooked therefore really place at the end of the Neolithic period – a genuine "time machine" at its best! At the beginning of the 17th century, he showed a tremendous outburst, which is known as *Nova Cygni 1600*. After about six years as a star of the third magnitude, the brightness decreased to <5^m. Apart from a few minor episodic outbursts, the luminosity increased again in the 18th century, until it reached the current, slightly variable value of about +4.7^m to +4.9^m.

P Cygni is the *prototype* for the already presented *P Cygni profiles* in *Table 2* (Alnitak) and *Table 10* (Alnilam). Such spectral features are found in nearly all spectral classes and are a reliable sign for a huge amount of radially ejected matter by the star. Not surprisingly this effect is sometimes also visible in the spectra of Novae and Supernovae.

direction to earth
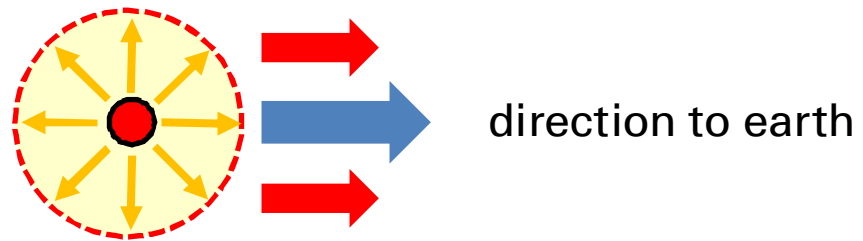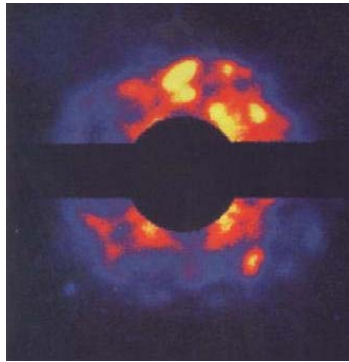
The left image shows parts of the expanding star shell, taken with the *HST*. The star in the center is covered here. The chart above right shows how the resulting *P Cygni profiles* are generated. In the direction of the *blue arrow* a small part of the expanding shell of gas moves right in our direction, so the resulting *absorption lines* appear blueshifted by the Doppler Effect. The *red arrows* symbolise the light, generated by the ionised shell areas, ejected sideways, and therefore are visible as emission lines. Both phenomena cause now the overall layout of the spectral line with a blue-shifted absorption part, which transits continuously into the mostly more intensive, red shifted emission peak. As already demonstrated in *Table 2* and in [30], the difference $\Delta\lambda$ between the two peaks enables the estimation of the expansion velocity of the shell (here some 200 km/s).

<u>Profile to the right (900L):</u> The "original" *P Cygni* star shows a higly impressive *Hα* emission line. Therefore the other spectral features appear strongly compressed, so they are barely recognisable. The blue absorption part of this line is strongly stunted. In contrast to this, the helium emission at λ 6678 shows here and in the lower profile of *Table 13* (900L) a textbook-like *P Cygni profile* – the same does *Hδ* in the upper profile of *Table 13* (200L). To show the other lines, overprinting here the telluric absorptions, the profiles in *Table 13* are strongly zoomed in the vertical intensity axis. The top of the *Hα* emission is therefore cutted. Noteworthy, that the continuum appears significantly elevated in an area of some 100 Å around *Hα*.
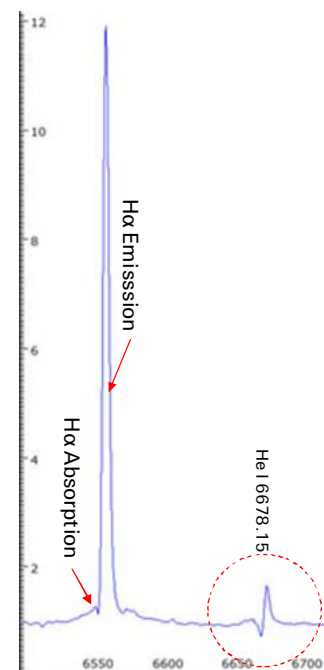
<u>Table 13</u>: Overview and detailed spectrum of *P Cygni* (34 Cyg)

Overview spectrum (200L grating, recorded September 16, 2009) and a higher resolved profile around the Hα line (900L grating, recorded June 22, 2010). The line identification is based on [341].

<u>Table 13 A:</u> Detailed spectrum of *P Cygni* (34 Cyg)

Higher resolved profile sections (900L grating), recorded May 07, 2011) in the green and blue area of the spectrum. The line identification in the range >λ 4100 is based on [341], in the range of <λ 4100 according to [341a], [341b].

<u>Remarks:</u>

What appears in these profiles as absorptions turns out at a higher resolution in most cases as emission lines or P Cygni profiles!

TABLE 13

Telluric O$_2$

He I 6678.15

Hα Emission

Si II 6371.36
Si II 6347.1

Telluric O$_2$

Fe III /Si II 5979
Fe III/ Si II

He I 5875.6

Ni I/Si II

P Cygni 34 Cyg
B2 Ia pe

Fe III 5156.12

Si II 5056
He I 5015.68

He I 4921.93

Hβ Emission

He I 4713.37

He I 4471.69

Fe II/ Fe III

Hγ Emission

Hδ Emission

I=0.5

He I 6678.15

N II 6610.58

C II 6582.85
C II 6578

Hα Emission

Hα Absorption

Si II 6371.36

Si II 6347.1

Telluric O$_2$

I=0.5
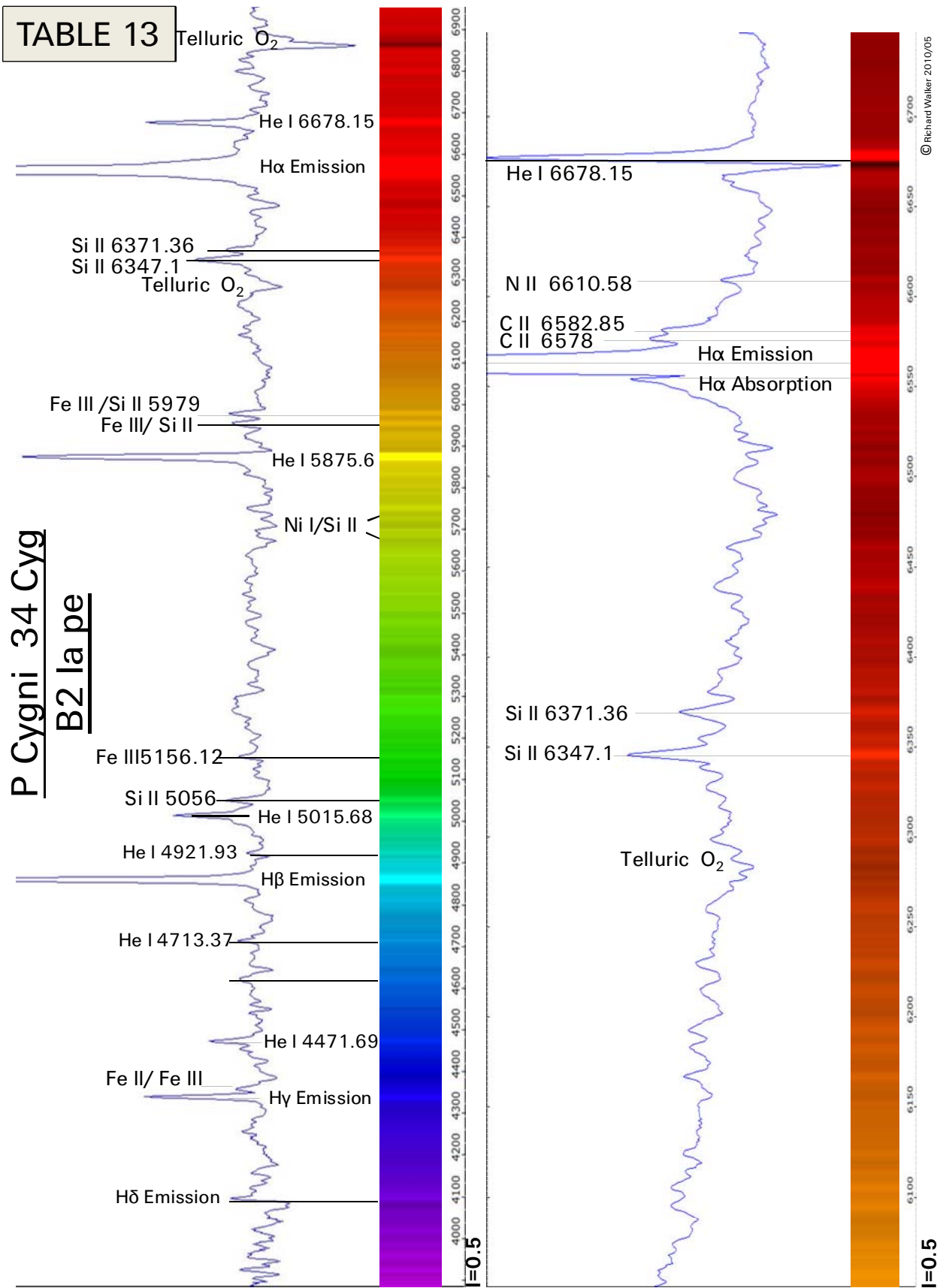
TABLE 13 A

P Cygni 34 Cyg
B2 la pe

N II 4643
N II 4631
N II 4621
N II 4614
N II 4601

Si III 4575
Si III 4568
Si III 4553

Al III/N II 4529/30
Al III 4513

Mg II 4481
He I 4471.69

Fe III 4431
Fe III 4420

Fe III 4396
He I 4388

O II 4353/59
O II 4346/49

Hγ 4340.47

Si II/Fe II 4285/87

S III 4254
N II/FeII 4242/44

Fe III 4165/67

He I 4144

He I 4121

Hδ 4101.74

NII/FeIII 4235 - 42

He I 4026

He I 4009.27
N II 3995
O II 3973

Hε 3970.07

He I 3965

Ca II 3933 interstellar
He I 3927

H8 3889.05

4600
4500
4400
4300
4200
4100
4000
3900

1.5
1.4
1.3
1.1
0.9
0.8
0.7
0.6
I=0.5

Fe III 6048
Fe III 6033

Fe III 5999

Fe III /Si II 5979
Fe III/Si II 5954/58

Fe III 5930

Na I 5890/96   interstellar

He I 5875.6

DIB interstellar
N II 5767
N II 5747/55
N II 5711   Si III 5740
Al III 5696
N II 5686
N II 5680   N II 5667
N II 5667

Fe II 5546V ?

Fe II 5376

Fe II 5334

Fe III 5272-80
FeII/ I 5260/62V
Fe III 5243

Fe III 5194

Fe III 5156   He I 5048

Fe III 5128

Fe III 5087
Fe III 5074

Si II 5056

Si II 5041

He I 5015.68

N II 4994 - 5011

He I 4921.93

N II 4895

Hβ 481.33

Si III 4813/20

C I 4262 ?

He I 4713.37

6000
5900
5800
5700
5600
5500
5400
5300
5200
5100
5000
4900
4800

1.4
1.1
0.9
0.8
I=0.5

11 Be Stars

Be stars form a large subgroup of the spectral *class B*, and all of them show a *high rotation speed*. A small number is still to find in the early *A-class*. These stars are mostly located on or near the *Main Sequence* of the *HRD*. A few Be-stars only have reached the giant stage with an upper limit of *luminosity class III*. The first Be-star, *γ Cassiopeiae,* was discovered in 1868 by Father *Angelo Secchi*, who wondered about the "bright lines" in this spectrum. The suffix *e* (*Be*) suggests that emission lines occur here. Due to the

University Western Ontario

sometimes temporary only occurrence of the Be stage, the suffix *e* for emission lines is missing in some stellar classification databases.

In contrast to the stars, showing *P Cygni profiles* due to expanding matter (*Table 13*), the *Be stars* develop, often just episodically, a *rotating circumstellar disk* of gas in the equatorial plane. The mechanism is not yet fully understood. This phenomenon is accompanied by *H I* and *He I* emissions in the spectrum, as well as strong infrared and *X-ray* radiation. Outside such episodes, the star can seemingly spend a normal "life" in the *B class*.

The approximately 450 ly distant *Dschubba,* dominant member in a quadruple star system, has mutated since about 2000 from the *B0.3 IV* spectral type in to a Be-star and developed a typical circumstellar disk of gas. The apparent rotation speed of the central star is approximately 180 km/s [505].The spectra in *Table 14* show the state of the gas disk at different dates. The Hα emission line was taken on August 18, 2009. Its intensity is significantly lower than by *P Cygni*, but although still so high, that the interesting, much weaker double peak profile of the helium line at λ 6678, could be overlooked. To make such details visible, the profiles in *Table 14* are strongly

zoomed in the intensity axis. The chart shows, how this double peak arises due to a combination of Doppler- and perspective effects. The intensities of *V* and *R*, as well as the distance between the two peaks, inform about the apparent "current" state of the disk. For detailed information with examples and formulas refer to [30] and [31].
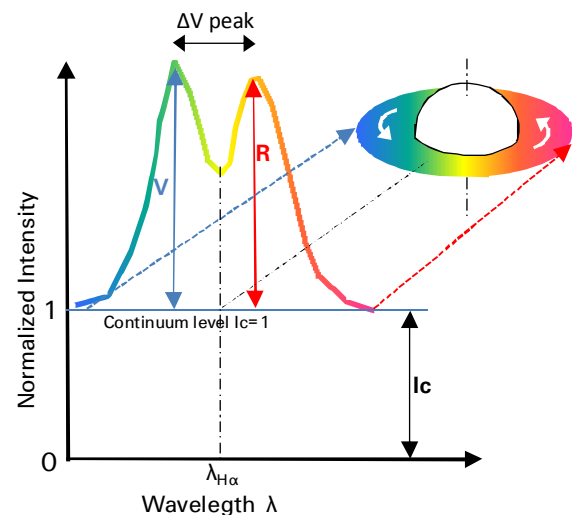
The main interest of the research seems to be focused on these spectral features. Anyway here are even more remarkable effects to see. Also *Hβ* shows an emission line, which grows up here in the middle of a broad *photospheric absorption* line of the central star [250]. Such spectral features are therefore called *emission-* or *shell cores* [2]. However *Hγ, Hδ* and *Hε* appear at this resolution as "normal" absorption lines, a suggestion for amateurs, to observe these lines with higher resolutions. Further at about λ 3700 the profile shows a kind of double peak emission. A similar structure within this wavelength domain was commented in [702] by *H.A. Abt* as a "Disk Line". In [2] a six-stage classification system is presented according to *Lesh*. The more lines of the *H* Balmer series show up as emission lines, the more intense the *Be* phenomenon is classified. Following the required excitation energies [eV], for some of the *H* Balmerlines, starting from the ground state $n = 1$: *Hα*: 10.2, *Hβ:* 12.1, *Hγ:* 12.7, *Hδ:* 13.0

<u>Table 14</u>: Be- star *Dschubba* (δ sco) B0.3 IV   V = 2.32^m

Overview spectrum (200L grating) and higher resolved profiles (900L grating) around the *Hα* and *Hβ* lines, further a zoomed detail of the Helium doublepeak at λ 6678.

TABLE 14

Telluric O$_2$

He I 6678.15

Hα 6562.82

Telluric O$_2$

N II 5932/42
Na I 5889.95
He I 5876

He I 4921.93
Hβ 4861.33

He I 4713.15
C III/ O II/He I

He I 4471.48

He I 4387.9
Hγ 4340.47

Hδ 4101.74

Hε 3970.07

H8 3889.05
H9 3835.38
H10
H11

Dschubba δ Sco B0.3 IV

He I 6678.15

R

>

He I 6678.15

Hα 6562.82

?

He I 4921.93

Hβ 4861.33

I=0.8

I=0.5

I=0.8
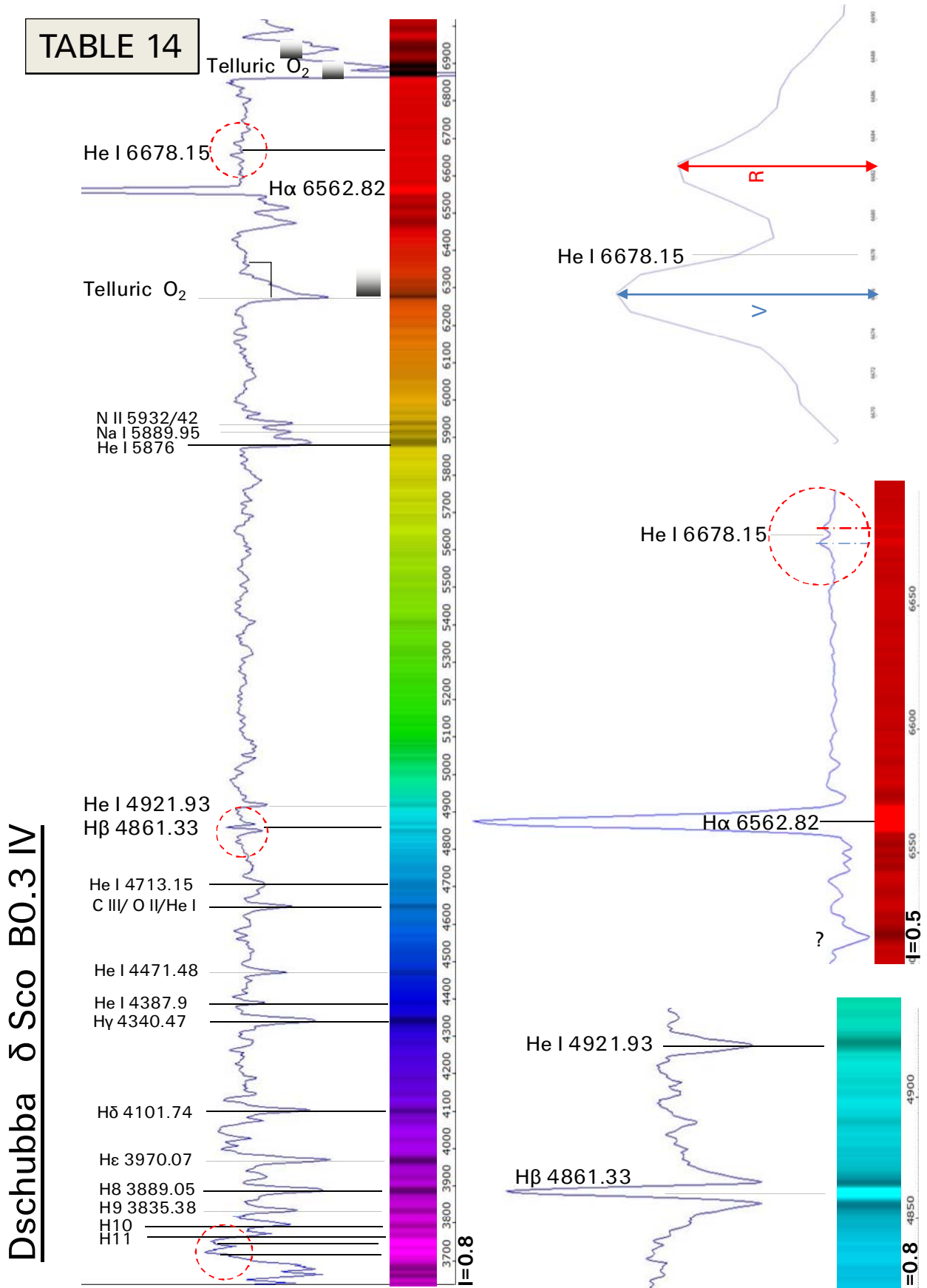
Table 14 A: Be- Star *Tsih γ Cassiopeiae* B0 IVe (610 Lj)   V = 2.47^m

Overview spectrum (200L grating). The apparent rotation speed of the central star is typically very high, ~300 km/s. The spectrum was taken on April 9, 2011. In contrast to *δ sco* much more lines are here in emission. Some of them are caused by Fe. The *He I* line at λ 6678 is hidden within a broad absorption and barely visible in this lowly resolved profile. The red profile represents the actual intensity ratios with the dominant *Hα* and *Hβ* emission. The blue one is strongly zoomed to make the fine lines visible.

TABLE 14 A

©Richard Walker 2011/03

He I 6678.15

Hα 6562.82

Telluric O$_2$

N II 5932/42
Na I 5889/95   Interstellar
He I 5876

Tsih γ Cas
B0 IV e

Fe I/II 5362-65 **V**
Fe I/II 5317-20 **V**
Fe I/II 5278-80 **V**
Fe I/II 5230-34 **V**
Fe I/II 5195-96 **V**
Fe I/II 5168-69 **V**

He I 5016

He I 4922

Hβ 4861.33

He I 4713

C III/ O II/He I

He I 4471

He I 4388
Hγ 4340.47

He I 4143.76
Hδ 4101.74
C III/O II 4068-76
He I 4025.5
Hε 3970.07
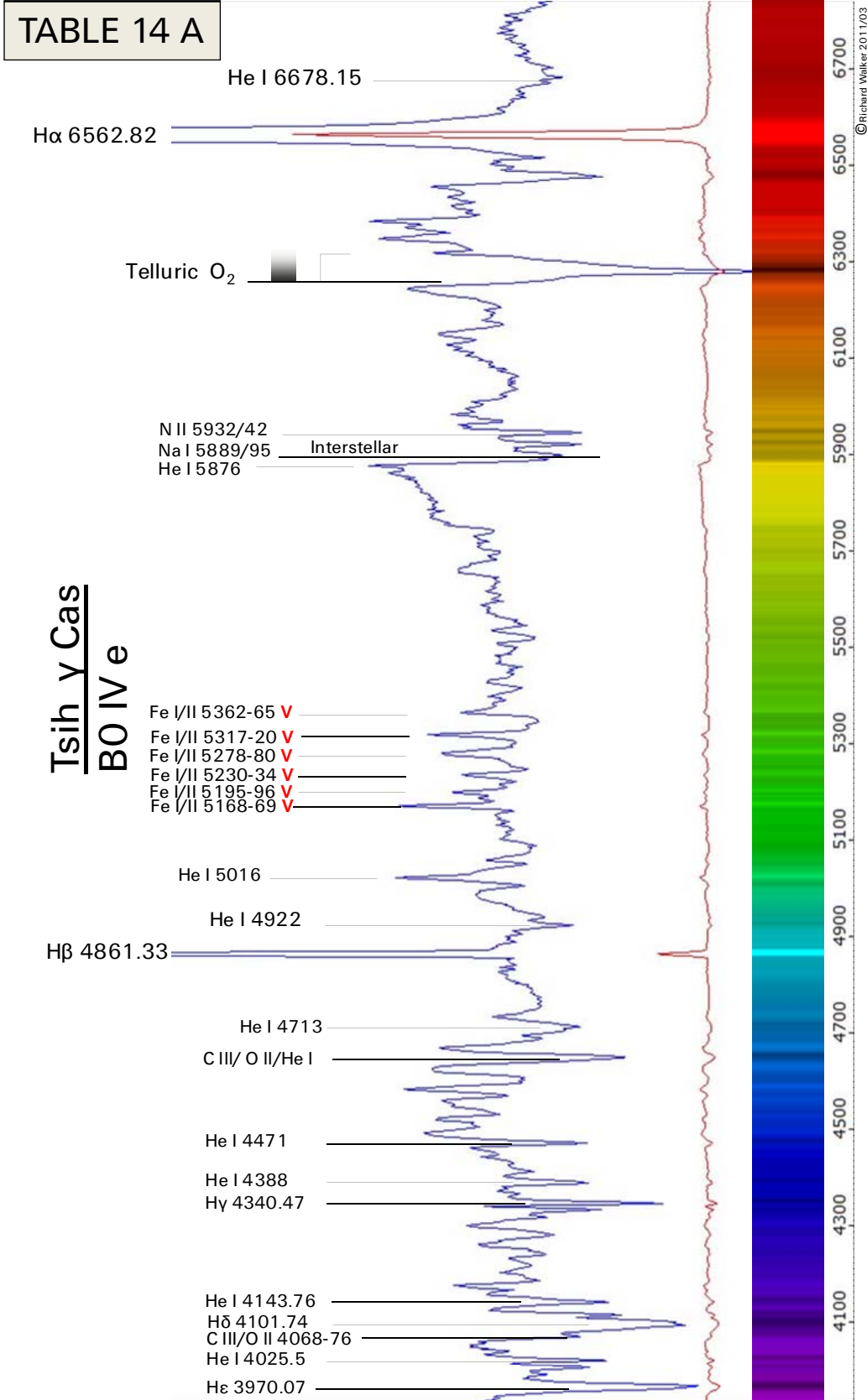
12 Be Shell Stars

During the *Be* phase a star can pass in some cases also the extreme *shell stage*. In this case it forms not only a disk, but rather a large scale, low density shell ("pseudo photosphere" [2]), which has similar characteristics like the photosphere of the supergiants with a luminosity class of approximately I-II. Accordingly, only few emission lines are showing up here, however much more very narrow but strikingly intense absorption lines with low FWHM values. Prototype for this star category is *ζ Tauri*. Also *28 Tauri* (Pleione) is undergoing this extreme shell stage from time to time. Sometimes the suffix *pe* is added to the spectral classification of such stars.

Table 15: Comparison Be Shell star *ζ Tauri,* and Be star *δ scorpii.*
ζ Tauri (HD 37202), *B4 IIIpe* [505], V_{var}= 2.88^m – 3.17^m

The approximately 417 ly distant *ζ Tauri* has a surface temperature of some 22,000 K. The apparent rotation speed of the central star is some 330 km/s, which is not unusual high for this type of star. It forms the main component of a binary system with a much smaller *B*-component of spectral class G8III. The orbital period is some 0.36 years, the distance between the components some 1 AU. The behavior of the spectral lines is sometimes very volatile. According to [505] the width of the H-lines may change within some 10 minutes – not unusual for *Be* shell stars! The spectral class of *ζ Tauri* is specified inconsistently by different datasources. So it's classified by [2] with *B2 IIIn shell,* instead of *B4 IIIpe* according to [505].

The Montage of the two spectra in *Table 15* shows the difference between the two stars. In contrast to *δ scorpii, Hα* is the only recognisable *emission line* in the spectrum of *ζ Tauri* (200L grating). The following profile (900L grating) shows *Hα* as an asymmetrical double peak emission line. Their shape can change within a very short time – a highly rewarding monitoring project for amateur astronomers!
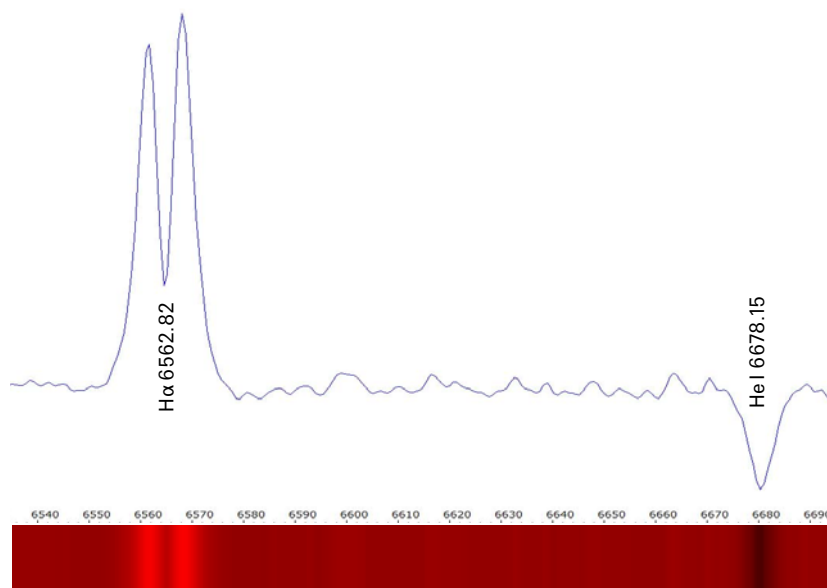
Unlike to *δ scorpii* the spectrum of *ζ Tauri* shows the *He I* line at λ 6678 and the *Hβ* line at λ 4861 *not* as emission- but relatively intensive absorption lines. (marked in *Table 15* with red ellipses). Furthermore all absorptionlines appear much more intensive compared to *δ scorpii,* corresponding approximately to those of early B Giants. Striking however is the strong absorption around the *He I* line at λ 5016. Due to the strong zoom in the vertical intensity axis, the peaks of the *Hα* emissions appear here "cutted". Their real intensity is similar in both spectral profiles.

TABLE 15

He I 6678.15

Hα 6562.82

Telluric O₂

N II 5932/42
Na I 5889/95   Interstellar
He I 5876

δ Sco
B0.3 IVe

ζ Tauri
B4 IIIpe

He I 5016

He I 4921.93
Hβ 4861.33

He I 4713.15
C III/ O II/He I

Si III

He I 4471.48

He I 4387.9
Hγ 4340.47

O II
Fe II ?

O II/CIII
He I 4143.76
Hδ 4101.74
C III/O II 4068-76
He I 4025.5
Hε 3970.07
He I 3926.53
H8 3889.05
H9 3835.38
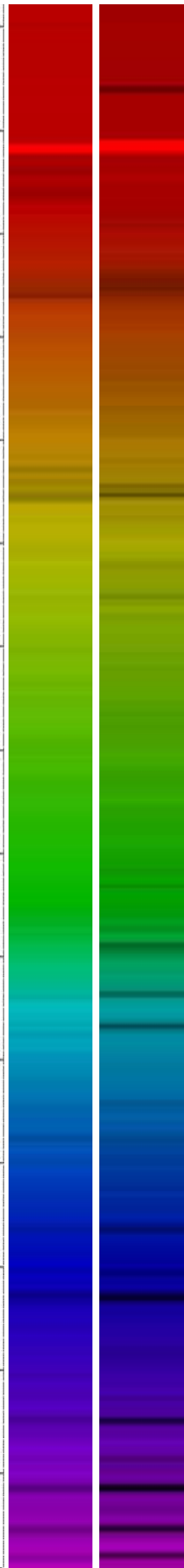
©Richard Walker 2011 1/03

13 Herbig Ae/Be− and T Tauri Protostars

13.1 Overview

The <u>*Herbig Ae/Be objects*</u> represent the birth stage of the stellar spectral classes A − O. For the later F − M types these are the <u>*T Tauri stars*</u>, which are still subdivided into *Classical T Tauri Stars (*<u>*CTTS*</u>*)* with intense emission lines and *Weak T Tauri stars (*<u>*WTTS*</u>*)* with predominantly absorption lines. The limit is determined here by the equivalent width *EW* of the Hα emission line. According to [2] the object is a *CTTS* if EW > |10Å| and according to other authors EW > |5Å|.
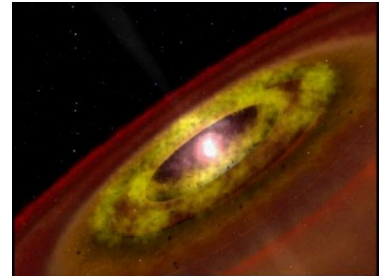
These so-called *YSO* (Young Stellar Objects) are formed from contracting gas and dust clouds. Due to this gravitational process the temperature in the center rises until the onset of the hydrogen fusion. Finally the star begins to shine. From now on, within the rough time frame of several hundred thousand to millions of years, it approaches from top, downward to the main sequence of the HRD. Therefore, these objects are also called *PMS stars* (Pre-Main Sequence) [2].

In this phase, the material forms a rotating accretion disk, which at least temporarily veils the central star. A part of the so-called *accretion flow* doesn't hit the emerging protostar [275]. It is deflected and ejected on both side of the disk, forming a cone-shaped, bipolar nebula (graphics Wikipedia). At some distance from the proto star, this jet may collide with interstellar matter, forming rather short living, nebulous structures, so-called *Herbig Haro* objects. These are named after *George Herbig* and *Guillermo Haro*. A detailed and illustrated presentation of these effects can be found in [275].
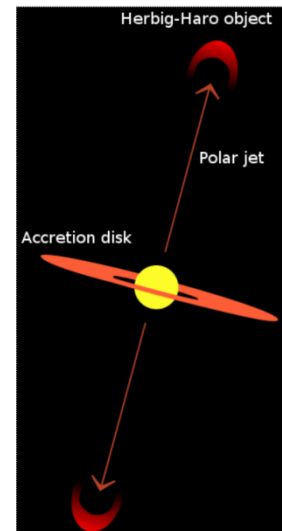
The highly irregular optical brightness variations proof, that the PMS stars are still very unstable. In a later phase planets are formed from the residual, protoplanetary disk material.

13.2 Spectral Characteristics of PMS Stars

This striking instability becomes also evident in the spectrum. Typically, it shows emission lines of the H-Balmer series, as well as the Ca II H- and K Fraunhofer lines. Depending on the state of the accretion disk, and our perspective on the object, in addition numerous Fe I and Fe II lines, as well as Ti II may show up [270]. Mainly late *WTTS* T Tauri stars sometimes generate more or less pure absorption spectra, which enable a fairly accurate classification of the star.

Gray Corbally [2] presents a classification system for Herbig Ae/Be stars with the following main criteria:

− The presence and intensity of emission lines of the H-Balmer series
− The presence and a possible λ shift of so-called *Shell Cores*, mainly observed by the Balmer series. These are emission lines, arising from rotationally broadened, photospheric absorption sinks.
− The presence of emission lines of ionised metals, particularly the *Fe II (42) Multiplet*
− The appearance of the Fe II (42) multiplet as *emission lines*, *absorption lines, or P Cygni profiles* (see below)
− Strenght of the Balmer Decrement

<u>Table 17</u>: NGC 2261 („Hubble's Variable Nebula") with *R Monocerotis*

R Monocerotis (ca. 2500 ly) is a *Herbig Ae/Be* star. Of its bipolar nebula from our perspective only one of the two conical halves is visible as NGC 2261 (Bild: HST). The star itself and the second symmetrical half of the nebula remain hidden behind the accretion disk. The brightness of R Monocerotis varies between ca. $10-12^m$. Only recently it became clear that this well-hidden object is a Herbig Ae/Be star of spectral type B0. Like most of the representatives of early spectral classes, R Monocerotis is also orbited by a smaller companion.

In the 1970's it was still considered by many authors as a T Tauri object of middle spectral class. In such cases, the spectral type can with reasonable accuracy be determined only with today's methods and means.

The spectrum in table 17 was taken on March 12, 2012 in the brightest tip of the nebula, near the not directly visible R Mon. With the 50 µm slit of DADOS at the C8, an exposure time was applied of 4x780 seconds: Atik 314L, −10° C, 2x2 binning mode. As for table 85 (M1), it was here also necessary, to record separately the disturbing light pollution spectrum just outside the nebula and to subtract it afterwards from the NGC 2261 signal (with Fitswork).

The most striking features are the strong H Balmer lines, which are seen here in emission. The Balmer Decrement in this profile yields Hα/Hβ ≈ 5. For such objects, this selective reddening of the profile is significantly influenced by the density of the circumstellar dust cloud and poses even an important classification criterion (see above). The high degree of dust occultation is probably one reason why here almost exclusively emission lines can be seen. C.A. Grady et al [273] noted the correlation between the intensity of the Fe I and Fe II emissions, and the degree of dust occultation, combined with the associated infrared excess. Striking in this profile appears further the so called *Fe II (42) Multiplet* at λλλ 4923, 5018 und 5169 [2]. This feature can also be found in the spectra of Novae and Supernovae as well as in Active Galactic Nuclei (AGN). Herbig already noted in the 1960's that the short-wave K-line of the two Ca II emissions mostly appears more intense.

Here it was also confirmed, that the spectrum, taken in a wider area of the NGC 2261 nebula, looks similar to a profile, recorded very close to R Monocerotis. Thus NGC 2261 is apparently rather a reflection and than an emission nebula. The quality of the obtained noisy profiles however is insufficient for this publication. The line identification is inter alia based on [2] and [270].

This highly interesting object is also very popular amongst astrophotographers who record the short-term brightness variations in spectacular series of images. On January 26, 1949 NGC 2261 became famous, because Edwin Hubbel him self photographed this nebula as the official First Light Object of the new 5m telescope at Mount Palomar Observatory!

<u>Table 18</u>: T Tauri HD 284419, Prototype of the T Tauri Stars

T Tauri is a *Classical T Tauri Star CTTS* with higly intense emission lines. This clearly demonstrates here the EW value of Hα: $EW_{Hα}$ ≈ −87A. At first glance, the two profiles of Table 17 and 18 look very similar. The Fe II (42) multiplet however is here much weaker, but the Ca II emission significantly stronger. T Tauri is classified as *G5 Ve,* much later than Type A. This can only be recognized here at the CH absorption band (γ ~4300).

A highly interesting detail are the forbidden [O I] line, the strikingly intense sulfur lines [S II] and the Hγ emission, which at the time of recording on March 27, 2012 appeared as <u>*Inverse P Cygni profiles*</u>*!* These indicate large-scale contraction movements within the

accretion disk, headed towards the star – this in contrast to the normal P Cygni profiles, which are always a reliable sign for an expansion. The Doppler analysis showed here contraction velocities of some 600 km/s (formula and example see Table 2).

According to AAVSO the apparent brightness of the object at the time of recording was ~10^m. The spectrum in Table 18 was taken with DADOS and the 25µm slit; exposure time 3x724 seconds: Atik 314L, −10°C, 2x2 binning mode. As for table 17, it was here also necessary, to record separately the disturbing light pollution spectrum just outside the nebula and to subtract it afterwards from the T Tauri signal (with Fitswork).

At T Tauri, as a by-product of this star birth, a closely neighboring *Herbig Haro object* is to observe. Here it is the variable nebula NGC1555, named after *John Russell Hind* (1823-95) visible in large telescopes next to T Tauri (image: CDS).

TABLE 17

(Recorded March 12. 2012)

NGC 2261 / R Monocerotis

O$_2$ telluric

[S II] 6718/33

Hα 6562.82

[O I] 6364

[O I] 6300

Zoom in the intensity axis

Original Profile

Fe II 5316

Fe II Multiplet

Fe II 5169

Fe II 5018

Fe II 4923

Hβ 4861.33

Fe II 4629

Fe II 4508 - 84

Hγ 4340.47

Fe II 4296

Fe II 4174

Fe I 4036 ?

Fe I 4006 ?

Ca II 3968

Ca II 3934

I=0.0
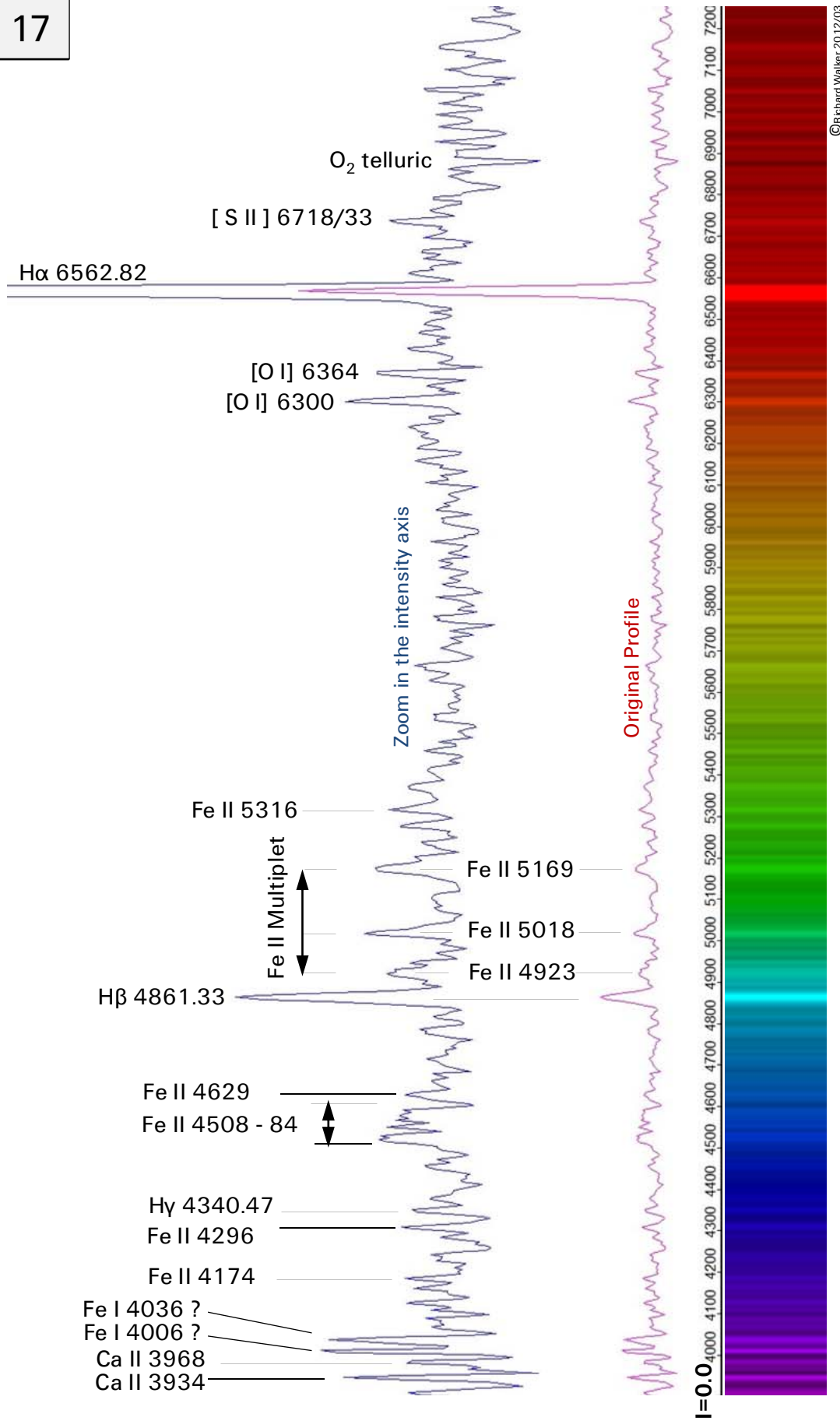
TABLE 18

©Richard Walker 2012/03

T Tauri HD 284419   (Recorded March 27. 2012)

O₂ telluric

[S II] 6718/33

Hα 6562.82

[O I] 6364

[O I] 6300

Inverse
P Cygni Profiles

Zoom in the intensity axis

Original Profile

Fe II Multiplet

Fe II 5169

Fe II 5018

Fe II 4923

Hβ 4861.33

Hγ 4340.47

CH 4299 - 4313

Hδ 4101.74

Ca II 3968

Ca II 3934

I = 0.0

7000 6900 6800 6700 6600 6500 6400 6300 6200 6100 6000 5900 5800 5700 5600 5500 5400 5300 5200 5100 5000 4900 4800 4700 4600 4500 4400 4300 4200 4100 4000
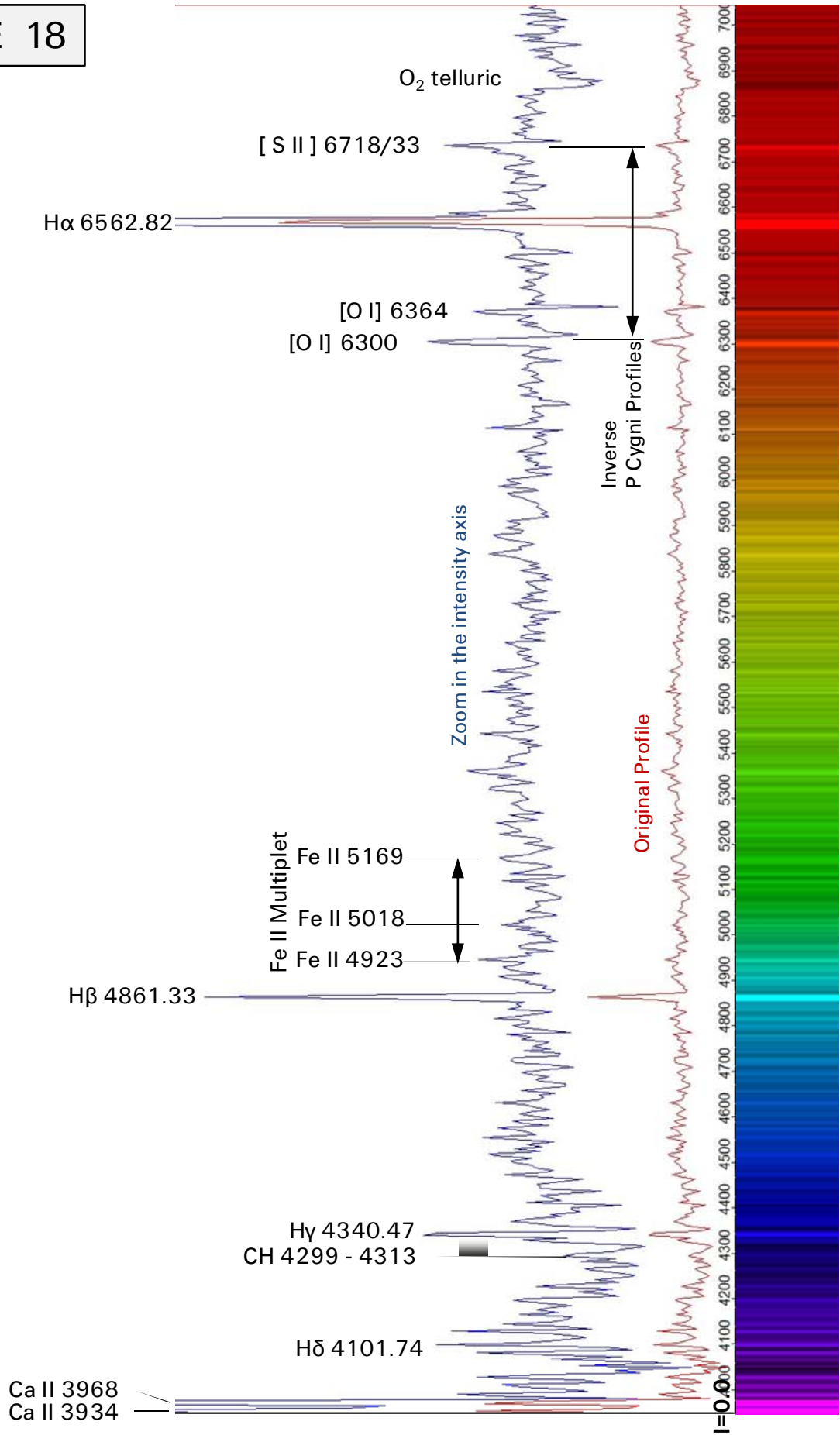
14 Spectral Class A

14.1 Overview

Several of the best known and most striking, bright white stars, like *Sirius, Vega, Castor, Deneb, Denebola, Altair*, and most of the stars in the *Great Bear* are classified as *A-types*. In this and all the following later classes, the single stars on the *Main Sequence* will pass at the end of their life a *Giant phase*, combined with an impressive "farewell tour" through almost the entire HRD. They will end their lives as extremely dense *White Dwarfs*. During this final process some of them will eject a photogenic *Planetary Nebula*.

14.2 Parameters of the Early to Late A-Class Stars

The following table shows the data exclusively for the *Main Sequence Stars* of the *A*-class, compared to the Sun (☉) and according to [701]. Compared with the enormously broad *B*-Class, the low mass range (factor 1.5) is striking here. Nevertheless impressive is the huge influence of this relatively small mass difference on the luminosity and life expectancy.

Mass M/M☉	Stay on main sequence [y]	Temperature photosphere [K]	Radius R/R☉	Luminosity L/L☉
3 – 2	440M – 3bn	10,000 – 7,500	2.7 – 1.7	55 – 8

14.3 Spectral Characteristics of the A-Class

Since the beginning of spectroscopy in the 19th century this class has fascinated by their impressive hydrogen lines, but otherwise very "tidy" and esthetically looking spectra. This was at least one reason for numerous false hypotheses. Father *Angelo Secchi* already classified these spectra in the mid-19th Century as *"Type I"* (see appendix 33.3). Edward Pickering labeled these in his later refined system as *"A-Type"*. Today, this class has still Pickering's *"A-label"*, but unconspicuously in the upper middle of the MK−stellar classes.

These distinctive and clear spectra are very well suited as a didactic introduction to the practical spectroscopy. Moreover, the pattern of the strong *H*-Balmer lines is an excellent aid for first calibration attempts. This feature gains intensity since the late *B*-class and reaches its maximum in type A2 [1]. Quantum mechanically, this can be explained with the surface temperature of about 9,800 K. This way the hydrogen atoms are thermally excited so that a maximum number of electrons stay already on the level *n2,* the "takeoff level" for the electron transitions in the shell system n2 − n∞ of the H-Balmer series [30].

From here on, the later *A*-classes are characterised by a gradual, but still moderate intensity loss of the *H*-Balmer series. Conversely, the two Fraunhofer *H* + *K* lines of *Ca II* become significantly stronger. The Fraunhofer *K*-line penetrates now deeper into the continuum peak between *Hε* and *H8* and exceeds between *A7* and *F0* the intensity of the hydrogen absorption. Within the same range also the growing Fraunhofer *H*-line (λ 3968) overprints now the weakening *Hε* absorption. In the late *A*-classes the "Blue Wing" of the *Hγ* line shows a small kink. At the latest in the *F0* class, it's revealed as the fast growing molecular *CH-absorption* of the Fraunhofer *G*-band (in the following graph marked with red arrow).

Higher resolved spectra show immediately that the first impression of the "simple spectrum" is deceptive. The continuum between the hydrogen lines is interrupted by numerous metal absorptions. The absorptions of neutral atoms become now more intensive at the expense of the singly ionised ones. In the early subclasses, a few *He I* lines still appear but very faintly. The intensity maximum of the real continuum moves here already to the "blue" short wave edge of the visible spectrum. The graph shows the theoretical

continuum for a synthetic *A5V* standard star (Vspec *Tools/Library*). Marked with red arrows are the two above-mentioned details.
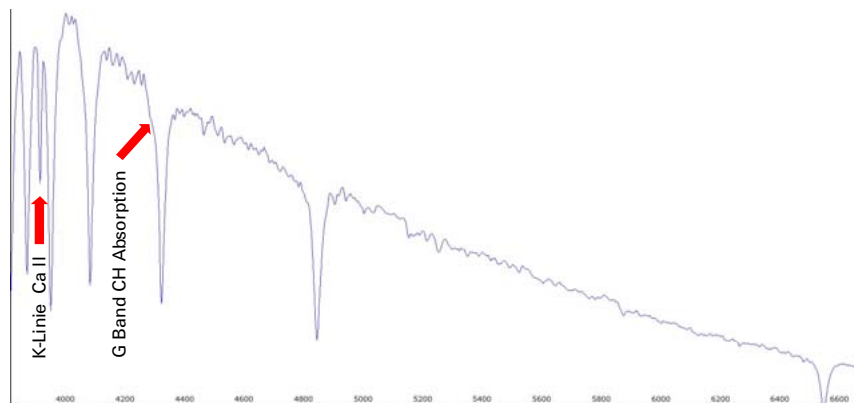
14.4 Commented Spectra

Table 20: Castor (α Gem) and Altair (α Aql)

The development within the A-subclasses is demonstrated here by a montage of two overview spectra (200L grating), representing an early and late subtype.

Castor (52 ly) is a very rare 6-fold star system. The two brightest components can be resolved even in smaller amateur telescopes (own picture by C8, and Meade DSI II). They dominate the spectrum and their early *A*-classifications, *A1Vm* and *A2Vm*, are very similar. The surface temperature – some 9,800 K – is therefore similar as for *Sirius* (*A1Vm*).
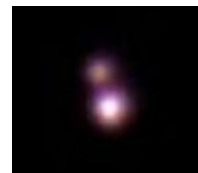
Altair (17 ly) is an *A7V Main Sequence Star* of the late *A*-Class. Correspondingly lower is therefore the surface temperature of some 7,550 K. For this late *A*-class it shows an extremely high apparent rotation speed of 210 km/s [506]. The equatorial diameter is therefore enhanced by about 22% (interferometric survey in 2007 by J. Monnier et al.).

Table 21: Detailed spectrum of Sirius A (α CMa)

Sirius A (8.6 ly), spectral type *A1 Vm* with a surface temperature of about 9,880 K, is similar to Vega and Regulus, a Dwarf star on the *Main Sequence* of the *HRD*. It forms the main component of a binary system with *Sirius B* (White Dwarf).
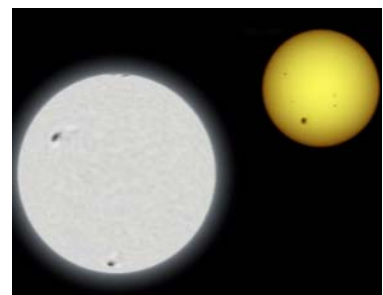
The table shows an overview spectrum (200L grating) and two higher-resolved profiles in the blue/green and red wavelength domain (900L grating). Within the blue/green part most of the interesting metal absorptions are concentrated. They look very slim, compared to the huge *H*-Balmer lines. Here, as well as in the spectrum of castor, the so-called *magnesium triplet* apperars, still faintly, for the first time at λ 5168 – 83 (Fraunhofer **b**).

Sirius is one of the metal-rich stars, which are labeled with the suffix [m] (see *Table 23*). Computer graphic Wikipedia: *Sirius* compared in size to the *Sun*.

Its apparent rotation speed of about only 13 km/s is unusual low for the early *A*-Class. According to [1] however, such statistical outliers correlate significantly with an overabundance of metals.

The line identification is based amongst others on [1], [5], [50], [51], [52],

TABLE 20

© Richard Walker 201 0/05

Hα 6562.82

Altair α Aql
A7 V

Na I 5895.92
Na I 5889.95

Ca I/Fe I 5587-90

Castor α Gem
A1 Vm / A2Vm

Fe II 5316.61
Fe II 5276.0
Fe II 5234.62
Mg I 5169-83

Fe II 5018.43

Fe II 4923.92

Hβ 4861.33
Cr II 4824.13
Ti II 4767.3

Fe II 4630/34
Mg I 4703.98

Fe II/Cr II 4584 - 88
Fe II/Ti II 4550
Fe I/Ti II 4526 - 29
Mg II 4481
Ti II 4468
Fe II 4384-85

Hγ 4340.47
CH 4299 - 4313

Ca I 4226.73
Ti II/Fe II 4172

Hδ 4101.74

Fe I/Mn I 4030-33

Hε 3970.07
Ca II 3933.66
H8 3889.05

I=0.3

I=0.4

TABLE 21

Hα 6562.82

Telluric O$_2$

Na I 5895.92
Na I 5889.95
He I 5876

Sirius α CMa
A1 Vm

Hβ 4861.33

Fe II 4630/35

Mg II 4481

Fe II 4384-85

Hγ 4340.47

Hδ 4101.74

Hε 3970.07

I=0.4

Fe II/Cr I 4666

Fe II 4634.6
Fe II 4629.9
Cr II 4617/19

Cr II 4588
Fe II 4583.8
Ti II 4571.97

Fe II 4556
Fe II 4550
Fe II 4541
Fe II 4534
Fe II 4520/23
Fe II 4515
Fe II 4508
Ti II 4501.27
Fe II 4489/91
Mg II 4481
Ti II 4470

Fe II 4451
Ti II 4444

Fe II 4416.8
Ti II 4400.63
Ti II 4395.04
Fe II 4384-85
Ti II 4375.35
Fe II 4366.17

Hγ 4340.47

Sc II/Ti II 4314
Ti II 4307.9
Fe II 4303.2
Ti I 4289

Fe I 4271-72
Fe II/Cr II 4258/62
Fe I 4250 - 51
Cr II 4242.38
Fe II 4233.17
Ca I 4226.73
Sr II 4215.77

Fe I 4198.31
Fe I 4187.04
Fe II/Cr II 4178-79
Fe II 4173.1

Fe I 4152 - 61

Fe I 4143-44

Si II 4128/31

Hδ 4101.74

Sr II 4077.71
Fe I 4071.74
Fe I 4067.6
Fe I 4062.4
Mn I 4055.54
Fe I 4045.82
Mn I 4031 - 36
Ti II/V II 4023/24
Cr II/Ti I 4012
Fe I 4002/05

Hε 3970.07

Cr II 3945
Ca II 3933.66

I=0.6

Fe II 5316.61

Fe II 5276.0

Fe II 5234.62
Fe I 5227.19 V

Fe II 5197.6

Mg I 5183.60
Mg I 5172.68
Mg I 5167.32

Fe II 5100.66 V

Si II 5056.02

Si II 5041.06

Fe II 5018.43

Fe II 5002/4

Fe I 4957 V

Fe I 4933 V
Fe II 4923.92

Fe II 4890 V

Hβ 4861.33

Cr II 4824.13

Ti II 4807

Ti II 4793

I=0.6

<u>Table 22:</u> Luminosity effect on spectra of the early A-class: *Vega* (α Lyr), *Ruchbah* (δ Cas) and *Deneb* (α Cyg).

<u>Vega</u> (25 ly) is classified with *A0V* and is, like our Sun, a so-called *Dwarf* on the *Main Sequence* of the *HRD*. Its surface temperature is about 9,500 K its apparent rotational speed at the equator with some 15 km/s is very low. However, recent interferometrical studies show that's why we see *Vega* almost "Pole on" and the *effective* rotational speed is >200 km/s.

<u>Ruchbah</u> (100 ly) is classified with *A5 III-IV*. Thus it's moving in the *HRD* on the way from the *Main Sequence* to the *Giant Branch*. Its surface temperature is about 8,400 K. Its rotation speed is indicated by *Kaler* [506] with 113 km/s, an inconspicuous value for this class.

<u>Deneb</u> (2,000 ly) is classified with *A2 Ia* and thus belongs to the *Supergiants*. The surface temperature is about 8,500 K. The apparent rotation speed is indicated with about 21 km/s. This *Supergiant* was during its former stay on the *Main Sequence*, an early *B*- or even a late *O*-star [506].

The comparison of these three equally normalised spectra shows clearly a *decrease* of the *intensity* and *width* of the *H*-lines by *increasing* luminosity. Conversely the metal lines in the *Giant* become more intense, what is expected due to the less dense stellar atmosphere and thus a lower *pressure* and *collision broadening*. Due to the relatively moderate $v \sin i$ values the *rotational broadening* has here not a dominant influence on the appearance of the profiles.

<u>Table 23:</u> Different metal abundance of *Vega* and *Sirius*

The comparison of the "metallicity" between Vega and Sirius has been the subject of numerous professional studies in the past, such as [703], [704]. Besides the different metal abundance these two stars are almost equally classified and have also a similarly low, apparent rotation speed. Differences in the spectrum must therefore primarily be caused by the different metal abundance, which predestines the two bright stars for such investigations.

At this resolution (900L grating) it can immediately be noticed, that the *Ca II* line (Fraunhofer *K* at λ 3933) in the *Vega* spectrum is *much intenser*, even though the star is classified slightly earlier than *Sirius*. This is already visible, even without measuring of the

EW values. But most, *if not all* other metal absorptions, are significantly stronger in the profile of *Sirius*. The graph shows the shape of the so-called *"Curve of Growth"* according to *Keith Robinson* [3]. We are interested here only in the approximately linear range, covering the area of the *unsaturated* spectral line in the left part of the graph. Here the *EW* of a particular spectral line is nearly proportional to the number of atoms of the corresponding element within a certain gas mixture.
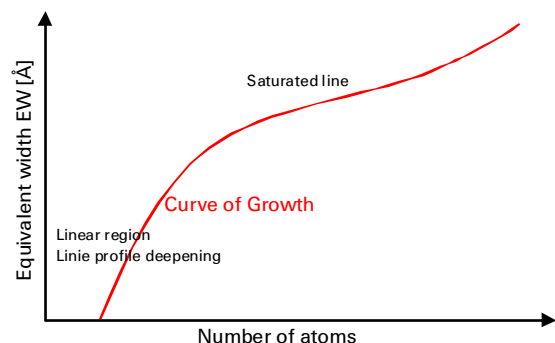
A Chinese study by *H. M. Qiu* et al. [703] summarises that *Sirius*, with a Fe/H ratio of +0.5 is relatively metal rich, *Vega* with a ratio of −0.57, however, is relatively metal poor. Here is also confirmed that for *Sirius Ca* and *Sc* are *underabundant* and vice versa *Fe overabundant*. According to this study this *deficit* of *Ca* and *Sc* and the *overabundance* of *Fe* are generally used as defining markers for metal rich *Am stars*. The Fraunhofer *Ca II* line (λ 3934) also serves in various other studies as an important indicator of metal abundance.

TABLE 22

Deneb α Cyg
A2 Ia

Ruchbah δ Cas
A5III-IV

Vega α Lyr
A0 V

©Richard Walker 2010/05

Deneb

Ruchbah

Vega

Effect of the luminosity on spectra of the A-class

Fe II/Cr I 4666

Fe II 4634.6
Fe II 4629.9
Cr II 4617/19

Cr II 4588
Fe II 4583.8

Fe II 4550

Fe II 4520/23
Ti II 4501.27
Mg II 4481
Ti II 4470

Ti II 4444

Fe II 4416.8
Ti II 4395.04
Fe II 4384-85
Fe II 4366.17
Fe II 4352
Hγ 4340.47

Sc II/Ti II 4314
Fe II 4303.2

Fe I 4271-72

Fe II 4233.17
Ca I 4226.73

Fe II 4178.9
Fe I 4173.1

Si II 4128/30

Hδ 4101.74

Sr II 4077.71
Fe I 4067.6
Fe I 4045.82

Zr II/Ti II 4024/28

Fe I 4002/05

Hε 3970.07

Ca II 3933.66

4700
4600
4500
4400
4300
4200
4100
4000

TABLE 23

Vega α Lyr
A0 V

Sirius α CMa
A1 Vm

© Richard Walker 2010/05

Comparison of metallicity Vega vs. Sirius

Fe II/Cr I 4666

Fe II 4634.6 V
Fe II 4629.9
Cr II 4617/19

Cr II 4588
Fe II 4583.8

Fe II 4550

Fe II 4520/23

Ti II 4501.27 V

Mg II 4481
Ti II 4470

Ti II 4444

Fe II 4416.8

Ti I 4395.04
Fe II 4384-85

Hγ 4340.47

Sc II/Ti II 4314

Fe I 4271 - 72

Fe II 4233.17
Ca I 4226.73

Fe II 4178.9
Fe I 4173.1

Fe I 4143-44
Si II 4128/30

Hδ 4101.74

Sr II 4077.71

Fe I 4062.4

Mn I 4055.54

Fe I 4045.82

Fe I 4005.25

Hε 3970.07

Ca II 3933.66

4700

4600

4500

4400

4300

4200

4100

4000

Vega

Sirius

15 Spectral Class F

15.1 Overview

The *F*-class is located directly above the *G*-category, where our Sun is classified. It includes several well-known, bright yellow shining stars like *Procyon*, *Caph (β Cas), Porrima (γ Vir), Mirfak (α Per), Canopus* in the southern sky and even the *Pole Star*. On the *Giant Branch* of the *HRD* we find here several pulsation variables, belonging to the categories of *δ Cephei* and *RR Lyrae*.

15.2 Parameters of the Early to Late F-Class Stars

The following table shows the data exclusively for the *Main Sequence Stars* of the *F*-class, compared to the Sun (⊙) and according to [701].

Mass M/M⊙	Stay on main sequence [y]	Temperature photosphere [K]	Radius R/R⊙	Luminosity L/L⊙
1.6 − 1.1	3bn − 7bn	7,200 − 6,000	1.6 − 1.2	6.5 − 2.0

15.3 Spectral Characteristics of the F-Class

The H-Balmer lines are now much weaker and the Fraunhofer *H + K* lines (*Ca II*) become the dominant features, so that the Fraunhofer *H* absorption now clearly displaces the *Hε* line. Towards the late subclasses the *neutral* elements, e.g. *Fe I, Cr I,* replace now increasingly the absorption of the *ionised* ones.

The *Ca I* line at λ 4227 clearly intensifies, as well as the *G-band* (*CH* molecular) which surpasses within the *F*-Class the intensity of the neighboring *Hγ* line. This striking "line double" can therefore only be seen here so it forms essentially the unmistakable "Brand" of the *F*-class! The *Magnesium Triplet* (λλ 5168−83) becomes here stronger, compared to the *A*- Class.

At this resolution, at the latest since the early *A*-class, most of the absorptions are formed by *several* metal lines of slightly different wavelengths, so called "blends". These can only be resolved with high-resolution spectrographs. Labeled here are therefore only the chiefly involved elements, causing these blends. In *Table 30*, one of the absorption lines within the *Procyon* profile is summarily labeled with *Fe I/Ca I 4454 − 59* (small graph below right). The large graph left shows a highly resolved profile (*Spectroweb* [59]) in the same wavelength domain. Obviously the imagination of isolated single lines must be abandoned!

26: Fe I 4454.380Å
29: Ca I 4454.779Å
40: Ca I 4455.887Å
45: Fe I 4456.628Å
51: Ti I   4457.427Å
57: Fe I 4458.080Å
63: Fe I 4459.117Å
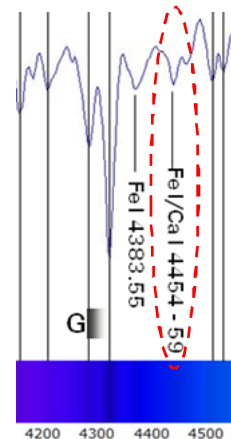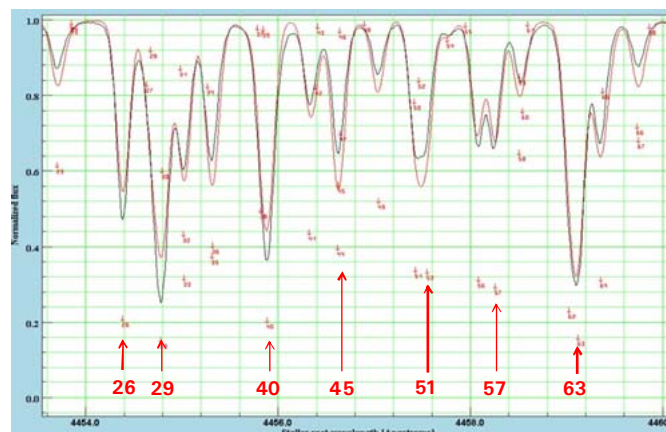
The intensity maximum of the real continuum is now clearly located within the visible range of the spectrum. The graph shows the theoretical continuum for a synthetic *F5 V* standard star *(Vspec/Tools/Library)*. Highlighted with a red circle is here the "Line-double" of the *G-band* and *Hγ*, the striking "Brand" of the *F*-class.
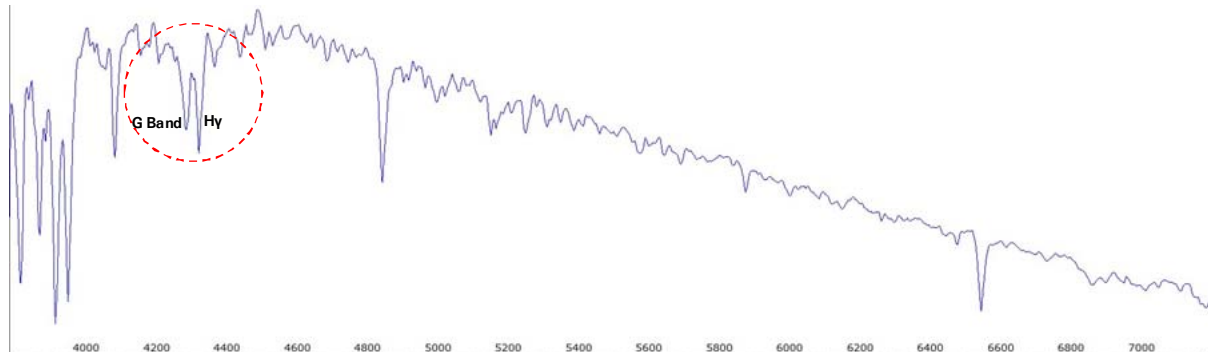
15.4 Commented Spectra

Tafel 30:   Adhafera (ζ Leo) und Procyon (α CMi)

The development of the *F*-subclasses is demonstrated here by two superposed overview spectra (200L grating) representing an early and middle subtype.

Adhafera (260 ly), classified as *F0 III*, is located at the top of the *F*-class and has already reached the Giant stage (III). The surface temperature is about 7,030 K and its apparent rotation speed some 84 km/s [506]. Even within this early *F*-class, the Fraunhofer-*H* and *K* lines have already *surpassed* the intensity of the *H*-Balmer series, where the *K*-line at λ 3968 has overprinted the *Hε* absorption.

Procyon (11 ly) is classified as *F5 IV-V* and thus representing approximately the "center" of the *F*-class. Like *Sirius*, it has a white dwarf companion. The luminosity class IV-V reveals that it has begun to leave the *Main Sequence* in the *HRD* towards the *Giant Branch*. The apparent rotation speed is only some 6 km/s. The surface temperature with about 6,630 K is expectedly lower than for the earlier classified *Adhafera*. At the first glance this has little effect on the spectral profile.

The most noticeable and important difference relates to the "Brand" of the *F*-class - the increasing intensity of the *CH* molecular absorption band (at λ 4300) and conversely the shrinking of the neighboring *Hγ* line. Further the growing intensity of the *Ca I* line (λ 4227), at this resolution clearly visible only by the somewhat colder *Procyon*. Some further differences may be caused by the difference in luminosity class.

Line identification:

The line identification is based amongst others on [1], [5], [51], [52], [59]

TABLE 30

Adhafera ζ Leo
F0 III

Procyon α CMi
F5 IV-V

© Richard Walker 2010/05

Hα 6562.82

Telluric O₂

Na I 5895.92
Na I 5889.95

Ca I/Fe I 5587-90

Fe I 5404 - 15
Fe I 5328.53
Fe I/Ca I 5270
Fe I/Ti II 5227
Mg I 5183.60
Mg I 5172.68
Mg I 5167.32
Fe I/Ni I 5079-81
Fe I 5041
Fe II 5018.44
Fe I 4983
Fe I 4957
Fe II 4923.92

Hβ 4861.33

Mn I 4754
Ti II 4708
Fe II/Sc II 4666/70

Fe II/Cr II 4585/88
Ti II 4550/56
Fe I/Ti II 4520 - 34

Fe I/Ca I 4454 - 59
Fe I 4383.55

Hγ 4340.47

CH 4299 - 4313
Ca I 4226.73
Fe II/Ti II 4172-73

Hδ 4101.74

Mn I 4031-36

Ca II 3968.47
Ca II 3933.66
H8 3889.05

H9 3835.38

G

I=0.3

G

I=0.5

Table 31: Effect of the luminosity on spectra of the *F*-class: *Porrima* (γ Vir), *Caph* (β Cas) and *Mirfak* (α Per).

Porrima (39 ly) is classified with *F0V* and is, like our Sun, a *Dwarf* on the *Main Sequence* of the HRD. Its surface temperature is about 7,100 K and its apparent rotation speed remains here unknown.

Caph (55 ly) is classified with *F2 III-IV*, thus moving from the *Main Sequence* to the *Giant Branch* in the HRD. Its surface temperature is about 6,700 K. His apparent rotation speed is reported by *Kaler* [506] with 70 km/s.

Mirfak (600 ly) is classified with *F2 Ib* and therefore one of the *Supergiants*. The surface temperature is about 6,180 K. The apparent rotation speed is reported with 18 km/s. Mirfak is a former *Main Sequence Star* of the *B*-Class [506].

The comparison of these three equally normalised spectra shows no striking differences between the luminosity classes. A difference regarding the intensity and width of the H-lines is here *visually* not recognisable. The metal lines of the *Supergiant Mirfak* are somewhat more intensive than in the profile of the *Giant Caph*. Between *Caph* and the *Main Sequence Star Porrima* differences are hardly discernible.

TABLE 31

Effect of the luminosity on spectra of the F-class

Mirphak α Per F2 Ib

Caph β Cas F2 III-IV

Porrima γ Vir F0 V

©Richard Walker 20 10/05

Mirphak

Caph

Porrima

Ti II 4708

Fe II/Sc II 4666/70

Cr II 4634.1

Fe II 4629.34

Cr II/Fe II 4618-20

Fe II/Cr II 4585/88

Fe II 4583.83

Ti II 4572

Ti II 4564

Fe II 4550/56

Ti II 4534

Fe II 4508

Ti II 4501

Fe II 4490

Mg II 4481

Ti II 4470

Ca I 4454.78

Ti II 4444

Ca I 4435

Fe I/II/Ti II 4415-18

Ti II 4400

Ti II 4395.04

Fe I/II 4384-85

Ti II 4368

Fe II/Cr I 4352

Hγ 4340.47

Fe I 4326

Sc II/Ti II 4314

CH/Fe II 4299-13

Cr I/Ti II 4290

Fe I 4271-72

Zr II 4258

Sc II 4247

Fe II 4231-33

Ca I 4226.73

Sr II 4215.52

Fe I/V II 4202

Y II/V II/Fe II 4177-79

Fe II/Ti II 4172-73

Ti II 4154

Zr II 4149

Fe I 4143

Si II 4128/30

Fe I/II 4118/22

Hδ 4101.74

Fe I 4084

Sr II 4077.71

Fe I 4064

Mn I 4055

Fe I 4045

Mn I 4031-36

Zr II 4024

Fe I 4002/05

Fe I 3997

Fe I/YII 3983

Ca II 3968.74

Ca II 3933.66

4700
4600
4500
4400
4300
4200
4100
4000

16 Spectral Class G

16.1 Overview

The yellow shining stars of the *G*-class have, from a spectroscopic view, a special status, because their spectra are more or less similar to that of our Sun, which is probably one of the best explored and documented. *α Centauri* in the southern sky is with *G2V* equally classified as the Sun. It shows therefore nearly the same surface temperature like our central star. In the northern sky *Muphrid (η Boo)* with *G0 IV* is classified relatively close to the Sun. Otherwise among the bright stars no further similar classified can be found. *Capella* with its two binary components of *G5IIIe* and *G0III* is already settled on the *Giant Branch* of the *HRD*. The same applies for *Sadalsuud (β Aqr)* with *G0Ib*.

Other well-known *G*-stars can only be found in the classes *G7* and later, such as *Kornephoros* (β Her), *γ Leo*, *γ Per*, *δ Boo*, *Vindemiatrix* (ε Vir).

16.2 Parameters of the Early to Late G-Class Stars

The following table shows the data exclusively for the *Main Sequence Stars* of the *G*-class, compared to the Sun (☉) and according to [701].

Mass $M/M_\odot$	Stay on main sequence [y]	Temperature photosphere [K]	Radius $R/R_\odot$	Luminosity $L/L_\odot$
1.05 − 0.9	7 bn − 15 bn	6,000 − 5,500	1.1 − 0.85	1.5 − 0.66

Striking is the percental *very low mass range*, which is covered by the *G*-class. Nevertheless, the life expectancy and luminosity of the star respond almost grotesquely sensitive to this difference. Our Sun with a surface temperature of about 5,800 K (G2V) belongs to the early *G*-class, spending some 7 billion years on the *Main Sequence*.

16.3 Spectral Characteristics of the G-Class

The Fraunhofer *H + K* lines of ionised *Ca II* become here impressively strong achieving theoretically the maximum intensity in the *late G classes*. This becomes also evident in the chart in sect. 6. In the solar spectrum (G2V) they are by far the strongest lines generated by the star itself. For *Main Sequence Stars* of the *G*-Class, the *K*-line is always slightly more intense than the *H*-line.

The *H*-Balmerseries becomes significantly weaker, so these lines are now surpassed even by various metal absorptions. Therefore they lose from here on their function as welcome orientation marks, e.g. for the calibration and line identification.The intensity of the so-called *Magnesium Triplet* (λλ 5169-83) has increased during the *F*-Class and achieves a considerable strength here, so with "*b*" it's even labeled with its own Fraunhofer letter. The *Ca I* line by λ 4227 also impressively gained intensity since the early *F* classes and becomes here a striking spectral feature also with an own Fraunhofer letter"*g*".

In general, the trend here continues by growing intensity of *neutral metals* e.g. *Fe I* and the Fraunhofer-D lines *(Na I)*. Towards the later subclasses they increasingly replace the absorption of the ionised elements. Due to the dominance of fine metal lines, the spectra become now more and more complex. Therefore, our Sun is not really a suitable object for beginners. The temperature here is sunken to such a low level that simple and robust *diatomic* molecules can survive in these stellar atmospheres. Most prominent of such features is the Fraunhofer *G*-band of the *CH molecule*, which already surpassed in the late *F*-class the intensity of the *Hγ* line. Further mentionable are also the strong *CN* and *CH*

absorption bands in the violet area, overprinting here the *H8* and *H9* Balmer lines beyond recognition. In highly resolved spectra now finer absorption bands of carbon monoxide *CO* appear. The intensity maximum of the real continuum shifts now to the green part of the visible spectrum, hence the evolution has optimised our eyes to this wavelength domain (Sun *G2V*). The graph shows the theoretical continuum for a synthetic *G5 V* standard star *(Vspec/Tools/Library)*. Highlighted with a red arrow is here the area on the violet side of the H+K Fraunhofer lines, where strong molecular *CN* and *CH* absorption bands overprint the former *H8-* and *H9*-Balmer lines.
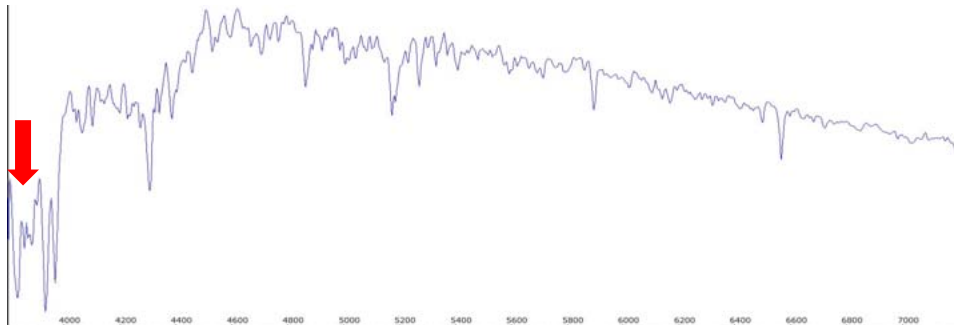
16.4 Commented Spectra

Table 40: *Muphrid* (η Boo) und *Vindemiatrix* (ε Vir)

The development of the *G*-subclasses is demonstrated here by two superposed overview spectra (200L grating) representing an early and late subtype.

Muphrid (37 ly) with *G0 IV* has already moved away from the *Main Sequence* towards the *Giant Branch* in the *HRD*. Of all naked eye visible stars in the northern sky, it's the closest "class neighbor" to the Sun (*G2V*). Its surface temperature is about 6,100 K, i.e. slightly hotter than our central star − hence the earlier classification. It's a part of a spectroscopic binary. The *B*-component however, is so small that, in contrast to *Spica*, no splitting of the spectral lines can be observed (SB1 system). *Muphrid* is classified by several sources as above average metal rich. Nevertheless, the suffix *m* is missing here in the classification.

Vindemiatrix (103 ly) with *G8 IIIab* is a late representative of the *G*-class and has already developed to the Giant stage. Its apparent rotation speed is <17km/s [505] what is usual for this class. According to [506] *Vindemiatrix* was formerly a *B*-class *Main Sequence Star*.

The comparison of these spectra demonstrates mainly the intensity loss of the *H*-Balmer lines, well visible by the *Hβ* line. The profile of *Vindemiatrix* shows also a massively shrunken *Hγ* line which is now difficult to identify, particularly besides the now dominant *G*-band (CH). Otherwise, no spectacular changes can be seen. However in highly resolved spectra, significant intensity differences of individual lines would be detectable, particularly within the blends.

Table 41 and 42:   The Sun, spectra recorded from reflected daylight.

Our central star (G2V), with a surface temperature of ca. 5,800 K, is a normal *Dwarf* on the *Main Sequence*. On these tables the Sun is documented with an overview spectrum (200L grating) and three higher-resolved profiles in the blue, green and red domain (900L grating). The Sun has a very low rotation speed of just below 2 km/s, which is usual for middle and late spectral types. The increased thickness of the convective shell generates strong magnetic fields with a considerable breaking effect on the stellar rotation. The image shows a picture in the *Hα* light by the SOHO satellite. Line identification: is based mainly on [80], [81], [59].

TABLE 40

© Richard Walker 2010/05

Hα 6562.82

C

Ca I 6362

Ca I 6161

D₁,₂

Na I 5895.92
Na I 5889.95
Ca I 5857

Muphrid η Boo
G0 IV

Vindemiatrix ε Vir
G8 IIIab

Ni I 5476.91
Fe I 5429.7
Fe I 5405

Fe I 5328

E

Fe I/Ca I 5270

Mg I 5183.60
Mg I 5172.68
Mg I 5167.32

b

Fe I/ Fe II/Ti I

Fe I 4920

Hβ 4861.33

F

Fe I/ Mn I 4754 - 58

Mg I 4703.98

Fe I/ Ti I 4668
Cr I/Fe I/Ni I 4646 - 49

Ti II/ Fe II 4550

Fe I/Ca I 4526 - 29

Fe I

Ca I/ Mn I/ Fe I 4452 - 64

Fe I 4405

Fe I 4383.55

Hγ 4340.47

CH 4299 - 4313

G

Ca I 4226.73

CH /Fe I

Fe I

Hδ 4101.74

h

Fe I/Mg I/Co I 4058

Ca II 3968.47

H

Ca II 3933.66

K

CN/CH Absorption

I=0.5

I=0.4

TABLE 41

Telluric O$_2$ A

Telluric H$_2$O

Telluric O$_2$ B

Hα 6562.82 C

Telluric O$_2$ a

Na I 5895.92 D$_1$
Na I 5889.95 D$_2$

Sun G2V

Fe I 5405
Fe I 5328
Fe I/Ca I 5270 E

Mg I 5183.60
Mg I 5172.68
Mg I 5167.32 b

Fe I/ Fe II/Ti I

Hβ 4861.33 F

Fe I/ Mn I

Mg I 4703.98
Fe I/ Ti I 4668 d

Fe I/Ca I 4526 - 29

Ca I/ Mn I/ Fe I 4452 - 64

Fe I 4383.55 e
Hγ 4340.47 f G
CH 4299 - 4313 g
Ca I 4226.73

Hδ 4101.74 h

Ca II 3968.47 H
Ca II 3933.66 K
CN/CH Absorption

I=0.3

Fe I 4768
Fe I/ Mn I 4754 - 58
Fe I 4737
Ni I 4715
Fe I/Mn I 4709
Mg I 4703.98
Fe I 4691
Fe I 4679
Fe I/ Ti I 4668 d
Fe I/Cr I 4655
Cr I/Fe I/Ni I 4646 - 49
Fe I 4638

Cr I 4580.07
Fe I,II/Ca I 4584 - 86
Ti I/Mg I 4572
Ti II 4563.76
Ti II/ Fe II 4550
Ti I,II 4534 - 36
Fe I/Ca I 4526 - 29
Ti I 4501.27
Fe I 4494.57
Fe I,II 4490
Fe I 4482.25
Ti II/Fe I 4469
Ca I/ Mn I/ Fe I 4452 - 64
Fe I 4443
Ca I 4434.96
Fe I 4415.13
Fe I 4404.75
Fe I 4383.55 e
CH/ Cr I/ Sc II 4375
CH/Cr I/ Mg I 4352 f
Hγ 4340.47
Fe I/CH 4325
CH 4299 - 4313 G
Ti I/Fe I/CH 4290 - 91
Fe I/CH 4271 -72
Cr I 4254.3
Fe I 4260.48
Fe I 4250
Fe I/CH 4236 g
Ca I 4226.73
Fe I/Sr II 4216
CH 4201
Fe I 4202.03
Fe I 4188
Fe I,II/ Ti I,II
Mg I 4167.27
Fe I 4154 - 57
Fe I 4143.87
Fe I 4132 - 34
Fe I/ V I 4128
Fe I/CO 4119
Fe I 4109.81
Hδ 4101.74 h
CO 4092.39
Fe I 4084
Sr II 4077.71
Fe I 4071.74
Fe I 4063.6
Fe I/Mg I/Co I 4058
Fe I 4045
Fe I/Mn I 4030 - 33
Fe I 4005.25
Fe I 3996-98
Fe I 3983.9
Ca II 3968.47 H
Ti I/Fe I 3956
Ca II 3933.66 K
Fe I 3922.91

I=0.2

TABLE 42

Fe I/Sc II 5658 - 59
Fe I 5624.55
Fe I 5615.65
Fe I/Ca I 5601 - 03
Fe I/Ca I/Ni I 5587 - 89
Fe I 5572.85
Fe I 5555.71
Fe I 5544
Fe I,II 5535
Mg I 5528.4
Ca I 5512.98
Fe I 5488
Ni I 5476.91
Fe I 5463
Fe I 5455.61
Fe I 5446.92
Fe I 5434.23
Fe I 5429.7
Fe I 5424.07
Fe I 5405
Fe I 5397.13
Fe I 5393.17
Fe I 5383.37
Fe I 5371.49
Cr I/Ca I 5349
Fe I 5340 - 41
Fe I 5324.19
Fe I 5328
Cr I 5297 - 98
Fe I 5282 - 84
Ca I/Cr I/Fe I 5262-64
Fe I/Ca I 5270
E
Cr I 5254.92
Fe I 5250-51
Fe I 5243
Fe I 5232.95
Fe I 5227
Fe I 5216-17
Cr I 5206 - 08
Fe I 5192
b1
Magnesium Triplet
Mg I 5183.60
Mg I 5172.68
Mg I 5167.32
b2
Fe I 5148
Fe I 5139 - 42
Fe I 5125
Fe I 5108 - 10
Fe I 5099
Fe I 5079
Fe I 5065
Fe II 5050 - 52
Fe I 5041
Fe I 5027 -28
Fe II 5018.43
Fe I/Ti I 5012 - 15
Fe I 5006
Fe I/Ni I 5000 - 03
Fe I/Ti I 4982 - 84
Fe I 4957.6
Fe I 4946.39
Fe I 4939
Fe I /Ball 4934
Fe I 4919-20
Fe I 4910
Fe I 4903.32
Fe I 4891
Fe I 4872
Hβ 4861.33
F
Ni I 4855.41
Cr II 4848.24
Fe I 4840
Mn I 4823.51
Fe I 4800
Fe I 4772.82
Mn I 4766

Hα 6562.82
C
Telluric O2
a
Sun G2V
Ca I 6169/70
Ca I 6162
Fe I 6137
Ca I 6122.22
Ca I 6102.72
Fe I 5914.16
D1
Na I 5895.92
Na I 5889.95
D2
Ca I 5857
Fe I 5753.38

© Richard Walker 2010/05

17 Spectral Class K

17.1 Overview

The stars of the orange yellow shining *K*-class includes familiar names such as *Pollux, Aldebaran, Arcturus, Hamal, Alphard*, as well as the lighter, yellow bright orange component of the famous double star *Albireo A* (K3 II).

17.2 Parameters of the Early to Late K-Class Stars

The following table shows the data exclusively for the *Main Sequence Stars* of the *K*-class, compared to the Sun (☉) and according to [701].

Mass M/M☉	Stay on main sequence [y]	Temperature photosphere [K]	Radius R/R☉	Luminosity L/L☉
0.8 – 0.6	>20bn	5,250 – 4,000	0.8 – 0.65	0.42 – 0.10

Striking is also here the percental low mass range, which is covered by this class. All *K*-class dwarfs stay longer on the *Main Sequence* than the estimated age of the universe of some 13.7 billion years. This means that in the entire universe, not a single star of this class is migrated to the *Giant Branch*! The luminosity of the *K- Main Sequence Stars* is so low that they are only visible at relatively short distances. Therefore, all above listed "highlights" of this class are located on the *Giant Branch*. These massive stars were classified much earlier during their former stay on the *Main Sequence*. Their parameters are therefore far outside of the table values above. Here they spend only a relatively short time before they explode as a *SN* or end up as *White Dwarfs*.

Only a *few real K- Main Sequence Stars are visible* with the naked eye. In the northern sky the best-known is probably the only 11 ly distant binary *61 Cygni*, with a total apparent brightness of just 4.8^m and the spectral classes *K5V* and *K7V* (see *Table 52*). The Wikipedia graphic shows the size of the two *K*-class components compared to the Sun.
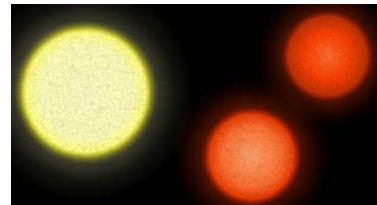
17.3 Spectral Characteristics of the K-Class

The temperature of this class is considerably lower than in the G-category, but still as high as within the solar sunspots. Correspondingly, the spectra of the early K-class look still very similar as in the whole G-category. The following chart shows in the blue short-wave domain the superimposed profiles of Pollux (blue) and Sun (green). Already Fraunhofer has noticed the striking similarity of the two spectra.
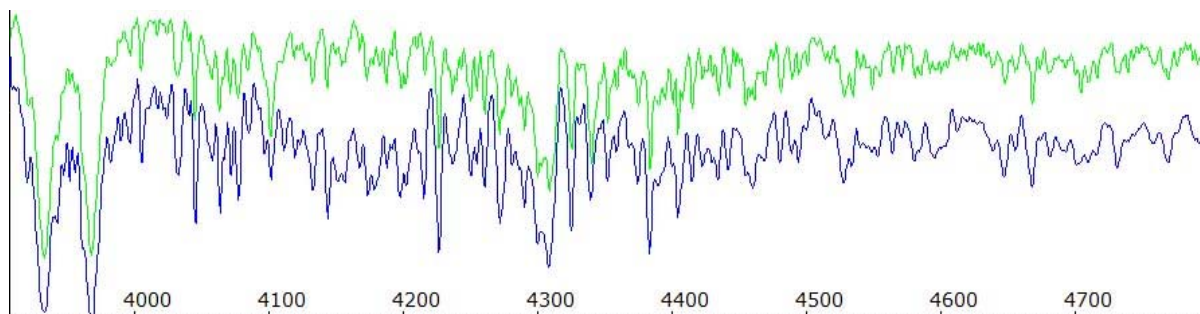
On a glance, the two profiles look indeed very similar, although *Pollux* (K0 IIIb) is a *Giant* and the *Sun* (G2V) is still a *Main Sequence Star*. Apparently the trend continues that the luminosity-related differences in the profiles become increasingly smaller towards later spectral classes.

Within the G- and early K-subclasses apparently no spectacular changes of spectral characteristics take place. Considered more in detail, several differences in the line intensity and in the shape of the continuum become visible. Now the spectral lines are mainly caused due to neutral atoms or by simple *diatomic* molecules. The intensity of the neutral metals continues to increase. The neutral calcium *Ca I* at λ 4227 has excelled the G-Band in the class *K5* (detail in Table 50 marked in red). The G-Band becomes now very faint and about at *K5* it's even splittet into several discrete lines. The H-Balmer series is now very weak and difficult to identify, except of the *Hα*- and the considerably shrunken *Hβ* line. The *Magnesium Triplet* still appears quite prominently.

In the spectra of the later K-subclasses a remarkable break occurs and the similarity to the solar spectrum gets increasingly lost. Since the class K5 and later, particularly in the long wave-(red) part of the spectrum, titanium oxide (TiO) bands appear and start to overprint the telluric H_2O and O_2 absorptions. Therefore already Father *Angelo Secchi* noticed *Aldebaran* (K5III) as a transition star for the appearance of the impressive *TiO* band spectra.

In use are only the classes *K1 - K5* and *K7*.   *K6*, *K8* and *K9* have not yet been allocated. The intensity maximum of the real continuum is shifted here into the red region of the visible spectral range. The graph shows the theoretical continuum for a synthetic *K4 III* standard star *(Vspec/Tools/Library)*.
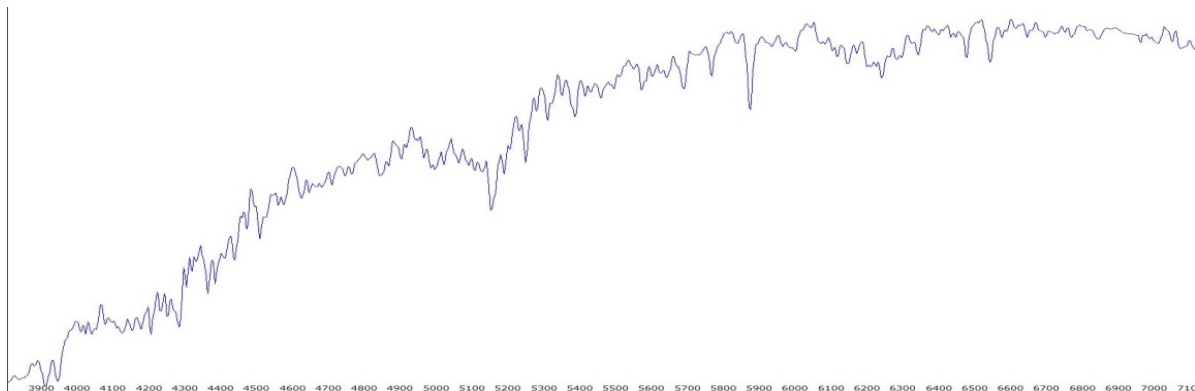
17.4 Commented Spectra

<u>Table 50:</u> *Arcturus* (α Boo) and *Alterf* (λ Leo)

The development of the *K*-subclasses is demonstrated here by two superposed overview spectra (200L grating) representing an early and late subtype.

<u>*Arcturus*</u> (37 ly), classified with *K1.5 III Fe−0.5*, is an early *K*-star and stays on the *Giant Branch* of the *HRD*. Its surface temperature is about 4,290 K. The suffix indicates a relative *underabundance* of *iron*. Compared to the Sun the Fe/H ratio of Arcturus is only about 20% [506]. The graph shows the proportions of *Arcturus* compared to the Sun. The apparent rotation speed is given in [505] with <17km/s. Like *Pollux* also the spectrum of *Arcturus* is very similar to that of the Sun. The main differences are in the intensity of individual lines, as already pointed out above.
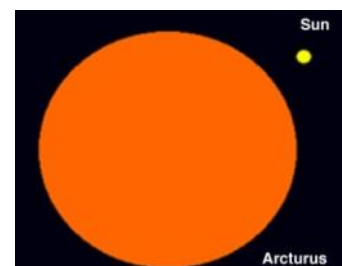
Alterf (320 ly) is a *K5 III* giant of the later *K*-class. Its surface temperature is 3,950 K, almost 340 K lower than that of *Arcturus*. The apparent rotation speed is indicated in [505] with <17 km/s. Such low values are normal for late spectral types and have no detectable effect on the spectra of this resolution.

Particularly the short-wave side of the *Alterf* profile is still dominated by discrete absorption lines, which are mostly the same, as seen in the spectra of *Pollux* and *Arcturus*. However the shape of the continuum in the yellow-red range is already similar to that of *Betelgeuse* and *Antares*, albeit much less intense. This shows the beginning influence of the molecular *TiO* absorption. At this spectral resolution, these absorption bands can be reliably identified only in the near infrared part, close to the telluric A-line which is *outside* of the chart in *Table 50*. The following detailed spectrum of *Aldebaran*, however, shows complementarily this section. With *K5 III* this star has the same spectral class like *Alterf*. The spectrum shows here clearly the absorption bands of titanium oxide *TiO* and calcium hydride *CaH*.
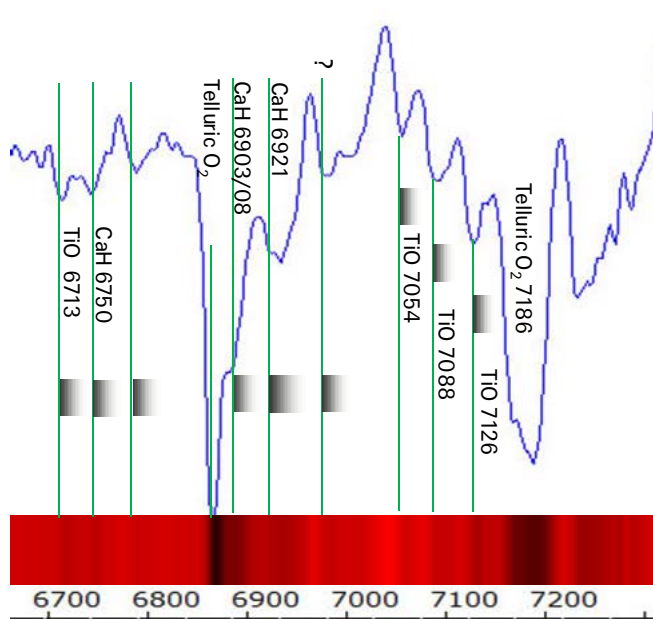
Table 51: *Pollux* (α Gem)

Pollux (34 ly) is classified as *K0 IIIb*, an early *K*-star already established on the *Giant Branch* of the *HRD*. Its surface temperature is about 4,770 K. The apparent rotation speed is given in [505] with <17km/s. On this table *Pollux* is documented with an overview spectrum (200L grating) and a higher resolved profile in the blue area (900L grating).

The line identification is based amongst others on [1], [5], [50], [52], [53], [55], [58], [59]

TABLE 50

© Richard Walker 2010/05

Arcturus α Boo
K1.5 III Fe-0.5

Alterf λ Leo
K5 III

Hα 6562.82

Fe I 6358.7

Ti I 6258-61

Ca I 6162

Na I 5895.92
Na I 5889.95
Ca I 5857

Fe I 5781/88

Fe I 5587

Fe I 5429.7
Fe I 5405
Fe I 5371.49
Fe I 5328

Cr I 5297 - 98

Fe I/Ca I 5270

Fe I 5227
Mg I 5183.60
Cr I 5204 - 08
Mg I 5172.68
Magnesium
Mg I 5167.32
Triplet

Fe I 5125
Fe I 5083
Fe I 5041
Fe I/Ti I 5002-13
Ti I 4981.73
Ba II 4934.1
Fe I 4919-20
Fe I 4889-91
Hβ 4861.33

Mn I 4783
Fe I/Mn I 4766 - 68
Mg I 4703.98
Fe I/ Ti I 4668
Cr I 4646

Fe I 4734

V I/Ca I 4580 - 94

Ti I/Fe I 4526 - 29

Fe I 4482 - 95

Ca I/ Fe I 4455 - 59
Fe I 4427-35
Fe I 4405
Fe I 4383.55
Hγ 4340.47
CH 4299 - 4313
Fe I/CH 4271 -72
Ca I 4226.73
CH /Fe I
Fe I
Fe I 4144-48

Hδ 4101.74

Fe I 4072
Fe I 4046
Ti I 4025
Ca II 3968.47
Ti I 3990 - 99
Ca II 3933.66

C

D₁
D₂

E

b

F

G
g

h

H
K

I=0.1

I=0.4

TABLE 51

Pollux β Gem
K0 IIIb

© Richard Walker 2010/05

Left panel:

Hα 6562.82 — C

Fe I 6358.7

Ca I 6161

Na I 5895.92 — D
Na I 5889.95

Fe I 5781

Fe I 5587
Mg I 5530
Ti I 5514
Ni I 5476.9
Fe I 5429.7
Fe I 5397 - 06
Fe I 5371
Fe I 5328
Cr I 5298
Fe I/Ca I 5270 — E
Fe I 5227
Magnesium Triplet Mg I 5183.60
Mg I 5172.68
Mg I 5167.32 — b
Fe I 5099
Fe I 5080
Fe I 5041
Fe I/Ti I 5002-13
Ti I 4982
Fe I 4958
Fe I 4938 - 40
Fe I 4920.5
Fe I 4889
Hβ 4861.33 — F
Mn I 4784
Fe I/Mn I 4767 - 68
Fe I 4734 - 36
Mg I 4703.98
Fe I/ Ti I 4668 — d
Cr I 4646
V I/Ca I 4580 - 86
Ti I/Fe I 4526 - 29
Fe I
Ca I/ Fe I 4455 - 59
Fe I 4427-31
Fe I 4404.75
Fe I 4383.55
Hγ 4340.47 — G
CH 4299 - 4313
Fe I/Cr I 4271 -72
Ca I 4226.73
Fe I
Fe I
Fe I 4144-48
Hδ 4101.74
Fe I/Mg I/Co I 4056-58
Ca II 3968.47 — H
Ca II 3933.66 — K

I=0.4

Right panel:

Fe I/Mn I 4767 - 68
Fe I/ Mn I 4754-58
Fe I 4734 - 36
Ni I/Ti I 4715
Mg I 4703.98
Ti I 4682
Fe I 4679
Fe I/ Ti I 4668
Ti I 4656
Cr I 4646
Cr I 4638
Fe I/Cr I 4600 - 02
V I/Ca I 4586
V I/Ca I 4580
Ti I/Mg I 4572
Cr I 4565
Ti I 4533 - 36
Ti I/Fe I 4526 - 29
Ti I/Fe I 4512 - 14
Fe I 4494.56
Fe I 4490
Fe I 4482.25
Ti II/Fe I 4469
Ca I/ Fe I 4455 - 59
Fe I 4442-48
Fe I 4427-31
Fe I 4415.13
Fe I 4404.75
Fe I 4383.55
Fe I 4375
Cr I 4359.6
Fe I/Cr 4352-53
Hγ 4340.47
Fe I 4325
CH 4299 - 4313 — G
Ti I/Fe I 4290 -96
Fe I/Cr I 4271 -72
Fe I 4260.48
Cr I 4255.5
Fe I 4250
Fe I/CH 4234-36
Ca I 4226.73
Sr II 4215.52
Fe I 4202.03
CN 4179 - 97
Fe I 4185
Fe I 4171-75
Mg I 4167.27
Fe I 4154 - 57
Fe I 4144-48
Fe I 4132 - 34
Fe I/Co I 4119
V I 4111.77
Hδ 4101.74
Fe I/Mn I 4084
Fe I/Sr II 4075-78
Fe I 4071.74
Fe I 4063.6
Fe I/Mg I/Co 4056-58
Fe I 4045.81
Mn I 4030 - 36
Ti I/II 4025
Fe I 4005.25
Fe I/Ti I 3998
Ti I 3989.76
Fe I 3983.9
Ca II 3968.47
Fe I 3956.68
Ca II 3933.66

I=0.2

<u>Table 52:</u> Luminosity effects on spectra of the late *K*-class: *Alsciaukat (α Lyncis)* and *61 Cygni B*.

<u>*61 Cygni B*</u> (11 ly) is the weaker of two binary components. With *K7 V* it's classified as an ordinary *Dwarf* on the *Main Sequence*. The surface temperature is some 4,120 K, its apparent rotation speed is <2km/sec. The two components belong to the few true *Main SequenceStars* of the *K*-class which are spectroscopically accessible to moderate sized telescopes.

<u>*Alsciaukat*</u> (220 ly): This star with the jaw-breaking, Arabic name is classified with *K7 III*, and thus a *Normal Giant*. Its surface temperature is about 3,860 K. Its apparent rotation speed could not be found. Its slight variability suggests that it stands just before a long-period, Mira-type variable stage [506].

The comparison of the two equally normalised spectra shows in this section a similar profile shape for the different luminosity classes. In each section, however, clear differences and even different lines are visible. The spectrum of *Alsciaukat* shows at this resolution (according to BSA) clearly the splitting of the former Fraunhofer *G* -band into *three* discrete absorption lines: *Ti I* (λλ 4301 and 4314) and *Fe I* (λ 4308).

<u>Table 53:</u> *Aldebaran* (α Tau)

Complementary to *Table 52* some higher-resolved detail spectra of the *K*-star Aldebaran (66 Lj) in the green and red region are added here (900L grating). *Aldebaran* with *K5 III* represents the later *K*-class and is established on the *Giant Branch* of the *HRD*. Its surface temperature is about 4,010 K. The apparent rotation speed is given in [505] with <17km/s. The graphic shows the proportions of *Aldebaran* compared to the Sun.
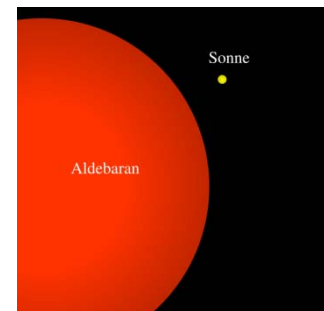
TABLE 52

Effect of the luminosity on spectra of the K-class

Alsciaukat α Lyncis
K7 III ab
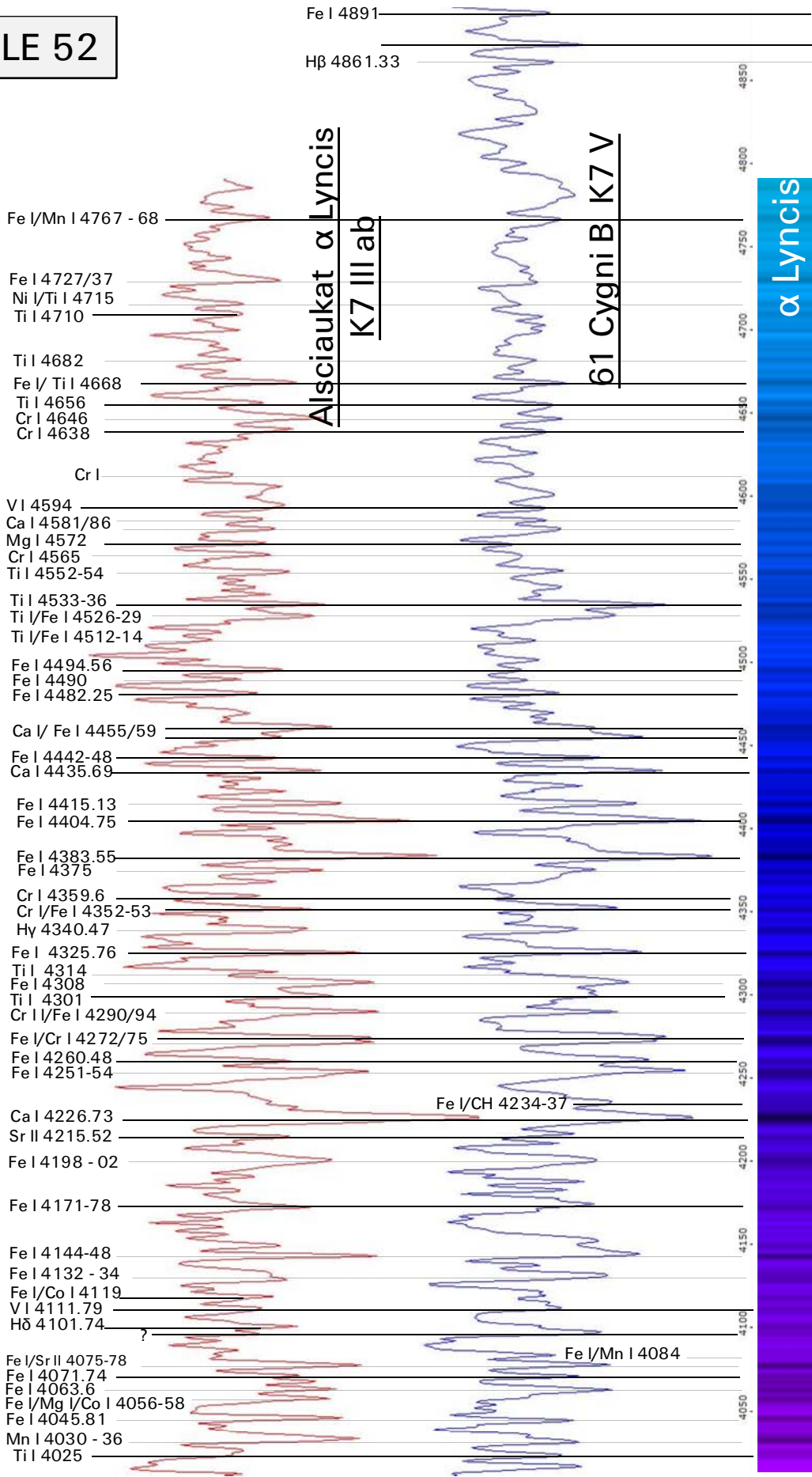
61 Cygni B K7 V

α Lyncis

61 Cygni B

© Richard Walker 2010/05

Fe I 4891
Hβ 4861.33

Fe I/Mn I 4767 - 68

Fe I 4727/37
Ni I/Ti I 4715
Ti I 4710

Ti I 4682
Fe I/ Ti I 4668
Ti I 4656
Cr I 4646
Cr I 4638

Cr I

V I 4594
Ca I 4581/86
Mg I 4572
Cr I 4565
Ti I 4552-54

Ti I 4533-36
Ti I/Fe I 4526-29
Ti I/Fe I 4512-14

Fe I 4494.56
Fe I 4490
Fe I 4482.25

Ca I/ Fe I 4455/59

Fe I 4442-48
Ca I 4435.69

Fe I 4415.13
Fe I 4404.75

Fe I 4383.55
Fe I 4375

Cr I 4359.6
Cr I/Fe I 4352-53
Hγ 4340.47

Fe I 4325.76
Ti I 4314
Fe I 4308
Ti I 4301
Cr II/Fe I 4290/94

Fe I/Cr I 4272/75

Fe I 4260.48
Fe I 4251-54

Ca I 4226.73

Fe I/CH 4234-37

Sr II 4215.52

Fe I 4198 - 02

Fe I 4171-78

Fe I 4144-48
Fe I 4132 - 34
Fe I/Co I 4119
V I 4111.79
Hδ 4101.74
?

Fe I/Sr II 4075-78

Fe I/Mn I 4084

Fe I 4071.74
Fe I 4063.6
Fe I/Mg I/Co I 4056-58
Fe I 4045.81
Mn I 4030 - 36
Ti I 4025

4850
4800
4750
4700
4650
4600
4550
4500
4450
4400
4350
4300
4250
4200
4150
4100
4050

TABLE 53

Aldebaran α Tau

K5 III

Na I 5895.92
Na I 5889.95

Cr I 5791
Fe I 5781

Fe I 5763
Fe I 5753.38

V I 5727

Fe I 5698

Fe I/Sc II 5658-59

Fe I 5624.55
Fe I 5615.65
Fe I/Ca I 5601-03
Fe I/Ca I/Ni I 5587-89
Fe I 5572.85

Fe I 5544/47
Mg I 5528.4

Ti I 5514
Fe I 5507
Fe I 5501
Fe I 5497
Fe I 5481
Ni I 5476.91

Fe I 5455.61
Fe I 5446.92
Fe I 5434
Fe I 5429.7

Cr I/Fe I 5410
Fe I 5405
Fe I 5397.13
Fe I 5390

Fe I 5371.49

Cr I 5346/48
Fe I 5340-41
Fe I 5328
Fe I 5324.19

Fe I 5303
Fe I 5307
Cr I 5298
Fe I 5282-84
Fe I/Ca I 5270
Fe I/Ca I/Cr I 5262-64
Fe I 5255
Fe I/Cr I 5247
Fe I 5250
Fe I 5242
Fe I 5232.95
Fe I 5227

Cr I 5204/08
Fe I 5192
Mg I 5183.60
Mg I 5172.68

Magnesium
Triplet

5850
5800
5750
5700
5650
5600
5550
5500
5450
5400
5350
5300
5250
5200

Hα 6562.82

Ti I 6258/59/61
V I 6243

Ca I 6169/70
Ca I 6162

Ca I 6137
Ca I 6122.22
Ca I 6102.72

Na I 5895.92
Na I 5889.95

6650
6600
6550
6500
6450
6400
6350
6300
6250
6200
6150
6100
6050
6000
5950
5900

© Richard Walker 2010/05

18 Spectral Class M

18.1 Overview

Some of the orange-red shining stars of the *M*-class are well-known names such as *Betelgeuse, Antares, Mirach (β And), Scheat (β Peg), Ras Algheti (α Her), Menkar (α Cet), Tejat Posterior (μ Gem)*. Some late types of this class are long period variables such as *Mira* (M7IIIe).

18.2 Parameters of the Early to Late M-Class Stars

The following table shows the data exclusively for the *Main Sequence Stars* of the *M*-class, compared to the Sun (⊙) and according to [701].

Mass M/M⊙	Stay on main sequence [y]	Temperature photosphere [K]	Radius R/R⊙	Luminosity L/L⊙
0.5 − 0.08	>100bn	3,850 − 2,600	0.63 − 0.17	0.08 − 0.001

Striking is here the huge percental increase of the covered mass range compared to the earlier classes *A, F, G, K*. The "late half" of this class already touches the range limit of the *Brown Dwarfs*, which are seperately classified with *L, T* and *Y* (not yet be treated here). As the *K*- also the *M*-Dwarfs stay longer on the *Main Sequence* than the estimated age of the universe of some 13.7 billion years. This means that in the entire universe, not a single star of the *M*-class is migrated to the *Giant Branch* in the *HRD*! All with the naked eye visible *M*-type stars are former class *B* to *G Main Sequence Stars* which spend here only a relatively short time until the end of their *Giant Stage*. Their parameters are therefore far outside of the table values above.

With the naked eye, <u>no real M-type Main Sequence Stars are visible</u>, although they provide 76% of the Sun's near neighbors! The most famous and apparently "brightest" representative is in the southern sky *Proxima Centauri* with the spectral class *M5 Ve*. With a distance of 4.22 ly it's the very nearest neighbor to the Sun, but reaching an apparent magnitude of only 11^m! Therefore, it was discovered very late in 1915. The graphic (Wikipedia) shows the proportion of *Proxima Centauri* compared to the *Sun*. Its diameter was determined with the *HST* to about 200,000 km. His life expectancy on the *Main Sequence* is estimated to some 4 trillion years! Whether our universe then still exists − in whatever form − must be answered by cosmological models.

18.3 Spectral Characteristics of the M-Class

The Fraunhofer *H + K* lines remain striking in the entire *M*-class. In addition to the *Hα* line neutral calcium *Ca I* at λ 4227 and the sodium double line at about λλ 5890/95, are the dominant *discrete* absorptions, which are still visible at this resolution. The once prominent *G*-band breaks now up in at least three discrete lines (BSA). The main features here are undoubtedly the huge absorption bands of *titanium oxide TiO*. Their intensity rises significantly towards the late subclasses, overprinting now thousands of neutral, atomic absorption lines which would otherwise visible here [1]. Although they show up already in the late *K*-classes, they form here the unmistakable "Brand" of the *M*-category. Much less frequent and with smaller intensity we find here a few absorption bands of *CaH* (calcium hydride) and *MgH* molecules (magnesium hydride). In the late *M*-subclasses the lower

temperature allows even the formation of further *diatomic* molecules like *vanadium oxide* (*VO*) and *molecular hydrogen H$_2$*.

The wavelengths of the *absorption bands* are defined by the "*most distinct edges*" the so called *band heads* of the profile. As a result of this characteristic, sawtooth-shaped curve, these *edges* are much more diffuse than discrete absorption lines, which show in theory approximately a Gaussian bell shape. The wavelength values for the individual bands can sometimes vary, depending on the source, up to 2 Å! These absorption bands are therefore totally inappropriate for a precise calibration of the spectrum, based on known lines. Only the calibration with the lamp can meet here reasonable standards.

The intensity maximum of the real continuum is shifted here into the infrared range of the spectrum. Therefore the telluric *H$_2$O* and *O$_2$* absorptions in the red range of the spectrum are almost completely overprinted by the stellar molecular bands. The graph shows the theoretical continuum for a synthetic *M5 III* star *(Vspec/Tools/Library)*.

Due to the specific radiation characteristics, influenced by the massive gaps in the continuum, the M class stars are considerably far away from an ideal black body radiator.
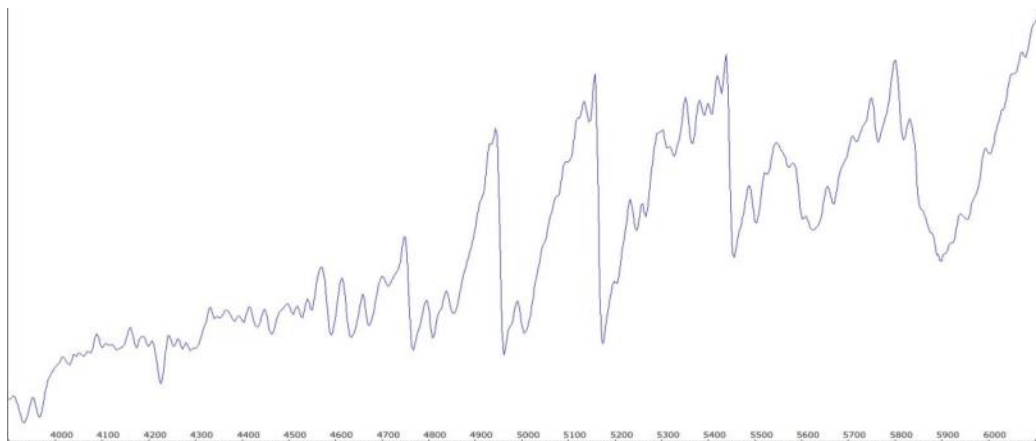
18.4 Commented Spectra

Table 60: *Antares (α Sco)* and *Ras Algethi (α Her)*

The development of the *M*-subclasses is demonstrated here by two superposed overview spectra (200L grating) representing an early and late subtype.

Antares (450 ly) is a *Supergiant* of the early *M*-Class with *M1.5 Iab* and the dominant component of a binary star system. Its surface temperature is about 3,600 K. The apparent rotation speed is given in [505] with <20 km/s. The graphic shows the proportions of *Antares*, compared to *Arcturus* and the Sun.

Ras Algethi (400 ly) is a multiple star system. The spectrum is dominated by the *Supergiant* classified as *M5 II* and represents a later M-Type. As expected its surface temperature of 3,300 K is lower than by the earlier classified Antares. *Ras Algethi* is smaller than *Antares*, but also surrounded by a cloud of gas and dust.
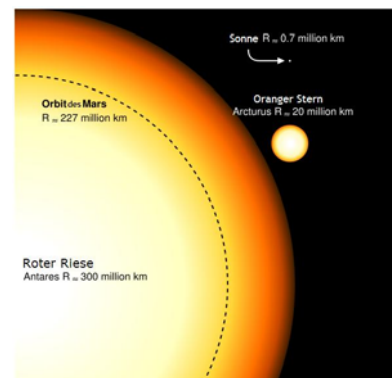
The line identification is based amongst others on [1], [5], [50], [52], [53], [55], [58], [59]

Due to lack of further detailed information to spectral features within the *M*-Class, for the time being no higher-resolved spectra are attached and commented here.

TABLE 60

Telluric O₂

CaH 6903/08/21
Telluric O₂
CaH 6750

Hα 6562.82
Ba II/Ti I/Fe I/Ca I

CaH 6390

Antares α Sco
M1.5 Iab-Ib

Na I 5895.92
Na I 5889.95

Ni I 5476.91
Fe I 5429.7
Fe I 5405
Fe I 5371.49
Fe I 5328
Cr I 5297 - 98
Fe I/Ca I 5270
Cr I 5204 - 08
Mg I 5167/72/84

Magnesium
Triplet

Fe I/Cr I 5125
Fe I 5080
Fe I/Ti I 5012-13
Fe I 5002 - 08

Ba II 4934.1
Fe I 4920.5
Hβ 4861.33
MgH 4780
Fe I/Mn I 4767 - 68

Fe I/ Ti I 4668
Cr I/Fe I/Ni I 4646-49

V I/Ca I 4580 - 94
Ti I/Fe I/Cr I 4526 - 29

Ca I/ Fe I 4455 - 59

Fe I 4383.55
Hγ 4340.47
Fe I/Ti I 4301- 4314
Fe I 4251 - 54
Ca I 4226.73
Fe I 4198 - 02
Fe I 4171 - 78

Fe I 4072
Fe I 4046
Ti I 4025

Ca II 3968.47
Ca II 3933.66

Fe I/V I 4405

K H

I=0.4

TiO 7126
TiO 7088
TiO 7054

TiO 6815
TiO 6782
TiO 6715
TiO 6681
TiO 6651

TiO 6569

TiO 6478

TiO 6384
TiO 6358

TiO 6268

TiO 6180
TiO 6159

TiO 5998
TiO 5968

TiO 5847
TiO 5814
TiO 5760

TiO 5668
TiO 5597/03

TiO 5497
TiO 5448/51

TiO 5359
TiO 5308

TiO 5240

TiO 5167

Ras Algethi α Her
M5 Ib-II

TiO 5020
TiO 5003
TiO 4955

TiO 4847
TiO 4804
TiO 4761-63

TiO 4704
TiO 4668
TiO 4626
TiO 4584

TiO 4548
TiO 4506
TiO 4462

TiO 4422

I=0.0

19 Spectral Sequence on the AGB

19.1 Evolution of the Stars on the Asymptotic Giant Branch (AGB)

The following simplified presented sequence is applicable for stars with 1 to 8, depending on the source, even up to about 10 solar masses.

Red Giant Branch RGB

After leaving the *Main Sequence* the star moves in the *HRD* first up to the right on the *Red Giant Branch* (RGB). In this phase, the hydrogen fusion zone grows outwards on a shell around the increasing helium core. Thus the radius and the luminosity of the star dramatically increase, while the density and temperature of the atmosphere substantially decrease.

Horizontal Branch HB

The so-called *helium flash* stops abruptly this ascent on the *RGB*. This event is triggered by the nuclear ignition of the helium core, which was formed during the *RGB* phase. From now on by helium fusion and other highly complex nuclear processes, carbon and oxygen is formed in the core of the star. As a result, the star first moves somewhat to the left and down on the *Horizontal Branch (HB)*.

Asymptotic Giant Branch AGB

In a later phase, the helium begins to "burn" within a shell around the core of carbon and oxygen and in addition triggers now the hydrogen fusion in a further outer shell of the star. This multiple or alternating "shell burning process" causes now the rise of the expanding and unstable star along the *AGB*. At one solar mass the stellar radius reaches now some 1.5 AU and the luminosity is about 10,000 times that of the former *Main Sequence Star*.

Post AGB Phase

In the final stage these stars eject their outer shells as a *Planetary Nebula* (see sect. 24), which is excited to the emission of light by the remaining, extremely hot core. These objects initially show similar spectra like *Wolf Rayet Stars* (sect. 8). Later on, they cool down and end as *White Dwarfs* on the stellar "cemetery" in the lower part of the *HRD*. The following chart (excerpt from the *HRD*) shows schematically the *Post-Main Sequence* Evolution for stars of about 1, 5 and 10 solar masses.
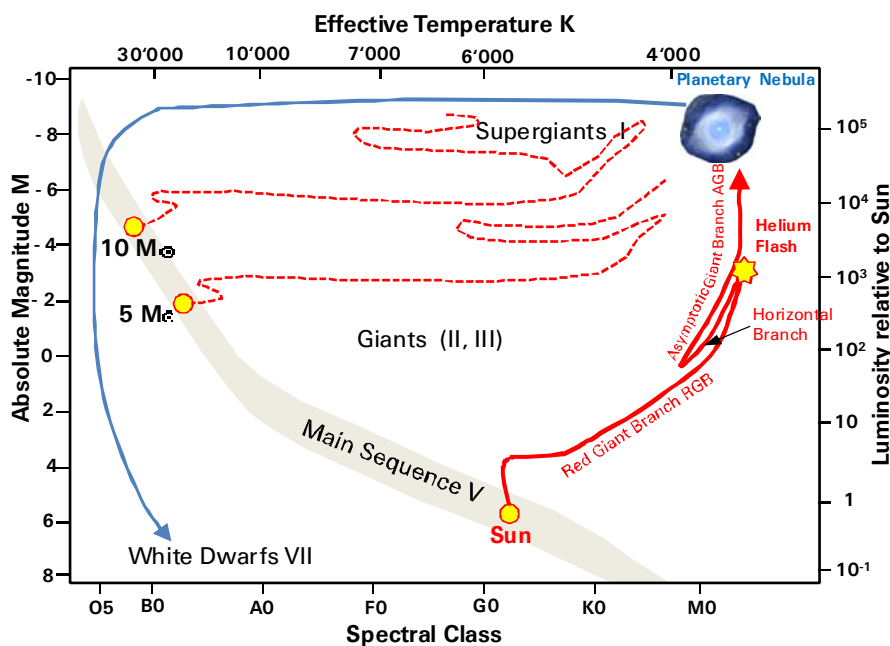
19.2 The Spectral Sequence of the Mira Variables on the AGB

This sequence consists of stars in their unstable *AGB* phase, limited to the range of about 1 − 2 solar masses and the spectral class *M* as well as to some late *K*-types. This category is for amateur astronomers not only interesting for photometric monitoring, but also in terms of spectral analysis. The astrophysical context is still not fully understood and shown here strongly simplified, mainly based on [2].

Once arrived on the *AGB* the star becomes unstable, as a result of the above mentioned complex fusion processes. It starts now pulsating and pushing off a lot of material. Therefore most but not all of these stars, show now the behavior of long-period *Mira Variables*. Current theories postulate at this stage strong, so-called *Thermal Pulses*, which trigger deep convective *"dredge up"* processes inside the star. As a result, carbon, and products of the nuclear *S*−process, is conveyed to the stellar surface (e.g. barium, lithium, zirconium, technetium, etc.). During its ascent on the *AGB* the star passes the following sequence of spectral classes (schematic diagram):
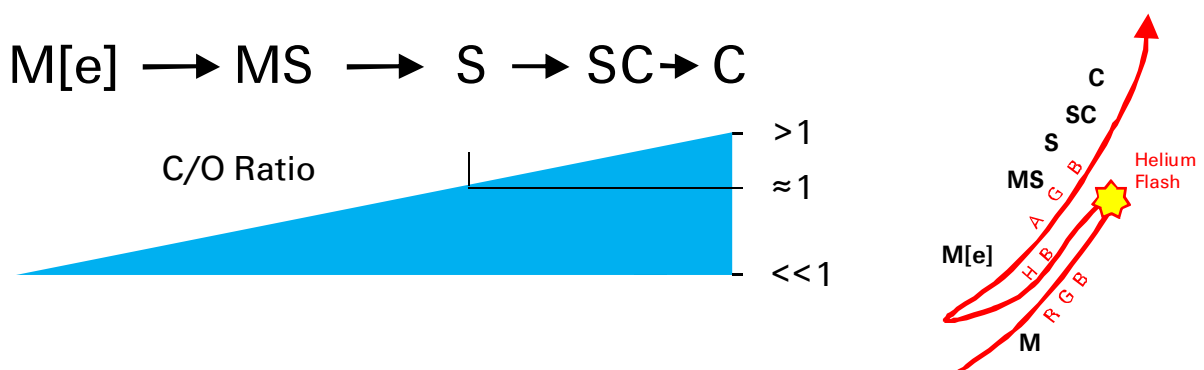
On this course the oxygen in the stellar atmosphere is not only bound by the formation of metal oxides (eg *TiO, ZrO, YO*). The rest of it combines now with the rapidly increasing carbon mainly to *CO* molecules [1]. Thus the *oxygen content* is now continuously reduced. It's expressed in this context as ratio of carbon to oxygene C/O.

In the M(e) phase, at the "bottom" of the *AGB*, the stellar atmosphere is still *oxygen-rich* $C/O \approx 0.5$. Here *TiO* absorptions still dominate the profile, usually associated with individual atomic emission lines. Therefore I added the "index" (e) to this class to distinguish it clearly from the relatively stable, only hydrogen "burning" giants of spectral types *K* to *M* on the *RGB*.

Within the MS to S classes the stellar atmosphere increasingly shows an oxygen deficiency. Therefore absorption of diatomic zirconiumoxide *(ZrO)* displaces now more and more the former dominating titanoxide bands *(TiO)*. In the area of spectral class S, the ratio becomes $C/O \approx 1$ and therefore no more unbound oxygen exists in the stellar atmosphere.

Above the spectral class S becomes $C/O > 1$. This creates a *carbon excess*, which accumulutates in a circumstellar cloud. This dominates now impressively the star's spectrum. Thus, in the intermediate SC -class, and increasingly in the following C- Class moderately high resolved spectra only show absorptions of diatomic carbon molecules (*CH*, *CN*, and C_2). Increasingly here also show up atomic lines of *S*−process products, but also impressive absorptions of *Na I*.

Once arrived at the top of the *AGB* the star ejects due to intense thermal pulses its outer shell as a photogenic *Planetary Nebula.*

20 M(e) Stars on the AGB

20.1 Overview

The unstable M(e) stars on the AGB still have an oxygen-rich atmosphere ($C/O < 1$) and are usually long-period variable of type *LPV (Long Period Variable)* or *Mira Variable*. The period of the brightness variation is in the order of about 100 to 1000 days. Prototype of this class is *Mira (o Ceti)*. This instability leads to shock waves in the stellar atmosphere, which expands and contracts by the rhythm of the brightness variations (radius up to a factor 2!).

As a result of this spectacular process the star loses continuously matter, as documented by recent photographs of *Mira*. The star produces on its way through the galaxy an impressive trace of stellar material, which can be seen in the ultraviolet region on a length of about 13 ly. This spectacular image was taken with GALEX (Galaxy Evolution Explorer, NASA), recorded in August 2008: http://www.nasa.gov/mission_pages/galex/.
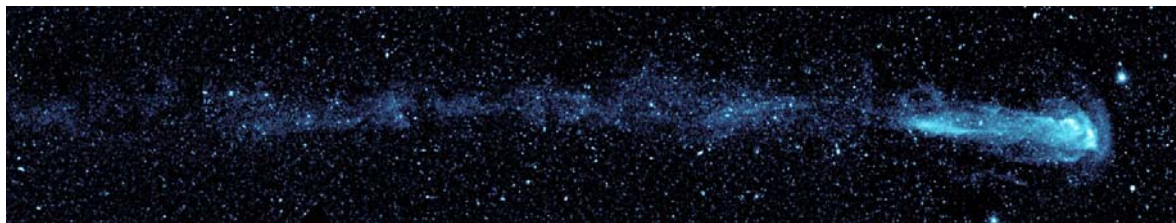

20.2 Spectral Characteristics of the M(e) Stars on the AGB

Parallel to the "pulsations" of the stellar atmosphere, emission lines of variable intensity appear in the spectrum, predominantely the short wave *H*−Balmerlines on the "blue side" of *Hγ*. The maximum intensity mostly shows *Hδ* (see Table 63). According to the *Balmer decrement* the *Hα, Hβ* and *Hγ* emissions are in fact much more intensive. But higly intense *TiO* absorption bands overprint here completely *Hα* and *Hβ* and strongly diminish *Hγ*. According to [1] this is evidence that the emission lines are formed in much deeper layers of the stellar atmosphere as the titanium oxide absorptions. The spectral type of the star itself is often variable within the range of decimal subclasses. Apart from the emission lines no further differences to a normal *M*- star can be detected in a moderately resolved spectrum.

20.3 Commented Spectra

Table 63: A montage of two overview spectra (200L grating). Comparison of the *M(e)* star *Mira, (o Ceti, M7 IIIe, alternatively M5e−9e [505])* and the ordinary *M-Type* star *Ras Algethi (α Her, M5 II)*, which is still located on the *RGB (*see *Table 60).*

Mira A, probably one of the most popular variables, forms the dominant component in a binary system with *Mira B (VZ Ceti).* It shows an impressive brightness variation $V_{var} \approx 3^m - 10^m$, with a period of about 331 days (LPV). In some cases it becomes much brighter than 2.0^m. Its spectacular variability was discovered in 1639 by *Holwarda*. The *HST* image (NASA) shows *Mira* in a phase with a slightly oval shape. Thanks to its diameter of > 500M km, the star (by interferometry) can still be recorded as a disc at a distance of about 300 ly!
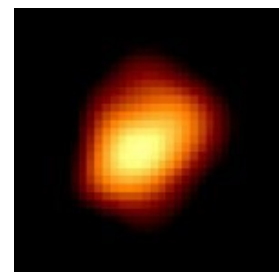
Apart from some differences in the intensity of *TiO* bands, the emission lines *Hδ* and *Hγ* are essentially the only spectral differences that distinguish the *AGB* star *Mira* from the *RGB* star *Ras Algethi*. *Hδ* is here in fact significantly more intensive than *Hγ* what was already explained above. The profile was recorded December 13, 2010 (JD 2455544.46), some 60 days after the maximum brightness, V ≈ 4.1m (AAVSO).

TABLE 63

Mira

© Richard Walker 2011/03

TiO 7126
TiO 7088
TiO 7054

Telluric O$_2$
TiO 6815
TiO 6782
TiO 6715
TiO 6681
TiO 6651
TiO 6569
TiO 6478
TiO 6384
TiO 6358
TiO 6268
TiO 6180
TiO 6159
TiO 5998
TiO 5968
TiO 5847
TiO 5814
TiO 5760
TiO 5668
TiO 5597/03
TiO 5497
TiO 5448/51
TiO 5359
TiO 5308
TiO 5240
TiO 5167
TiO 5003/20
TiO 4955
TiO 4847
TiO 4804
TiO 4761-63
TiO 4704
TiO 4668
TiO 4626
TiO 4584
TiO 4548
TiO 4506
TiO 4462
TiO 4422
Hγ 4340.47
Ca I 4226.73
Hδ 4101.74
Ca II 3968.47
Ca II 3933.66

Ras Algethi α Her
M5 Ib-II

Mira o Ceti
M7 IIIe, M5e – M9e

21 Spectral Class S on the AGB

21.1 Overview and Spectral Characteristics

The spectrum of a star is influenced on the further ascent along the *AGB* by:

− the *increase of carbon* in the stellar atmosphere
− the consequential *decline of the oxygen content*
− "dreged up" *S−process products* (eg, zirconium, lithium, etc.)

This development changes at first the spectral type *M(e)* in to the intermediate class *MS*. If at all, then only small differences are detectable here with moderate resolution spectrographs. However at higher resolution appear first signs of zirconium oxide (ZrO). within the still dominant *titanium oxide* bands. The share of *ZrO* increases now continuously up to the extreme types of the spectral class *S*, where *ZrO* almost entirely replaces the *TiO* absorption. In [2] this effect is explained with the higher affinity of *ZrO* to oxygen, and the greater temperature resistance of this molecule. The dissociation energy of *ZrO*, (and also of *LaO* and *YO*), is **>**7eV, in contrast to *TiO* **<**7eV.

21.2 The Boeshaar − Keenan S−Classification System

The spectral class *S* is specified with the following format. It forms a temperature sequence, analog to the normal *M*-giants on the *RGB*. Since all *S*-stars are already giants, a luminosity class is usually not indicated.

$$\text{S}\textcolor{red}{\text{X}}/\textcolor{blue}{\text{n}}\text{(e)}$$

X: stands for the temperature sequence of the *M*-class from 1 − 9 (some 3,800−2,500 K).
n: *C/O index* on a scale of 1 − 10, estimated from the relative intensities of *TiO* and *ZrO*. The *C/O ratio* itself can not be obtained directly from the spectrum. It can only be estimated by means of the *C/O index* (table values according to *Scalo, Ross*)
(e) indicates that the spectrum sometimes shows emission lines.

This classification can be supplemented with characteristic elements/molecules showing up in the spectrum. The following table shows the spectral class *S* between the intermediate classes *MS* an *SC*, based on [140] and [2], where also detailed classification details can be found.

Spectraltype with *C/O Index*	Criteria for the *C/O Index*	~ *C/O* Ratio	Comment
MXS	*TiO* still dominates, some signs for *ZrO* bands are recognisable in higly resolved spectra		Transition class from *M(e)* to *S*
SX/1	*TiO* >> *ZrO, YO*	< 0.95	Spectralclass *S*
SX/2	*TiO* > *ZrO*	0.95	
SX/3	*TiO* ≈ *ZrO, YO* intensive	0.96	
SX/4	*ZrO* > *TiO*	0.97	
SX/5	*ZrO* >> *TiO*	0.97	
SX/6	*ZrO* very intensive, no *TiO* recognizable	0.98	
SX/7 = SC X/7	*ZrO* weaker, intensive *Na* lines	0.99	
SC X/8	No *ZrO* recognizable, intensive *Na* lines	1.00	Transition class from the *S*− to the carbon stars
SC X/9	Very intensive Na lines, C_2 very weak	1.02	
SC X/10 = C-N	Intensive Na lines, C_2 weak	1.1	

21.3 „Intrinsic" and „Extrinsic" („Symbiotic") S-Stars

According to [2], this classification system does not explain the whole *S*−Class and carbon stars. Many *non*− or only *slightly variable S*−stars, which lie often outside the AGB, show *no*

short-living and unstable ^{99}Tc (technetium) isotopes in the spectrum – hence called *"Tc - poor "*. This affects at least 40% of all registered *MS* and *S* types [160]. A recent, still debated scenario postulates a mass transfer, which brings the *ZrO* from a nearby companion star in to the stellar atmosphere. Therefore these special types are also called *"extrinsic"* or *"symbiotic"*. Textbook example is the relatively bright and only slightly variable (V ≈ 5.2^m) *BD Camelopardalis (Table 66a)*. In fact, such objects are relatively hot and form components of close binary systems. These properties, as well as a low variability and the absence of ^{99}Tc in the spectrum, are currently the main distinguishing characteristics of an *"extrinsic"* *S*-class star. In such cases the spectral classification is sometimes supplemented by *"symbiotic"* or *"extrinsic"*.

In contrast, the *S*–Type stars on the *AGB* show *thermal pulses*, are usually *highly variable* and classified as *"Tc - rich"* or *"intrinsic"*. Intrinsic means, that the elements and molecules, responsible for the *S*-classification, are produced by the star itself.

21.4 Hints for the Observation of *S*–Class Stars

On the *AGB* the stellar atmospheres meet the condition $C/O \approx 1$ only during a very short period. Therefore *S*–classified stars are very rare. For our galaxy, only some 1300 are registered [160]. In the amateur literature unfortunately *Chi Cygni* is very often proposed as a "showcase object" of the *S*–Class stars, whose brightness can reach up to 3.3^m. Regrettably it has a very low *C/O* index, like all other bright *S*–stars. The disappointment is respectively great for beginners, when in low-resolution spectra, if at all, only weak signs of zirconium can be seen. But there are some members with a high *C/O* index, reaching a maximum brightness up to some 7^m. At this stage they become recordable with slit spectrographs at guided telescopes of medium aperture, including *R Cygni* HD185456 and *R Geminorum* HD 53791 – further also *R Lyncis* HD 51610, *U Cassiopeiae* HD 4350, *S Ursae Maioris* HD 110813 and *V Cancri* 70276. For the observation planning, the current brightness level for most of the variable *S* stars is displayed by *AAVSO* [507].

21.5 Commented Spectra

<u>Table 65:</u> For comparison, a montage of two broadband spectra (200L grating) is presented. *M(e)* star *Mira (o ceti)* (see *Table 63*) and the *S*–class star *R Cygni (S4/6e)* with a very high *C/O Index = 6*. The comparison of the two profiles shows impressively the transition from the spectral type *M(e),* dominated by *TiO* bands to an extreme *S*–type star which shows *ZrO* absorptions only.

<u>R Cygni</u>, HD185456 (distance?), is strongly variable, according to *AAVSO*: V$_{var}$ ≈ 7.5^m – 13.9^m, and shows a period of about 429 days *(LPV)*. The maximal and minimal brightness may differ considerably, compared between the individual periods. In the oxygen-rich *Mira* atmosphere the prominent *TiO bands* are still dominating. In the profile of *R Cygni,* due to the strong lack of oxygen, only impressive *ZrO* absorption bands, atomic lines of *S*–process elements, as well as a strong *Na I* absorption can be seen. Following a number of other physical effects (see [2]), the outer layers of the atmosphere become more "transparent" by the extreme *S*–Class. Therefore all emission lines of the *H-Balmer series* show up here – *Hα* however, significantly dampend, compared to the law of the Balmer decrement. In the *Mira* profile only *Hα* and *Hβ* are in emission. The identification of the ^{99}Tc *I* lines (marker for the "intrinsic" type) at λλ 4238, 4262 and 4297 is uncertain at this low resolution. The profile was taken on April 3, 2011 (JD 2455654.56) in the region of the maximum brightness V ≈ 7.5m (AAVSO) with the Celestron C8, 4x240 seconds. The detailed *ZrO* line identification was chiefly enabled by [141] - in second priority by [2].

TABLE 65

©Richard Walker 2011/03

Fe ?

TiO 7126
TiO 7088
TiO 7054

ZrO 6988
ZrO 6933

Telluric O$_2$
TiO 6815
TiO 6782
TiO 6715
TiO 6681
TiO 6651

ZrO 6778/87
ZrO 6743

TiO 6569

Hα 6562.82

TiO 6478

VO 6532
ZrO 6475/81/94
ZrO 6447/55

ZrO 6412/18

TiO 6384
TiO 6358

ZrO 6378/84
ZrO 6350

TiO 6268

ZrO 6294
ZrO 6261
ZrO 6229
ZrO 6201
ZrO 6154
ZrO 6132/36

TiO 6180
TiO 6159

ZrO 6054/63
ZrO 6023/27
ZrO 5983

TiO 5998
TiO 5968

Na I 5890/96

TiO 5847
TiO 5814

ZrO 5839/49

ZrO 5860/70

TiO 5760

ZrO 5748/54

ZrO 5718/24

TiO 5668
TiO 5597/03

ZrO 5629
ZrO 5593
ZrO 5545/51
ZrO 5515

ZrO 5539
ZrO 5485/90

TiO 5497
TiO 5448/51

ZrO 5456/63

ZrO 5432/37

ZrO 5404/07
ZrO 5375/79
ZrO 5332
ZrO 5298/5305

TiO 5359
TiO 5308

TiO 5240

ZrO 5246

TiO 5167

TiO 5003/20
TiO 4955

MgO 5007

Hβ 4861.33

TiO 4847
TiO 4804
TiO 4761-63

ZrO 4827
ZrO 4792
ZrO 4737

TiO 4704
TiO 4668
TiO 4626
TiO 4584
TiO 4548
TiO 4506
TiO 4462
TiO 4422

ZrO 4641
ZrO 4620
Sr I 4607
Ba II 4554

ZrO 4471

Hγ 4340.47

Tc I ?
Tc I ?

Ca I 4226.73

Hδ 4101.74

Mira o Ceti
M5e – M9e

R Cygni
S4/6e

7200
7000
6800
6600
6400
6200
6000
5800
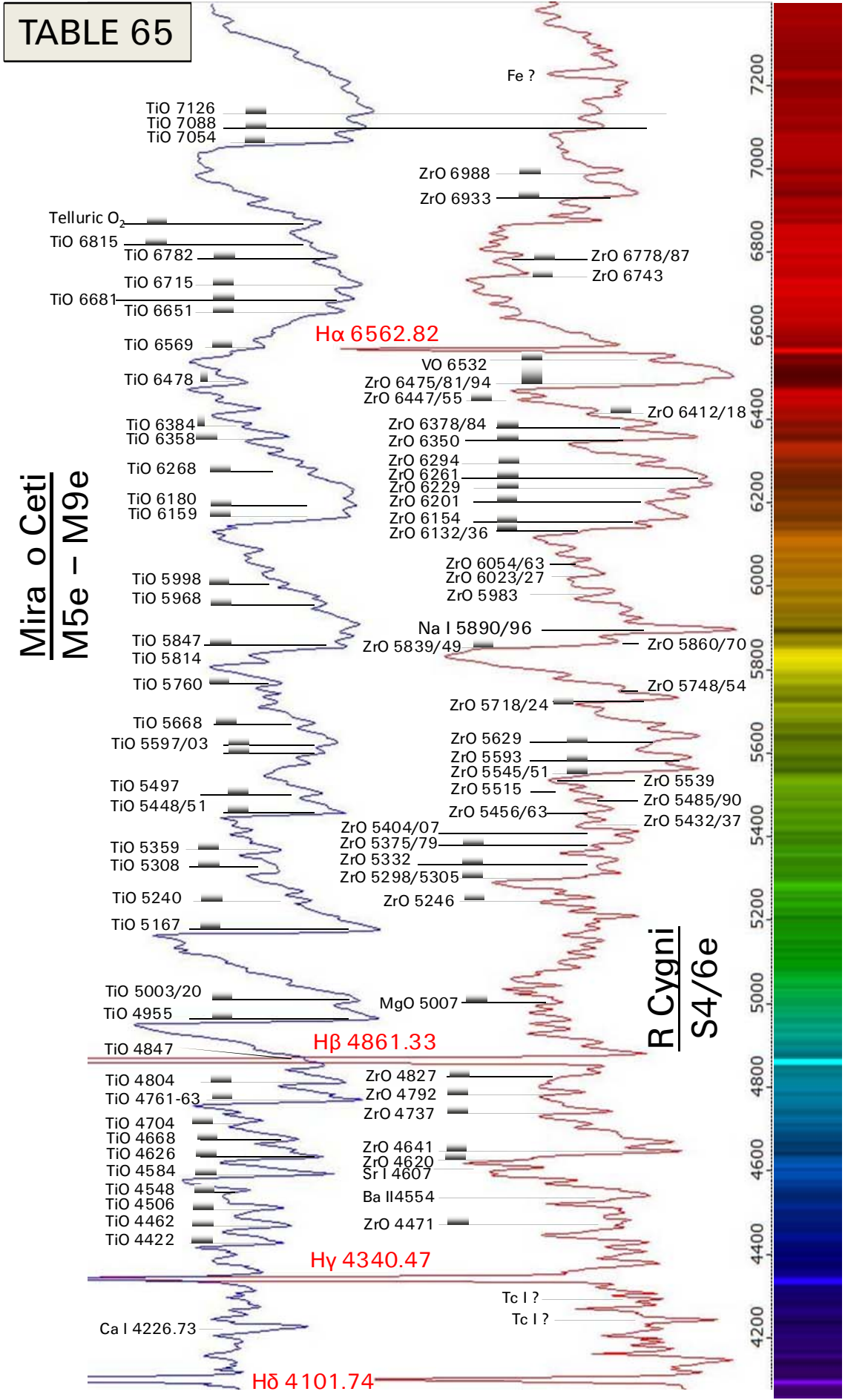5600
5400
5200
5000
4800
4600
4400
4200

<u>Table 66:</u> A montage of three broadband spectra (200L grating) is presented to demonstrate the spectral development within the *S*−Class. To optimise the clarity, only the prominent lines are labeled here.

<u>*Omicron1 Orionis*</u> *(4 Ori)* HD 30959, (540 ly).

This star, with an apparent magnitude of about 4.74^m, is only slightly variable. With *M3.2S* it forms the transition class between the *M(e)* and *S*−types. Alternatively, the star is also classified as *S3.5/1−*. According to the very low *C/O* index *ZrO* is barely visible in this low-resolution spectrum. TiO bands here still dominate the profile.

<u>*Chi Cygni*</u> HD 187796, (340 ly).

With a classification of *S6/1e* (alternatively *S7/1.5e*), the *C/O* index is here only slightly higher compared to *Omicron1 Orionis*. Thus the zirconiumoxide absorptions can overprint here the still dominant TiO bands only within a few small sections of the profile at λλ 5298/05, 5375/79, 5839/49 and 6475/81/94 (blend with *TiO* λ 6478). This star shows with $V_{var} ≈ 3.3^m − 14.3^m$, the highest brightness variation of all known variables − period length about 408 days *(LPV)*.

<u>*R Cygni*</u> *HD 185456*.

As already shown in *Table 65*, the *ZrO* absorptions have fully overprinted here the *TiO* bands, due to the high *C/O* Index.

<u>Observation hint</u>: *R Cygni* is easy to find. It's located just nearby of *Theta Cygni,* HD 185395 (V≈ 4.5^m).

<u>Table 66 A</u>: Shows a montage of two broadband spectra (200L grating) to compare an ˝intrinsic˝ and an ˝extrinsic˝ *S*−class star. Both stars have nearly the same spectral classification. Despite of some minor differences the two profiles run almost identically − regardless of the suspected different origin of the *ZrO* in the stellar atmospheres.

The <u>intrinsic *HR Pegasi*</u>, HD 216672, (970 ly), is only slightly variable $V_{var} ≈ 6.1^m − 6.5^m$ with a periode of some 50 days (Type *SR*, semi-regular). It is classified as *S4/1+* with a very low *C/O* Index.

The <u>extrinsic *BD Camelopardalis*</u>, HD 22649, (510 ly), is only slightly variable V≈ 5.1^m. It forms a component of a close binary system, is classified as *S3.5/2 symbiotic* and therefore relatively hot.

TABLE 66

Chi Cyg
S7/1.5e

R Cygni
S4/6e

4 Ori
M3.2S

TiO 7126
TiO 7088
TiO 7054

ZrO 6988
ZrO 6933

Telluric O$_2$

TiO 6815

ZrO 6778/87
ZrO 6743

TiO 6715
TiO 6681
TiO 6651

TiO 6569

Hα 6562.82

TiO 6478

ZrO 6475/81/94

VO 6532

TiO 6358

ZrO 6378/84
ZrO 6350

TiO 6180
TiO 6159

ZrO 6132/36

Na I 5890/96

ZrO 5839/49

TiO 5847
TiO 5814

TiO 5668

ZrO 5718/24

ZrO 5629

TiO 5597/03

ZrO 5545/51

TiO 5448/51

ZrO 5404/07

ZrO 5375/79
ZrO 5298/5305

TiO 5167

ZrO 5246

TiO 5003/20
TiO 4965

Hβ 4861.33

TiO 4761-63

ZrO 4792
ZrO 4737

TiO 4626
TiO 4584

ZrO 4641
Sr I 4607
Ba II 4554
ZrO 4471

Hγ 4340.47

Tc I ?
Tc I ?

Ca I 4226.73

Hδ 4101.74

7200
7000
6800
6600
6400
6200
6000
5800
5600
5400
5200
5000
4800
4600
4400
4200

TABLE 66 A

©Richard Walker 2011/03

HR Pegasi S4/1+

BD Camelopardalis S3.5/2 symbiotic

TiO 7126
TiO 7088
TiO 7054

Telluric O₂

TiO 6815

TiO 6715
TiO 6681
TiO 6651

TiO 6569

TiO 6478 — ZrO 6475/81/94

TiO 6358

TiO 6180
TiO 6159

Na I 5890/96

TiO 5847
TiO 5814

TiO 5668

TiO 5448/51

TiO 5167

TiO 5003/20

TiO 4965

TiO 4761-63

TiO 4626

TiO 4584

7100
6900
6700
6500
6300
6100
5900
5700
5500
5300
5100
4900
4700
4500

22 Carbon Stars on the AGB

22.1 Overview and Spectral Characteristics

The final stage of the stellar evolution on the *AGB* is formed by the deeply red shining carbon stars, in most of the cases also *Mira Variables or „Carbon Miras".* In the atmosphere of a star, finally moving to the upper part of the *AGB*, the *C/O* ratio becomes $C/O > 1$. This results in a *carbon excess* which accumulates in a circumstellar cloud, dominating now impressively the star's spectrum. Thus, in the intermediate class *SC*, and increasingly in the following *C*–Class, moderately high resolution spectra show now predominantely absorptions of diatomic carbon molecules. In addition to *CH* and *CN* the so-called *Swan bands* due to C_2 are particularly striking – discovered in 1856 by the Scot *William Swan*. (see also *Table 110*). Further visible are atomic lines of *S*–Process products and impressive absorptions of *Na I*. Angelo Secchi was the first to discover that the intensity gradient of the C_2 *Swan bands* is reversed [▆▆▆] in contrast to other molecular absorptions, such as *titanium-* and *zirconium oxide*. For this feature, he created the separate spectral class IV. (see appendix 33.3).

22.2 Competing Classification Systems

The phenomenon of carbon stars is still far from being fully understood (see e.g. [106]). For the *S*–class, in spite of ongoing disputes exists a generally accepted and consistently applied classification system. However for the carbon stars – the situation is still confusing and unsatisfactory. The "*Revised MK-System 1993*", propagated in most of the textbooks, is applied obviously rarely. Its precursor from the 1960's, the so-called *MK*–*C system*, however, very often! Surprisingly frequent one can see even classifications according to the much older *Harvard system*, with the *R* and *N* classes.

22.3 The Morgan Keenan (MK) – C System

This simple, old classification system is still very popular, both in many professional publications, as well as in most of the stellar databases. It uses the following format:

$$C\textcolor{red}{X,n}$$

X: defines on a scale of 0 – 7, the position of the star in the temperature sequence. This scale is temperature equivalent to the spectral classes from *G4* to *M4* (see table below). The system appears to have been extended down to *C9* (e.g. *WZ Cas*).

n: This index rates on a scale from 1 – 5, the intensity of the C_2 *Swan bands*. In individual cases, appropriate supplements may be added, for example, (e) for emissionlines, further also intensive lines of *S*–Process elements.

C0	C1	C2	C3	C4	C5	C6	C7
G4-G6	G7-G8	G9-K0	K1-K2	K3-K4	K5-M0	M1-M2	M3-M4
4500	4300	4100	3900	3650	3450		

This classification system squeezes the entire complex class of carbon stars in one seven-stage temperature sequence, supplemented just with one single intensity index!

Example*: C 2,5* indicates a stellar temperature, equivalent to the spectral *G9 – K0*, combined with very intense C_2 Swan bands.

22.4 The „Revised MK System 1993"

In 1993, the old "C system" was revised to the "Revised MK System 1993" and adapted to new findings [107]. It comprises five sub-classes (!), ordered by spectral symptoms – whose astrophysical background however remains widely unclear. Perhaps this could be one reason why the acceptance of this complex system, even some 20 years after its introduction, seems to be still limited. The "Keenan 1993 system" uses the following format:

$$C\text{-Sub X n}$$

Sub: corresponds to the subclass of the carbon star according to the following table
X: defines the position of the star in the temperature sequence of the C–Class. This forms a parallelsequence to the spectral classes from $G4$ to $M4$ (see table)
n: Various indices as listed below.

Sub-class	Supposed status [106]	Criteria, spectral symptoms
C–R	Intrinsic	Intensive *Swan bands (C$_2$)* in the blue part of the spectrum. Considerable flux in the blue/violet area – decreasing with lower temperatures. Later types show weaker H – Balmerlines, $H\beta$ line serves as a temperature indicator. S–process elements show average intensity. Intensity of $^{12}C^{13}C$ Band head at λ 4737 is above average.
C–N	Intrinsic	S–Process elements are exceptionally intensive. Early C–N types show a tendency to *Merril Sanford Bands* (*SiC2* silicon carbide).Strong, broad and diffuse absorption, or even a barely detectable flux in the blue range $\lambda < 4400$. *Swan bands C_2* weaker than with the C–R types
C–J	Intrinsic	Very intensive *Swan bands (C$_2$)* and *CN* absorptions, further *Merril Sanford bands* (*SiC2*) and an *infrared excess*.
C–H	Extrinsic	Dominant *CH* absorptions in the blue/violet area. Fraunhofer G band at λ 4300 exceptionally- and S–Process elements above average intensive.
C–Hd	?	*Hd* indicates *Hydrogene deficient*. Hydrogen lines or *CH* absorptions weak or even absent. *CN* and *Swan bands (C2)* above average intensive, very often irregular *R Crb Variables*, showing sudden dramatic brightness dips, due to veiling of the photosphere by circumstellar dust clouds.

Temperatur equivalent of the *Main Sequence*	~Temperatur range [K]	C–R- Sequence	C–N- Sequence	C–H- Sequence
G4 – G6	4500	C–R0		C–H0
G7 – G8	4300	C–R1	C–N1	C–H1
G9 – K0	4100	C–R2	C–N2	C–H2
K1 – K2	3900	C–R3	C–N3	C–H3
K3 – K4	3650	C–R4	C–N4	C–H4
K5 – M0	3450	C–R5	C–N5	C–H5
M1 – M2		C–R6	C–N6	C–H6
M3 – M4			C–N7	
M5 – M6			C–N8	
M7 – M8	~2500		C–N9	

This classification can be supplemented with the following indices [107], [2]:

Index	Specification
C_2 − Index	Intensity of the molecular C_2 *Swan bands* Scale 1 − 5
CH − Index	Intensity of the molecular *CH* absorption. Scale 1 − 6.
MS − Index	Intensity of the *Merril Sanford Bands (SiC$_2$),* Scale 1 − 5
J − Index	Intensity ratio of the C_2 molecular absorption with the Isotopes $^{12}C^{13}C$ and $^{12}C^{12}C$, Scale 1 − 5.
Elements	In some cases, for strong lithium and sodium lines index values are specified

Not included in this system is the still *not* understood class of the *dC* carbon dwarf stars located on the *Main Sequence*.

22.5 Function of these subclasses in the evolution of carbon stars

Current professional publications provide a rather diffuse picture about the functions of these subclasses within the evolution of carbon stars. Many details, so e.g. about the *"dredge up"* processes, are obviously far from being fully understood. Further the theoretical modeling of *"carbon atmospheres"* $C/O > 1$ seems to be difficult.

Analog to the *S*−Class also carbon stars on the *AGB* are referred as *"intrinsic"*. It's assumed, that the subclass *C−N*, as well as the late representatives of *C−R*, form the last development stage of the *AGB* sequence. These subgroups show a behavior like *M*-giants with very similar spectra. Furthermore they are also so-called *"Low Mass Objects"* with ≤ 3 solar masses, typically show a *mass loss* and all of them are *Variables*.

Early representatives of C−R Type shows in contrast, neither variability nor a significant mass loss. Further they seem *not* to be AGB stars and show a behavior like *K*-giants. One of the discussed scenarios postulates a star on the *Horizontal Branch* (*HB*) with a helium "burning" core. However it remains here a mystery how the formed carbon will be conveyed to the surface. A further hypothesis is a former binary system whose masses fused into one single star.

The position of the *C−J* class on the AGB is unclear. It's argued that these *"Low Mass Objects"* could be descendants of the *C−R* class on the *AGB*.

The *C−H* class seems to be "extrinsic". Most representatives are on the *Horizontal Branch* (*HB*) and components of close binary stars. This suggests a mass transfer scenario similar to the extrinsic *S*−Class.

22.6 Merrill Sanford Bands (MS)

Already at the beginning of the 20th Century in spectra of certain carbon stars, in the range of some λλ 4640 to 5200, intensive absorptions attracted attention, which for a long time could not be interpreted. The most intense bandheads are at λλ 4977, 4909, 4867, 4640 and λ 4581. These absorption bands are named after the two explorers, who first described these in 1926. Not until 1956 *Kleman* could prove with laboratory spectra, that these bands are caused by *SiC$_2$* silicon carbide. For this purpose he heated silicon in a graphite tube up to 2500 K.

P. J. Sarre et al. have also shown [109] that the *Merril Sanford Bands* are generated in cooler layers of the stellar atmosphere, far beyond the photosphere. *Merril Sanford Bands* are most common in the entire *C−J* and the early *C−N* classes.

22.7 Commented Spectra

The majority of carbon stars is part of the sub-class *C−N*, documented here with some examples. The spectral classes are here indicated in the old *MK−C system*, according to Stephenson's 1989 catalog [500]. If available [107], also the classification, corresponding to the *"Revised MK System 1993"*, is specified.

Table 67: A montage of three broadband spectra (200L grating) is presented to demonstrate the difference between the profiles of differently classified carbon stars.

WZ Cassiopeiae: HD 224855, spectralclass *C9,2 Li* or *C-N7 III: C_2 2 Li 10.*
J2000 RA: 00h 01' 16''   Dec: +60° 21' 19" V_{var} ≈ +6.5 − 8.5^m

WZ Cas (1,500 ly) is an extremely late classified, cool *Supergiant* (2,500 K). It's the dominant component of a binary star system, impressively contrasting with its white-blueish shining companion star (*V ≈ 8^m, A0*). It's located in the constellation Cassiopeia (Photo: www.astro.sci.muni.cz/).

Besides the rather weak *Swan bands* (here classified with index value 2), this spectrum is dominated by the striking, almost fully saturated (!) *Na I* line. Further by the impressive absorption of *lithium Li I* (λ 6708), whose intensity is rated here with 10. Therefore *WZ Cassiopeiae* is often called "Lithium star" [348]. According to [349] this intense *Li I* absorption line was the first evidence of *Lithium* outside the solar system, found by *McKellar* 1941 − a small but anyway interesting detail in the history of science! Further the profile is dominated by *CN-* und *C_2*-absorption bands and the *H*-Balmerlines are barely recognisable here. The spectrum was recorded with the Celestron C8 − exposure: 3x85 sec. The line identification is based amongst others on [100], [104], [110], [348], [349].

Z Piscium: HD 7561, spectral class *C7,3* or *C-N5 C_2 4*
J2000   RA: 01h 16' 05''   Dec: +25° 46' 10" V_{var} ≈ max. +6.8^m

This star is a *Supergiant* with a surface temperature of some 3,000 K and located some 1,500 ly distant in the constellation *Pisces* [105]. With *C7,3* it's classified earlier than *WZ Cas (C9.2)*. The carbon absorptions are here much intenser and the *Na I* line somewhat weaker, but still very impressive! Instead of the exceptional *Lithium* line (λ 6708) the undisturbed *CN a*bsorption at λ 6656 is visible here.

The spectrum was recorded with DADOS 50µm slit and the Celestron C8/ 3x60sec. The line identification is based amongst others on [100], [104], [110], [348].

W Orionis: HD 32736, spectral class *C5,4*
J2000   RA: 5h 05' 59"   Dec: +1° 11' 27" V_{var} ≈ max.+5.88^m

The luminosity class of this carbon giant (some 700 ly distant), is difficult to determine [506]. *Merrill Sanford Bands* are striking here. In the profiles of the two other, much later classified carbon stars, these absorption bands of triatomic *SiC_2 silicon carbide* are hardly recognisable. The spectrum was recorded with DADOS 25µm slit and Celestron C8/ 5x42 sec. The line identification is based amongst others on [100], [104], [110], [107], [109] [348].

Table 67a: *W Orionis*. Higher resolved spectrum (900L grating) in the wavelength domain of the *Merrill Sanford Bands*. The line identification is based here additionally on [108].

TABLE 67

CN 7283

CN 7119

CN 6955

WZ Cassiopeiae C 9.1

Z Piscium C 7.3

W Orionis C 5.4

Li I 6708
CN 6656

Ca 6572

CN 6502

CN 6355

CN 6259
CN 6206
C_2 6168 C_2 6191
C_2 6122
C_2 6059
C_2 6005

Na I 5895.92
Na I 5889.95

CN 5749

C_2 5636
C_2 5585
C_2 5541
C_2 5502

Ti I 5426.26
Mn I 5394.67

Sc I 5301.94
CN 5255
Cr I 5206.04
C_2 5165
C_2 5130

Ba II 4934.1

Merill Sanford Bands

SiC_2 4977
SiC_2 4957
SiC_2 4909
SiC_2 4867
SiC_2 4832
SiC_2 4807
SiC_2 4767

C_2 4737

WZ Cas   Z Psc   W Ori

© Richard Walker 2011/04

TABLE 67A

$C_2/Sc\ I\ 5302$

CN 5255

Fe I/Ni I/V II 5215-16
Fe I/Cr I/La II 5205
$SiC_2\ 5198$
$SiC_2\ 5192$

$C_2\ 5165$

$C_2\ 5130$

$C_2\ 5095-110$

$C_2\ 5041$

$C_2\ 5020$
$C_2\ 5006$

$SiC_2\ 4977$ $SiC_2\ 4981$

$SiC_2\ 4957$

Ba II 4934.1

$SiC_2\ 4909$

$SiC_2\ 4867$

$SiC_2\ 4851$

$SiC_2\ 4832$

$SiC_2\ 4807$

$SiC_2\ 4767$

$SiC_2\ 4750$

$C_2\ 4737$

Merrill Sanford Bands

W Orionis   C 5.4

Merrill Sanford Bands

5300

5200

5100

5000

4900

4800
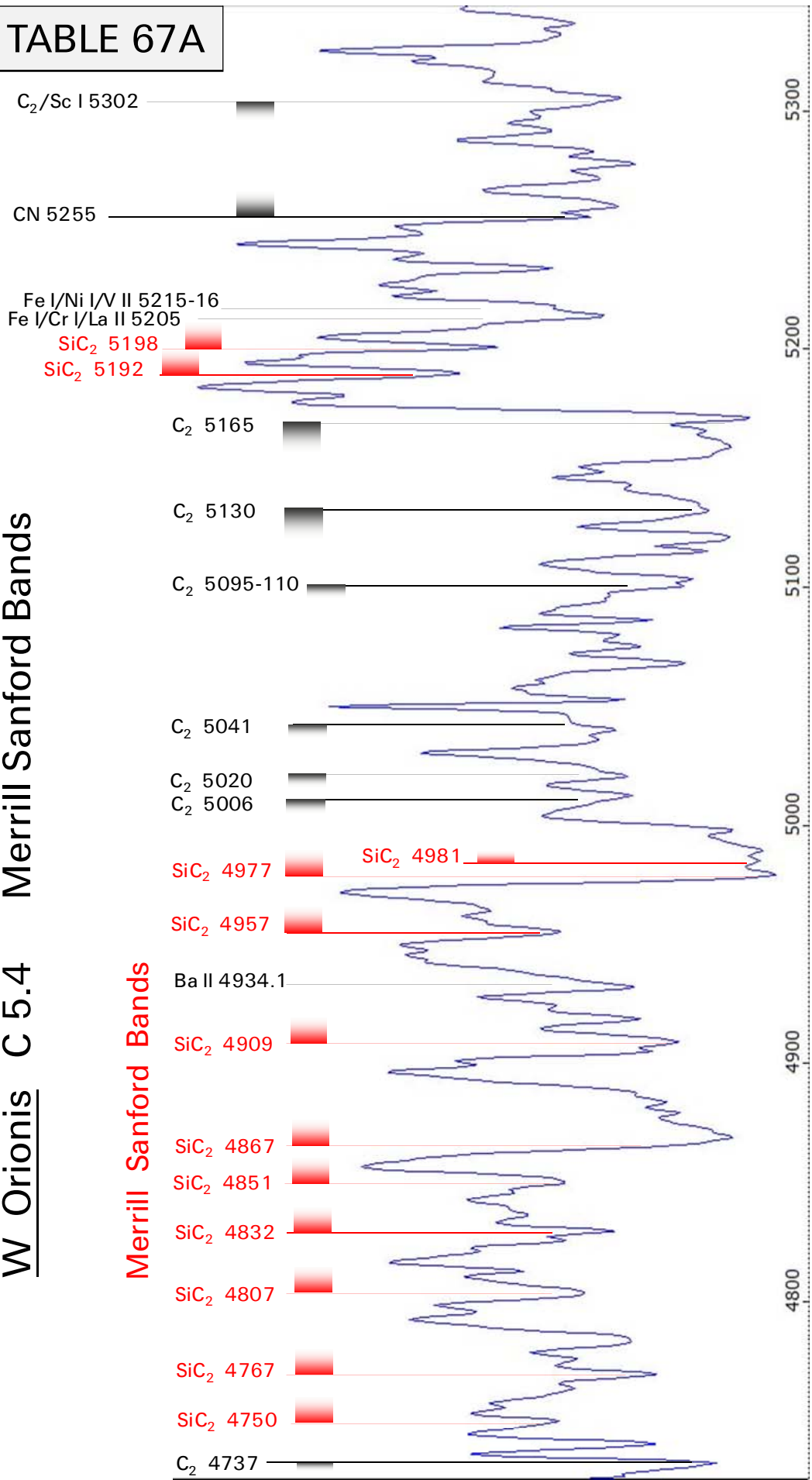
23 Spectra of Extragalactic Objects

23.1 Introduction

It's impossible with amateur equipment, to record spectra of single stars within external galaxies. However it's possible to record *composite spectra* of galaxies and quasars! In contrast to profiles of individual stars the composite (or integrated) spectra show the superposed characteristics of hundreds of billions individual star spectra. Using Doppler spectroscopy thus also the radial velocities, respectively the z-values of such objects can be measured. Further by "edge on" galaxies the rough distribution of the rotation speed within the galactic disk can be estimated [30].

On a professional level, this has been practiced successfully since the beginning of the 20th century and has contributed substantially to our present understanding of the universe. The first, who tried this with M31, was in 1912 *Vesto M. Slipher* at the Lowell Observatory in Flagstaff Arizona. He was able to measure the *blue shift* of the spectrum and derived a radial velocity of −300 km/s. Further he detected the rotation of this "nebula". The fact that M31 is a galaxy outside the Milky Way was proved only later in the early twenties. Further, he also noted that most of the other galaxies appearing *red shifted* and thus are removing from us. Hubble used these shift measurements later for the correlation with the distance (Hubble constant).

Very soon it was recognised that such composite- or integrated spectra have a similar content of information as those of individual single stars. They also show profiles e.g. with or without emission lines, chiefly depending on the kind and activity of the galactic nuclei. The relative similarity of the galactic composite spectra to those of single stars, was a powerful argument in the historical dispute (mainly between *H. Shapley* and *H. Curtis*), that galaxies are not dust or gas nebulae like M42 (see *Tables 80/80A*), but extremely distant, huge clusters of individual stars!

The characteristics of the spectra are also quite well correlated with the morphological types of galaxies (see graph of the so-called tuning-fork diagram). Such spectral profiles are amongst others powerful means to determine e.g. the content of stars, and the development state of the galaxy [301].
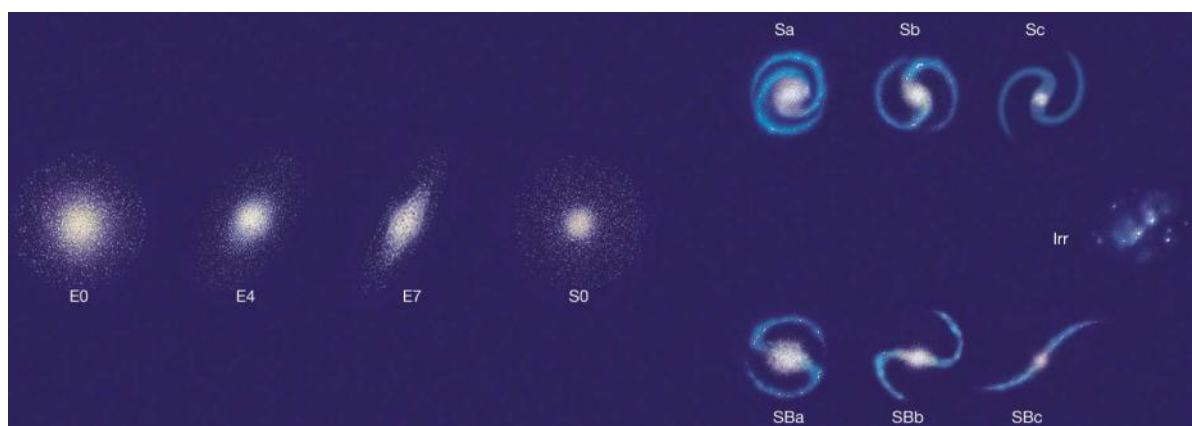
In this edition, for the time being, only a composite spectrum of our neighboring galaxy M31 is presented. Later on spectra of other galaxies and quasars are planned.
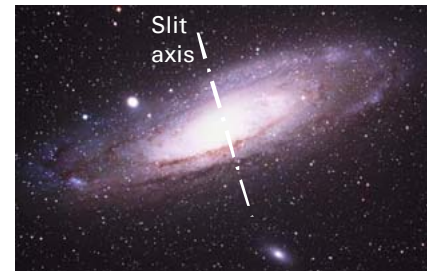
Table 70: Andromeda Galaxy M31/NGC224

The table shows heliocentric parameters according to NED [501], other sources [*] and Evans, N.W. Wilkinson (2000) [1].

Velocity	Redshift z	Distance	Morphology *	Diameter *	Mass [1]
−300km/s	−0.001	2.6M ly	Sb	141,000 ly	$1.23 \cdot 10^{12} M_\odot$

Table 70 shows a composite spectrum of M31. The slit axis of the DADOS spectrograph was adjusted nearly parallel to the apparently smaller crossaxis of the galaxy, since no rotation effects are intended to show here [30].

According to [301] composite spectra of the galaxy types *Sa − Sab* are dominated mainly by *developed Giant stars*. As a matter of fact the pseudo-continuum of the recorded *M31* spectrum fits here best to that of a single star of the late G−class! For a comparison, the *M31* profile is therefore shown here superposed with the pseudo-continuum of *Vindemiatrix* (ε Vir). The most dominant common features are the *Fraunhofer G-band*, the *Calcium T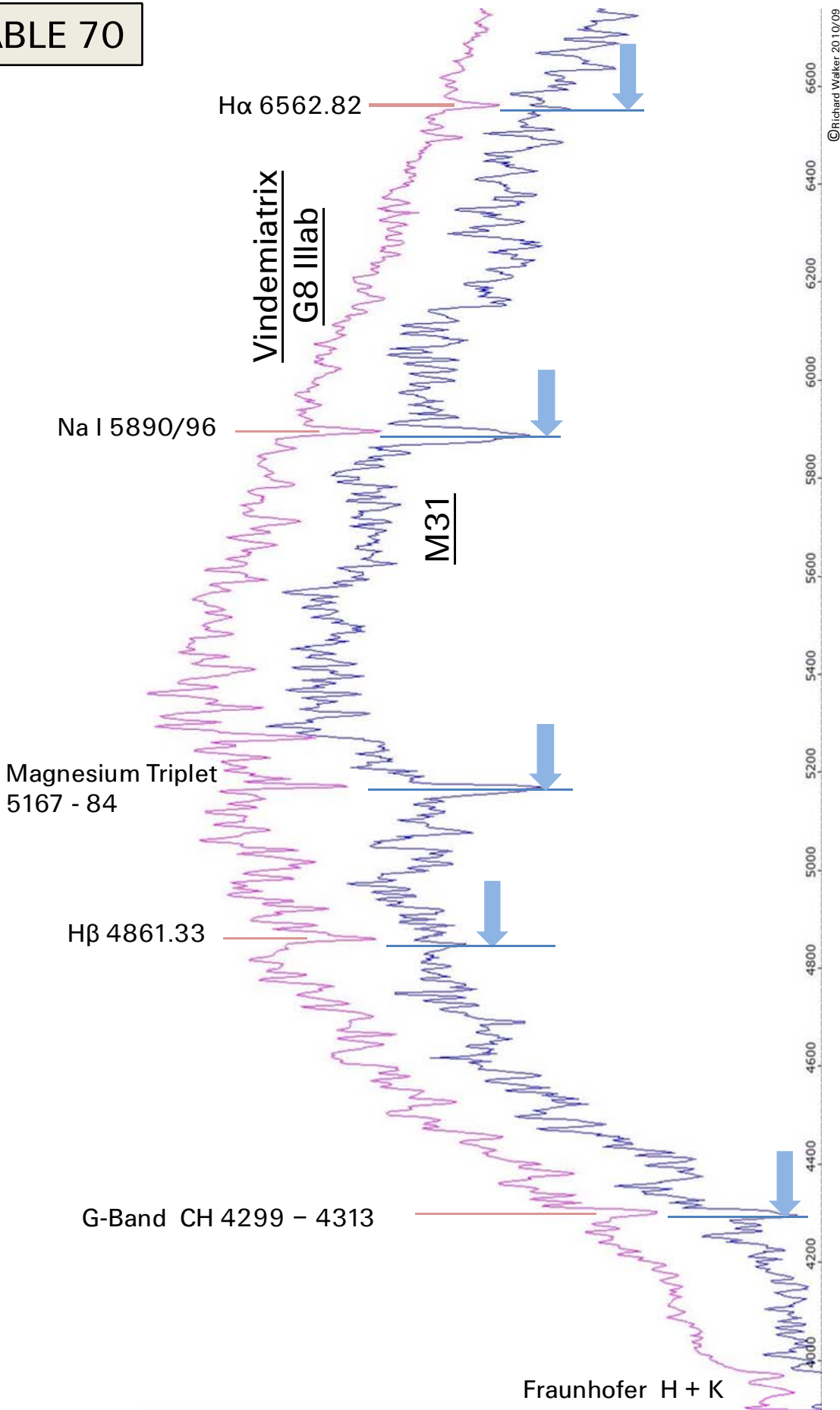riplet*, and the *Sodium Double Line* (Fraunhofer D line). The *H*-Balmer lines are only faintly visible in absorption. According to [301], this finding fits rather to *elliptical galaxies (type E)*. For the type *Sa−Sab* also few emission lines, caused by a younger stellar population, should sporadically be recognisable. However this is not detectable in this spectrum of M31.

The profile was recorded in the Nasmith focus of the 90 cm CEDES Cassegrain Telescope in Falera − exposure: 3x340 sec. Clearly visible here is the expected blueshift of several Angstroms by the *absolutely* wavelength-calibrated *M31* profile, compared to the *relatively* calibrated spectrum of ε Vir, based on known lines.

Comparison of Spectra: Galaxis M31 vs. Vindemiatrix G8 IIIab

TABLE 70

Vindemiatrix
G8 IIIab

M31

Hα 6562.82

Na I 5890/96

Magnesium Triplet
5167 - 84

Hβ 4861.33

G-Band CH 4299 − 4313

Fraunhofer H + K

©Richard Walker 2010/09

24 Spectra of Emission Nebulae

24.1 Short Introduction and Overview

Reflection nebulae are interstellar gas and dust clouds which passively reflect the light of the embedded stars. *Emission nebulae* however are shining actively. This process requires that the atoms are first ionised by hot radiation sources with at least 25,000K. The density of the nebulae is so extremely small that on earth it can be generated only as the best ultra-high vacuum. In [30], sect. 20, these processes are explained more in detail. The requirements for the development of *emission nebulae* are mainly met by the following astronomical "object classes":

H II Regions:

Textbook example is the Orion Nebula *M42* (Photo: NASA). Here extremely hot stars of the O- and early B class ionise – in addition to helium, oxygen and nitrogen – primarily hydrogen atoms of the surrounding nebula. This requires UV photons, above the so-called Lyman limit of 912 Å and corresponding to an ionisation energy of >13.6 eV. This level is only achievable by very hot stars of the O- and early B-Class. Such H II regions tend to have a clumpy and chaotic structure and may extend over dozens of light years. They show a high star formation rate and can still be detected even in distant galaxies. The reddish hue is caused by the dominant Hα emission.

Planetary Nebulae PN – The most significant sub-group of the emission nebula

In the central part of these much higher energetic objects are mostly extremely hot white dwarfs with up to > 200,000K. This is the final stage of stars at the end of the AGB (sect. 19 – 22) with originally <8 solar masses. They ionise the atoms of their rather slowly expanding former stellar envelopes (some 20-40 km/s). Photo: NGC 6543 Cat's eye nebula (NASA). About 10% of central stars show similar spectra in the final stage like Wolf Rayet stars, and thus have WR-classifications (WRPN).Their absolute magnitude however is considerably lower. PN often show an ellipsoidal shape, in some cases with a regular fine structure. The reasons for the numerous other existing forms are only partially understood.

Super Nova Remnants SNR

SNR show a striking filamentary structure. The main part of the ionisation energy is provided here by the collision of the rapidly expanding stellar envelope (a few 1000 km/s) with the interstellar matter. Photo: M1 Crab Nebula (NASA). The shells around the Wolf-Rayet Stars are excited in a similar way (sect. 8), such as the *Crescent Nebula NGC 6888*.

In the center of SNR the remaining Neutron Star or Pulsar emits a wind of relativistic electrons with nearly light speed. It is deflected or slowed by magnetic fields within the plasma or electric fields around the ions. Such energy losses are compensated by emitted photons, causing broadband *Synchrotron-* or *Bremsstrahlung*, predominantly in the X-ray domain.

## 24.2 Common Spectral Characteristics of Emission Nebulae

Besides of the chemical composition the local state of the plasma is determined by the power of the UV radiation as well as the temperature T_e and density N_e of the free electrons. By recombination the ions recapture free electrons which subsequently cascade down to lower levels, emitting photons of well defined discrete frequencies (fluorescence effect). According to the Plank formula: $\Delta E = h \cdot \nu$, the frequency of the emitted photon ν [nu:] is exactly proportional to the energy difference ΔE between the levels, of the downward electron transition. For these reasons, *emission nebulae* generate, similar to a gas discharge lamp, predominantly "quasi monochromatic" light, not as a continuum, but rather as several discrete emission lines. Accordingly effective are therefore specifically designed, narrow band nebula filters. With the exception of SNR, emission nebulae show only a very faint continuum radiation.

Since the main part of the light is concentrated on a few, more or less intense emission lines, these objects can be still detected even at extreme distances. The brightest [O III] lines become photographically visible just after very short exposure times. In all types of emission nebulae physically the same ionisation processes are responsible for the line formation, albeit with very different excitation energies. This explains the very similar appearance of the spectra. The graph below shows a section of the emission spectrum of M42 with two noticeable features:

1. The intensity ratio of the brightest [O III] lines is always: $I(5007)/I(4959) \approx 3$.

2. The intensity ratio between the hydrogen lines, called *Balmer Decrement D*, represents the quantum-mechanically induced intensity loss of these lines in the direction of decreasing wavelength. Detailed description see [30], sect. 18.

Important for astrophysics is the intensity ratio $D = I(H\alpha)/I(H\beta)$. The theoretically calculated value for thin gases is $D_{Th} \approx 2.85$. The steeper the curve, the greater is the selective interstellar extinction (reddening) of light by dust particles, what in Photometry is called *red color excess*. As a result, the lines at shorter wavelengths are increasingly shown too short. Most of the galactic PN, reachable for amateurs, show values of $D \approx 3.0 - 3.3$ [203]. Therefore, for a rough determination of the excitation class this effect can be neglected, especially as the diagnostic lines are relatively close together (see below). However, there are stark outliers like NGC 7027 with D ≈ 7.4 [14]. For extragalactic objects D becomes > 4, which in any case requires a correction of the intensities ("Dereddening") [204], (procedure see [30] sect. 19).
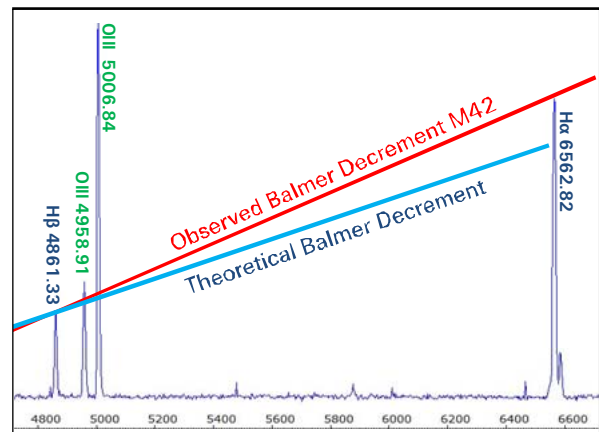
24.3 Emission Line Diagnostics and Excitation Classes E

Since the beginning of the 20th Century numerous methods have been proposed to determine the excitation classes of emission nebulae. The 12-level "revised" *Gurzadyan* system [14], which has been developed also by, *Aller*, *Webster*, *Acker* and others [204, 205, 206] is one of the currently best accepted and appropriate also for amateurs. It relies on the simple principle that with increasing excitation class, the intensity of the forbidden [O III] lines becomes stronger, *compared* with the H-Balmer series. Therefore as a classification criterion the intensity sum of the two brightest [O III] lines, relative to the Hβ emission, is used. Within the range of the low excitation classes E: 1−4, this value increases strikingly. The [O III] lines at λλ4959 and 5007 are denoted in the formulas as N_1 and N_2.

For low Excitation Classes E1 − E4: $I_{N1+N2}/I_{H\beta}$

Within the transition class E4 the He II line at λ4686 appears for the first time. It requires 24.6 eV for the ionisation, corresponding to about 50,000K [202]. That's almost twice the energy as needed for H II with 13.6 eV. From here on, the intensity of He II increases continuously and replaces the now stagnant *Hβ* emission as a comparison value in the formula. The ratio is expressed here logarithmically (base 10) in order to limit the range of values for the classification system:

For middle and high Excitation Classes E4 − E12: $\log(I_{N1+N2}/I_{He\,II\,(4686)})$

The 12 *E*-Classes are subdivided in to the groups *Low* ($E = 1 − 4$), *Middle* ($E = 4 − 8$) and *High* ($E = 8 − 12$). In extreme cases 12^+ is assigned.

Low		Middle		High	
$E-$Class	$I_{N1+N2}/I_{H\beta}$	$E-$Class	$\log(I_{N1+N2}/I_{4686})$	$E-$Class	$\log(I_{N1+N2}/I_{4686})$
E1	$0 − 5$	E4	2.6	E9	1.7
E2	$5 − 10$	E5	2.5	E10	1.5
E3	$10 − 15$	E6	2.3	E11	1.2
E4	>15	E7	2.1	E12	0.9
		E8	1.9	E12$^+$	0.6

24.4 Remarks to the Determination of Excitation Classes and Recording of Spectra

The determination of the low E classes 1−4 is easy, since the Hβ line, compared to the [O III] emission, is relatively intense. At level E4 the He II line (λ 4686) starts very weak, requiring very low-noise spectra, and a strong zoom into the intensity axis.

Quite easy to record are spectra from the very small disc-shaped and blue-greenish shining PN. Thus they are very quickly to localize within a stellar group and the exposure time for the bright representatives takes only a few minutes (200L reflection grating). The brightest [O III] line appears often just after a few seconds on the screen (eg NGC 6210). The intensity of the lines is here integrated along the very short, exposed part of the slit. But along this very short appearing diameter the individual lines show considerably different intensities (see sect. 24.7). Furthermore, during long exposure times, small changes in the slit position with respect to the nebula are to observe as a result of inadequate seeing and/or guiding quality. Tests have shown that several spectra of the same object may show significantly different results including for the Balmer Decrement. Anyway the influence on the excitation class was observed as quite low! The picture shows the small sliver of the *Spirograph Nebula* (IC 418) on the 25 micron slit (PHD Guiding). Between the green autoguiding cross and the slit the bright central star is visible.

By contrast the large appearing nebulae as M27 and M57 require, with the C8 and the Meade DSI III, at least 20−30 minutes of exposure time (without binning) and a totally cloud- and haze-free section of the sky. But they allow a selective recording of spectra within specific areas of the nebula, and to gain an intensity curve along the quite long exposed part of the slit (sect. 24.7). In this case, tests with several spectra of the same object showed consistent results.

24.5 The Excitation Class as an Indicator for Plasma Diagnostics

Gurzadyan (among others) has shown that the excitation classes are more or less closely linked to the evolution of the PN [14], [206]. The study with a sample of 142 PN showed that the E-Class is a rough indicator for the following parameters; however in the reality the values may scatter considerably [13].

1. The age of the PN
    Typically PN start on the lowest E- level and subsequently step up the entire scale with increasing age. The four lowest classes are usually passed very quickly. Later on this pace decreases dramatically. The entire process takes finally about 10,000 to > 20,000 years, an extremely short period, compared with the total lifetime of a star!

2   The Temperature T_{eff} of the central star
    The temperature of the central star also rises with the increasing E-Class. By repelling the shell, increasingly deeper and thus hotter layers of the star become "exposed". At about E7 in most cases an extremely hot White Dwarf remains, generating a WR-like spectrum. This demonstrates impressively the table of the PN in sect. 31. Hence, for T_{eff} [K] the following rough estimates can be derived:

E-Class	E1-2	E3	E4	E5	E7	E8-12
T_{eff} $[K]$	35,000	50,000	70,000	80,000	90,000	100,000 – 200,000

3. The Expansion of the Nebula
    The visibility limit of expanding PN lies at a maximum radius of about 1.6 ly (0.5parsec), because from here on the dilution becomes too great [202]. With increasing E-class, also the radius of the expanding nebula is growing. Gurzadyan [206] provides mean values for R_n [ly] which however may scatter considerably for the individual nebulae.

E-Class	E1	E3	E5	E7	E9	E11	E12+
R_n $[ly]$	0.5	0.65	0.72	1.0	1.2	1.4	1.6

24.6 Emission Lines identified in the Spectra of Nebulae

The appearance and intensity of emission lines in the spectra of the individual Nebulae are different. Therefore here follows a compilation with identified emission lines from *Plasma Recombination Lasers in Stellar Atmospheres* [200] and *Frank Gieseking* [202]. So-called "Forbidden lines" are written within brackets [].

Ne III 3869 [Ne III] 3967.5 He I 4026.2 [S II] 4068.6 Hδ 4101.7 C II 4267.3 Hγ 4340.5
[O III] 4363.2 He I 4387.9 He I 4471.5 He II 4541.6 [Mg I] 4571.1 [N III] 4641] He II 4685.7
[Ar IV] 4740.3 Hβ 4861.3 He I 4921.9 [OIII] 4958.9 [OIII] 5006.8 N I 5198.5 He II 5411.5
[Cl III] 5517.2 [Cl III] 5537.7 [O I] 5577.4 [N II] 5754.8 He I 5875.6 [O I] 6300.2 [S III] 6310.2
[O I] 6363.9 [Ar V] 6434.9 [N II] 6548.1 Hα 6562.8 [N II] 6583.6 He I 6678.1 [S II] 6717.0
[S II] 6731.3 [He II] 6890.7 [Ar V] 7006.3 He I 7065.2 [Ar III] 7135.8 He II 7177.5 [Ar IV] 7236.0
[Ar IV] 7263.3 He I 7281.3

24.7 Commented Spectra

Because spectra of emission nebulae barely show a continuum, the profiles in the following tables are slightly shifted upwards to improve the visibility of the scaled wavelength axis. The presentation of the following objects is sorted according to ascending excitation classes. For most of the PN, the problem of distance estimation is still not really solved. The information may therefore vary, depending on the sources up to >100%! Correspondingly inaccurate are therefore also the estimated diameters of the nebulae!

By pushing off the envelope and the progressive "exposing" of increasingly hotter, inner stellar layers, central stars of PN may generate spectra, *simulating* substantially more massive and luminous stars. This applies, for example, for all O-, early B- and WR-classifications! However the progenitor stars of planetary nebulae are limited to maximum 8 solar masses, corresponding to the middle B class.

Table 80	Orion Nebula M42, NGC1976	Object type: HII region	Excitation class: **E1**

T80 shows the emission spectrum of M42 (ca. 1400 ly) taken in the immediate vicinity of the trapezium θ^1 *Orionis.* Main radiation source is the C- component, a blue giant of the rare, early spectral type O6 (see Table 3) with a temperature of ca. 40,000K [207]. Together with the other stars of the early B-Class, it is capable to excite the surrounding nebula with the criterion value $I_{N1+N2}/I_{H\beta} \approx 5$ up to the border area between the classes E1 and E2. The *Hβ* line is here just slightly surpassed by the [O III] (λ 4959) emission. Due to the enormous apparent brightness the object is spectrographically easy accessible and requires only modest exposure times. (10x30 seconds).

Table 80A	Orion Nebula M42	Intensity profiles within the central part of the nebula

T80A shows for the [O III] (λ5007) and *Hβ* emission lines the intensity profiles along the entire length of the slit array (some 2.5 ly), within the central region of the nebula (Photo M42: HST). The ratio of these intensities demonstrates indirectly the course of the excitation class. Thanks to the linear arrangement of the three slits, DADOS allows for 2-dimensional appearing objects an improvised "Long-slit" spectroscopy, which enables to gain spectral information, combined with the spatial dimension. These profiles have been generated with Vspec and spectral stripes, rotated by 90° with the IRIS software. On the narrow bridges between the individual slits the intensity curve is supplemented with dashed lines. After recording of the spectra in each case a screenshot of the slit camera was taken to document the exact location of the slit array within the nebula.

The different width of the three slits (50/25/30 μm) plays a little role for this purpose, since just the intensity course is recorded and IRIS averages anyway the gray values within the whole slit width. The slit array was positioned on two places within the central part of M42 and approximately aligned in the North-South direction. The western section runs through the *C- component* of the brightest Trapezium star *Θ₁ Orionis C* (Table 3) and ends at the so called *Orion Bar*. The eastern section runs along the *Schröter-Bridge,* through the *Sinus Magnus* and finally also the impressive *Orion Bar*, southeast of the *Trapezium*. The intensity scales of the profiles are normalised on the spectral peak value of [O III] = 1 within the *Orion Bar and* the peak of Hβ on the local ratio there of [O III]/Hβ ≈ 2.5.

Striking is the dramatic increase of intensity within the area of the Trapezium and in the huge ionisation front of the *Orion Bar*. The latter marks the end of the ionised H II region or the so called *Stromgren Radius*. At the end of this transition zone the nebula is heated up to just several 100 K, by the remaining UV photons with energies <13.6 eV which, below this Lyman limit, could not be absorbed by the ionisation processes within the H II area. Outside this transition zone follow chemically increasingly complex molecular clouds [404].

Also remarkable is the sharp drop of the intensity within the dark cloud in the *Sinus Magnus* and the slight increase in the range of the *Schröter Bridge*. The C- component of θ_1 *Orionis* produces here about 80% of all photons [223]! Without it, only a much smaller part of the nebula would be ionised, i.e. the corresponding Strömgren Radius R_s would be significantly shorter. Calculated for a relatively "dense" gas (relative to H II regions) of $10^3\,cm^{-3}$ and an O6 star with 43,600K yields $R_s \approx 3$ ly (0.9pc). For B0 stars this value drops to $R_s \approx 1.2$ly (0.36pc) [404]. The lower the density of the nebula the greater will be the *Strömgren Radius*, because comparatively lesser photons will be absorbed within the same route.

| Table 81 | Spirograph Nebula IC 418 | Object type: PN | Excitation class: **E1** |

Spectrum of IC 418 (ca. 2500 ly). The central star has here a temperature of only 35,000K [207]. It is still unstable, highly variable within short periods of time and therefore just able to excite this nebula with the criterion value $I_{N1+N2}/I_{H\beta} \approx 2.8$ to the lowest class E1 (Gurzadyan: E1 [206]). This is still lower than in the H II region M42. Further Hβ here even outperforms the intensity of [O III] (λ 4959). Accordingly, the PN stage must be still very young and also the diameter of the ionized shell is estimated to just 0.2 ly [207]. The complex spirograph pattern in the nebula is still not understood. Exposure time with the C8 is 3x170 seconds. Photo: HST.

| Table 82 | Turtle Nebula NGC 6210 | Object type: PN | Excitation class: **E4** |

Spectrum of NGC 6210 (ca. 6500 ly). The central star has here a temperature of ca. 58,000K [207] and is classified as O7f. It excites this nebula with the criterion value $I_{N1+N2}/I_{H\beta} \approx 14$ slightly below the threshold of class E4 (~consistent to Gurzadyan: E4 [206]). In the spectrum appears here, only very weak, the He II line (λ 4686). In some cases, this line can also be emitted directly from the central star [206]. Exposure time with the C8 is 4x45 seconds. Photo: HST.

| Table 83 | Saturn Nebula NGC 7009 | Object type: PN | Excitation class: **E8** |

Spectrum of NGC 7009 (ca. 2000 ly). The central White Dwarf has a temperature of ca. 90,000K [207]. It excites this nebula with the criterion value $\log(I_{N1+N2}/I_{He\,II\,(4686)}) \approx 1.9$ up to the class E8. (Gurzadyan: slightly different: E7 [206]). The blue profile is strongly zoomed in the intensity to make the weaker lines visible. Striking are here, despite the high excitation class, still intense H emissions and a too low Balmer decrement of D <2.8, (possible influences sect. 24.4). This PN is the first whose expansion could be detected photographically. [202]. Exposure time with the C8 is 7x240 seconds. Photo: HST
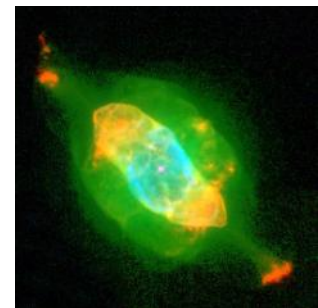
| Table 84 | Ring Nebula M57, NGC 6720 | Object type: PN | Excitation class: **E10** |

T84 shows the emission spectrum of M57 (ca. 2300 ly) approximately in the center of the Ring Nebula. The central White Dwarf has a temperature of ca. 150,000K [207]. It excites this nebula with the criterion value $\log(I_{N1+N2}/I_{He\,II\,(4686)}) \approx 1.4$ up to the class E10 (consistent to Gurzadyan: E10 [206]).

Accordingly weak are here the hydrogen lines relative to [O III]. The Hα line here just reaches parity with the weaker [N II] (λ 6548) emission. The much stronger [N II] (λ 6584) line however is the second-most intense emission behind [O III] (λ 5007). Therefore the reddish color within the ring of M57 predominantly originates from [N II] instead of the by far weaker Hα line.

The broadband spectrum (left) was taken with the 90cm CEDES Cassegrain Telescope in Falera, slit width: 25µm, exposure time 5x340 seconds. This was obviously too short to show the weak classification line *He II* (λ 4686). However, this was later achieved with the

C8, the low-resolution 50µm slit and an exposure time of 3x1270 seconds (excerpt of the spectrum to the right). This reflects the high effort, required for these large appearing PN (in this case 86"x72"). Typical for this high excitation class are the old age of about 20,000 years, and the large extent of the nebula of about 1.4 ly.

Table 84A	M57, Intensity profile along the longitudinal axis of the Ring Nebula

T84A shows for the strongest emission lines [O III] and [N II], the intensity profile along the entire 50µm slit, positioned on the longitudinal axis of the Ring Nebula. This profile has been generated with Vspec and a spectral stripe, rotated by 90° with the IRIS software.

| Table 85	M1, NGC 1952	Object type: SNR	Excitation class: **E >5**

T85 shows the emission spectrum of the Supernova Remnant (SNR) M1 (ca. 6300 ly). The 50µm slit runs in ~N−S direction through the central part of this young SNR. The causal supernova explosion was observed and documented in 1054 by the Chinese. Today, the diameter of the expanding nebula reaches approximately 11 ly.

Vesto Slipher in 1913 recorded the first spectrum of M1. At that time he already noticed a massive split up of the most intense emission lines. Unaware of the nebula expansion, he interpreted this spectral symptom incorrectly as the newly discovered *Stark effect* caused by the interaction with electric fields. 1919 exposed R.F. Sanford, the M1 spectrum with the 2.5m Hooker Telescope, and at that time the "fastest" film emulsions, while no fewer than 48 hours! The result he describes sobering as "dissapointingly weak", a well clear indication that even today this can't be really a beginner object. The expansion of the nebula was found not untill 1921 by C.O. Lampland, by comparing different photographic plates!

With the C8, a 200L grating and an Atik 314L camera, cooled to −20°C with 2x2 binning mode, after all still 2x30 minutes were needed to record a spectrum of passably acceptable quality. As an annoying side effect of the long exposure time, light pollution and airglow (Table 96) was recorded in a comparable intensity to the signal of M1, despite a quite passable rural sky with a visible magnitude of maximum about 4−5^m. This disturbing spectrum was therefore recorded separately, just outside the nebula, and afterwards subtracted with Fitswork from the M1 signal.

This apparently almost 1,000 years old expanding shell is meanwile so diluted that it has become optically transparent. This show also the redshifted peaks of the splitted, well shaped emission lines, often appearing of similar intensity like the blue-shifted, but in some cases however significantly weaker.

The chart at right explains the split up of the emission lines due to the Doppler Effect. The parts of the shell which move towards earth cause a blue shift of the lines and the retreating ones are red shifted. Thereby, they are deformed to a so-called velocity ellipse. This effect is seen here at the noisy [O III] lines of the M1 spectrum − below the 50µm slit, on the top the 25µm slit.
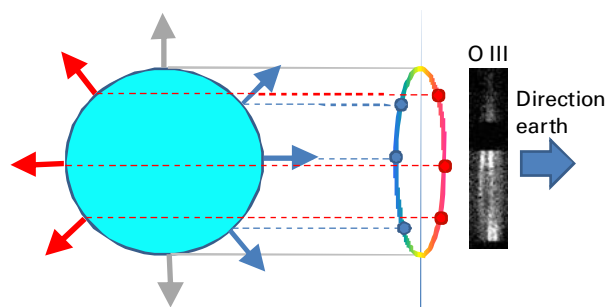
At this low resolution the red-shifted peak of the [O III] (λ 4959) emission forms a blend with the blue-shifted peak of the [O III] (λ 5007) line. Due to the transparency of the *SNR*, with the split up of Δλ, as already shown in Table 2 and in [30], the total expansion velocity of the matter can be determined, related on the diameter of the shell (here, about

1800km/s). The *radial velocity* is obtained finally by halving this value. The radial velocity of this young SNR yields just below 1000 km/s − about 50 times higher than in PN.

By contrast, the envelopes of Wolf Rayet stars (Table 5), P Cygni (Table 13/13A) and to an extreme extent also of Novae and Supernovae, are so dense that we see only the *hemisphere* of the expanding shell, heading towards the earth. In these cases we measure *directly* the *radial velocity*, applying the Doppler formula.

Even more spectral symptoms show that SNR are a special case within the family of the emission nebula. In the center of the nebula (Profile **B**), due to synchrotron and bremsstrahlung processes (see [30]) a clear continuum is visible, which is very weak in the peripheral regions of the SNR (**A**). The latter profile was even slightly raised to make here readable the labeling of the wavelength axis. In contrast to the SNR it is difficult to detect a continuum in the spectra of *PN* and H II regions.

The line intensities I of the profiles $B_{1,2}$ were adapted relative to the continuum heights (I/I_c), to become roughly comparable with those of profile **A**. Apparently in profile **A** and **B** the emissions in the range around λ 6500 are of similar intensity. However, in the peripheral area of the nebula (profile **A**), the [O III] lines around λ 5000 are several times stronger. Obviously the conditions for forbidden transitions are here much more favourable than in the vicinity of the high-energy pulsar, the stellar remnant of the SN explosion. This statement is relativized by the uncertainty, whether and to what extent the rudimentary subtraction of light pollution has affected the course of the continuum.

Due to shock wave induced collisional excitation the strikingly intense sulfur doublet (λλ 6718/33) becomes clearly visible. This feature is only weak in PN and almost completely absent in H II spectra. This also applies to the [O I] line at λ 6300. Anyway at this resolution it can hardly be separated from the [O I] airglow line at the same wavelenght (see sect. 27).

24.8 Distinguishing Characteristics in the Spectra of Emission Nebulae

Here, the main distinguishing features are summarised again. Due to the synchrotron and bremsstrahlung *SNR* show, especially in the X-ray part of the spectrum, a clear continuum. X-ray telescopes are therefore highly valuable to distinguish SNR from the other nebula species, particularly by very faint extragalactic objects. For all other types of emission nebulae the detection of a continuum radiation is difficult.

In the optical part of *SNR* spectra, the [S II] and [O I] lines are, relative to Hα, more intense than at PN and H II regions, due to additionally shock wave induced collision ionisation. The [S II] and [O I] emissions are very weak at PN and allmost totally absent in H II regions [204].

In SNR the electron density N_e is very low, ie somewhat lower than in H II regions. It amounts in the highly expanded, old *Cirrus Nebula* to about 300 cm^{-3}. By the still young and compact *Crab Nebula* it is about 1000 cm^{-3} [204]. By PN, N_e gets highest and is usually in the order of 10^4 cm^{-3} [204]. In the H II region of M42, N_e is within the range of 1000−2000 cm^{-3} [224]. The determination of N_e and T_e from the line intensities is presented in [30].

In H II regions, the excitation by the O- and early B-class stars is relatively low and therefore the excitation class remains in the order of just ca. E = 1-2. Planetary nebulae usually pass through all 12 excitation classes, following the evolution of the central star.

In this regard the SNR are also a highly complex special case. By very young SNR, eg the Crab Nebula (M1), dominate higher excitation classes whose levels are not homogeneously distributed within the nebula, according to the complex filament structure [222]. The diagnostic line He II at λ 4686 is therefore a striking feature in some spectra of M1, ([222] and Table 85).

TABLE 80

Excitation class E1

Criterion $I_{N1+N2}/H\beta \approx 5$ →

Orion Nebula M42

Classification lines

[N II] 6583.6

Hα 6562.82

He I 5876

[O III] 5006.84

[O III] 4958.91

Hβ 4861.33

Hγ 4340.47

TABLE 80A

Pons
Schröteri

Trapezium

Θ₁ Ori C

Orion Bar   Ionization Front

W

N

Sinus
Magnus

~ 1.6′

Θ₂ Ori A

Intensity Profiles [O III], Hβ
<u>Trapezium Area</u>

Θ₁ Ori C

Intensity

[O III]

Hβ

Trapezium

Orion Bar

Intensity Profiles [O III], Hβ
<u>Sinus Magnus</u>

Intensity

[O III]

Hβ

Pons Schröteri

Sinus Magnus

Orion Bar

Nebula Sectors
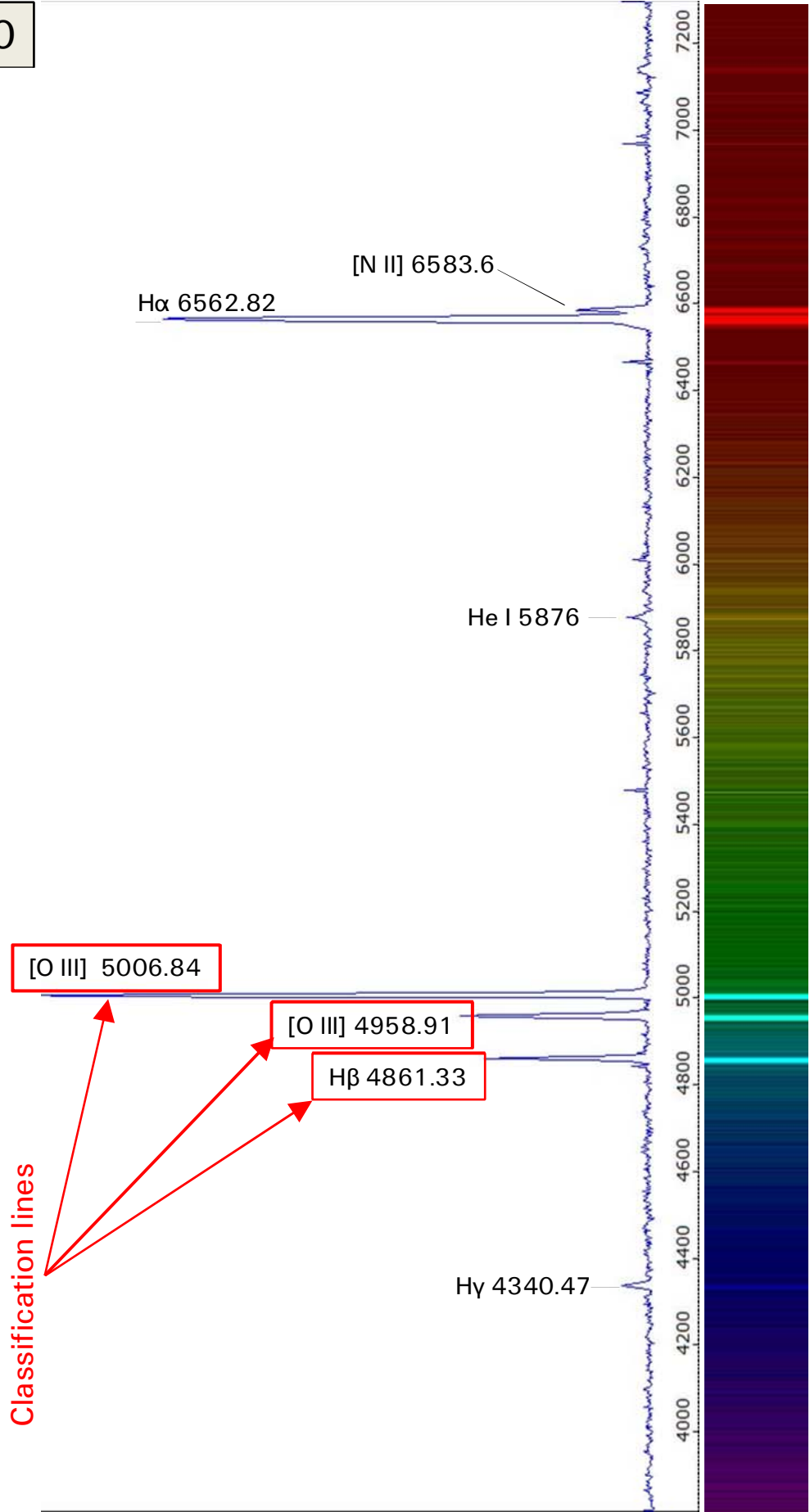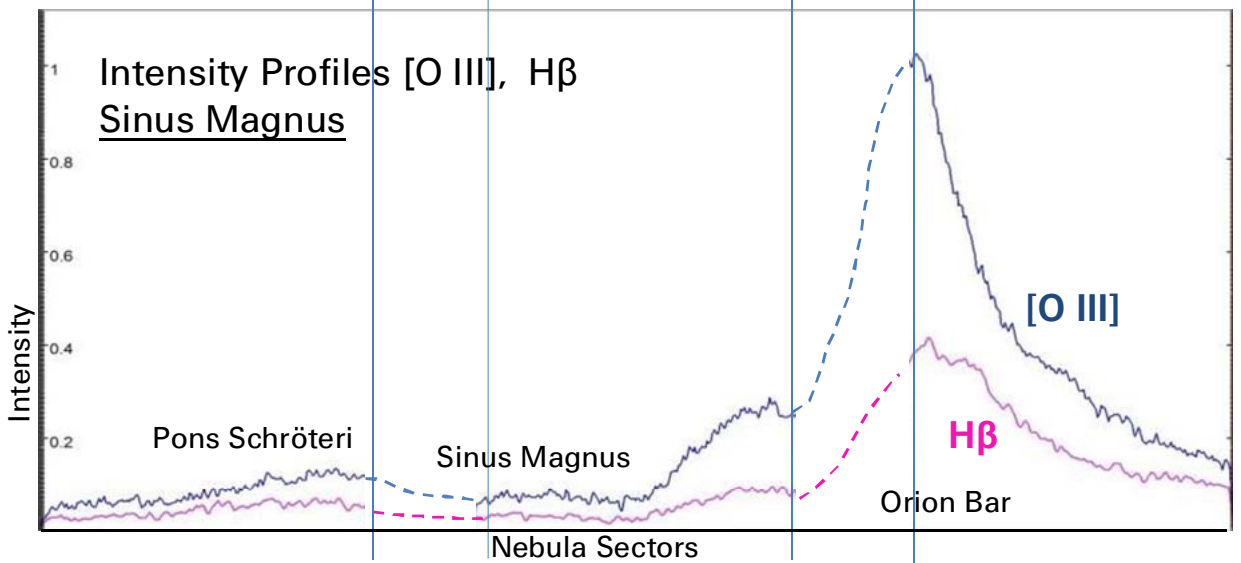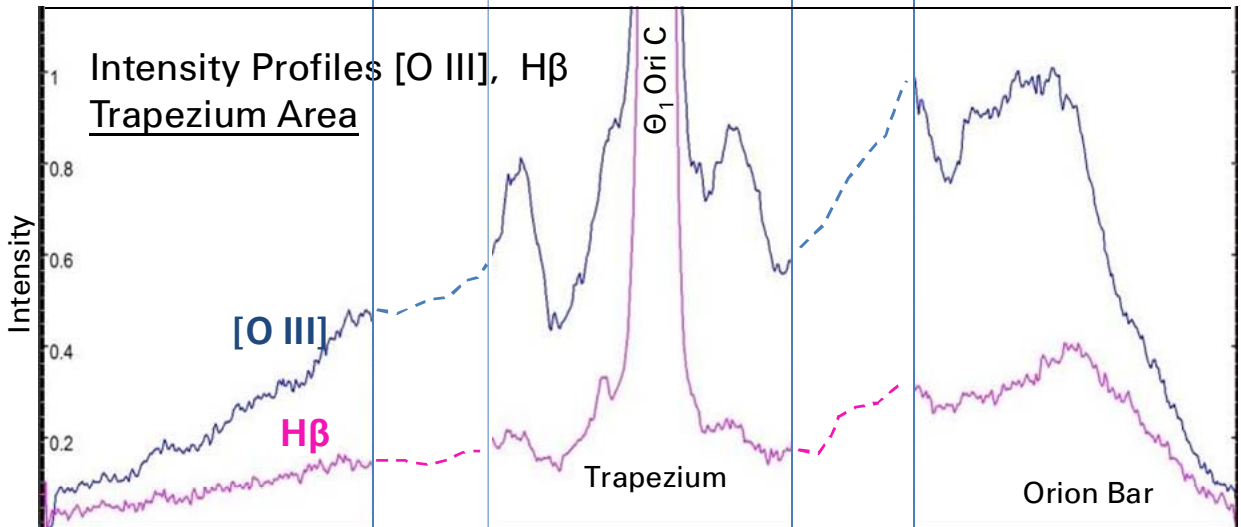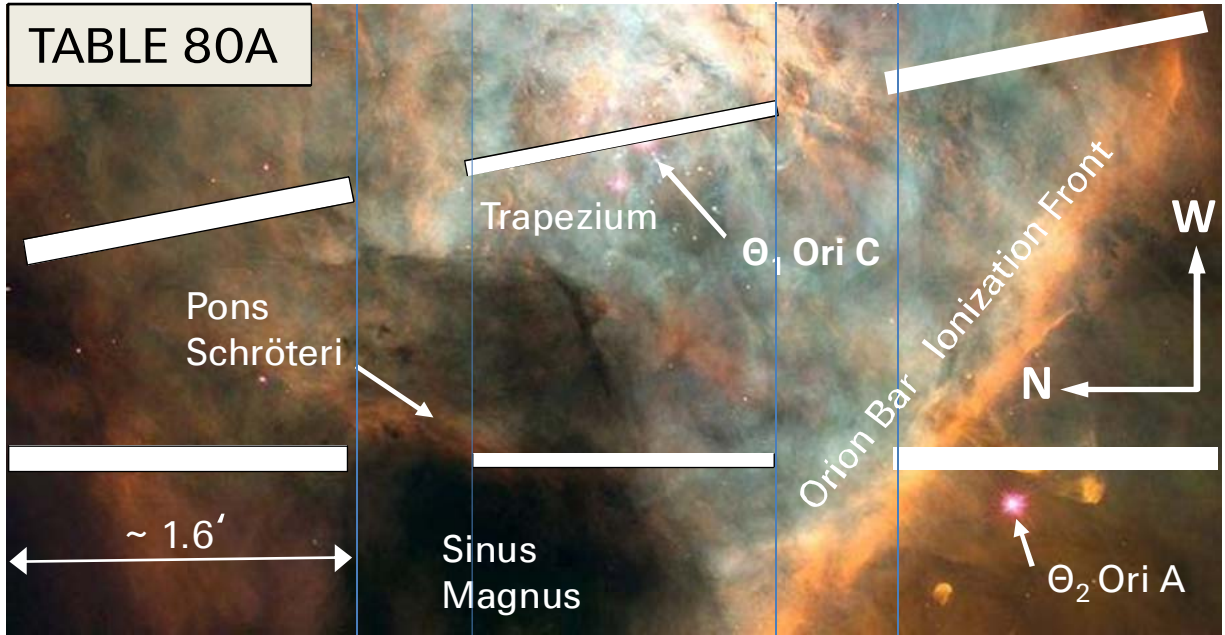
TABLE 81

Spirograph Nebula IC 418

Criterion I_{N1+N2} /Hβ ≈ 2.8 ➔ Excitation Class E1

Classification lines

[Ar III] 7135.8 —
He I 7065.2 —

7000

6800

[S II] 6717 / 31 —
He I 6678.1 —

[N II] 6583.6
Hα 6562.82

6600

[N II] 6548.1 —

6400

[O I] 6300.2 —

6200

6000

He I 5876 —

5800

[N II] 5754.8 —

5600

5400

5200

5000

[O III] 5006.84

[O III] 4958.91

Hβ 4861.33

4800

4600

He I 4471.5 —

4400

Hγ 4340.47 —

4200

Hδ 4101.74 —

TABLE 82

[O III] 5006.84

[O III] 4958.91

Hβ 4861.33

He II 4685.7

Classification lines
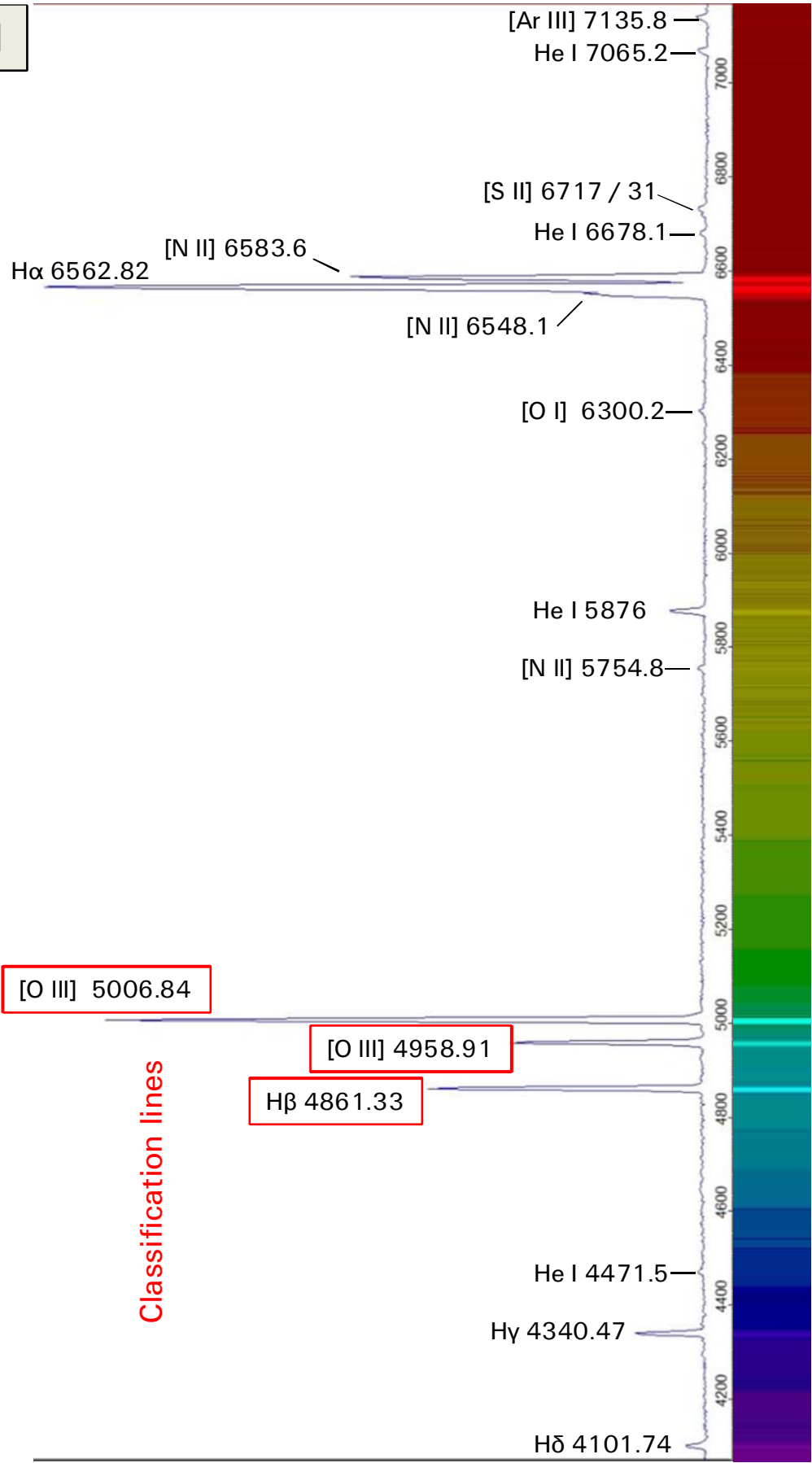
Turtle Nebula NGC 6210

Criterion I_{N1+N2} /Hβ ≈ 14 → Excitation Class E3

[N II] 6583.6

Hα 6562.82

He I 5875.6

[Cl III] 5517.3

[O III] 5006.84

[O III]4958.91

Hβ 4861.33

He II 4685.7

Hγ 4340.5

[Ne III] 3869
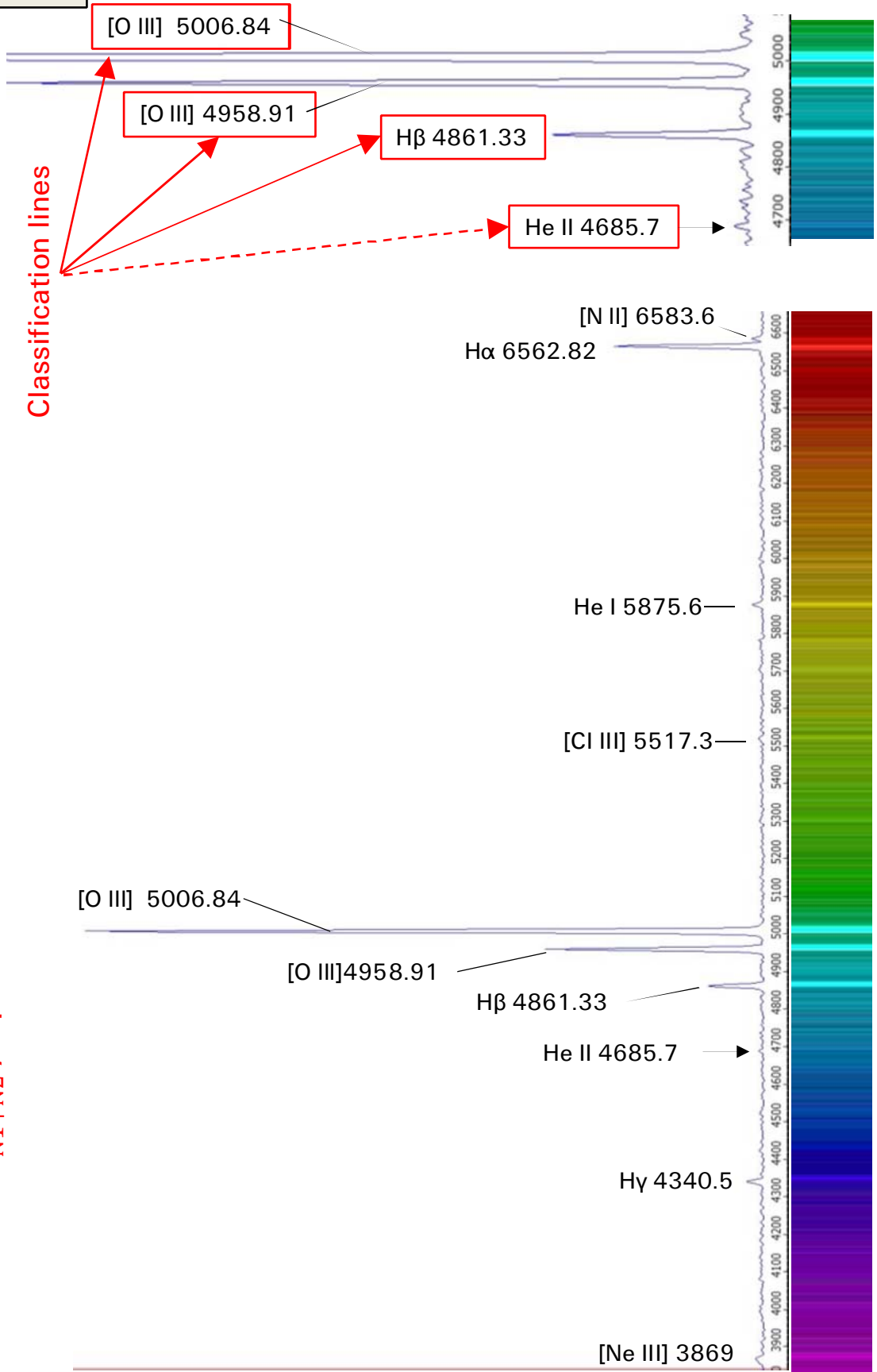
TABLE 83

Saturn Nebula NGC 7009

Criterion $\log\left(I_{N1+N2}/I_{He\,II\,(4686)}\right) \approx 1.9$ ↑ Excitation class E8

Classification lines

[N II] 6583.6

Hα 6562.82

He I 5875.6

[O III] 5006.84

[O III] 4958.91

Hβ 4861.33

[Ar IV] 4740.3
[Ar IV] 4711.34

He II 4685.7

[N III] 4641

He I 4471.5

[O III] 4363.2

Hγ 4340.5

Hδ 4101.74

[Ne III] 3967.47

[Ne III] 3868.76

©Richard Walker 2011/12

TABLE 84

© Richard Walker 2010/05

[O III] 5006.84

[O III] 4958.91

Hβ 4861.33

He II 4685.7

Classification lines
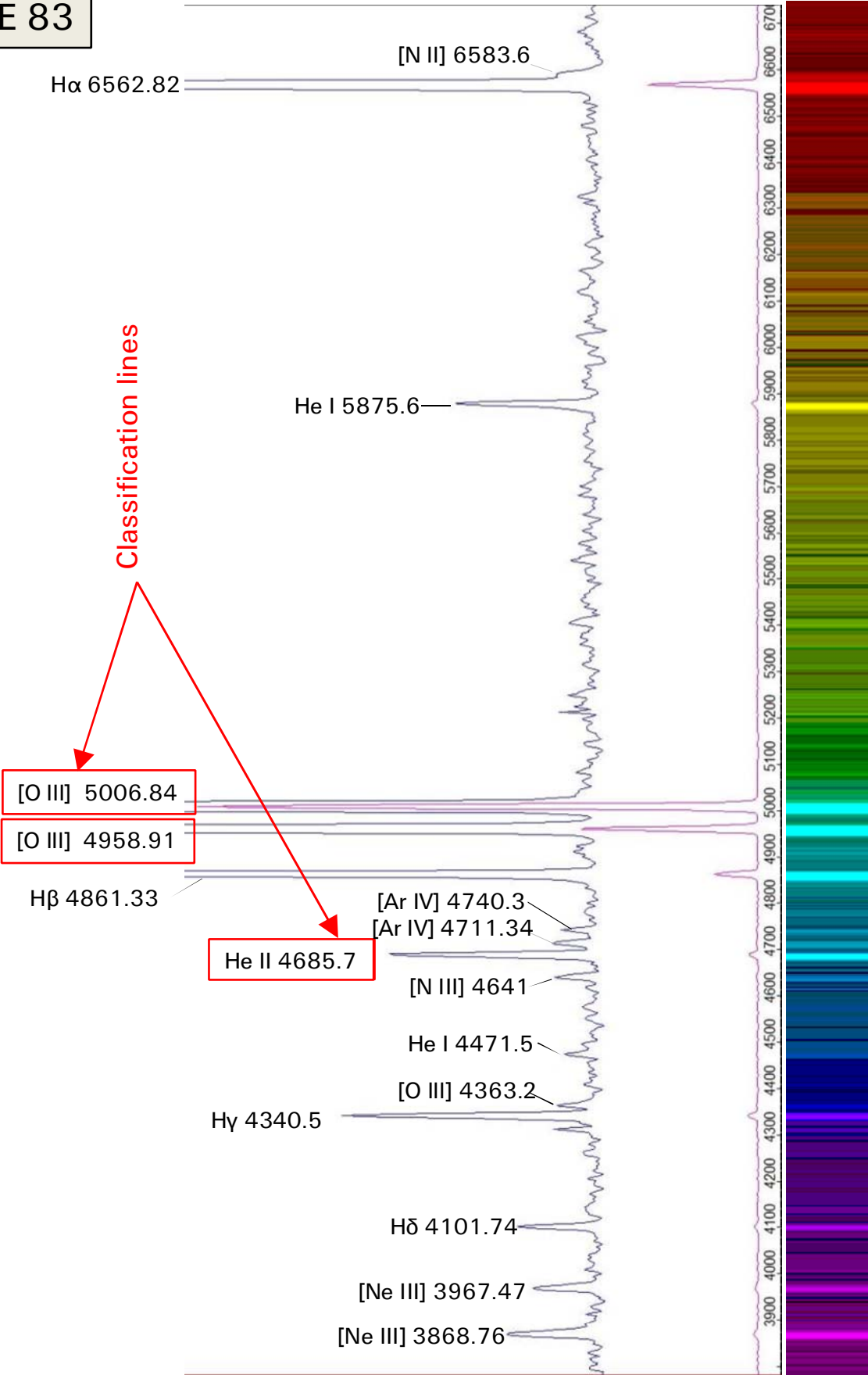
Ring Nebula M57

Criterion $\log\left(I_{N1+N2}/I_{He\,II\,(4686)}\right) \approx 1.4$ ➔ Excitation Class E10

[S II] 6732.7
[S II] 6718.3

[N II] 6583.6

Hα 6562.82

[N II] 6548.1

[O I] 6363.88

[O I] 6300.23

[O I] 5577.4

[O III] 5006.84

[O III] 4958.91

Hβ 4861.33
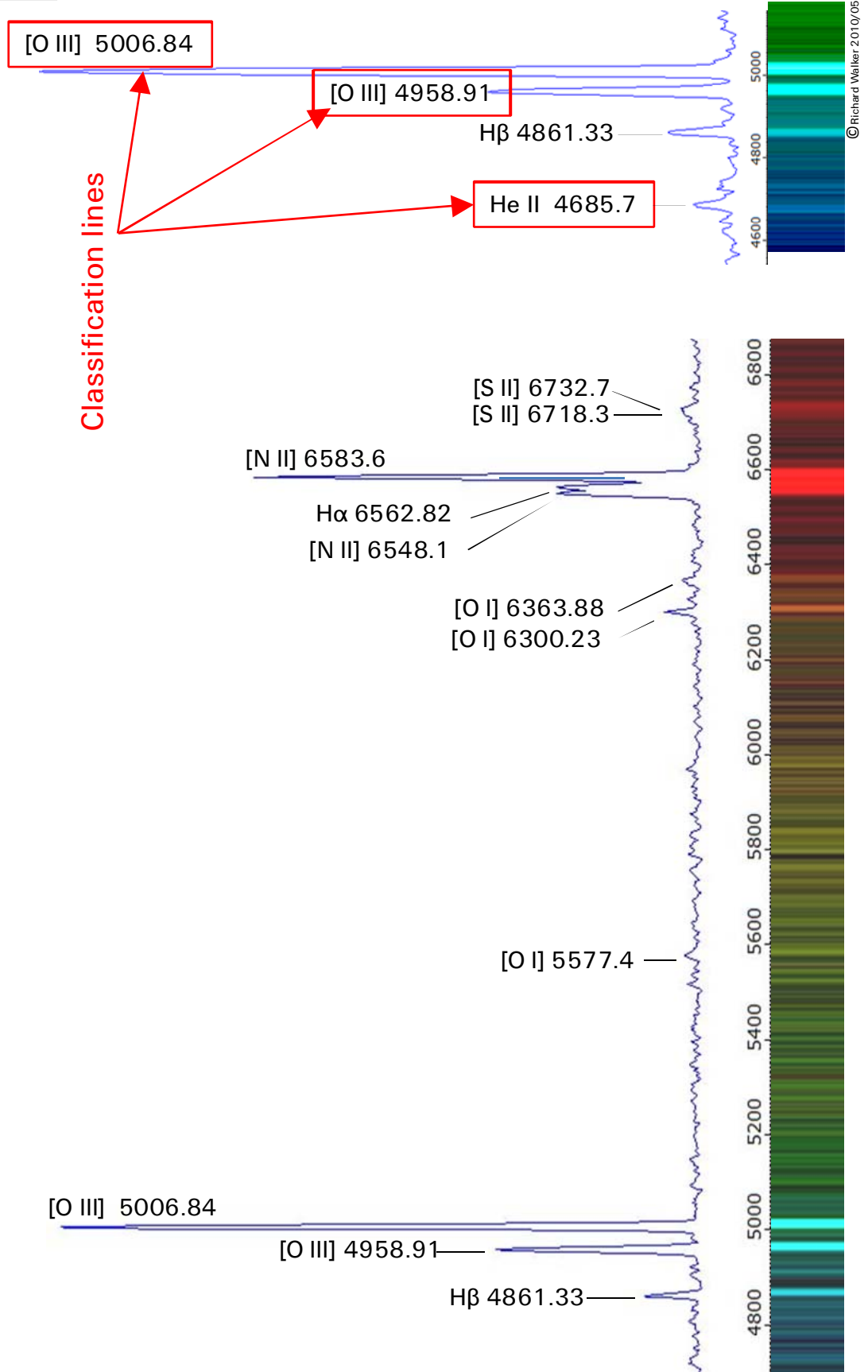
TABLE 84A

Ring Nebula M57

Longitudinal section through M57. The 50µm slit of DADOS is approximately aligned with the longitudinal axis of the nebula. With Vspec the Intensity profiles of the strongest emissions [O III] and [N II] are generated along the entire length of the slit. The scales of the two profiles are normalized on the peak value of [O III] = 1, proportional to their line intensity in the spectrum. [N II] chiefly generates the reddish yellow edge part of the nebula, [O III] mainly produces the turquoise-blue color in the center of the Nebula (Photo: HST).

Intensity Profile [O III] λ 5007

Intensity Profile [N II] λ 6584
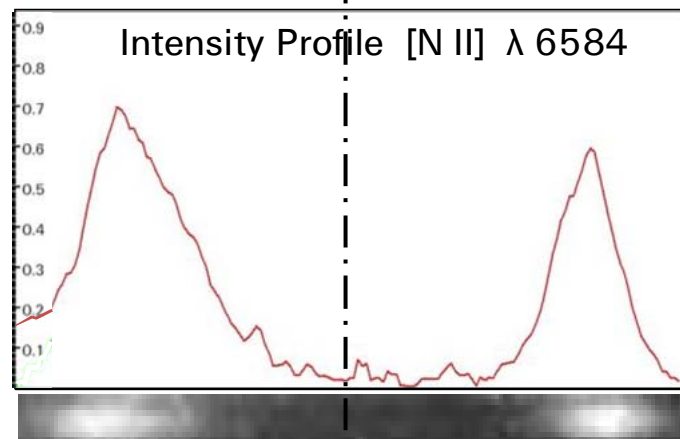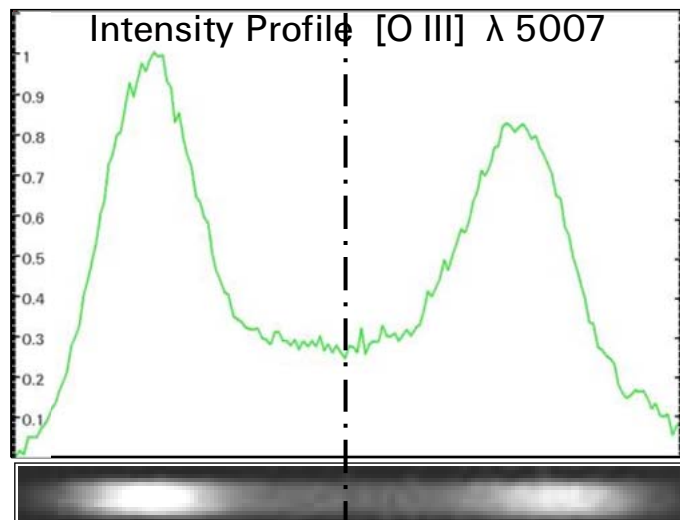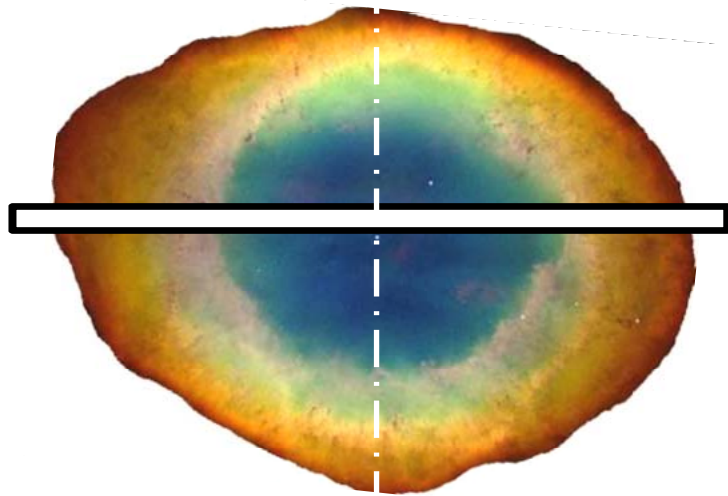
TABLE 85

SNR M1 / NGC 1952

Excitation class E > 5

50μ Spalt

N

W

B

A

B₂

Δλ ≈ 41Å

[S II] 6732.7
[S II] 6718.3

[N II] 6583.6
Hα 6562.82

Δλ ≈ 30Å

[O I] 6300.23

He I 5875.6

A

B₁

Δλ ≈ 31Å

Δλ ≈ 28Å

[O III] 5006.84

[O III] 4958.91

Hβ 4861.33

He II 4685.7

4600 4700 4800 4900 5000 5100 5200 5300 5400 5500 5600 5700 5800 5900 6000 6100 6200 6300 6400 6500 6600 6700 6800

©Richard Walker 2012/02
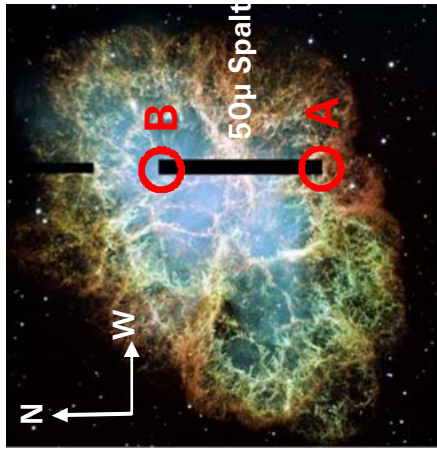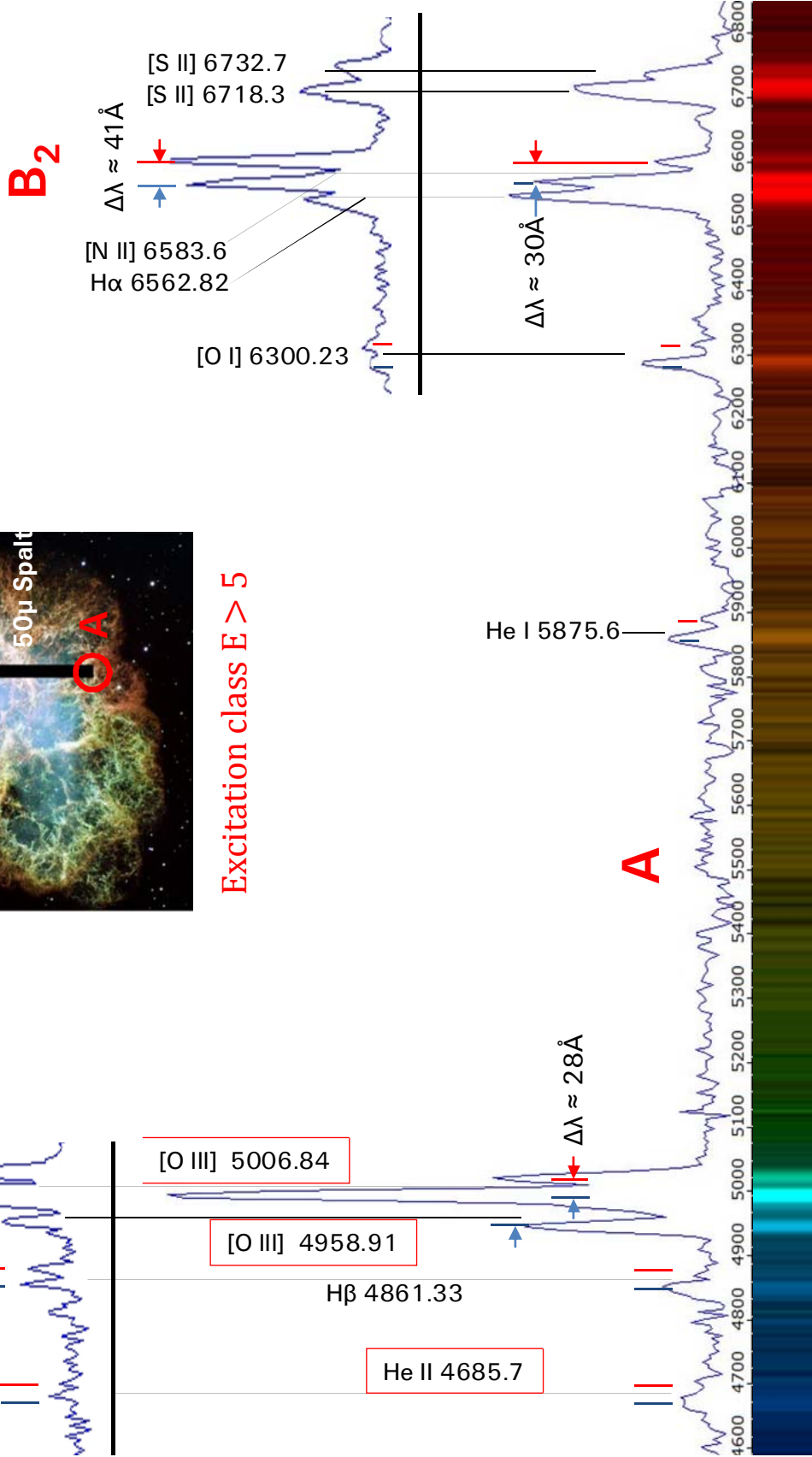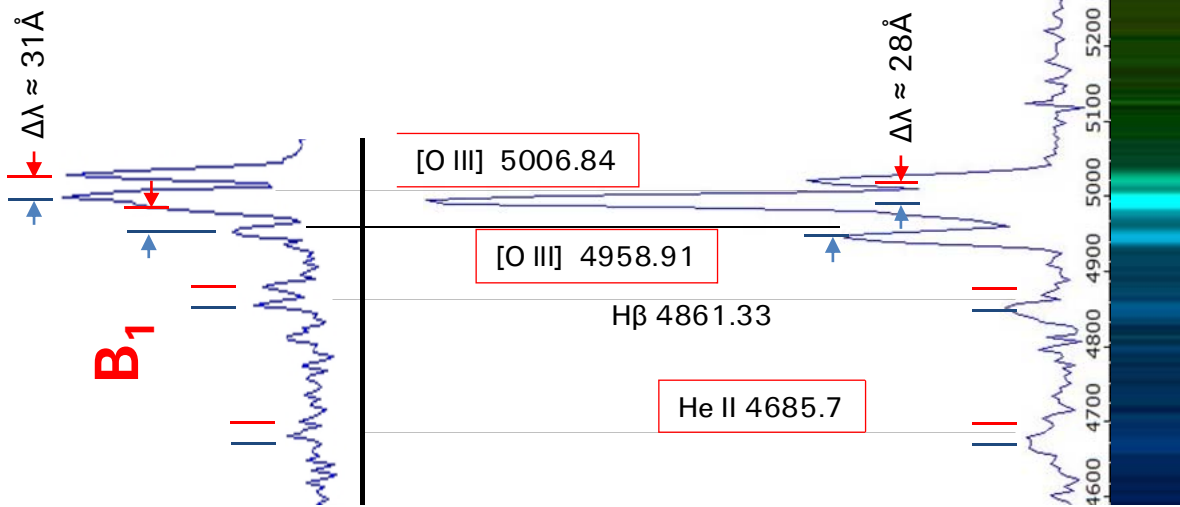
25 Reflexion Spectra of Solar System Bodies

25.1 Overview

The objects in our solar system are not self-luminous, and visible only due to reflected sunlight. Therefore, with exception of comets, these spectra always show, not surprisingly, the absorption lines of the Sun. On the other hand the spectral *continua* of the reflected profiles are overprinted, because certain molecules, e.g. CH_4 (methane) in the atmospheres of the large gas planets, are reflecting or absorbing the light differently strong within specific wavelength ranges. According to their characteristics the planetary reflection spectra are separated here into two tables, each compared with the continuum of the sunlight. All profiles (200L grating) have been equally normalised. During the recording of the spectra all objects had an elevation above the horizon of some 30-40°.

Table 90: Reflection spectra of *Mars* and *Venus*

The extremely dense atmosphere of *Venus* generates on the surface a pressure of about 90 bar, ie approximately 90 times as high as on *Earth*. It consists of about 96% carbon dioxide *(CO_2)*. The remaining shares are mainly nitrogen *(N_2)*, water vapor (H_2O), and sulfur compounds in the form of sulfur dioxide *(SO_2)* and sulfuric acid *(H_2SO_4)*.

The extremely thin atmosphere of *Mars* consists similar to *Venus*, to about 96% of CO_2, but here under a surface pressure of only 0.006 bar, i.e. <1% of the value on the surface of the *Earth*. Here particularly the rocky surface of the planet might determine the reflective properties. In the displayed range the spectra neither of *Venus* nor *Mars* show significant deviations from the shape of the Sun's spectral continuum. In higher resolved spectra, of course experts can recognise and analyse differencies.

Table 91: Reflection spectra of *Jupiter* and *Saturn*

The outer atmosphere of *Jupiter* consists of about 89% hydrogen and10% helium, the rest mainly of methane and ammonia.

Saturn's outer atmosphere is composed slightly different. It consists of about 93% hydrogen and only close to7% of helium. Further appear some traces of methane, ammonia and other gases.

Impressive to see are here, concentrated in the near-infrared range, the very broad methane *(CH4)* and ammonia (NH3) absorption gaps in the spectral continuum. In this wavelength domain, these differences are most pronounced visible in the areas of 6200 and λ 7300.

Table 94: Comet C/2009 P1 Garradd

Comets, like all other objects in the solar system, reflect the sunlight. However on its course into the inner solar system core material increasingly evaporates, flowing out into the coma, and subsequently into the mostly separated plasma- and dust tails. The increasing solar wind, containing highly ionised particles (mainly protons and helium cores), excites the molecules of the comet. Thus the reflected solar spectrum gets more or less strongly overprinted with molecular emission bands, − chiefly due to vaporised carbon compounds of the cometary material. The most striking features are the C_2 Swan bands, above all, the band heads at λλλ 5165, 5636 and 4737 (see also sect. 28.2 and the comments on Table 110). Further frequently occurring emissions are CN (cyan) at λλ 4380 and 3880, NH2 (Amidogen Radicals), and C_3 at λ 4056. Sometimes also Na I lines can be

detected. Only slightly modified is the solar spectrum, recorded from sunlight, which has been exlusively reflected by the *dust tail*. A comprehensive catalog of cometary emission line can be found in [210] and additional data also in [110].

All these facts and the associated effects create complex composite spectra. The influence of the possible components depends primarily on the current intensity of the core eruptions, as well as on our specific perspective, regarding the coma, as well as the plasma- and dust tail.

In Table 94, the coma profile of C/2009 P1 Garradd is presented, taken on November 17 2011, 1730 GMT. Exposure time with the C8: 3x900s. Shown is a montage of the comet profile together with the C_2 Swan bands, generated with a butane gas burner. This comparison clearly shows that in this spectrum of comet Garradd only two of four C_2-bandheads at λλ 5165 and 4715th are visible. The missing two are overprinted by molecular CH, CN and NH_2 emissions. Absorptions of the solar spectrum are hardly recognisable here. This became clear by a test superposition of the comet profile and the solar spectrum.

At the bottom of Table 94 the influence regions of different molecules on the emissions of the spectrum, are presented, according to the tables of [210]. Those are based on spectral profiles, which were obtained with a high-resolution Echelle spectrograph (R ~ 40,000). It is noticeable that, apart from some isolated emissions, overlappings of the influence regions can barely be found.

.

TABLE 90

Reflection spectra of Mars and Venus compared to the daylight

Sun (daylight)

Mars (CO_2, Gestein)

Venus (CO_2, N_2)

Telluric O_2

Telluric H_2O

Telluric O_2

Hα 6562.82

Na I 5980/96

Magnesium Triplet

Hβ 4861.33
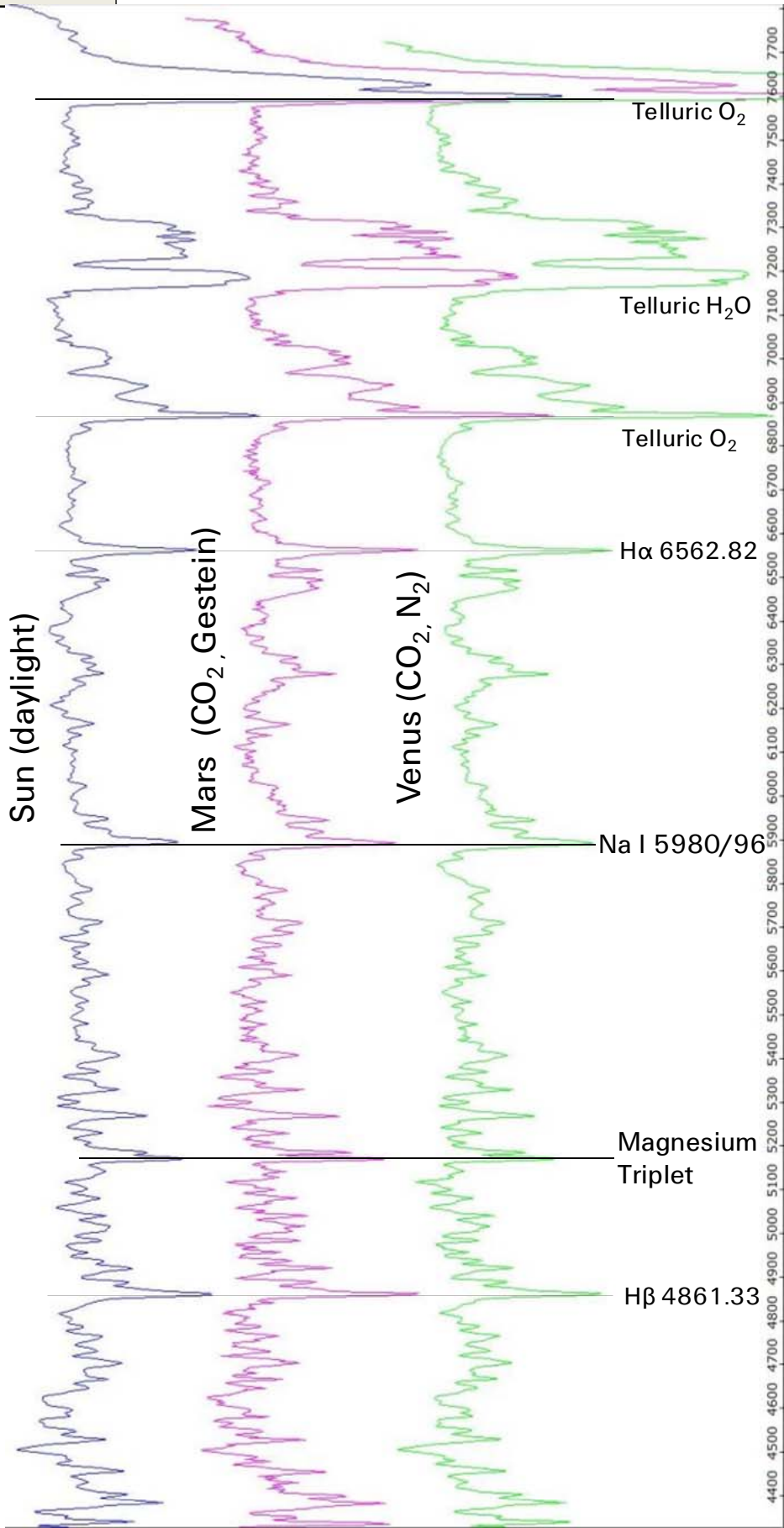
TABLE 91

Reflection spectra of Jupiter and Saturn compared to the daylight

Sun (daylight)

Jupiter (H_2, He, CH_4, NH_3)

Saturn (H_2, He, CH_4, NH_3)

Telluric O_2

CH_4

Telluric H_2O

CH_4

CH_4

Telluric O_2

NH_3

Hα 6562.82

NH_3

CH_4

Na I 5980/96

Magnesium Triplet

Hβ 4861.33

TABLE 94

Coma-Spectrum Comet C/2009 P1 Garradd (November 17, 2011, 1730 GMT)

P1 Garradd

Air GlowO$_2$ 6300 / H$_2$O

NH$_2$/C$_2$

Air Glow O$_2$ 5577

NH$_2$/C$_2$

NH$_2$/C$_2$

Butane Torch

C$_2$ 5165
C$_2$ 5130

Swan Bands

C$_2$ 4737

C$_2$ 4715
C$_2$ 4685

C$_2$/CH 4383/85

Hg I 4358.34   telluric

CH 4315

CH
CN

C$_3$

C$_3$

C$_3$ 4056

C$_3$

CN 3880

©Richard Walker 2012/03

NH$_2$

C$_2$

NH$_2$

C$_2$

NH$_2$

C$_2$

NH$_2$

C$_2$

CH

CN

C$_3$

CN

Influence zones of the individual molecule emission bands [2 10]

26 Telluric Molecular Absorption

<u>Table 95:</u>   Overview on the most dominant absorptions caused by the earth's atmosphere.

Between ca. λλ 6,200 – 7,700 it literally swarms with molecular H_2O- und O_2 absorption bands, caused by the earth's atmosphere. Few of them appear in the form of discrete lines even beyond λ 5,700, unfortunately pretending the presence of stellar absorptions. On *Table 90* the solar spectrum within the domain of λλ 6,800 – 7,800 is shown (900L grating). These features appear here so impressively that Fraunhofer has labeled them with the letters A and B. At that time he could not know that these lines do not originate from the Sun, but arise due to absorption in the earth's atmosphere.

For astronomers, they are only a hindrance, unless they need fine water vapor lines of known wavelength to calibrate the spectra. These "calibration marks" are generated by complex molecular vibration processes, appearing as a very broad scattered absorption swarm.

The atmospheric physicist deduces from the H_2O absorptions moisture profiles of the troposphere. The O_2 bands (Fraunhofer A and B) allow him conclusions about the layer temperatures of the atmosphere [180].

For the "average amateur" important is just the awareness, that the line identification within this area requests great caution. In most of the cases only the *Hα* line overtops unambiguously the "jungle" of the telluric absorption lines and bands. This is particularly the case for the early spectral classes, where the maximum of the stellar radiation occurs in the ultraviolet or blue part of the spectrum. Exceptions are here *Wolf-Rayet* and *Be-stars* and those which show mass loss due to strong *P Cygni profiles*. In the latter two cases, at least the helium line *He I* at λ 6678 can additionally be identified.

Stars of the late *K* and all *M*-classes, as well as the carbon stars, predominantly radiate in the infrared part of the spectrum. Therefore particularly intense *titanium oxide (TiO)* absorption bands are capable to overprint these telluric lines. Further the reflection spectra of the large gas planets show mainly here the impressive gaps in the continua of their spectral profiles.

These telluric bands and lines can be reduced to a certain extent with a relatively large effort – e.g. by subtraction of synthetically produced standard profiles of the telluric lines (see *Vspec* manual) and further by comparison with profiles of standard stars. Complicating facts are the influences by weather conditions, elevation angle of the object etc. For further information refer to [180], [181].

TABLE 95

Most significant spectral absorptions due to the earth atmosphere

Fraunhofer **A**
O_2 Absorption
7594 – 7684

H_2O Absorption
7168 - 7394

Fraunhofer **B**
O_2 Absorption
6867 – 6944

I= –0.2

© Richard Walker 2010/05
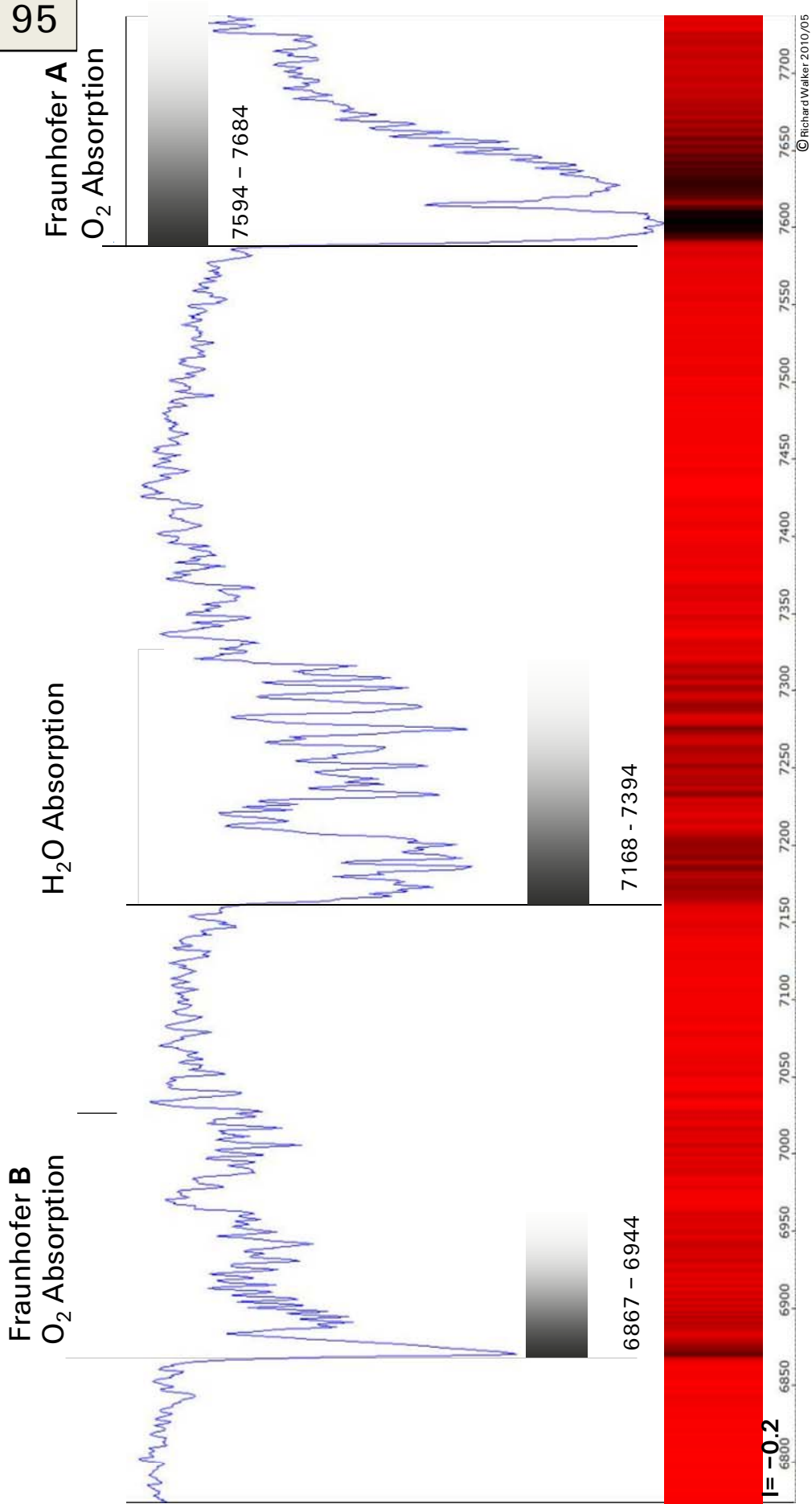
27 The Night Sky Spectrum

27.1 Introduction

Mainly due to light pollution and airglow the night sky is significantly brightened and the astronomical observations thereby seriously hampered.

The _light pollution_ is mainly caused by street lamps and other terrestrial light sources. The light is chiefly scattered by molecules and particles in the mesopause (altitude ca. 80 – 100km).

The _airglow_ is produced during the day in the atmosphere by photoionisation of oxygen as a result of solar UV radiation and chemical reaction chains. At night recombination takes place, causing emission lines at discrete frequencies. Really striking here are only two of the O I lines at λλ 5577.35 and 6300.23. The latter is visible just under a very good night sky, and therefore lacking in the spectrum of Table 96. Airglow however includes also the rotational and vibrational bands of OH molecules in the near infrared range, detected in 1950 by A. B. Meinel. Further influence, particularly over the continuum of the night sky spectrum, has the diffuse galactic light (DGL), the integrated starlight (ISL) and the reflected zodiacal light (ZL). The latter may also contribute elements of the solar spectrum. (www.caltech.edu)

27.2 Effects on the Spectrum

Depending on the quality of the night sky, at long to very long exposure times the emissions of airglow and light pollution can disturbingly superimpose the recorded signal of the examined object, example see M1, Table 85 and 96. The effects of airglow to the spectrum are much less harmful than the light pollution, which can consist of dozens of emission lines, depending on the type of terrestrial light sources in the wider surroundings, as well as meteorological factors. Under a perfect night sky, only the airglow is visible in the spectrum.

27.3 Countermeasures

In such cases helps the recording of the night sky spectrum in the immediate vicinity of the examined object (with the same exposure time). This must then be subtracted from the object spectrum, eg with Fitswork.

27.4 Comments to Table 96

This night sky spectrum was recorded to clean the disturbed spectrum of M1 (Table 85). It was taken at my home (Rifferswil Switzerland) about 610m above sea level, under a rather moderately good rural sky with a limiting magnitude of about 4–5^m and an elevation angle of approximately 50°. For such long exposures (30 Minutes) the C8 was equipped with a long dew cap to reduce the influence of scattered light from the surrounding area. The lighting of the residential area consists of gas discharge lamps, of which some but not all spectral lines appear in the spectrum. Major roads with sodium vapor lamps are some 100m distant without a direct line of sight. As the most harmful source of pollution in literature consistently high-pressure sodium vapor lamps are referred, since they produce a bell-shaped emission around the Fraunhofer D Lines λ 5890/96 D (see also Table 104). This feature can hardly be effectively filtered out without impairing of the wanted signal. Not surprisingly the famous sky contamination act („La Ley del Cielo"), affecting the islands of Tenerife and La Palma, severely limits the use of high-pressure sodium vapor lamps [190]!

TABLE 96

Night Sky Spectrum
Rifferswil Switzerland

OH Meinel Bands: Molecular Rotational- and Vibrational Bands

Na I 6154/65

6115 Ar II / Xe II

High-Pressure Sodium Vapor

Na I 5890/96

HG I 5790
HG I 5770

Na I 5683/88

[O I] 5577.35 Airglow

?

Hg I 5460.75
Xe II 5419.15

M1 Spectrum + Light Pollution

M1 Spectrum

O₂ Lines

[O I] 4802 ?

Hg I 4358.34

©Richard Walker 2010/05
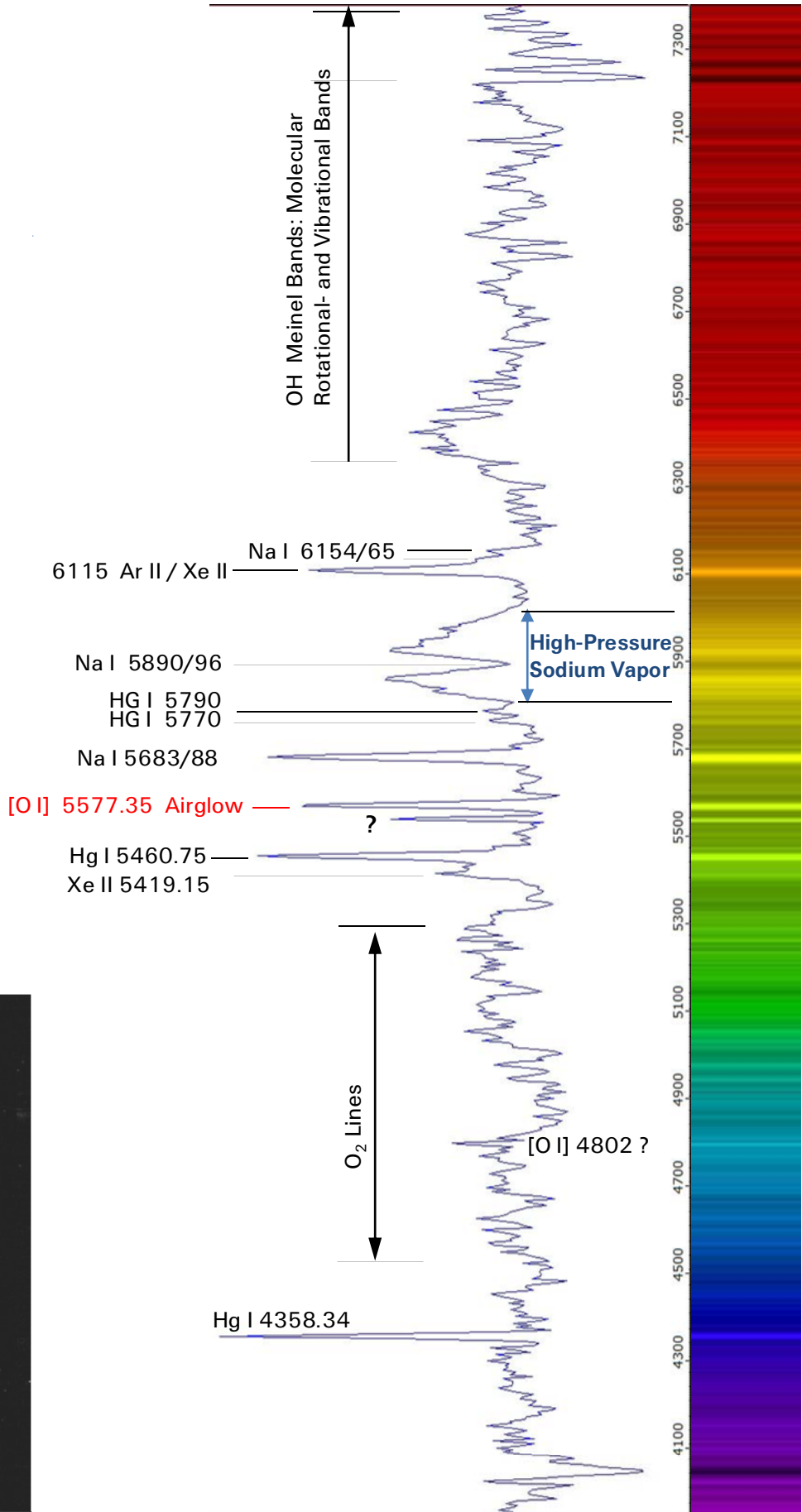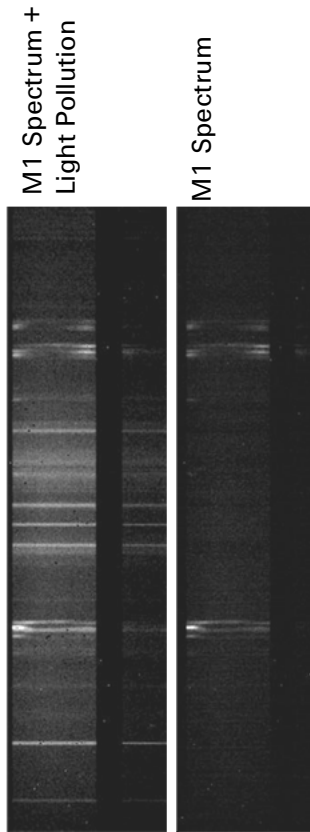
28 Terrestrial Lightsources

28.1 Spectra of Gas Discharge Lamps

Gas discharge lamps play a key role for astronomers. They can be useful, for example to calibrate the spectral profiles - but also represent a disturbing source e.g. by light pollution from the road- and municipal lighting. For beginners they are also usefull exercise objects to study the spectra – particularly during cloudy nights.

Table 101: *Neon glow lamps*

The orange glowing neon glow lamps are used as indicator lights, e.g. for stoves, flat irons, connection plug boards etc. They produce a large number of emission lines, mainly in the red region of the spectrum. Their wavelengths are known with high accuracy. These properties make them very popular as calibration lamps among the amateurs. The disadvantage is that the intense lines are limited to the red region of the spectrum. Further they can only be operated with mains voltage of 230V, therefore posing a safety risk and requiring specific electrotechnical safety measures. With very long exposures, especially in the green area further emissions will appear, but coupled with the disadvantage that the most intense neon lines in the red range of the spectrum become oversaturated at low to moderately high-resolution spectrographs. Such lines can therefore no longer be used for calibration purpose within the same profile. For the calibration of broadband spectra (red to blue) or higher-resolved profiles within the blue range, low cost solutions according to tables 103 and 106 are preferred. In the professional sector or on the senior amateur level, relatively expensive hollow cathode lamps are used, producing a fine raster of eg iron-argon emission lines.

Table 102: *Energy saving lamp ESL Osram Sunlux*

Amateurs often use ESL as a complement to the neon lamps, which are limited to the red part of the spectrum. These lamps contain several gases and substances performing different tasks – among other things, fluorescent substances, usually so called *rare earth* metals. The mixture depends largely on the color, the lamp should produce. Anyway for calibration purposes usefull are only the intense lines of the auxiliary gases, e.g. Argon (Ar), Xenon (Xe), and Mercury (Hg). Unfortunately, some of these line positions are located very close together and are therefore difficult to distinguish, such as Ar II (6114.92) and Xe (6115.08).

Table 103: *Xenon strobe tube*

Better-suited for the broadband calibration of profile graphs, is the spectrum of a xenon strobe light, e.g. kit K2601 from *Velleman*. This kit is designed primarily as position lamp for model aircraft as well as for lighting effects on stages, dancefloors, in shop windows etc. The flicker frequency for the calibration purpose must be adjusted to the maximum and the lamp requires some 15 seconds warmup time to produce accurately the specified lines. This lamp generates some 50 useful lines, distributed over the entire range from the near infrared to violet (about λλ 8,000 – 3,900). In the infrared domain further emissions are available, but not documented here. Most emission lines are produced by *xenon*. However the shortwave-end of the spectrum is dominated by lines of *rare earths*. The xenon tube gets very hot during operation. Further it requires also mains voltage of 230V. Therefore an appropriate housing is needed.

Table 104: *High pressure sodium vapor lamp for street lighting*

This lamp is widely used for street lighting. The sodium generates light in the domain of the Fraunhofer D1, and D2 line. Due to the high gas pressure it's not a real monochromatic light. The continuum, as a result of *pressure and collision broadening*, as well as *self*

absorption effects, shows a bell-like shape. Added auxiliary gases, for example Xenon, can produce some discrete lines in the spectrum.

<u>Table 105:</u> *High power Xenon lamp*

Such high pressure gas discharge lamps are used for lighting of stadiums, position lamps on mountain tops etc.

The line identification in Table 102 – 105 is based on Vspec (*Tools/Elements/elements),* as well as on data sheets from the lamp manufacturers.

<u>Table 106:</u> Glow Starter ST 111 from OSRAM, (4–80W, 220V–240V)

Another alternative for broadband calibration and detailed analysis in the blue range of spectra are modified glow starters for fluorescent lamps. They contain a small gas discharge lamp, which is not used there as light source but as a bimetal switch. For our special purpose it must be wired with a series resistor (details see [34]). OSRAM declares the composition of the gas with hydrogen *H* and argon *Ar*. The light output in the blue range of the spectrum is relatively weak and may require somewhat longer exposure times. For 110V mains, appropriate starters may be used also from other suppliers. The necessary series resistors must be determined by tests. The current must be limited to the extent, that a reasonable light output is achieved without closing the bimetal switch. In the case of ST111 40-80W, ~24 kΩ was evaluated. Rainer Ehlert from Mexiko tested the 110V type "Fulgore" and evaluated the same resistor value!

TABLE 101

Spectrum Neon Glow lamp

TABLE 102

Spectrum ESL Osram Sunlux

Ar 6114.92 Å
Xe 6115.08 Å ?

Ar 6307.66 Å

Hg 5769.6 Å

Hg 5790.66 Å

Hg 5460.75 Å

Xe 5419.15 Å

Hg 4358.33 Å

Hg 4046.57 Å

Hg 4077.83 Å
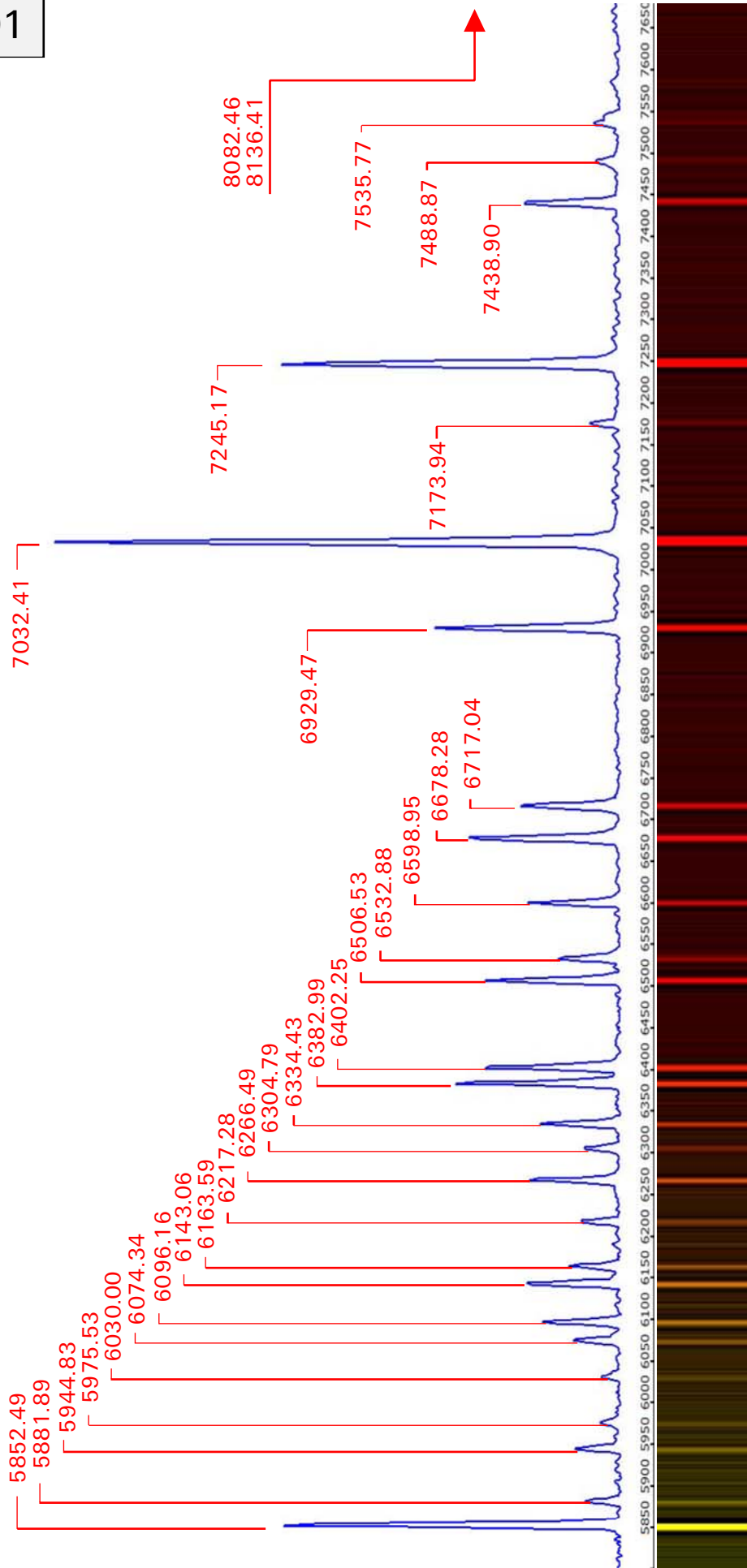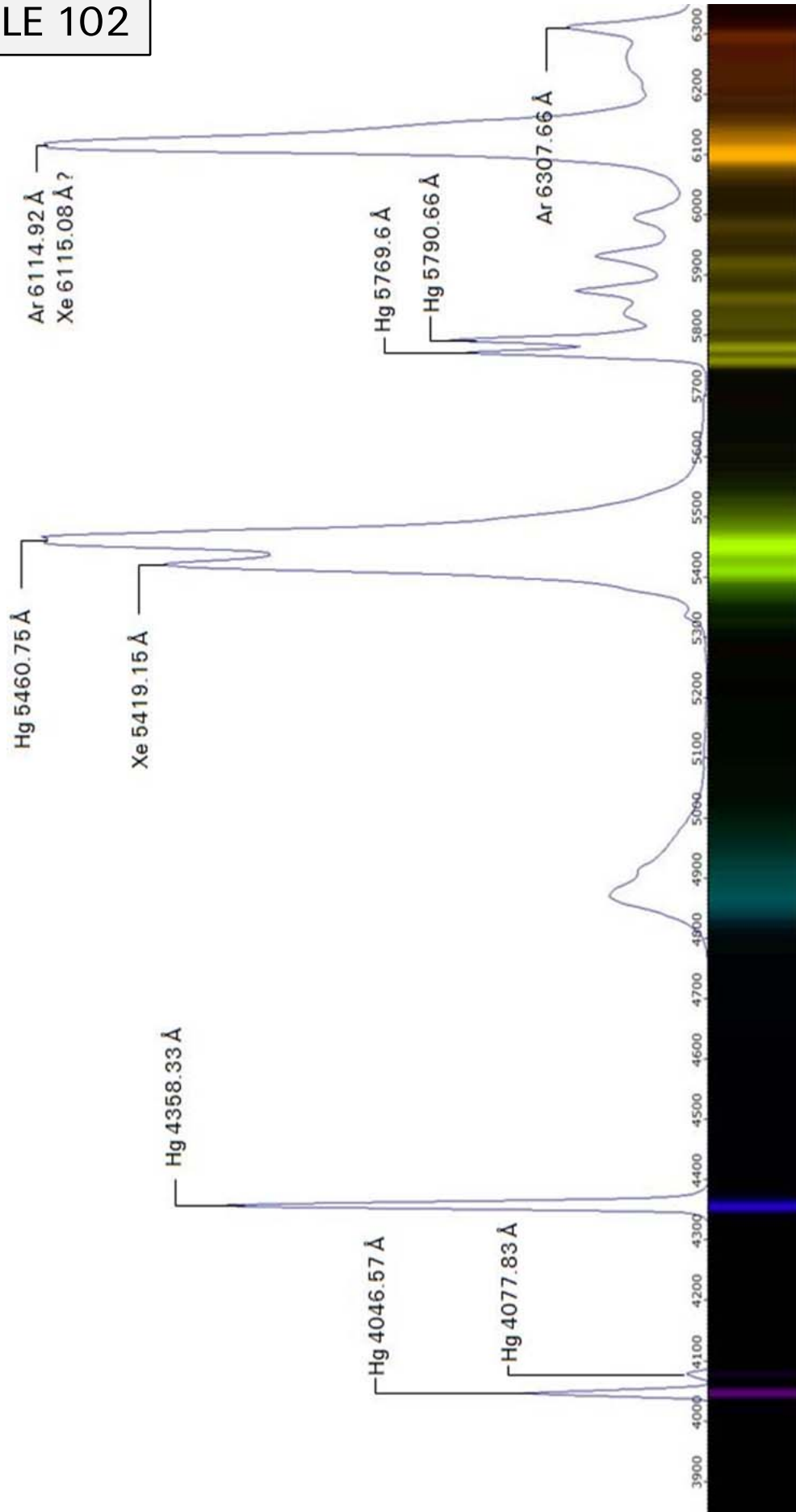
TABLE 103

Spectrum of the Xenon Strobotube 27 WS   Kit: Velleman   K2601

Xe 6182.42

Xe 6097.59

Xe 6051.15
Xe 6036.2

Xe 5976.46

Xe 5934.17

Xe 5893.29
Xe 5875.02

Xe 5824.8

Xe 5751.03

Xe 5699.61

Xe 5667.56

Xe 5616.67

Xe 5531.07

Xe 5472.61
Xe 5460.39
Xe 5438.96

Xe 5419.15

Xe 5372.39

Xe 5339.33

Xe 5292.22

Xe 5261.95

Xe 5191.37

Xe 5125.7

Xe 5080.62

Xe 5028.28

Xe 4988.77
Xe 4971.71

Xe

Lines lacking wavelength indications are not fit for calibration purposes

Xe 8061.34
Xe 7967.34
Xe 7887.4

Xe 7642.02

Xe 7393.79

Xe 7284.34

Xe 7119.6

Xe 6976.18

Xe 6882.16

Xe 6827.32

Xe 6728.01

Xe 6668.92

Xe 6595.01

Xe 6469.7

Xe 6318.06

Xe 6182.42

Xe 4843.29
Xe 4828.04

Xe 4807.02

Xe 4734.15

Xe 4673.7

4624.9 Ce?

4525.31 La?
4501.52 Cs?

4384.43 Cs?

4193.8 Ce?

4080 Ce?

3952.54 Ce?

©Richard Walker 2010/07

TABLE 104

High pressure sodium vapor lamp

Ar I 7067.21 Å

Ar I 6170 Å
Na I 6175 Å

Na 5890 / 5896 Å

Xe I 5696 Å
Na I 5688 Å

Ar I 5212 Å
Xe I 5239 Å

Xe I 4988/91 Å
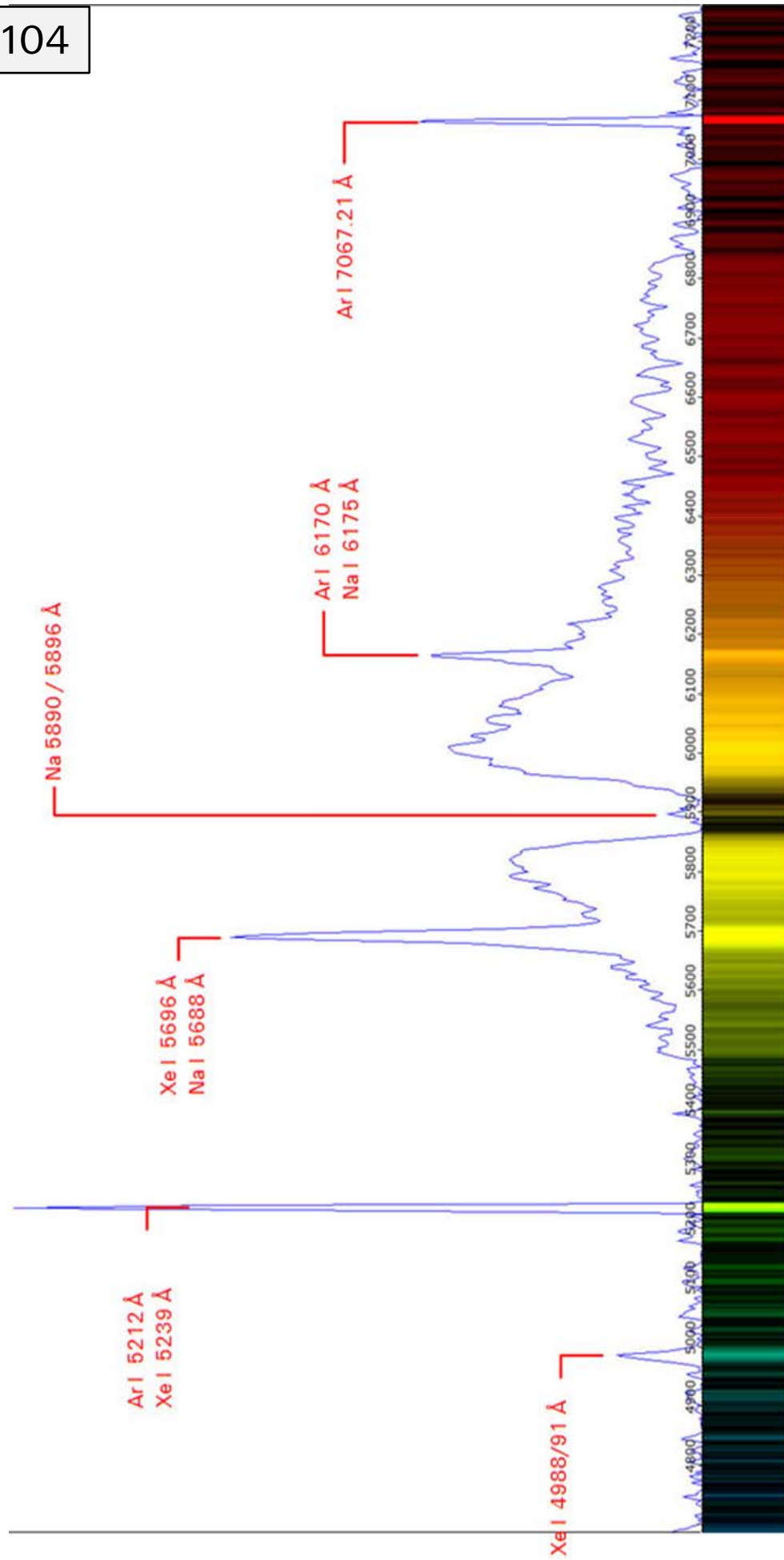
TABLE 105

Xenon high power lamp
Position lamp on the summit of Mt. Rigi

Xe: Xenon
Y: Yttrium fluorescence material
Zr : Zirconium (Getter material)
Tm: Thulium (activation of the luminescent substance)
Dy: Dysprosium (color optimization emission spectrum)
Ne: Neon
Sc: Scandium (color optimization emission spectrum)

Y I 5893.93 Å
Xe I 5893.29 Å

Tm I 5685.19 Å
Dy I 5685.58 Å

Sc I 5020.14 Å

Zr I 6160.20 Å

Ne I 6402.25 Å
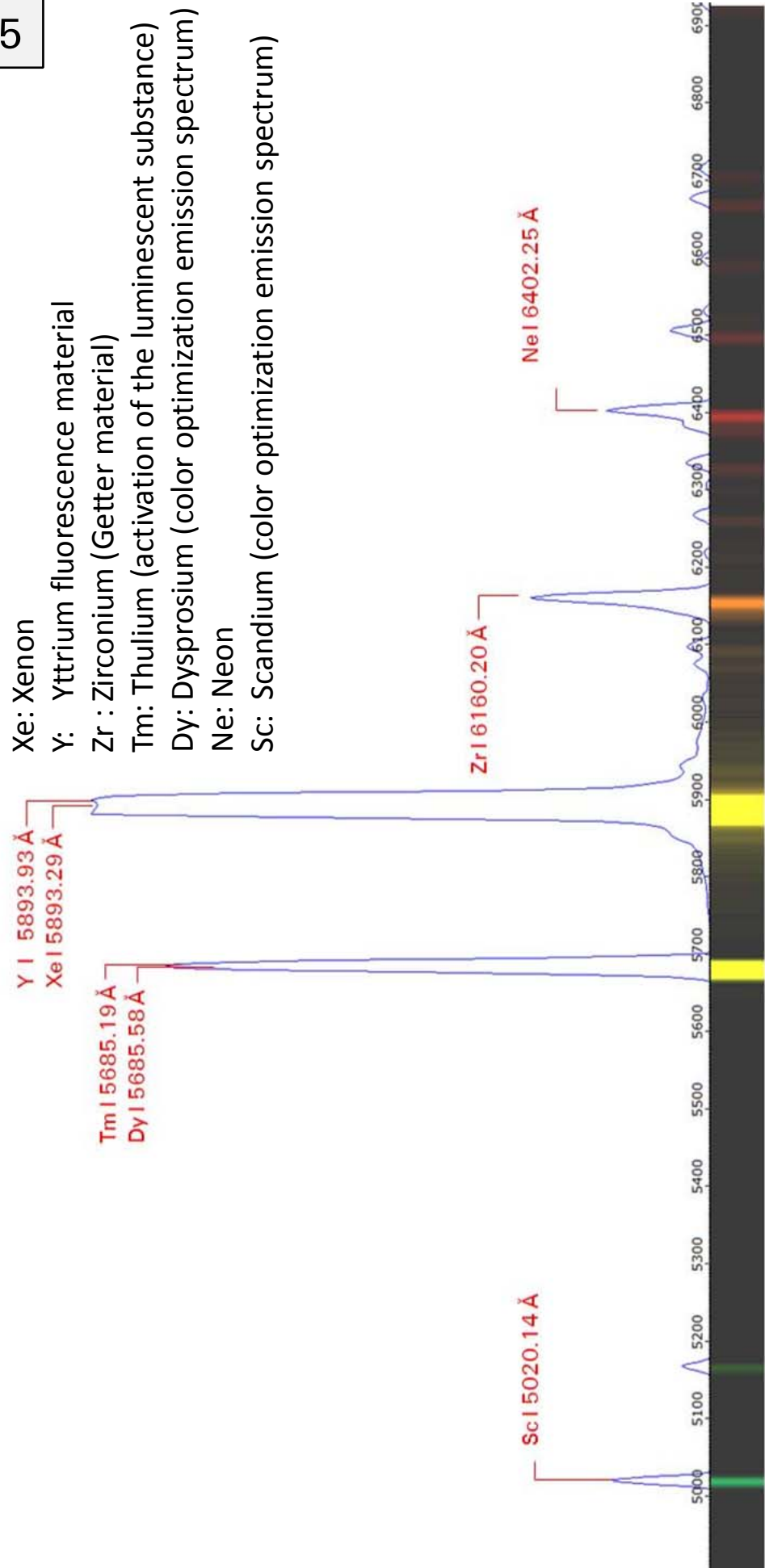
TABLE 106

Spectrum Glow Starter OSRAM ST 111 4-80W   Grating: 900L/mm

Ar 4764.78
Ar 4735.91
Ar 4726.87
Ar 4657.9
Ar 4609.57
Ar 4589.89
Ar 4579.35
Ar 4545.05
Ar 4510.73
Ar 4481.81
Ar 4474.76
Ar 4448.88
Ar 4426.0
Ar 4400.99
Ar 4379.67
Ar 4370.75
Hγ 4348.06
Ar 4340.47
Ar 4300.1
Ar 4277.53
Ar 4259.36
Ar 4237.22
Ar 4228.16
Blend
Ar 4190.71
Ar 4158.59
Ar 4131.72
Ar 4103.91
Blend mit Hδ
Ar 4072
Ar 4052.9
Ar 4042.89
Ar 4013.86
Ar 3994.79
Ar 3979.36
Blend
Ar 3928.6 →

Grating: 200L/mm

Blend
Ar 7635.11
Blend
Ar 7383.98
Ar 7272.94
Ar 7147.04
Ar 7067.22
Ar 6965.43
Ar 6871.29
Ar 6752.83
Ar 6677.28
Hα 6562.85
Ar 6416.31
Ar 6172.28
Ar 6032.13
Ar 5606.73
Ar 5495.87
Ar 4965.08
Hβ 4861.33
Ar 4806.02
Ar 4764.87
Ar 4657.9
Ar 4609.57
Ar 4545.05
Ar 4510.73
Blend
Blend
Ar 4277.53
Ar 4200.67
Ar 4158.59
Ar 4072.0
Blend

28.2 Spectra of Gasflames

Table 110: *Swan Bands* in comparison to the following spectra:
butane gas torch, *comet Hyakutake* and carbon star *WZ Cassiopeiae*

The Swan Bands, already described in sect. 22, are of great importance for astrophysics. They are generated e.g. in the cool atmospheres of carbon stars as <u>*absorption bands*</u> and in the comets of the solar system as <u>*emission bands*</u>. Molecular band spectra are generated by complex rotational and vibrational processes of heated molecules [3]. The required exitation energy to generate *Swan Bands* is relatively low. Therefore this spectral detail can be easily simulated by the intense combustion of hydrocarbons with do it yourself equipments from the hardware store!

Table 110 shows the *Swan Bands*, generated with a *butane torch*. The wavelengths of the most intensive *band heads* are λλ 6191, 5636, 5165, 4737 and 4383. Further a number of *fainter C_2* absorptions are still recognisable, with wavelengths according to [110]. Some of these lines are also visible in the profiles of the carbon stars in *Table 65*.

In this *table,* spectra of the butane gas flame (C_4H_{10}), comet *Hyakutake* and the carbon star *WZ Cassiopeiae* (excerpt from *Table 67*) are superposed. The shape of the *Hyakutake* profile (March 28, 1998) was transfered to and accordingly scaled up in the drawing from an ESO/Caos project http://www.eso.org/projects/caos/.

Striking are the amazingly similar *emission spectra* of the comet *Hyakutake* and the *butane gas flame* within the domain of the *C_2 Swan bands!* That's why for both cases the same physical process is taking effect. *WZ Cassiopeiae* shows the *Swan Bands* in *absorption* instead of *emission*. Therefore the shape of this profile runs inversely to the others.

The line identification is based amongst others on [110], [210].

Tests with acetylen flames (C_2H_2), carried out in the workshop of Urs Flükiger, yielded similar results (Photo below).
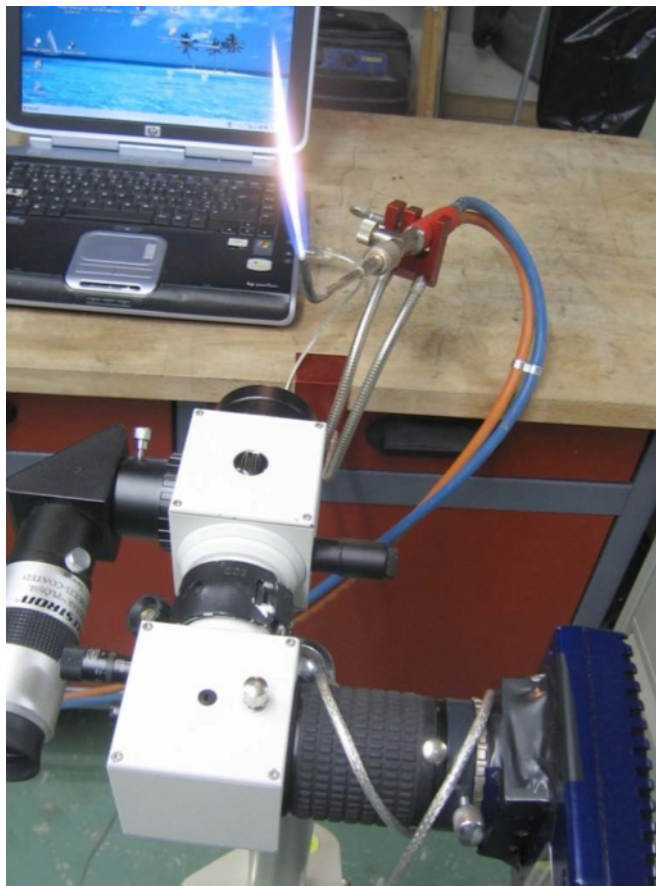
TABLE 110

Swan Bands: Butane torch, Comet Hyakutake and WZ Cas

Butane torch

C$_2$ 6191

C$_2$ 5636
C$_2$ 5585
C$_2$ 5541
C$_2$ 5502

C$_2$ 5165

C$_2$ 5130

Swan Bands

Comet Hyakutake

C$_2$ 4737
C$_2$ 4715
C$_2$ 4698
C$_2$ 4685

C$_2$ /CH 4383/85

CH 4315

CH 3900/3880

WZ Cassiopeiae
carbon star

©Richard Walker 2010/05
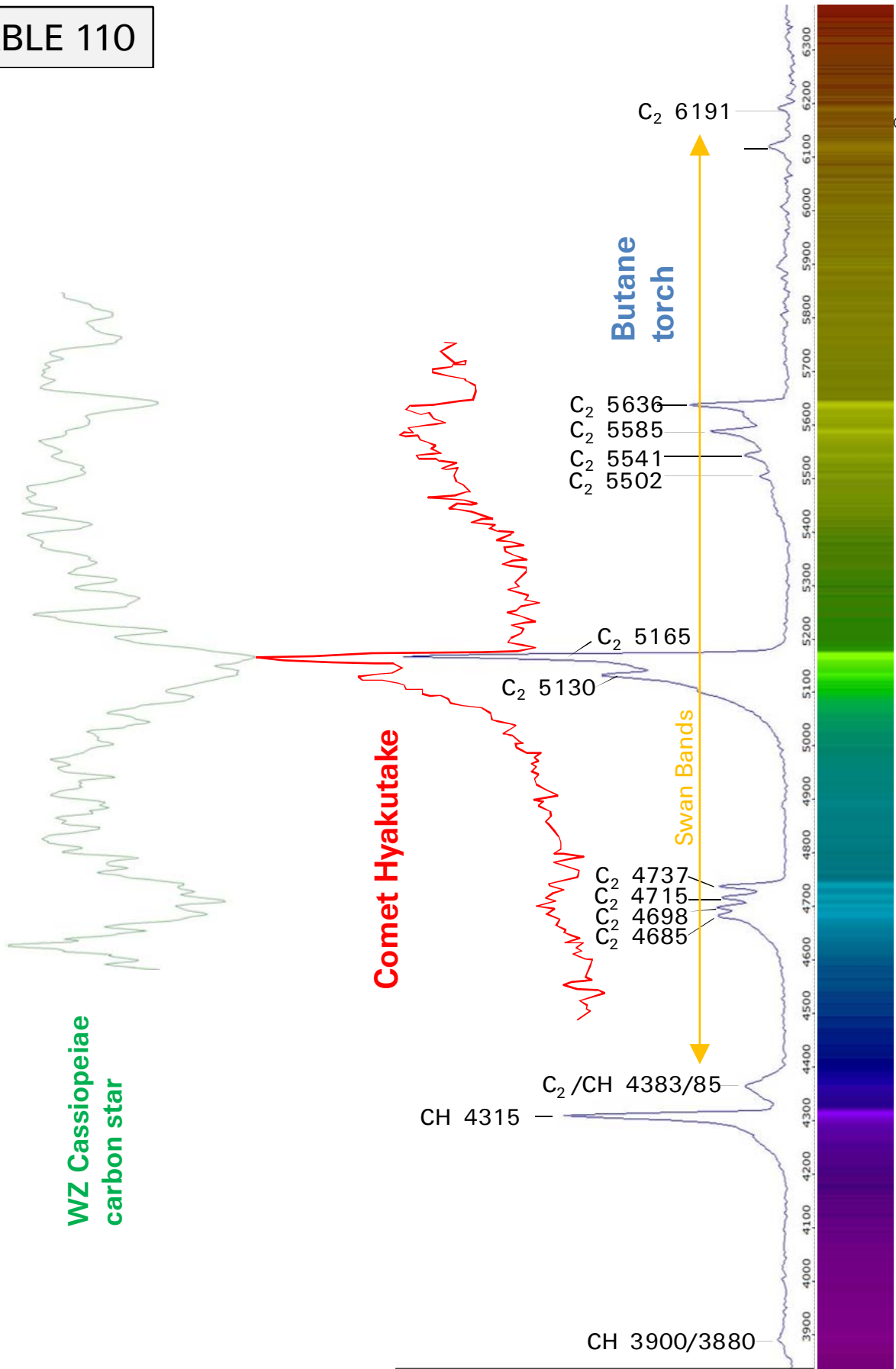
29 Spectral Classes and $v \sin i$ − Values of Important Stars

Stars of the spectral classes *O, B, A, F, G, K, M* observable from Central Europe:

Spectral class	Luminosity class	Appar. magn	$v \sin i$ [km/s]	Bayer designation	Proper name
O8	III	3.5		λ Ori A	Meissa
O9	III	2.8	130	ι Ori	Nair al Saif
O9.5	Ib	2.1		ζ Ori A	Alnitak
	II	2.2		δ Ori A	Mintaka
	V	3.7	94	σ Ori A	

B0	Ia	1.7	87	ε Ori	Alnilam
	IVe	2.5	300	γ cas	
	V	2.8	24	τ Sco	
B0.5	Ia	2.1	82	κ Ori	Saiph
	IV	2.3	181	δ Sco	Dschubba
	V	2.6		β Sco	Acrab
	IV	2.9	153	ε Per	Adid
	V	3.4	46	η Ori	Algiebbah
B1	V	1.0	159	α Vir	Spica
	II-III	2.0	36	β CMa	Mirzam
	Ib	2.9	59	ζ Per	Menkib
	III	3.2	28	β Cep	Alfirk
B2	III	1.6	59	γ Ori	Bellatrix
	IV	2.8	3	γ Peg	Algenib
B3	IV	2.0	201	σ Sgr	Nunki
	IV	3.4	19	ε Cas	Segin
B5	Ia	2.5	45	η CMa	Aludra
	IIIe	3.0	259	δ Per	
B6	III	3.2	31	ζ Dra	Aldhibah
	III	3.7	215	17 Tau	Electra
	IVe	4.2	282	23 Tau	Merope
B7	V	1.4	329	α Leo	Regulus
	III	1.7	71	β Tau	Alnath
	IIIe	2.9	215	η Tau	Alcyone
B8	IIpe	3.4		β Lyr	Sheliak
	Ia	0.1	33	β Ori	Rigel
	V	2.1	65	β Per	Algol
	IIIp Hg Mn	2.6	41	γ Crv	Gienah Corvi
	Ve	2.9	276	β Cmi	Gomeisa
	III	3.9	39	20 Tau	Maia
	III	3.6	212	27 Tau	Atlas
	Ve			β Cyg	Albireo B
	III	3.2	68	φ Sgr	
	IVp Mn Hg	2.1	56	α And	Alpheratz
B9	III	3.2	76	γ Lyr	Sulafat

Spectral class	Luminosity class	Appar. magn	$v \sin i$ [km/s]	Bayer designation	Proper name
A0	Va	0.0	15	α Lyr	Vega
	p Cr	1.8	38	ε UMa	Alioth
	IV	1.9	32	γ Gem	Alhena
A1	Vm	-1.46	13	α CMa A	Sirius A
	V	1.9		α Gem A	Castor A
	V	2.4	39	β UMa	Merak
	V	3.8	96	ε Aqr	Albali
A2	Ia	1.25	21	α Cyg	Deneb
	Vm	2.9		α Gem B	Castor B
	IV	1.9	37	β Aur	Menkalinan
A3	V	2.1	121	β Leo	Denebola
	III-IV	2.8		α Lib A	Zubenelgenubi
	V	3.4	173	ζ Vir	Heze
A4	IV	2.6	181	δ Leo	Zosma
A5	V	2.6	79	β Ari	Sharatan
	III	2.1	219	α Oph	Ras Alhague
	III-IV	2.7	113	δ Cas	Ruchbah
A7	V	0.8	242	α Aql	Altair
	V	2.4	246	α Cep	Alderamin
	III	3.0	139	γ Boo	Seginus
A9	III	3.8	141	γ Her	

F0	Iae	3.0	29	ε Aur A	Alanz
	III	3.4	84	ζ Leo	Adhafera
	IV	3.5	111	δ Gem	Wasat
	V	2.8		γ Vir	Porrima
F2	III-IV	2.3	70	β Cas	Caph
F5	IV-V	0.4	6	α CMi	Procyon
	Ib	1.8	18	α Per	Mirfak
	Ib-II	2.0	17	α Umi	Polaris
F6	IV	3.4	93	α Tri	Mothallah
F8	Ia	1.9	28	δ CMa	Wezen
	Ib	2.2	20	γ Cyg	Sadr
	V	3.6	3	β Vir	Zavijah

G0	IV	2.7	13	η Boo	Muphrid
	Ib	2.9	18	β Aqr	Sadalsuud
	III	0.1		α Aur	Capella B
G1	II	3.0	<17	ε Leo	Raselased
G2	V	-26.75	1.9	SOL	Sun
	V	-0.27		α Cen A	Rigil Kentaurus
	Ib-IIa	2.8	13	β Dra A	Rastaban
	Ib	3.0	<17	α Aqr	Sadalmelik
G5	II	2.7	<17	β Crv	Kraz
	III3e	0.1		α Aur A	Capella A
G7	IIIa	2.8	<19	β Her	Kornephoros
G8	Ib	3.0	<17	ε Gem	Mebsuta

	III Fe I	3.5	< 19	δ Boo	
	IIIa Ba0.3 Fe-0.5	3.5	< 17	β Boo	Nekkar
G8	IIIab	2.8	< 17	ε Vir	Vindemiatrix

Spectral class	Luminosity class	Appar. magn	$v \sin i$ [km/s]	Bayer designation	Proper name
K0	IIIb	1.1	< 17	β Gem	Pollux
	IIIa	1.8	< 17	α Uma	Dubhe
	IIIa	2.2	21	α Cas	Shedar
	II - III	2.4		ε Boo	Izar
K1.5	III Fe-0.5	-0.0	< 17	α Boo	Arcturus
K2	III Ca-1	2.0	< 17	α Ari	Hamal
	IIIb CN1	2.7	< 17	α Ser	Unukalhai
	III	2.8	< 17	β Oph	Cebalrai
K3	IIIa	2.7		δ Sgr	Kaus Media
	II	2.7	< 17	γ Aql	Tarazed
	II	3.1		β Cyg A	Albireo A
K4	III	2.1	< 17	β Umi	Kochab
	III Ba0.5	3.5	< 17	β Cnc	Altarf
K5	III	0.9	< 17	α Tau	Aldebaran
	III	2.2	< 17	γ Dra	Eltanin
	V	5.2	<2	61 Cyg A	
K7	IIIab	2.2		α Lyn	Alsciaukat
	V	6.1	<2	61 Cyg B	

M0	IIIa	2.1		β And	Mirach
	III	3.1		μ Uma	Tania Australis
M0.5	III	2.7		δ Oph	Yed Prior
M1.5	Ia-Ib	1.0	<20	α Sco	Antares
	IIIa	2.4		β Peg	Scheat
M1-2	Ia-Iab	0.5		α Ori	Betelgeuse
	III	2.5		α Cet	Menkar
M3	III	3.3		η Gem	Propus
	IIIab	2.9		μ Gem	Tejat Posterior
	III	3.4		δ Vir	Auva
M5	Ib - II	3.1		α Her	Ras Algethi
M7	IIIe	3-10		o Cet	Mira (variable)

Lower case letters of the Greek alphabet

α	Alpha		η	Eta		ν	Ny		τ	Tau
β	Beta		θ	Theta		ξ	Xi		υ	Ypsilon
γ	Gamma		ι	Iota		o	Omikron		φ	Phi
δ	Delta		κ	Kappa		π	Pi		χ	Chi
ε	Epsilon		λ	Lambda		ρ	Rho		ψ	Psi
ζ	Zeta		μ	My		σ	Sigma		ω	Omega

30 Required Ionisation Energies for the Individual Elements

This table shows the required energies [eV], which are needed for the ionisation of a certain element, starting from the ground state $n = 1$. Source: [201].

Z	Element	Required excitation energy [eV] to reach the following ionisation stages							
		II	III	IV	V	VI	VII	VIII	IX
1	H	13.6							
2	He	24.6	54.4						
3	Li	5.4	75.6	122.5					
4	Be	9.3	18.2	153.9	217.7				
5	B	8.3	25.2	37.9	259.4	340.2			
6	C	11.3	24.4	47.9	64.5	392.1	490.0		
7	N	14.5	29.6	47.5	77.5	97.9	552.0	667.0	
8	O	13.6	35.1	54.9	77.4	113.9	138.1	739.3	871.4
9	F	17.4	35.0	62.7	87.1	114.2	157.2	185.2	953.9
10	Ne	21.6	41.0	63.5	97.1	126.2	157.9	207.3	239.1
11	Na	5.1	47.3	71.6	98.9	138.4	172.2	208.5	264.2
12	Mg	7.6	15.0	80.1	109.2	141.3	186.5	224.9	265.9
13	Al	6.0	18.8	28.4	120.0	153.7	190.5	241.4	284.6
14	Si	8.2	16.3	33.5	45.1	166.8	205.1	246.5	303.2
15	P	10.5	19.7	30.2	51.4	65.0	230.4	263.2	309.4
16	S	10.4	23.3	34.8	47.3	72.7	88.0	280.9	328.2
17	Cl	13.0	23.8	39.6	53.5	67.8	98.0	114.2	348.3
18	Ar	15.8	27.6	40.7	59.8	75.0	91.0	124.3	143.5
19	K	4.3	31.6	45.7	60.9	82.7	100.0	117.6	154.9
20	Ca	6.1	11.9	50.9	67.1	84.4	108.8	127.7	147.2
21	Sc	6.5	12.8	24.8	73.5	91.7	111.1	138.0	158.7
22	Ti	6.8	13.6	27.5	43.3	99.2	119.4	140.8	168.5
23	V	6.7	14.7	29.3	46.7	65.2	128.1	150.2	173.7
24	Cr	6.8	16.5	31.0	49.1	69.3	90.6	161.1	184.7
25	Mn	7.4	15.6	33.7	51.2	72.4	95.0	119.3	196.5
26	Fe	7.9	16.2	30.7	54.8	75.0	99.0	125.0	151.1
27	Co	7.9	17.1	33.5	51.3	79.5	102	129	157
28	Ni	7.6	18.2	35.2	54.9	75.5	108	133	162
29	Cu	7.7	20.3	36.8	55.2	79.9	103	139	166
30	Zn	9.4	18.0	39.7	59.4	82.6	108	134	174
31	Ga	6.0	20.5	30.7	64				

31 Bright Planetary Nebulae sorted by Excitation Classes

This table shows the Planetary Nebulae up to apparent magnitude 11m, sorted by excitation class E, according to *Gurzadyan* et al [206]. The temperatures of the central stars are from J. Kaler [207], the spectral classes from CDS / SIMBAD [500], magnitudes from Karkoschka or Wikipedia.

E	Catalogue	Popular Name	Constellation	App. mag.	Central Star Spectral class	Temperature T_{eff} [K]
1	IC418	Spirograph Nebula	Hare	9m3	O7fp	35,000
2	IC2149		Charioteer	10m6	O7.5	
2	IC4593		Hercules	10m9		35,000
2	IC4776		Archer	11m5		
2	IC4997		Archer	11m5		49,000
3	IC3568		Giraffe	11m5		57,000
4	NGC6210	Turtle	Hercules	8m8	O7f	58,000
4	NGC6790		Eagle	10m5		76,000
4	NGC6891		Dolphin	10m5		
5	NGC6543	Cat's Eye	Drache	8m1	O7+WR	80,000
5	NGC6803		Eagle	11m4		
7	NGC6884		Swan	10m9		87,000
7	NGC7009	Saturn Nebula	Water Bearer	8m3		90,000
7	NGC6572	Blue Racquetball	Serpent Bearer	9m0	Of+WR	100,000
7	NGC7293	Helix Nebula	Water Bearer	7m5	DA0	110,000
8	NGC1514		Bull	10m9	DB8	
8	NGC1535		River	10m6		
8	NGC3587	Owl Nebula	Great Bear	9m9		
9	NGC3132	South. Ring Nebula	Sails	8m2		
9	NGC6886		Arrow	11m4		168,000
9	NGC6741	Phantom Streak	Eagle	11m0		180,000
9	NGC3242	Ghost of Jupiter	Fem Water Snake	7m7		90,000
9	NGC3918		Centaur	8m5		
10	NGC7662	Blue Snowball	Chained Maiden	8m3		110'000
10	NGC7027		Swan	8m5	invisible	
10	NGC6853	Dumbbell Nebula	Fox	7m5	DO7	160'000
10	NGC2438		Puppis Stern	10m1		
10	NGC650	Small Dumbb. Nebula	Hero	10m1		
10	NGC6818		Archer	9m3		155'000
10	NGC6302	Bug Nebulal	Scorpion	9m6		
10	NGC6720	Ring Nebula	Lyre	8m8		150'000
10	NGC2392	Eskimo Nebula	Twins	9m1		65'000
11	NGC6826	Blinking Planetary	Swan	8m8		100'000
11	NGC2818		Compass	8m2		
11	NGC7008		Swan	10m7		
12	NGC1360		Furnace	9m4		
12+	NGC246		Sea Monster	10m9		
12+	NGC4361		Crow	10m9		

32 Terminology of the Spectroscopic Wavelenght Domains

Terminology for wavelength domains is used inconsistently in astrophysics [2] and depends on the context. Furthermore many fields of astronomy, various satellite projects etc. often use different definitions.

Here follows a summary according to [2], [11] and Wikipedia (*Infrared Astronomy*). Given are either the center wavelength λ of the corresponding photometric band filters, or their approximate passband.

Optical region UBVRI   λλ 3300 − 10,000 (Johnson/Bessel/Cousins)

Center wavelength		Astrophysical wavelength domain	Required instruments
λ [µm]	λ [Å]		
0.35	3,500	**U** − Band (UV)	Most optical telescopes
0.44	4,400	**B** − Band (blue)	
0.55	5,500	**V** − Band (green)	
0.65	6,500	**R** − Band (red)	
0.80	8,000	**I** − Band (infrared)	

Further in use is also the *Z−Band, some* λλ 8,000 − 9,000 and the *Y−Band, some* λλ 9,500 − 11,000 (ASAHI Filters).

Infrared region according to Wikipedia (*Infrared Astronomy*)

Center wavelength		Astrophysical wavelength domain	Required instruments
λ [µm]	λ [Å]		
1.25	10,250	**J** − Band	Most optical- and dedicated infrared telescopes
1.65	16,500	**H** − Band	
2.20	22,000	**K** − Band	
3.45	34,500	**L** − Band	Some optical- and dedicated infrared telescopes
4.7	47,000	**M** − Band	
10	100,000	**N** − Band	
20	200,000	**Q** − Band	
200	2,000,000	Submilimeter	Submilimeter telescopes

For ground based telescopes mostly the following terminology is in use [Å]:

− Far Ultraviolett (FUV):   λ <3000
− Near Ultra Violett (NUV):   λ 3000 − 3900
− Optical (VIS):   λ 3900 − 7000
− Near Infrared (NIR):   λ 6563 (Hα) − 10,000
− Infrared or Mid-Infrared: λ 10,000 − 40,000   (J, H, K, L − Band 1 − 4 µm)
− Thermal Infrared: λ 40,000 − 200,000 (M, N, Q − Band 4 - 20µm)
− Submilimeter: λ >200,000 (200 µm)

33 Appendix

33.1 Constellations

Constellation Latin genitiv	Abbrev.	Proper name
Andromedae	And	Chained Maiden
Antliae	Ant	Air Pump
Apodis	Aps	Bird of Paradise
Aquarii	Aqr	Water Bearer
Aquilae	Aql	Eagle
Arae	Ara	Altar
Arietis	Ari	Ram
Aurigae	Aur	Charioteer
Bootis	Boo	Herdsman
Caeli	Cae	Engraving Tool
Camelopardalis	Cam	Giraffe
Cancri	Cnc	Crab
Canum Venaticorum	CVn	Hunting Dogs
Canis Maioris	CMa	Great Dog
Canis Minoris	CMi	Lesser Dog
Capricorni	Cap	Sea Goat
Carinae	Car	Keel
Cassiopeiae	Cas	Seated Queen
Centauri	Cen	Centaur
Cephei	Cep	King
Ceti	Cet	Sea Monster
Chamaeleontis	Cha	Chameleon
Circini	Cir	Compass
Columbae	Col	Dove
Comae Berenicis	Com	Bernice's Hair
Coronae Australis	CrA	Southern Crown
Coronae Borealis	CrB	Northern Crown
Corvi	Crv	Crow
Crateris	Crt	Cup
Crucis	Cru	Southern Cross
Cygni	Cyg	Swan
Delphini	Del	Dolphin
Doradus	Dor	Dolphinfish
Draconis	Dra	Dragon
Equulei	Equ	Little Horse
Eridani	Eri	River
Fornacis	For	Furnace
Geminorum	Gem	Twins
Gruis	Gru	Crane
Herculis	Her	Hercules
Horologii	Hor	Clock
Hydrae	Hya	Female Water Snake
Hydri	Hyi	Male Water Snake
Indi	Ind	Indian

Constellation Latin genitiv	Abbrev.	Proper name
Lacertae	Lac	Lizard
Leonis	Leo	Lion
Leonis Minoris	LMi	Lesser Lion
Leporis	Lep	Hare
Librae	Lib	Scales
Lupi	Lup	Wolf
Lyncis	Lyn	Lynx
Lyrae	Lyr	Lyre
Mensae	Men	Table Mountain
Microscopii	Mic	Microscope
Monocerotis	Mon	Unicorn
Muscae	Mus	Fly
Normae	Nor	Carpenter's Square
Octantis	Oct	Octant
Ophiuchi	Oph	Serpent Bearer
Orionis	Ori	Hunter
Pavonis	Pav	Peacock
Pegasis	Peg	Winged Horse
Persei	Per	Hero
Phoenicis	Phe	Phoenix
Pictoris	Pic	Painter's Easel
Piscium	Psc	Fishes
Piscis Austrini	PsA	Southern Fish
Puppis	Pup	Stern
Pyxidis	Pyx	Compass
Reticuli	Ret	Reticle
Sagittae	Sge	Arrow
Sagittarii	Sgr	Archer
Scorpii	Sco	Scorpion
Sculptoris	Scl	Sculptor
Scuti	Sct	Shield
Serpentis	Ser	Serpent
Sextantis	Sex	Sextant
Tauri	Tau	Bull
Telescopii	Tel	Telescope
Trianguli	Tri	Triangle
Trianguli Australis	TrA	Southern Triangle
Tucanae	Tuc	Toucan
Ursae Maioris	UMa	Great Bear
Ursae Minoris	UMi	Lesser Bear
Velorum	Vel	Sails
Virginis	Vir	Maiden
Vulpeculae	Vul	Fox
Volantis	Vol	Flying Fish

33.2 Periodic Table of Elements

hydrogen 1 H 1.0079																	helium 2 He 4.0026
lithium 3 Li 6.941	beryllium 4 Be 9.0122											boron 5 B 10.811	carbon 6 C 12.01	nitrogen 7 N 14.007	oxygen 8 O 15.999	fluorine 9 F 18.998	neon 10 Ne 20.180
sodium 11 Na 22.990	magnesium 12 Mg 24.305											aluminium 13 Al 26.982	silicon 14 Si 28.086	phosphorus 15 P 30.974	sulfur 16 S 32.065	chlorine 17 Cl 35.453	argon 18 Ar 39.948
potassium 19 K 39.098	calcium 20 Ca 40.078	scandium 21 Sc 44.956	titanium 22 Ti 47.867	vanadium 23 V 50.942	chromium 24 Cr 51.996	manganese 25 Mn 54.938	iron 26 Fe 55.845	cobalt 27 Co 58.933	nickel 28 Ni 58.693	copper 29 Cu 63.546	zinc 30 Zn 65.39	gallium 31 Ga 69.723	germanium 32 Ge 72.61	arsenic 33 As 74.922	selenium 34 Se 78.96	bromine 35 Br 79.904	krypton 36 Kr 83.80
rubidium 37 Rb 85.468	strontium 38 Sr 87.62	yttrium 39 Y 88.906	zirconium 40 Zr 91.224	niobium 41 Nb 92.906	molybdenum 42 Mo 95.94	technetium 43 Tc [98]	ruthenium 44 Ru 101.07	rhodium 45 Rh 102.91	palladium 46 Pd 106.42	silver 47 Ag 107.87	cadmium 48 Cd 112.41	indium 49 In 114.82	tin 50 Sn 118.71	antimony 51 Sb 121.76	tellurium 52 Te 127.60	iodine 53 I 126.90	xenon 54 Xe 131.29
caesium 55 Cs 132.91	barium 56 Ba 137.33	57-70 *	lutetium 71 Lu 174.97	hafnium 72 Hf 178.49	tantalum 73 Ta 180.95	tungsten 74 W 183.84	rhenium 75 Re 186.21	osmium 76 Os 190.23	iridium 77 Ir 192.22	platinum 78 Pt 195.08	gold 79 Au 196.97	mercury 80 Hg 200.59	thallium 81 Tl 204.38	lead 82 Pb 207.2	bismuth 83 Bi 208.98	polonium 84 Po [209]	astatine 85 At [210]	radon 86 Rn [222]
francium 87 Fr [223]	radium 88 Ra [226]	89-102 **	lawrencium 103 Lr [262]	rutherfordium 104 Rf [261]	dubnium 105 Db [262]	seaborgium 106 Sg [266]	bohrium 107 Bh [264]	hassium 108 Hs [269]	meitnerium 109 Mt [268]	ununnilium 110 Uun [271]	unununium 111 Uuu [272]	ununbium 112 Uub [277]		ununquadium 114 Uuq [289]			

* Lanthanide series

lanthanum 57 La 138.91	cerium 58 Ce 140.12	praseodymium 59 Pr 140.91	neodymium 60 Nd 144.24	promethium 61 Pm [145]	samarium 62 Sm 150.36	europium 63 Eu 151.96	gadolinium 64 Gd 157.25	terbium 65 Tb 158.93	dysprosium 66 Dy 162.50	holmium 67 Ho 164.93	erbium 68 Er 167.26	thulium 69 Tm 168.93	ytterbium 70 Yb 173.04

** Actinide series

actinium 89 Ac [227]	thorium 90 Th 232.04	protactinium 91 Pa 231.04	uranium 92 U 238.03	neptunium 93 Np [237]	plutonium 94 Pu [244]	americium 95 Am [243]	curium 96 Cm [247]	berkelium 97 Bk [247]	californium 98 Cf [251]	einsteinium 99 Es [252]	fermium 100 Fm [257]	mendelevium 101 Md [258]	nobelium 102 No [259]

33.3 Some Excerpts of Historical and up to date Spectral Atlases

The very first *Spectral Atlas* was written by Father *Angelo Secchi* at the Vatican Observatory, illustrating his classification system. Many sources call him therefore "Father of the modern astrophysics". The tables with the hand drawn spectra are taken from the german translation of his book *Die Sterne, Grundzüge der Astronomie der Fixsterne* (1878). Courtesy by Martin Brunold [705].
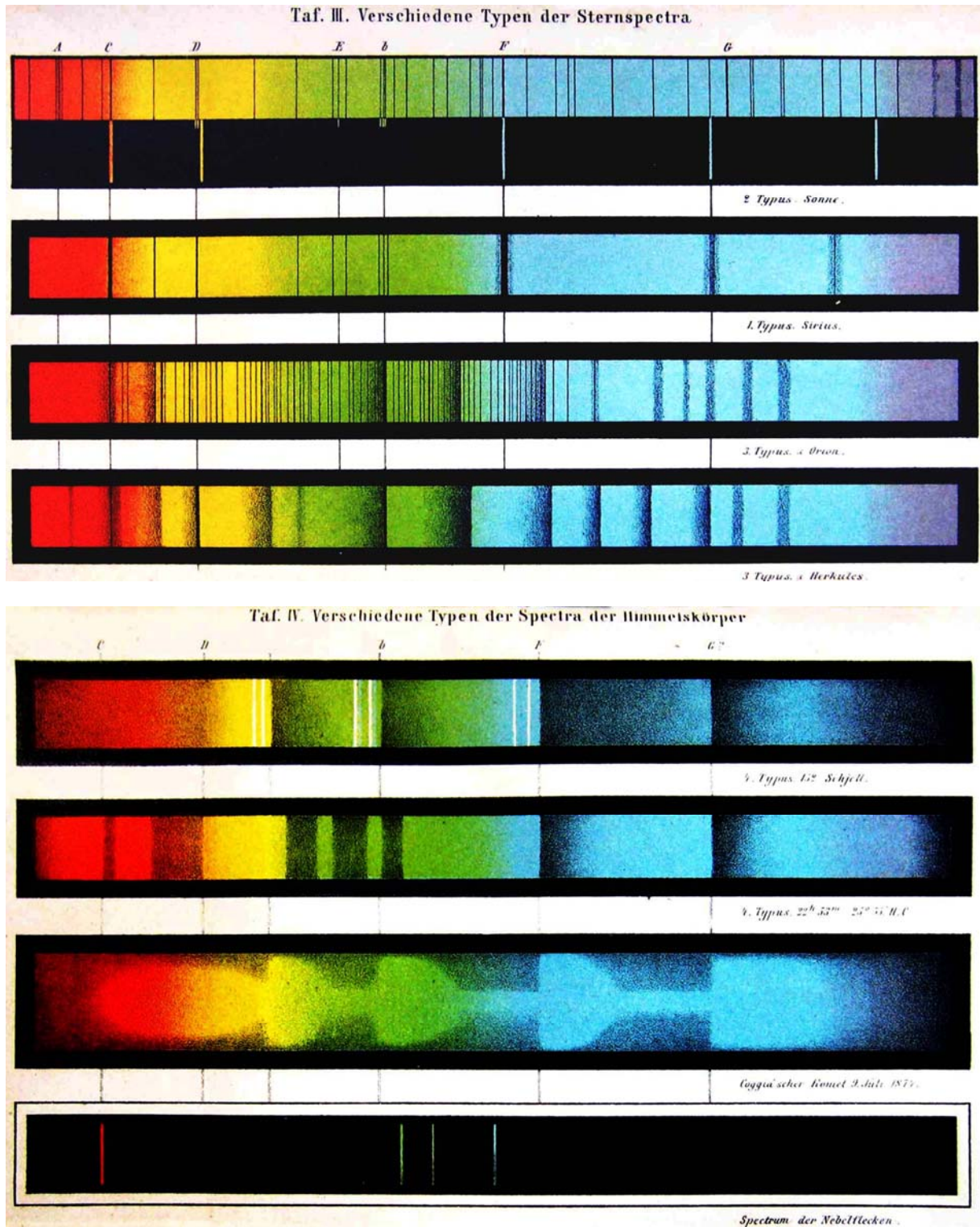
Excerpt from *An atlas of stellar spectra, with an outline of spectral classification,* Morgan, Keenan, Kellman 1943 [50].
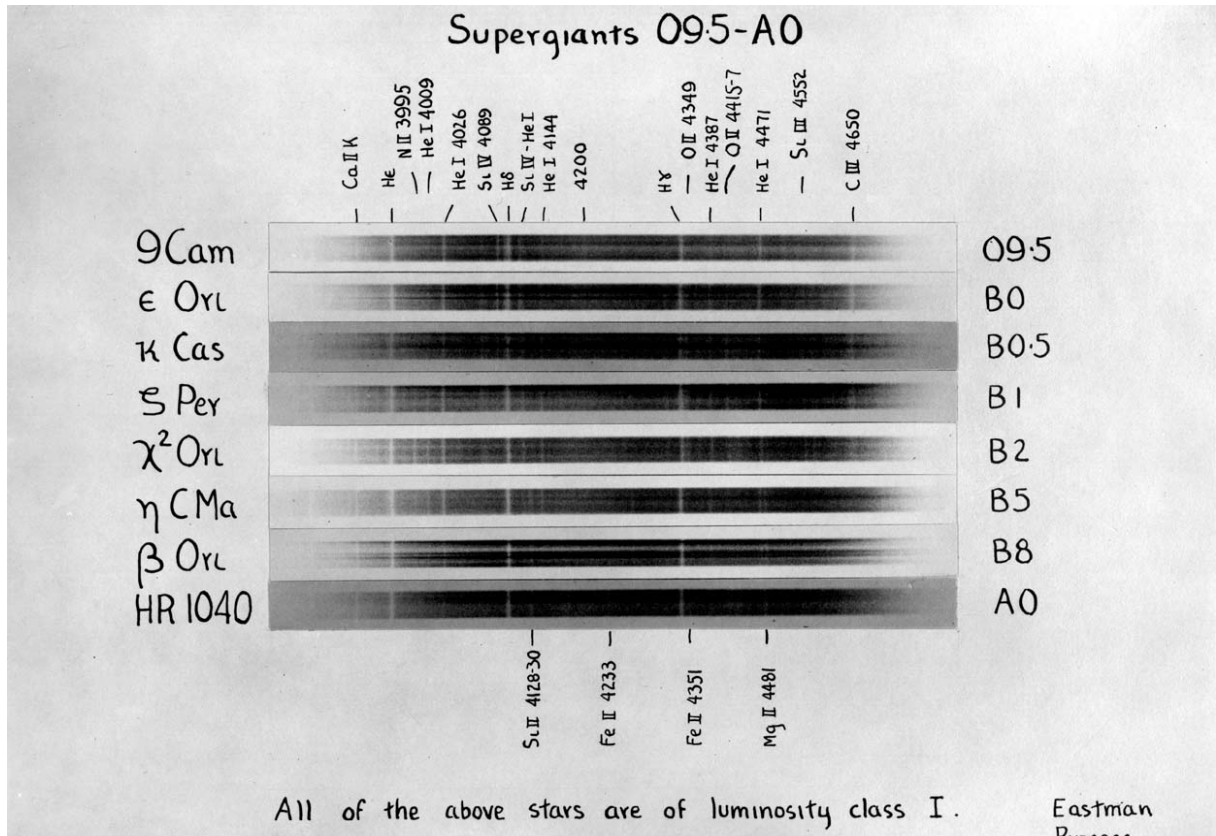
Excerpt from the *Bonner Spektralatlas* (out of print), 1975, Waltraut Carola Seitter (Collection Martin Brunold). The presentation of the spectra is here strictly ordered by luminosity classes (here Ia).
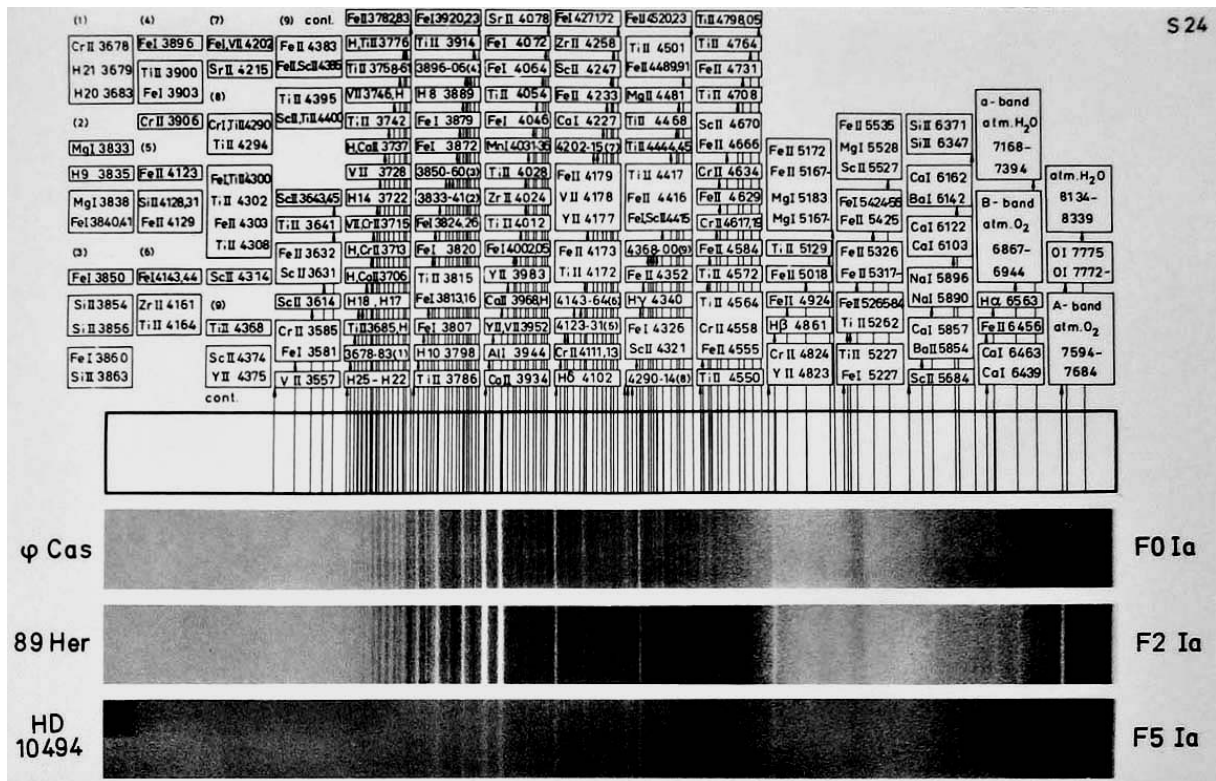
Excerpt from *Revised MK Spectral Atlas for Stars earlier than the Sun*
W.W. Morgan, H.A. Abt, and J.W. Tapscott, (1978)

LUMINOSITY EFFECTS NEAR A2

The Balmer lines of hydrogen — and the lines of Ti II and Fe II — are very sensitive to differences in luminosity near this spectral type.

↑ = strengthens toward brighter M.   ↓ = strengthens toward fainter M.   T = relatively unchanged with M.

A sensitive discriminant in use is the change in appearance of the line-pattern in the range of λλ 4383–4584: Mg II 4481 stands out over the numerous singly-ionized metallic lines surrounding it, at luminosity class V; it loses this preeminence on passing toward higher luminosity, and is no longer outstanding at A2 Ia.

Excerpt from *A Digital Spectral Classification Atlas*   R.O. Gray, (2000)

Luminosity Effects at B5
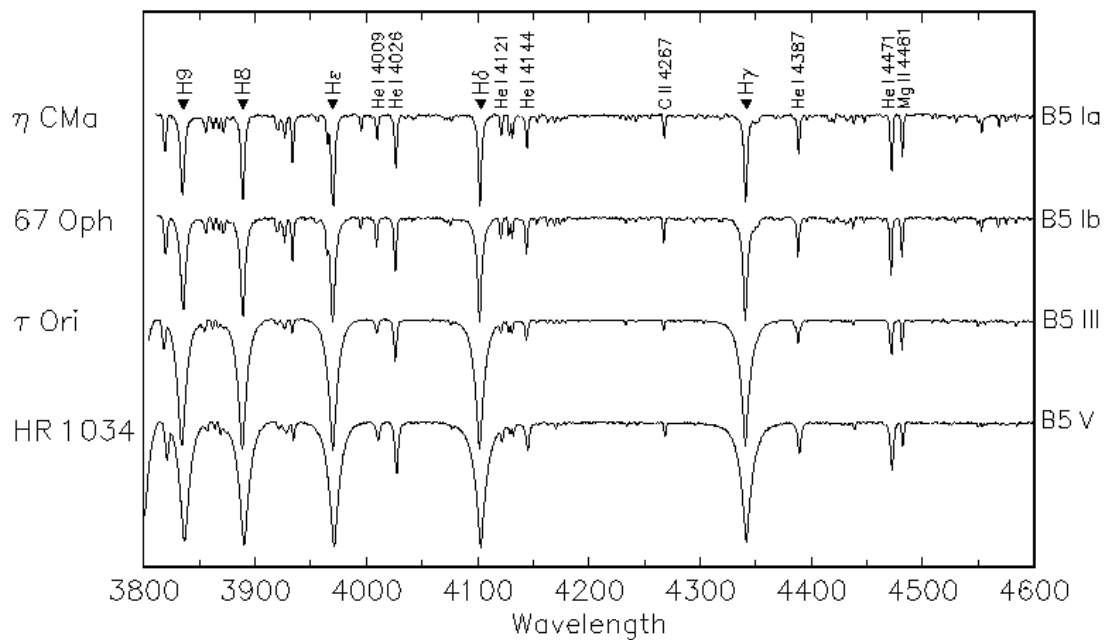
33.4 Instruments

Telescope: Celestron C8, aperture 8 Inch, focal length some 200 cm
                    Mount: Equatorial, Vixen Sphinx SXD

Spectrograph: DADOS, Baader Planetarium, Reflexion gratings 200 and 900L/mm,
Slit width: 25, 35 and 50µm

Camera: Meade DSI III Pro monochrom

Location: Rifferswil, Switzerland   Elevation: 610m above sea level

Below: Some spectra of Deep Sky Objects have been recorded with the CEDES Cassegrain Telescope of the *Mirasteilas* Observatory in Falera, Switzerland: aperture 90 cm, focal length 900 cm, and Nasmith Fokus. For more details refer to [706].
Martin Huwiler (left), technical head of the observatory.
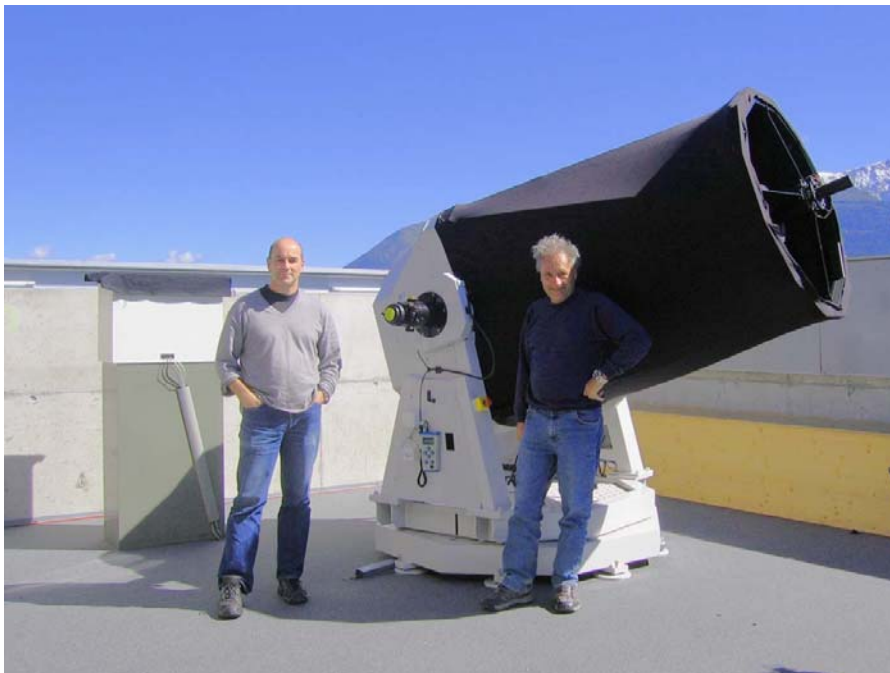
Finally sincere thanks are given to *Martin Huwiler,* for his valuable collaboration and support, as well as to the successful Asteroid hunter *Jose de Queiroz* for his kind hospitality during our stay!

34 Bibliography and Internet

Literature:

[1] James Kaler, *Stars and their Spectra*

[2] Richard Gray, Christopher Corbally, *Stellar Spectral Classification,* Princeton Series in Astrophysics

[3] Keith Robinson, *Spectroscopy, The Key to the stars*

[4] Stephen Tonkin, *Practical Amateur Spectroscopy*

[5] Waltraut Carola Seitter, *Atlas for Objective Prism Spectra – Bonner Spektralatlas*, Astronomisches Institut Bonn, Duemmler Verlag 1970/1975. Out of print today, but recently available as Download: http://www.archive.org/search.php?query=bonner%20atlas

[6] H.A. Abt, A.B. Meinel, W.W. Morgan, J.W. Tapscott, 1968. *An Atlas of Low Dispersion Grating Stellar Spectra*, Out of print.

[7] N. Houk, N. Irvine, D. Rosenbush, Univ. Michigan 1968. *An Atlas of Objective-Prism Spectra,* Out of print.

[8] Ginestet, N.; et al. 1992. *Atlas de Spectres Stellaires, Standards de Classification MK*, / Observatoire Midi-Pyrenees, Out of print.

[9] Jack Martin, *A Spectroscopic Atlas of Bright Stars,* Springer Verlag 2010

[10] Erich Karkoschka, *Atlas für Himmelsbeobachter*, 3. Auflage, Kosmos Verlag

[11] Brian D. Warner, *Lightcurve Photometry and Analysis*

[12] Ken M. Harrison, *Astronomical Spectroscopy for Amateurs*, Springer Verlag 2010

[13] J.-P. Rozelot, C. Neiner et al, *Astronomical Spectrography for Amateurs*, EDP Sciences: EAS Publication Series, Volume 47, 2011.

[14] G.A. Gurzadyan, 1997, *The Physics and Dynamics of Planetary Nebulae*, ISBN-13: 9783540609650

Internet Links:

<u>Author:</u>

The following scripts on the subject (in german) are downloadable under this link: http://www.ursusmajor.ch/astrospektroskopie/richard-walkers-page/index.html

[30] *Analysis and Interpretation of Astronomical Spectra, Theoretical Background and Practical Applications for Amateur Astronomers*

[31] *Das Aufbereiten und Auswerten von Spektralprofilen mit den wichtigsten IRIS und Vspec*

[32] *Kalibrierung von Spektren mit der Xenon Stroboskoplampe*

[33] *Emissionsspektroskopie mit Funken- und Lichtbogenanregung*

[34] *Kalibrierung von Spektren mit dem Glimmstarter ST 111 von OSRAM*

Spectral atlases and commented spectra:

[50] *An atlas of stellar spectra, with an outline of spectral classification,* Morgan, Keenan, Kellman (1943): http://nedwww.ipac.caltech.edu/level5/ASS_Atlas/frames.html

[51] *Revised MK Spectral Atlas for Stars earlier than the Sun* W.W. Morgan, H.A. Abt, and J.W. Tapscott, (1978), Yerkes Observatory, University of Chicago and Kitt Peak National Observatory http://nedwww.ipac.caltech.edu/level5/March02/Morgan/frames.html

[52] *Digital Spectral Classification Atlas* von R.O. Gray, (2000): http://nedwww.ipac.caltech.edu/level5/Gray/frames.html

[53] *Moderate-resolution spectral standards from lambda 5600 to lambda 9000* von Allen, L. E. & Strom, K. M: http://adsabs.harvard.edu/full/1995AJ....109.1379A

[54] Paolo Valisa, *Osservatorio Astronomico Schiaparelli, Varese*. http://www.astrogeo.va.it/astronom/spettri/spettrien.htm

[55] *An atlas of low-resolution near-infrared spectra of normal stars* Torres Dodgen, Ana V., Bruce Weaver: http://adsabs.harvard.edu/abs/1993PASP..105..693T

[56] *Contemporary optical spectral classification of the OB stars - A digital atlas* : N. R. Walborn, E.L. Fitzpatrick (1990) http://adsabs.harvard.edu/full/1990PASP..102..379W

[57] *An Atlas of yellow-red OB Spectra* N. R. Walborn (1980), http://articles.adsabs.harvard.edu/full/1980ApJS...44..535W

[58] *A Standard Stellar Spectral Sequence in the Red/Near Infrared Classes: K5 to M9*, Kirkpatrick et al. http://articles.adsabs.harvard.edu/full/1991ApJS...77..417K

[59] *The Interactive Database of Spectral Standard Star Atlases.* http://alobel.freeshell.org/ http://spectra.freeshell.org/SpectroWeb_news.html

[60] UCM: *Librerias de espectros estelares* http://www.ucm.es/info/Astrof/invest/actividad/spectra.html

Sun:

[80] Highly resolved solar spectrum, Bass2000 http://bass2000.obspm.fr/download/solar_spect.pdf

[81] Lunettes Jean Roesch (Pic du Midi), Highly resolved solar spectrum, recorded on the Jungfraujoch Switzerland, Université de Genève: http://ljr.bagn.obs-mip.fr/observing/spectrum/index.html

Carbon Stars:

[100] *A Moderate Resolution Spectral Atlas of Carbon Stars*, Cecilia Barnbaum, P. Keenan et al. http://articles.adsabs.harvard.edu/full/1996ApJS..105..419B

[101] *A High Resolution Spectral Atlas of Carbon Stars*, Cecilia Barnbaum, http://articles.adsabs.harvard.edu/full/1994ApJS...90..317B

[102] *The Chemical Composition of the Rare J-Type Carbon Stars*, Carlos Abia et al. http://arxiv.org/PS_cache/astro-ph/pdf/9912/9912025v1.pdf

[103] *Near-Infrared Spectra of 29 Carbon Stars, Simple Estimates of Effective Temperature*, Masuo Tanaka et al.   http://pasj.asj.or.jp/v59/n5/590508/590508.pdf

[104] *Radial Velocity Distribution and Line strengths of 33 Carbon Stars in the Galactic Bulge*, 1991, D. Tyson et al. http://articles.adsabs.harvard.edu/full/1991ApJ...367..547T

[105] *Carbon Stars, Hydrostatic Models and Optical/Near Infrared Interferometry*, S. Schneiderbauer, 2008, Univ. Vienna, http://othes.univie.ac.at/1627/1/2008-10-13_9940129.pdf

[106] *Understanding Carbon Star Nucleosynthesis from Observations*, 2003, C. Albia et al. http://www.publish.csiro.au/?act=view_file&file_id=AS03021.pdf

[107] *Revised MK Classification of the Red Carbon Stars*, 1993, P. Keenan http://adsabs.harvard.edu/full/1993PASP..105..905K

[108] *Photometric and Spectroscopic Investigation of a New Carbon Star in the Auriga Region*, 1978, M. Vetesnik, Brno University http://articles.adsabs.harvard.edu/full/1979BAICz..30....1V

[109] *SiC2 in carbon stars: Merrill Sanford Absorption Bands between 4100 and 5500A,* P. J. Sarre et al. http://articles.adsabs.harvard.edu/full/2000MNRAS.319..103S

[110] *Band-Head Wavelengths of C2, CH, CN, CO, NH, NO, O2, OH and Their Ions,* L. Wallace *1962* http://adsabs.harvard.edu/full/1962ApJS....7..165W

Spectral Class S:

[140] *Spectral types of S and SC stars on the revised MK system*, 1979, Keenan, & Boeshaar
http://articles.adsabs.harvard.edu/full/1980ApJS...43..379K

[141] *Molecular Spectra of pure S-Stars*, 1978, S. Wyckoff, R.E.S. Clegg
http://adsabs.harvard.edu/abs/1978MNRAS.184..127W

Evolution AGB Stars:

[160] *On the evolution and properties of AGB stars*, 1993, Martin Arnold Theodoor Groenewegen,
Universität Amsterdam http://dare.uva.nl/,   103726 in das Suchfeld eingeben.

Telluric Absorptions:

[180] *High Resolution Spectral Atlas of Telluric Lines*, G. Catanzaro, Universita die Messina.
http://webusers.ct.astro.it/gca/papers/telluric.pdf

[181] *A Method of Correcting Near-Infrared Spectra for Telluric Absorption.* W. D. Vacca et al.
http://www.journals.uchicago.edu/doi/pdf/10.1086/346193

Light Pollution and Airglow:

[190] *Measuring Light Pollution on La Palma*, Chris R. Benn, Isaac Newton Group, Spain
http://www.starlight2007.net/pdf/proceedings/C_Benn.pdf

[191] *The High-Resolution Light-polluted Night-Sky Spectrum at Mount Hamilton, California*, T. G.
Slanger P. C. Cosby et al. 2003:   http://adsabs.harvard.edu/abs/2003PASP..115..869S

[192] *Where the shadows lie – The dark skies of Chile*, Ferdinando Patat – ESO,
http://www.eso.org/~fpatat/science/skybright/zenit/zenit_paper.htm

Planetary Nebulae and Emissionsline Objects:

[200] *Emission Lines Identified in Planetary Nebulae*, Y.P. Varshni, et al., 2006 Univ. Ottawa
http://laserstars.org/
http://laserstars.org/data/nebula/identification.html

[201] *Gallery of Planetary Nebula Spectra*, Williams College
http://www.williams.edu/astronomy/research/PN/nebulae/
http://www.williams.edu/astronomy/research/PN/nebulae/legend.php

[202] *Planetarische Nebel*, Frank Gieseking, 6 articles, SUW 1983.

[203] *Balmer Line Ratios in Planetary Nebulae*, Osterbrock et al., Univ. Wisconsin 1963
http://articles.adsabs.harvard.edu/cgi-bin/nph-
iarticle_query?1963ApJ...138...62O&defaultprint=YES&filetype=.pdf

[204] *3D Spektrofotometrie Extragalaktischer Emissionslinienobjekte*, Dissertation J. Schmoll, AIP
http://www.aip.de/groups/publications/schmoll.pdf

[205] *An Evaluation of the Excitation Parameter for the Central Stars of Planetary Nebulae*, W. A.
Reid et al, Univ. Sydney 2010 http://arxiv.org/PS_cache/arxiv/pdf/0911/0911.3689v2.pdf

[206] *Excitation Class of Nebulae – an Evolution Criterion?* G. A. Gurzadyan, A.G. Egikyan, Byurakan
Astrophysical Observatory 1990 http://articles.adsabs.harvard.edu/full/1991Ap%26SS.181...73G

[207] *The Planetary Nebulae*, J. Kaler, http://stars.astro.illinois.edu/sow/pn.html

[210] *A HighResolution Catalogue of Cometary Emission Lines*, M.E Brown et al. 1996 Caltech
http://www.gps.caltech.edu/~mbrown/comet/echelle.html

[220] Optical Spectra of Supernova Remnants, Danziger, Dennefeld, Santiago de Chile 1975,
http://articles.adsabs.harvard.edu/full/1976PASP...88...44D

[221] Optical and Radio Studies of SNR in the Local Group Galaxy M33, Danziger et al. 1980, ESO
http://www.eso.org/sci/publications/messenger/archive/no.21-sep80/messenger-no21-7-11.pdf

[222] Emission-line spectra of condensations in the Crab Nebula, Davidson 1979
http://adsabs.harvard.edu/abs/1979ApJ...228..179D

[223] *ISM and Star Formation, The Orion Bar*, Harvard Astronomy 201b/2011
http://ay201b.wordpress.com/2011/05/01/the-orion-bar/

[224] *Complex ionized structure in the theta-2 Orionis region*, J. R. Walsh, Univ. Manchester, 1981
http://articles.adsabs.harvard.edu/full/1982MNRAS.201..561W

Wolf Rayet Stars:

[230] *C IV λ5806 in Wolf Rayet Stars*, Anne B. Underhill
http://articles.adsabs.harvard.edu//full/1988PASP..100.1269U/0001269.000.html

[231] *Atlas for Wolf-Rayet Stars*, Harvard Center for Astrophysics
https://www.cfa.harvard.edu/~pberlind/atlas/htmls/wrstars.html

[232] *The VII$_{th}$ catalogue of galactic Wolf–Rayet stars*, Karel A. van der Hucht
http://www.astro.uio.no/ita/grb/VIIWRCAT.pdf

[233] *Spectral Classification of Wolf-Rayet Stars*, W.A. Hiltner, R.E. Schild, 1965 Chicago
http://articles.adsabs.harvard.edu/full/1966ApJ...143..770H

[234] *Physical Properties of Wolf-Rayet Stars,* Paul A. Crowther,
http://www.stsci.de/wr140/pdf/crowther2006.pdf

Be Stars:

[250] *High and intermediate-resolution spectroscopy of Be stars*, J. Chauville et al. A&A 2002
http://www.aanda.org/index.php?option=com_article&access=standard&Itemid=129&url=/articles/aa/abs/2001/42/aa1599/aa1599.html

[251]: *Spectra of the Brightest Be stars and Objects Description*, A. Miroshnichenko, University of North Carolina, www.astrospectroscopy.de/Heidelbergtagung/Miroshnichenko2.ppt

[252] *Summary of Experiences from Observations of the Be-binary δ Sco*, A. Miroshnichenko, University of North Carolina, www.astrospectroscopy.de/Heidelbergtagung/Miroshnichenko1.ppt

[253] *Properties of the δ Scorpii Circumstellar Disk from Continuum Modeling,* A. Miroshnichenko et al.: University of North Carolina,
http://libres.uncg.edu/ir/uncg/f/A_Miroshnichenko_Properties_2006.pdf

[254] *High resolution emissionline spectroscopy of Be Stars*, Reinhard W. Hanuschik, Astronomisches Institut Universität Bochum.
http://articles.adsabs.harvard.edu/full/1986A%26A...166..185H

[255] *V/R Variations of Binary Be Stars,* S. Stefl et al. ESO 2007
http://www.arc.hokkai-s-u.ac.jp/~okazaki/Meetings/sapporo/361-0274.pdf

[256] *The Optical Counterpart of the X-ray Transient RX J0117.6-7330R.* Soria:, Siding Spring Observatory Coonabarabran, Australia http://articles.adsabs.harvard.edu/full/1999PASA...16..147S

[257] *Spektroskopische Beobachtungen der Hα- und der He I 6678-Emission am Doppelsternsystem δ Scorpii,* E. Pollmann: http://www.bav-astro.de/rb/rb2009-3/151.pdf

Herbig Ae/Be Stars:

[270] *Spectrophotometry of R Monocerotis*, K.H. Böhm et al. 1976, University of Washington
http://adsabs.harvard.edu/full/1976A%26A....50..361B

[271] *Spectroscopy of R Monocerotis and NGC 2261*, Alan Stockton et al. Univ. of Hawai 1974,
http://adsabs.harvard.edu/full/1975ApJ...199..406S

[272] *Toward Understanding the Environment of R Monocerotis from high Resolution Near-Infrared Polarimetric Observations,* M.A. Jolin et al. Université de Montréal, 2010
http://iopscience.iop.org/0004-637X/721/2/1748/fulltext/apj_721_2_1748.text.html

[273] *Iron Emission Lines in the Spectra of Herbig Ae/Be stars Viewed through Their Proto-Planetary Disks*. C.A. Grady et al. 183rd AAS Meeting, Washigton DC
http://articles.adsabs.harvard.edu/full/1993AAS...183.4109G

[274] *Spektroskopische Variationen des Herbig Ae/Be Sterns HD 163296*. Diploma Thesis Stefan Noll, University Heidelberg 1999,
http://www.lsw.uni-heidelberg.de/projects/hot-stars/Diplom_Noll.pdf

[275] *Carbon Monoxide Observations of R Monocerotis, NGC 2261 and Herbig Haro 39: The Interstellar Nozzle*. J Canto et al. Univ. Mexico 1980.
http://articles.adsabs.harvard.edu/full/1981ApJ...244..102C

T Tauri Stars:

[280] *Spectra of T Tauri Stars*, A. McKay
http://astronomy.nmsu.edu/

[281] *Understanding Stellar Birth Through the Photometric and Spectroscopic Variability of T Tauri Stars,* MW Eastwood, N. Mahmud, C.M. Johns, Rice University Houston Texas 2011,
http://www.as.utexas.edu/ugrad_symposium/?a=3

Extragalactic Objects:

[300] Caltech: Spektralatlasses for extragalactic Objekts
http://nedwww.ipac.caltech.edu/level5/catalogs.html

[301] *A Spectrophotometric Atlas of Galaxies*, Robert C. Kennicutt, Steward Observatory
http://articles.adsabs.harvard.edu/full/1992ApJS...79..255K

Monographs:

[340] *Time-series Analysis of Line Profile Variability in Optical Spectra of ε Orionis*, Gregory B. Thompson http://etd.ohiolink.edu/send-pdf.cgi/Thompson%20Gregory%20Brandon.pdf?toledo1249511358

[341] *Spektralatlas P Cygni*, O. Stahl, Landessternwarte Heidelberg
http://seds.org/Maps/Stars_en/Spectra/pcyg.html

[341a] *The Spectrum of P Cygni 1964,* L.S. Luud, Academy of Science Estonian SSR 1964
http://adsabs.harvard.edu/full/1967SvA....11..211L

[341b] *Of the Spectrum and Nature of P Cygni,* Maart de Groot, Astr. Inst. Nederlands, 1968
http://adsabs.harvard.edu/full/1969BAN....20..225D

[342] Christian Buil: *Vega Spectrum Atlas, a full commented spectrum*
http://astrosurf.com/buil/us/vatlas/vatlas.htm

[343] O.C. Wilson: *The Wolf-Rayet Spectroscopic Binary HD 190918*, Mount Wilson 1948
http://articles.adsabs.harvard.edu/full/1949ApJ...109...76W

[344] *A Study of the moderately wide Wolf Rayet Spectroscopic Binary HD190918*, A. Underhill et al. http://adsabs.harvard.edu/full/1994ApJ...432..770U

[345] Lesley A. Morgan 1971: *The Emission Line Spectrum of the Orion Nebula*...
http://articles.adsabs.harvard.edu/cgi-bin/nph-iarticle_query?1971MNRAS.153..393M&defaultprint=YES&filetype=.pdf

[346] S. V. Marchenko et al.: *The unusual 2001 Periastron Passage in the „Clockwork" Colliding Wind Binary WR 140*, http://www.stsci.de/wr140/pdf/marchenko2003.pdf

[347] *Multi Frequency Variations of Wolf Rayet System HD193793*, P.M. Williams et al. 1989
http://esoads.eso.org/abs/1990MNRAS.243..662W

[348] *Spectral Analysis of a Peculiar Star WZ Cassiopeiae*, Masanori Hirai, University of Tokyo,
http://adsabs.harvard.edu/full/1969PASJ...21...91H

[349] *The 6708 resonance line of Li I in the spectrum of the N-type variable star WZ Cassiopeiae*, McKellar 1941, http://articles.adsabs.harvard.edu//full/1941Obs....64....4M/0000004.000.html

[350] *Cyclic variability of the circumstellar disk of the Be star ζ Tau*, S. Stefl et al., ESO, http://arxiv.org/PS_cache/arxiv/pdf/0907/0907.2250v1.pdf

[351] *Visual/infrared interferometry of Orion Trapezium stars: preliminary dynamical orbit and aperture synthesis imaging of the θ1 OrionisC system*, S. Kraus, Y. Y. Balega et al. 2006, www.skraus.eu/papers/kraus.T1OriC.pdf

[352] *Spectrum variability of 68 Cygni, an O(f) star at the center of a ring nebula,* V. I Alduseva, A. A. Aslanov et al. 1982, *http://adsabs.harvard.edu/full/1982SvAL....8..386A*

Lectures and practica:

[400] *Versuchsanleitung zum Astrophysikalischen Praktikum, Grobe Klassifikation von Sternspektren*, Kiepenheuer Institut: http://www.kis.uni-freiburg.de/fileadmin/user_upload/kis/lehre/praktika/sternspektren.pdf

[401] F. Royer: *Rotation des étoiles de type A*, Vorlesung Ecole d'Astronomie de CNRS http://adsabs.harvard.edu/abs/1996udh..conf..159R

[402] *Vorlesung Astrophysik*, Max Planck Institut München: www.mpa-garching.mpg.de/lectures/TASTRO

[403] *Vorlesung Astrophysik,* Astrophysikalisches Institut Potsdam http://www.aip.de/People/MSteinmetz/classes/WiSe05/PPT/

[404] Astrophysics graduate course 25530-01 Lecture 6 and 7, Univ. Basel http://phys-merger.physik.unibas.ch/~cherchneff/Site_2/Teaching_at_UniBasel.html

Data files

[500] CDS Strassbourg: *SIMBAD Astonomical Database* http://simbad.u-strasbg.fr/simbad/

[501] *NASA Extragalactic Database (NED)* http://nedwww.ipac.caltech.edu/

[502] *The SAO/NASA Astrophysics Data System*, http://adsabs.harvard.edu/index.html

[503] *NIST Atomic Spectra Database*: http://physics.nist.gov/PhysRefData/ASD/lines_form.html

[504] Simulated emission spectra for all elements http://bmauclaire.free.fr/astronomie/spectro/simulation/noblet/index2.htm

[505] *The Bright Star Catalogue, 5th Revised Ed. (Preliminary Version) (Hoffleit+, 1991)* Datenzugang über http://www.alcyone.de/search_in_bsc.html

[506] James Kaler http://stars.astro.illinois.edu/sow/sowlist.html

[507] AAVSO, American Association of Variable Star Observers http://www.aavso.org/

Spectrographic software:

[550] IRIS: Webpage of *Christian Buil* http://www.astrosurf.com/buil/

[551] Vspec: Webpage of *Valerie Désnoux* http://astrosurf.com/vdesnoux/

[552] RSpec: Webpage of *Tom Field* http://www.rspec-astro.com/

[553] MIDAS, ESO http://www.eso.org/sci/software/esomidas//

Spectrographs and Cameras:

[600] SQUES Echelle Spectrograph, Eagleowloptics Switzerland,
http://www.eagleowloptics.com/

[603] DADOS Spectrograph, Baader Planetarium, Germany:
http://www.baader-planetarium.com/pdf_download.htm

[605] Shelyak Instruments: http://www.shelyak.com/

[606] Datasheet Sony Chip ICX285AL:
http://www.datasheetcatalog.org/datasheet/sony/a6803068.pdf

[607] SBIG Spectrograph DSS-7, http://ftp.sbig.com/dss7/dss7.htm

General links:

[700] Isabelle A. Grenier: *The Gould Belt, star formation and the interstellar medium*
http://arxiv.org/PS_cache/astro-ph/pdf/0409/0409096v1.pdf

[701] Gene Smith, University of California, San Diego*, Astronomy Tutorial, Stellar Spectra*
http://cass.ucsd.edu/public/tutorial/Stars.html

[702] H.A. Abt: *New Data on A-Type Disk stars*, The Astrophysical Journal 2007,
http://iopscience.iop.org/0067-0049/174/2/499/pdf/0067-0049_174_2_499.pdf

[703] H. M. Qiu et al.*: The Abundance Patterns of Sirius and Vega*, The Astrophysical Journal 2001
http://iopscience.iop.org/0004-637X/548/2/953/pdf/0004-637X_548_2_953.pdf

[704] U.K. Gehlich: *Differential Fine Analysis Sirius versus Vega*, Astronomy & Astrophysics, 1969
http://articles.adsabs.harvard.edu/full/1969A%26A.....3..169G

[705] Martin Brunold, CH-Abtwil http://www.astrolabe.ch/index.aspx

[706] *Mirasteilas,* Observatory, Falera http://www.sternwarte-mirasteilas.ch/

http://de.wikipedia.org/wiki/Sternwarte_Mirasteilas